respiration and in mitochondrial biogenesis (12). The expression of several antioxidant enzymes is also repressed by glucose, but in some cases this effect is only slight (reviewed by 1, 13). At high glucose levels, mitochondria are present with few cristae that are not well developed (14) and, as a consequence, this organelle is not very active. On the other side, when glucose is consumed from the culture medium, yeast suffers great physiological and biochemical changes in order to produce ATP mainly by oxidative phosphorylation and consequently more ROS are generated. Therefore, by changing the carbon source in the media, bioenergetics of yeast is profoundly affected.

Expression of peroxiredoxins is also affected by glucose in yeast (15,16). cTPxI (also known as Tsa1p) from *Saccharomyces cerevisiae* was the first peroxiredoxin described in a eukaryotic cell and is a very abundant protein (17, 18). Its importance in cell protection against peroxide insult has been demonstrated in several reports (5; 19), especially in cells with dysfunctional mitochondria (15). Furthermore, it was shown in a genome-wide screen that *TSA1* has an important role in the protection of yeast against accumulation of mutations and of chromosomal rearrangements (20). cTPxII (also known as Tsa2p) appears to be a duplication of cTPxI, since they share 86% of identity in their amino acid sequence and both are located in the cytosol (2,21). Contrary to cTPxI, the levels of cTPxII are very low under basal conditions (2,22). Here, we have analyzed the expression pattern of cTPxII and the viability of Δ cTPxII cells under several conditions. Additionally, the enzymatic properties of recombinant cTPxI and cTPxII were investigated in detail. Our results indicated that cTPxII, together with cTPxI and other antioxidants, is a key component of yeast defense against stress induced by organic peroxides, independently of the carbon source present in the media. Moreover, biochemical assays performed in cell extracts indicated that catalase cooperate with peroxiredoxins in the protection of yeast against H_2O_2 insult.

Experimental Procedures

Yeast strains and growth conditions

Saccharomyces cerevisiae yeast strains used in this study were BY4741 *(Mat a; His3Δ1; Leu2Δ0; Met15Δ0; Ura3Δ0)*, Δ cTPxI *(Mat α; His3Δ1; Leu2Δ0; Lys2Δ0; Ura3Δ0; YML028W : : Kan Mx4.)*, Δ cTPxII *(Mat a; His3Δ1; Leu2Δ0; Met15Δ0; Ura3Δ0; YDR453C : : Kan Mx4)*.

Cells were grown at 30°C in complete synthetic medium (23) containing glucose, glycerol or raffinose as carbon sources. For most analysis, except when expression of the *TSA2* gene was tested at different phases of growth, cells were collected at the mid-logarithmic phase, usually at $OD_{600nm} = 0.8$.

To obtain high amounts of cells adapted to growth under glycerol or raffinose as the carbon source, pre-cultures were grown overnight in glucose, harvested and transferred to the respective media. Cells were then cultivated for eight hours in glycerol or raffinose-containing media. This condition was sufficient to induce yeast adaptation from a fermentative to a respiratory condition (16).

Determination of peroxide tolerance

Tolerance of yeast cells to H_2O_2 or to TBHP was determined by the spot test. Inoculates were obtained from cells that were grown overnight in complete synthetic media with 2% glucose.

In the case of the experiments conducted in fermentative conditions, inoculates were diluted to $OD_{600nm} = 0.2$ in the next day. Afterwards, yeast was grown until cell density reached a value equivalent to $OD_{600nm} = 0.8$. Finally, cell cultures were diluted again to $OD_{600nm} = 0.2$ and then four subsequent 1/5 dilutions of these cell suspensions were

performed. 10 µl droplet of each dilution was plated onto complete synthetic medium plus agar with glucose 2%.

For experiments in respiratory conditions, inoculates were diluted in synthetic media containing glycerol with a cell density equivalent to $OD_{600nm} = 0.8$. Cells were then cultivated for eight hours in glycerol-containing media and then diluted to $OD_{600nm} = 0.2$. Four subsequent 1/5 dilutions of these cell suspensions were performed. 10 µl droplet of each dilution was plated onto complete synthetic medium plus agar with glycerol 2% and glucose 0.1%.

Plates were incubated for 30 or 48 hours when glucose or glycerol was used respectively as the carbon source. Peroxides were added to plates at the concentrations indicated in the figures.

Northern blot analysis

All the procedures were according to the membrane manufacturer's protocol and as described by Ausubel *et al.* (23). In summary, analyses were conducted on total yeast RNA extracted from cells under distinct growth conditions by the hot acid phenol and separated by electrophoresis on formaldeyde-agarose gels. The fractioned RNAs were transferred to a positively charged nylon membrane (Amersham) by capillary blotting and fixed. Probed membranes were exposed to Kodak films (X-OMAT). For probe preparation, a 600 bp *NdeI/BamHI* fragment containing the *TSA2* coding sequence was isolated from plasmid pPROEX/*TSA2*. Plasmidial DNA preparation, gel electrophoresis and purification were all carried out using standard methods. The resulting purified fragment was used to construct the *TSA2* ^{32}P-labeled probe by random-primed labeling. Ribosomal RNA, whose abundance was fairly constant under different growth conditions or among strain derivatives, was used as a loading control (15,16). The amount of rRNA in each well was determined by the

fluorescence of ethidium bromide bound to this nucleic acid and by nucleic acid absorbance at 260nm.

Construction of expression vectors for cTPxI, cTPxII, thioredoxin reductase and thioredoxin 1

TSA2 was PCR amplified from yeast genomic DNA, using the following forward 5'-TATCATATGGTAGCAGAAGTTCAAAAACAAGCC-3' and reverse 5'-TAGGATCCTTAATTATTGGCATTTTTG-3' primers. The underlined bases represent the *NdeI* and *BamHI* sites, respectively. The PCR product was cloned into the pGEM-Teasy vector (PROMEGA), resulting in the pGEM/*TSA2* plasmid. An *E. coli* DH5-alpha strain was transformed with pGEM/*TSA2* and white colonies were selected from LB-ampicillin-*X-gal* medium. Plasmid extraction was performed using the Rapid Plasmid Miniprep System Concert kit (GIBCO-BRL). p-PROEX (GIBCO-BRL) and pGEM/*TSA2* were first digested with *NdeI* and then with *BamHI*. Both p-PROEX and pGEM/*TSA2* digestion products were extracted from an agarose gel using the Rapid Gel Extraction Concert kit (GIBCO-BRL) and the *TSA2* fragment was ligated to the digested p-PROEX expression vector. The resulting p-PROEX/*TSA2* plasmid was sequenced with an Applied biosystems ABI Prism 377 96 apparatus to confirm that the construction was correct. An *E. coli* DH5-alpha strain was transformed with p-PROEX/*TSA2* and it was used for cTPxII expression and purification.

Expression vectors for Trr1, Trx 1 and cTPxI were similarly constructed after their genes were cloned respectively into *NdeI* and *BamHI* restriction sites of pPROEX, pET17b (Novagen) and pET15b (Novagen) expression vectors.

Protein expression and purification

The *E. coli* DH5-alpha strain transformed with p-PROEX/*TSA2* or with p-PROEX/*TRR1* were cultured (50 ml) overnight in LB + ampicillin medium (100 μg/ml), transferred to 1 liter of fresh LB + ampicillin medium and cultured further until the OD_{600} reached 0.6-0.8. IPTG was then added at a final concentration equivalent to 1 mM. After 3 hours of incubation, cells were harvested by centrifugation. The pellet was washed and suspended in the start buffer (20 mM phosphate buffer, pH 7.4). Two sonication cycles of 30 seconds (35% amplitude) followed by 30 seconds on ice were applied to the cell suspension. The cell extract was then kept on ice during treatment with 1% streptomycin sulfate for 15 minutes. The suspension was centrifuged at 31,500 x g for 30 minutes to remove nucleic acid precipitates and cell debris. cTPxI and Trx1 were expressed by similar protocols, but Bl21(DE3) strain was used as the host instead of DH5-alpha strain.

Cell extracts containing bacteria that expressed cTPxI, cTPxII or TRR1 were applied to a Hi-trap nickel-affinity column (Amersham, Uppsala, Sweden) or Talon cobalt-affinity resin (BD Biosciences Clontech, Palo Alto, CA, USA). The conditions for protein purification were optimized using the gradient procedure for imidazole concentration as described by the manufacturer. Trx1 (thioredoxin 1 protein) was purified by boiling bacterial extracts as described previously (24).

Determination of thioredoxin-dependent peroxidase activity

Thiol dependent peroxidase activities of cTPxI and cTPx II were measured by NADPH oxidation assay. NADPH oxidation was monitored at A_{340nm} in 1mL reaction mixtures containing 50mM Hepes-NaOH (pH 7.4), 100uM DTPA, 1mM azide, 0.225uM Trx2, 0.075uM TRR1, 2.1uM cTPxII and 0.18mM NADPH. The reaction was started by addition of 10 to 100uM of peroxide solution and the mixture was incubated at 30°C. Protein concentrations were determined using their absorbance at 280nm. The extinction coefficients

for cTPxI (ε_{280} = 22800 $M^{-1}.cm^{-1}$) and for cTPxII (ε_{280} = 26150 $M^{-1}.cm^{-1}$) were obtained by calculations performed through ProtParm tool (http://bo.expasy.org/tools/protparam.html).

Determination of peroxide consumption by yeast extracts

Cells were grown at 30°C in complete synthetic medium (23) containing 2% glucose and collected at log phase (OD_{600nm} = 0.8) and were harvested by centrifugation at 16000 x g for 5 minutes. The pellet was washed and suspended in 400ul of 50mM Hepes pH 7.4 / 50mM NaCl buffer containing 2ug/ml leupeptin and 1ug/ml pepstatin. Glass beads were added at the same volume of the sample. Two cycles of 6 minutes of vortex following of 6 minutes on ice were applied to cell suspension. The suspension was centrifugated at 16000 g for 5 minutes. Supernatants were collected and centrifugated again at 16000 g for 30 minutes in order to remove protein precipitates. The supernatants were collected for assay.

The remaining peroxide contents present in the supernatants were determined at different intervals by the FOX assay as described previously (25). Reactions were initiated by the addition of peroxide compounds and stopped at different intervals by the addition of 200 µM HCl to the reaction mixtures. H_2O_2 concentration in stock solutions was checked by its absorbance at 240 nm (ε_{240nm} = 43.6 $M^{-1}.cm^{-1}$).

The amount of proteins in yeast extracts were determined by the Bradford assay using bovine serum albumin as a standard and the reagents were purchased from BIO-RAD. Conditions used to measure H_2O_2 or organic hydroperoxide consumptions were markedly distinct and are indicated in the legend of the figures.

Catalase assays

Yeast cellular extracts were obtained as described in the previous section. Oxygen release due to catalase activity (see reaction 1) in yeast cellular extracts was specifically

determined using Clark electrode at 30°C (Yellow Spring). The saturating oxygen concentration, which corresponds to the full scale of the electrode, was taken to be 0.225 mM (26).

Results

Role of cTPx II in cell protection against peroxide insult.

Previous results have indicated that deletion of the cTPxII gene renders cells more sensitive to peroxide insult, but the effect observed was only slight (21). Here, a very systematic study was performed in which several peroxide concentrations and cell dilutions were analyzed. Moreover, the effect of the carbon source on the protective role of cTPxII was also investigated due to the catabolic repression exerted by glucose (reviewed by 12).

Cells were grown in synthetic medium to avoid the reaction of peroxides with extra-cellular components present in a rich medium such as glutathione (27). Since the rich media are not so well controlled as in the synthetic medium, reproducibility problems may occur when experiments are performed with different lots of components. Using this approach, a pronounced sensitivity of Δ cTPxII cells to TBHP treatment was found in both glucose (preferentially fermentative) and glycerol (respiratory supportive only)-containing media (figure 1). In glucose, at 1 mM TBHP concentration, wild type and mutant strains were similarly sensitive (figure 1). When higher concentrations of TBHP were added to the solid medium, both Δ cTPxI and Δ cTPxII cells were found to be much more sensitive than wild type cells. At 1.2 mM concentration of TBHP, wild type cells could be observed until the 1/125 dilution, whereas Δ cTPxI and Δ cTPxII cells had a significant growth only until the 1/5 dilution. Therefore in these conditions wild type cells were at least one order of magnitude more resistant to TBHP than mutant strains (figure 1). These results indicated that both cTPxI

and cTPxII, among other antioxidants, would be required to protect wild type *Saccharomyces cerevisiae* from TBHP treatment at doses higher than 1mM.

cTPxI and cTPxII appeared to be also very important for cell protection against TBHP treatment in glycerol as a carbon source. Under these conditions, the physiology of yeast is profoundly altered since several genes are repressed by glucose (14). Again, at TBHP doses lower than 1 mM, no significant decrease in viability was observed for Δ cTPxI or Δ cTPxII cells (data not shown). However, deletion of *TSA1* or *TSA2* rendered yeast cells more sensitive to TBHP at higher concentrations (figure 1). These results indicated that both cTPxI and cTPxII were important for yeast protection against TBHP, under both fermentative and respiratory conditions.

A systematic investigation was also performed in order to find a condition where cTPxII would be important for cell protection against H_2O_2 insult. Several conditions were tried and no clear sensitivity of Δ cTPxII cells to H_2O_2 was found when yeast was grown in both glucose-and glycerol-containing media (figure 2). In fact, in some conditions Δ cTPxII cells appeared to be even more resistant than wild type strain (cells grown in glucose and treated with 1,5mM H_2O_2). In contrast, in the same set of experiments a considerable effect was observed for Δ cTPxI cells exposed to H_2O_2 at 1.2 and 1.5 mM concentrations under both repressing and non-repressing conditions (figure 2). The data shown in figures 1 and 2 are representative of at least three experiments performed in the same conditions. In summary, the results presented so far indicated that both cTPxI and cTPxII are important for cell protection against TBHP.

Analysis cTPx II expression

A possible explanation for the specific sensitivity of Δ cTPxII cells to organic peroxide insult could be related to the pattern of *TSA2* expression, in case this gene is induced at higher levels by organic peroxide than by H_2O_2. Therefore, series of *Northern blot* experiments were

conducted to analyze *TSA2* expression. No *TSA2* transcript was detected, in any condition tested, when cells were not exposed to peroxides. However, addition of peroxides even at very low concentrations (0.1 mM for H_2O_2 and 0.3 mM for TBHP) induced strong expression of *TSA2* (figure 3). In contrast, cTPxI is a very abundant protein in the absence of peroxides and is only slightly induced by these oxidants (15,18,21). It is important to note that the probe used in our *Northern blot* experiments was very specific for the *TSA2* gene, since no band was detected in Δ cTPxII cells exposed to 0.3 mM peroxide for 15 minutes (figure 3).

The dose-response expression pattern of *TSA2* was very similar for cells exposed to H_2O_2 and for cells exposed to TBHP and could not explain the specific sensitivity of Δ cTPxII cells for organic peroxides. Therefore, *TSA2* expression was also analyzed as a function of time. Maximal *TSA2* expression was achieved at about 30 minutes of peroxide treatment, followed by a sharp decrease at 60 minutes of treatment (figure 4). Again, the time dependence of *TSA2* expression was very similar after treatments of cells with H_2O_2 and TBHP, in both glucose-or glycerol-containing media (figure 4). Only the induction of *TSA2* by H_2O_2 in cells grown on glucose differed slightly from the pattern described above. In this case, maximal expression was achieved at 15 minutes instead of 30 minutes (figure 4A).

The expression of *TSA2* was also analyzed in cells grown in media containing other carbon sources and other concentrations of glucose. As described above, transcripts were only detected when cells were treated with peroxides (figure 5A). Finally, expression of *TSA2* was measured as function of growth phase. At later phases of growth, a low amount of transcripts could be detected in the absence of peroxides, but levels of *TSA2* transcript increased greatly after peroxide treatment (figure 5B). The much higher induction of *TSA2* by peroxide treatment than induction by glucose exhaustion is in agreement with previous reports (22, 28).

Enzymatic properties of recombinant cTPxII

Since specific sensitivity of Δ cTPxII cells to TBHP could not be attributed to the pattern of *TSA2* induction by peroxides, the enzymatic properties of cTPxII was also analyzed. We hypothesized that cTPxII could be much more efficient in the removal of organic peroxides than in decomposition of H_2O_2. It was reported before that the enzymatic activity of cTPxII is higher for H_2O_2 than for TBHP using an assay based on NADPH oxidation (2). In this case, only one concentration of peroxide was analyzed (1mM). Although the enzymatic parameters of other yeast peroxiredoxins are known (29,30,31), K_m and K_{cat} for cTPxII and K_{cat} for cTPxI have never been established before. Therefore, we have analyzed the properties of cTPxII in detail and enzymatic parameters were determined. Additionally, the enzymatic data of cTPxI and cTPxII were compared using the same thioredoxin and thioredoxin reductase preparations.

cTPxII was slightly more efficient in the removal of H_2O_2 than in the removal of TBHP (figure 6) and all the three K_{cat}/K_m ratios for cTPxII were in the same order of magnitude (10^4 $M^{-1} \times s^{-1}$), (Table I). As described before (2), cTPxI was more efficient than cTPxII in the removal of H_2O_2 (figure 6A and Table I), however the catalysis of TBHP decomposition by cTPxI and cTPxII occurred with about the same efficiency (figure 6B). Since, cTPxII decomposed all the peroxides with approximately the same efficiency (Table I), it does not appear that the enzymatic properties of cTPxI and cTPxII can be implied with the specific sensitivity of Δ cTPxII cells to organic peroxides.

Peroxide removal activities in cellular extracts.

One alternative explanation for the specific sensitivity of Δ cTPxII cells to organic peroxides could be related to the enzymatic properties of other antioxidant enzymes than peroxiredoxins. For instance, catalase and cytochrome c peroxidase I are heme-dependent

proteins that only decomposes H_2O_2 through the catalysis of the reactions 1 and 3, respectively:

$2\ H_2O_2 \rightarrow 2\ H_2O + O_2$ (reaction 1)

2 cytochrome c (Fe^{+2}) + $H_2O_2 \rightarrow$ 2 cytochrome c (Fe^{+3}) + H_2O (reaction 3)

Therefore, it would be expected that the repertoire of antioxidant enzymes available to decompose H_2O_2 would be higher than the systems available to decompose organic peroxides. In fact, the ability of cellular extracts to decompose H_2O_2 was much higher than the removal activity of TBHP. Cellular extracts whose total protein concentration was equal to 0.25ug/ul decomposed a large amount of H_2O_2 added (figure 7A), whereas no removal of TBHP was detected in these conditions (data not shown). It is noteworthy to observe that almost all of the H_2O_2 consumption was inhibited by azide (data not shown), indicating that heme-dependent proteins, probably catalase, mediated this process (see discussion below). The total H_2O_2 removal activities of all yeast extracts were in the same order of magnitude, although extracts from Δ cTPxII cells have significantly higher capacity to decompose this oxidant (figure 7A).

Next, the catalase activities were specifically measured by oxygen release (see reaction 1). Very interestingly, catalase activity in Δ cTPxII cells was about two fold higher than the catalase activities in wild type and Δ cTPxI cells (figure 7B). As expected, oxygen release in all yeast extracts was fully inhibited by azide (data not shown).

Finally, the concentration of cellular extracts and the interval for the analysis peroxide consumption were increased in order to detect TBHP removal. After two hours, cellular extracts from Δ cTPxII cells decomposed less TBHP than wild type and Δ cTPxI cells (figure 8). Therefore, Δ cTPxII cells presented the highest H_2O_2 removal activity and the lowest TBHP removal ability which should be related with its high sensitivity to organic peroxides.

In summary, our results indicated that heme-dependent proteins, probably catalase, in Δ cTPxII cells are responsible, at least in part, for the high resistance of this strain to H_2O_2

(figure 2). Since heme-dependent peroxidases are specific for H_2O_2 (6), they could not cooperate with peroxiredoxins in the protection of Δ cTPxII cells to TBHP treatment, which could explain the results described in figures 1 and 2.

Discussion

In this work, we have reported an extensive analysis of the viability of yeast strains with deletions in the genes encoding cTPxI and cTPxII. Interestingly, Δ cTPxII cells were specifically sensitive to TBHP and resistant to H_2O_2 insult, whereas Δ cTPxI strain was more sensitive than wild type strain to both kinds of peroxides (figures 1 and 2). Some hypotheses were tested to explain this phenotype of Δ cTPxII cells: [1] TBHP would induce higher levels of cTPxII than H_2O_2 ; [2] cTPxII would be more efficient in the enzymatic removal of organic peroxides than in the enzymatic removal of H_2O_2 and [3] alteration of the levels of antioxidants other than cTPxI and cTPxII.

Since the pattern of *TSA2* induction by H_2O_2 and by TBHP were very similar (figures 3 and 4), hypothesis [1] could be ruled out. Enzymatic assays with recombinant peroxiredoxins were conducted in order to test hypothesis [2]. In our hands, cTPxII catalyzed the reduction of both organic hydroperoxides and H_2O_2, with almost same efficiency (10^4 M^{-1} x s^{-1}, Table I), indicating that hypothesis [2] is not valid either. As a matter of comparison, other thiol-dependent peroxidase from *Saccharomyces cerevisiae*, namely cTPxIII (also known as Ahp1, type II TPx or TSA II), is one order of magnitude more efficient in the removal of organic peroxides than in the removal of H_2O_2 (29).

cTPxI decomposed H_2O_2 more efficiently than cTPxII, although in both cases the catalysis were in the same order of magnitude (figure 6A, Table I). The catalysis of organic peroxides by these two proteins were also in the same range. These results indicate that cTPxI

and cTPxII behave similarly which is in agreement with the fact that these two proteins decomposed peroxides at comparable levels in yeast cells (21). As stressed before, these results were expected since cTPxI and cTPxII share 86% of identity (96% of similarity) in their amino acid sequence. However, in a previous report (2), it was shown that cTPxII had the lowest TBHP removal activity among the peroxidases studied which is in contrast with our results showing that cTPxI is only slightly more efficient than cTPxII in the removal organic peroxides (figure 6B, table I). This discrepancy is perhaps explained by the fact that only one peroxide concentration (1mM) was used in the experiments described by Park et al. (2). Since it is well known that peroxides at high concentrations inhibit peroxiredoxins (32), perhaps cTPxII is inhibited to a higher extend than cTPxI. In any case, it is important to emphasize that the kinetic parameters measured here are in the same range of the values obtained for others peroxiredoxins belonging to the 2-cys peroxiredoxin category (32)

Analyses of gene deletions is complex because several processes can be affected in null mutants besides the absence of the respective protein. As an example, deletion of *TSA1* promotes the induction of several genes related to the glutathione system (4). Therefore, an alternative hypothesis for the specific sensitivity of Δ cTPxII cells could be related with proteins other than cTPxI and cTPxII (hypothesis [3]). For instance, heme-dependent proteins, such as catalase and cytochrome c peroxidase, specifically catalyze the decomposition of H_2O_2 but not of organic peroxides (reviewed by 6). cTPxI is a very abundant protein and therefore at low peroxide concentrations it could cope with oxidative stress, especially in cells in the log phase (15,19). At high peroxide concentrations, other enzymes may be necessary to protect yeast. In the case of high levels of organic peroxides, it appears that cTPxII, together with cTPxI (among other antioxidants), would be responsible for the antioxidant protection. In the case of the oxidative stress insult by high levels of H_2O_2, catalase and cytochrome c

peroxidases may probably cooperate with cTPxI and cTPxII. Figure 9 summarizes this hypothesis and is described in more detail later.

To test the hypothesis of figure 9, peroxide removal activities were determined in several conditions and in several cellular extracts. Our results indicated that the capacity of yeast to decompose H_2O_2 is much higher than the removal of TBHP. After 10 minutes of incubation, no removal of organic peroxide could be detected, whereas about 40-66 % of H_2O_2 added was decomposed by yeast extracts (figure 7A). Very importantly, almost 100% of H_2O_2 decomposition observed in figure 7 was inhibited by azide, indicating an important role of heme-dependent proteins, probably catalase, since it was shown before that H_2O_2 decomposition, in the absence of reductants, was fully abolished in acatalasemic yeast strain (33). In fact, catalase activity was specifically detected in all yeast extracts due to its ability to release oxygen (figure 7B). Both H_2O_2 removal and catalase activity were significantly higher in Δ cTPxII, but not in Δ cTPxI strain (figure 7). We have tried to measure the mRNA levels of catalase T (cytosolic) and catalase A (peroxisomal) in the conditions of the assays described in figure 7, but no bands were detected, which is in agreement with previous reports that both catalases genes are repressed by glucose (34). In spite of repression of catalase expression, a considerable amount of catalase activity has been detected in media containing high levels of glucose by us (figure 7B) and by others (33). These findings probably reflect the fact that catalase possess very high specific activity (reviewed by 6).

In both Δ cTPxI and Δ cTPxII cells there are catalase and cytochrome c peroxidase available to decompose H_2O_2, but only the first strain is more sensitive than wild type cells to this oxidant (figure 2). Several factors may explain this phenomenon: (i) cTPxI is more abundant than cTPxII in basal conditions; (ii) catalase activity in Δ cTPxII was twice than the activity in Δ cTPxI strain (figure 7), (iii) cTPxI is more efficient than cTPxII in the removal of

H_2O_2 (Table I, figure 6A and reference 2) and (iv) transcription of *TSA2* gene is induced in Δ cTPxI cells, but *TSA1* mRNA levels are not increased in Δ cTPxII cells (21).

To measure TBHP consumption the amount of protein extracts were increased sixteen times in relation to the experiments of H_2O_2 decomposition. Analysis of TBHP removal (figure 8) was also in agreement with the hypothesis summarized in figure 9. Both wild type and mutant cells cannot account with catalase or cytochrome c peroxidase to decompose organic peroxides because these enzymes are specific for H_2O_2 (reviewed by 6). Thus, the repertoire of antioxidant enzymes available to decompose organic peroxides in *Saccharomyces cerevisiae* should be more limited and therefore this microorganism is probably more dependent on cTPxI and cTPxII to protect themselves from this oxidant. In fact, deletion of *TSA2* gene rendered yeast more sensitive to organic peroxides (figure 1) and reduced the capacity of this microorganism to decompose this oxidant (figure 8).

The mechanisms involved in cell susceptibility to peroxides appeared to be distinct in the Δ cTPxI and Δ cTPxII mutants (figure 9). Δ cTPxI cells are very sensitive to both kinds of peroxides probably because they do not possess cTPxI (a very abundant protein) to decompose these oxidants. It is interesting to note that Δ cTPxI cells have the highest THBP removal activity from all the strains studied including the wild type (figure 8). This phenomenon is probably related with the induction of several GSH-dependent enzymes (4), including the recently described mitochondrial glutathione reductase isoform (35).

In the case of Δ cTPxII, a significant up-regulation of catalases was observed (figure 7), which should contribute for the high resistance of this strain to H_2O_2 (figure 2). As a matter of fact, in some cases (cells grown in glucose and exposed to 1,5mM H_2O_2), Δ cTPxII strain was even more resistant than wild type cells. Interestingly, while Δ cTPxII cells were highly resistant to H_2O_2, they presented high TBHP sensitivity. The factors involved in this phenotype are not evident, but they should not solely depend on the absence of cTPxII

proteins because this peroxidase is not an abundant protein in basal conditions (22). Probably, proteins other than cTPxI and cTPxII are involved in this phenomenon. One of these proteins could be mitochondrial glutathione reductase that is present at low levels in Δ cTPxII cells (36). The low levels of reduced glutathione in the mitochondria of Δ cTPxII cells should limit the supply of reducing equivalents to PhGPx enzymes and therefore impair the decomposition of organic peroxides by this pathway (3,4). Besides cTPxI, cTPxII and PhGPx proteins, is important to mention that cTPxIII should also be very important for the protection of *Saccharomyces cerevisiae* against TBHP (figure 9) according to previous results (29,37).

The signaling network involved in the response of yeast to the different kinds of peroxides is very complex. In the case of mTPxI (also known as Prx1p), at least two different pathways are involved in the regulation of its expression: one dependent on heme and the other on cAMP as signaling agents (16). The zinc-finger transcriptional regulator Msn2p/Msn4p regulates the induction of mTPxI by carbon starvation, whereas other transcriptional regulator, Hap1, is involved in the induction of mTPxI by H_2O_2 (16). Recently, it was described that cTPxII expression is also regulated by Msn2p/Msn4p and by Hap1 among other transcriptional regulators (22,28). These results together with microarray data (38) indicate that expression of mTPxI and cTPxII may share at least part of the same regulatory pathways. Like mTPxI, cTPxII is highly inducible by peroxides. However, contrary to mTPxI, cTPxII was only weakly induced by glucose starvation (figure 5). *Western blot* studies conducted by *Hong et al.* (22) also indicated that cTPxII is more inducible by peroxides than by glucose exhaustion. *TSA2* expression as a function of growth was also performed on the JD7-7C strain used by Hong *et al.* (22) and again the same pattern of expression was observed (data not shown). The complexity of the yeast response to oxidative stress was further demonstrated by the fact that besides Hap1 and Msn2p/Msn4p, *TSA2* gene is regulated also by Yap1, Rox1p and by Hap2/3/5p (28 and 39). Moreover, the activity of

cTPxII can be modulated pos-translationally. This is because cTPxII interacts with CSR1, a protein involved in phospholipid transport (40).

Although the signaling pathways involved in the regulation of expression of antioxidants are not completely understood, the results presented in this report clearly show that cTPxI and cTPxII are key components of yeast defense against organic hydroperoxides and that catalases and peroxiredoxins cooperate in the protection of cells against H_2O_2 insult. Our results together with data from the literature indicate that although all the peroxiredoxin isoforms share the same enzymatic activity (thiol-dependent peroxidase), they are not totally redundant proteins. Since yeast has proved to be a good model to higher eukaryotes, this assumption may also be valid for the peroxiredoxin enzymes of these organisms.

References

01. Jamieson, D.J. (1998) *Yeast* **16**:1511-1527.

02. Park, S. G., Cha, M. K., Jeong, W., and Kim, I. H. (2000) *J. Biol. Chem.* **275**: 5723-5732.

03. Avery, A.M., and Avery, S.V. (2001) *J. Biol. Chem.* **276**: 33730-33735.

04. Inoue, Y., Matsuda, T., Sugiyama, K., Izawa, S., and Kimura, A. (1999) *J. Biol. Chem.* **274**: 27002-27009.

05. Chae, H. Z., Kim, I. H., Kim, K., and Rhee, S. G. (1993) *J. Biol. Chem.* **268**: 16815-16821.

06. Halliwell, B. and Gutteridge, J.M.C. (1999) in *Free Radicals in Biology and Medicine*, 3rd. Edition, Clarendon Press - Oxford.

07. Netto, L. E.S., Chae, H.Z., Kang, S.W., Rhee, S.G., and Stadtman, E.R. (1996) *J. Biol. Chem.* **271**: 15315-15321.

08. Izawa S, Maeda K, Sugiyama K, Mano J, Inoue Y, Kimura A. (1999) *J. Biol. Chem.* **274**: 28459-28465.

09. Carmel-Harel, O., and Storz, G. (2000) *Annu Rev Microbiol* **54**: 439-461.

10. Kuge, S., Arita, M., Murayama, A., Maeta, K., Izawa, S., Inoue, Y. and Nomoto, A. (2001) *Mol. Cell. Biol.* **21**: 6139-6150.

11. Delaunay, A., Isnard, A.D., and Toledano, M.B. (2000) *EMBO J.* **19**: 5157-5166.

12. Gelade, R., Van De Velde, S., Van Dijck, P., and Thevelein, J.M. (2003) *Genome Biol.* **4**: 233-237.

13. Moradas-Ferreira, P., and Costa, V. (2000) *Redox Rep.* **5**: 277-285.

14. Pon, L.; Schatz, G. (1991) in *Biogenesis of Yeast Mitochondria in the Molecular and Cellular Biology of the Yeast Saccharomyces*. Chapter 7, Volume 1. *Genome dynamics,*

protein synthesis and energetics. (Broah, J.R., Pringle, J.R., Jones, E.W. Eds.) New York: Cold Spring Harbor Laboratory Press.

15. Demasi, A.P.D., Pereira, G.A.G., and Netto, L.E.S. (2001) *FEBS Letters* **509**: 430-434.

16. Monteiro, G., Pereira, G.A.G., and Netto, L.E.S. (2002) *Free Radic. Biol. Med.* **32**: 278-288.

17. Kim, I. H., Kim, K., and Rhee, S. G. (1989) *Proc. Natl. Acad. Sci. U S A.* **86**: 6018-6022.

18. Kim, K., Kim, I.H., Lee, Ki-Y, Rhee, S.G. and Stadtman, E.R. (1988) *J. Biol. Chem.* **263**: 4704-4711.

19. Ross, S. J., Findlay, V. J., Panagiota, M., and Morgan, B. A. (2000) *Mol Biol Cell* **11**: 2631-2642.

20. Huang, M.E., Rio A.G., Nicolas, A., and Kolodner, R.D. (2003) *PNAS* **100**: 11529-11534.

21. Wong, C.M., Zhou Y., Ng, R.W., Kung, H.F., and Jin, D.Y. (2002) *J. Biol. Chem.* **277**: 5385-5394.

22. Hong, S.K., Cha M.K., Choi Y.S., Kim W.C., and Kim I.H. (2002) *J. Biol. Chem.***277**: 12109-12117.

23. Ausubel, F. M., Brent, R., Kingstone, R. E., Moore, D. D., Seidman, J. A., Smith, J. A., and Struhl, K. (1994) Current Protocols in Molecular Biology. New York: John Wiley & Sons, Inc.

24. Chae H.Z., Chung S.J., and Rhee SG. (1994) *J. Biol. Chem.* **269**: 27670-27678.

25. Jiang, Z-Y., Hunt, J.V., and Wolff, S.P. (1992) *Anal. Biochem.* **202**: 384-389.

26. Robinson, J. and Cooper, J.M. (1970) *Anal. Biochem.*, 33:339-349.

27. Maris, A.F., Assumpção, A.L., Bonatto, D., Brendel, M., and Henriques J.A. (2001) *Curr. Genet.* **39**: 137-49.

28. Wong C.M., Ching Y.P., Zhou Y., Kung H.F., and Jin D.Y. (2003) *Free Radic. Biol. Med.* **34**: 585-97.

29. Jeong JS, Kwon SJ, Kang SW, Rhee SG, and Kim K. (1999) *Biochemistry.* **38**:776-783.

30. Pedrajas, J.R., Miranda-Vizuete, A., Javanmardy, N., Gustafsson, J.A., and Spyrou, G. (2000) *J. Biol. Chem.* **275**:16296-16301.

31. Verdoucq, L., Vignols, F., Jacquot, J.P., Chartier, Y., and Meyer, Y. (1999) *J. Biol. Chem.* **274**: 19714-22.

32.Wood Z.A., Poole L.B., Karplus P.A. (2003) *Science* **300**:650-653.

33. Izawa, S., Inoue, Y., and Kimura, A. (1996) *Biochem. J.* **320**:61-67.

3. Hortner, H., Ammerer, G., Hartter, E., Hamilton, B., Rytka, J., Bilinski, T., and Ruis, H. (1982) *Eur. J. Biochem.* ***128***: 179-184.

35.Outten C.E. and Culotta, V.C. (2004) *J. Biol. Chem.* **279**: 7785-7791.

36.Monteiro, G., Kowaltowski, A.J., Barros, M.H. and Netto, L.E.S. (2004) *Arch. Biochem. Biophys.* In press.

37. Nguyên-nhu, N.T., Knoops, B. (2002) *Toxicology letters.* **135**: 219-228

38. Gasch, A.P., Spellman, P.T., Kao, C.M., Carmel-Harel O., Eisen, M.B., Storz, G., Botstein, D., and Brown, P.O. (2000) *Mol. Biol. Cell.* **11**: 4241-4257.

39.Lee J., Spector D., Godon C., Labarre J. and Toledano M.B. (1999) *J. Biol. Chem.* **274**: 4537-4544.

40. Cha, M.K., Hong, S.K., Oh, Y.M. and Kim, I.H. (2003) *J. Biol. Chem.* **278**: 34952-34958.

Footnotes:

[1] The abbreviations used are: cTPxI , cytosolic thioredoxin peroxidase I protein also known as Tsa1p (YML028W); cTPxII, cytosolic thioredoxin peroxidase II protein also known as Tsa2p (YDR453C); cTPxIII, cytosolic thioredoxin peroxidase III also known as Ahp1, type II TPx or TSA II (YLR109W); mTPxI mitochondrial thioredoxin peroxidase I also known as Prx1 (YBL064C); FOX, Ferrous Oxidation Xylenol Orange Assay; GSH, Glutathione; mtGlr1, mitochondrial glutathione reductase isoform; phGPx, phospholipid glutathione peroxidase; RNS, reactive nitrogen species; ROS, reactive oxygen species; TBHP, *tert*-butylhydroperoxide; *TRR1*, Thioredoxin reductase I gene (YDR353W); Trr1, Thioredoxin reductase I protein (YDR353W); *TRX2*, thioredoxin 2 gene (YGR209C); Trx2, thioredoxin 2 protein (YGR209C); *TSA1*, cytosolic thioredoxin peroxidase I gene (YML028W) and *TSA2*, cytosolic thioredoxin peroxidase II gene(YDR453C).

Acknowledgments – We thank Dr. Maria Cristina Arias for help in the construction of expression vectors; Dr. Gisele Monteiro and Dr. Camila Oresco dos Santos for assistance in *Northern blot* experiments and Dr. Gisele Monteiro and Dr. Marilene Demasi for critical reading of the manuscript. We especially thank FAPESP and CNPq for financial support.

Figure Legends

Figure 1: **TBHP tolerance by yeast strains**. Tolerance was measured by the spot test as described in *Material and Methods*. The first spot on the left in each lane corresponds to the cell suspension diluted to OD_{600nm} = 0.2. Four subsequent 1/5 dilutions of cell suspensions were performed from left to right. Cell dilutions and carbon sources used are described at the top of the figure. Yeast strains and TBHP concentrations used are described at the side of the figure. This figure is representative of at least three similar experiments.

Figure 2: **H_2O_2 tolerance by yeast strains**. Tolerance was measured by the spot test as described in *Material and Methods*. The first spot on the left in each lane corresponds to the cell suspension diluted to OD_{600} = 0.2. Four subsequent 1/5 dilutions of cell suspensions were performed from left to right. Cell dilutions and carbon sources used are described at the top of the figure. Yeast strains and H_2O_2 concentrations used are described at the side of the figure. This figure is representative of at least three similar experiments.

Figure3: **Effect of peroxide dose on *TSA2* expression**. *Northern blot* analysis of RNA isolated from mid-logarithmic phase culture (OD_{600nm} = 0.8). All of samples were treated with peroxide for 15 minutes. Panels A and B refer to H_2O_2 treatment whereas panels C and D refer to TBHP treatment. Panels A and C refer to glucose as the carbon source whereas panels B and D refer to glycerol as the carbon source. This figure is representative of at least three similar experiments.

Figure 4: **Kinetics of *TSA2* induction by hydroperoxides.** *Northern blot* analysis of RNA isolated from mid-logarithmic phase cultures (OD_{600nm} = 0.8). Time zero corresponds to

untreated cells. Panels A and B refer to H_2O_2 (0,3mM) treatment whereas panels C and D refer to TBHP (0.5mM) treatment. Panels A and C refer to glucose as the carbon source whereas panels B and D refer to glycerol as the carbon source. This figure is representative of at least three similar experiments.

Figure 5: ***TSA2* expression under fermentative and respiratory conditions.** A. Effect of carbon source on *TSA2* expression. *Northern blot* analysis of *TSA2* from cells grown in media with different carbon sources which are described at the bottom of the figure. RNA was isolated from mid-logarithmic phase cultures (OD_{600nm} = 0.8). Where indicated, TBHP was added at 0.5 mM concentration. B. *TSA2* yeast gene expression during different growth phases. *Northern blot* analysis of RNA isolated from wild type cells. The growth phases are indicated at the bottom of the figure. Treated (0.5mM of TBHP) and untreated samples are indicated by + or – signals, respectively. The carbon source used in all samples was glucose. This figure is representative of at least three similar experiments.

Figure 6: **NADPH oxidation catalyzed by cTPxI and cTPxII.** NADPH oxidation was monitored as A_{340nm} in a 1mL reaction mixture containing 50mM Hepes-NaOH (pH7.4), 100uM DTPA, 1mM azide, 0.225uM Trx2, 0.075uM TRR1, 2.1uM cTPxII, 0.18mM NADPH and 20uM peroxide(A = H_2O_2 and B = TBHP). Reactions were incubated at 30°C and were initiated by peroxide addition. This figure is representative of at least three similar experiments (--- = without peroxiredoxin; —□— cTPxI; —x— cTPxII)

Figure 7: **Enzymatic assays in cellular extracts**. (A) H_2O_2 consumption in yeast extracts was determined at 10 minutes at 37°C, by the FOX assay as described in *Material and Methods*. Reactions were carried out in 50 mM HEPES buffer, pH 7.4, in the presence of DTPA (0.1

mM) and 0.25ug/ul of cellular extract. Reactions were initiated by addition of 200uM peroxide (H_2O_2 or TBHP). (B) Oxygen release by cellular extracts (0.25ug/ul) was determined using oxygraph at 30°C as described in *Material and Methods*. Reactions were initiated by H_2O_2 (100 uM) addition. Rates were determined by tracing a line over the initial slope. The differences between Δ cTPxII and wild type (but not between ΔcTPxI and wild type) were statistically significant for p values ≤ 0.05 (determined from paired t test) and are indicated with the symbol *.

Figure 8: **TBHP consumption by yeast cellular extract**. The amount of TBHP present in yeast cellular extracts (— wild type; ··· Δ cTPxII and ---Δ cTPxI) at different intervals was determined by the FOX assay as described in *Material and Methods*. Reactions were carried out in 50 mM HEPES buffer, pH = 7.4, in the presence of DTPA (0.1 mM) and cellular extract (4ug/ul). Reactions were initiated by the addition of TBHP (200uM). After incubation at 37°C , the absorbance was monitored at 540nm.

Figure 9: **Pathways of peroxide decomposition in yeast cells.** Upper yeast cells correspond wild type strain and lower yeast cells correspond to ΔcTPxII Strain. Abbreviations used in the figure: Cta1 (Catalase A), Ctt1 (Catalase T), Ccp1 (cytochrome c peroxidase), cTPxI (cytosolic thioredoxin peroxidase I), cTPxII (cytosolic thioredoxin peroxidase II), mTPxI (mitochondrial thioredoxin peroxidase I), cTPxIII (cytosolic thioredoxin peroxidase III), mtGlr1 (mitochondrial glutathione reductase), phGPxs (phospholipid glutathione peroxidases).

Table I – Enzymatic Parameters for peroxiredoxins

	cTPxI				cTPxII			
Peroxide	Vmax (uM/s)	Km (uM)	Kcat (s^{-1})	Kcat/Km ($M^{-1}.s^{-1}$)	Vmax (uM/s)	Km (uM)	Kcat (s^{-1})	Kcat/Km ($M^{-1}.s^{-1}$)
H_2O_2	0,66	12,0	0,31	$2,6x10^4$	0,39	13,8	0,18	$1,3 \times 10^4$
THBP	0,61	7,9	0,29	$3,6x10^4$	0,29	5,1	0,14	$2,7 \times 10^4$
CHP	0,56	17,1	0,26	$1,5x10^4$	0,28	4,5	0,14	$3,0 \times 10^4$

[a] Parameters were determined from data obtained in three experiments performed in the same conditions. Experimental conditions were described in figure 6. THBP = *tert*-butylhydroperoxide; CHP = cumene-hydroperoxide. (sem correção, cTPxI-co; cTPxII ni)

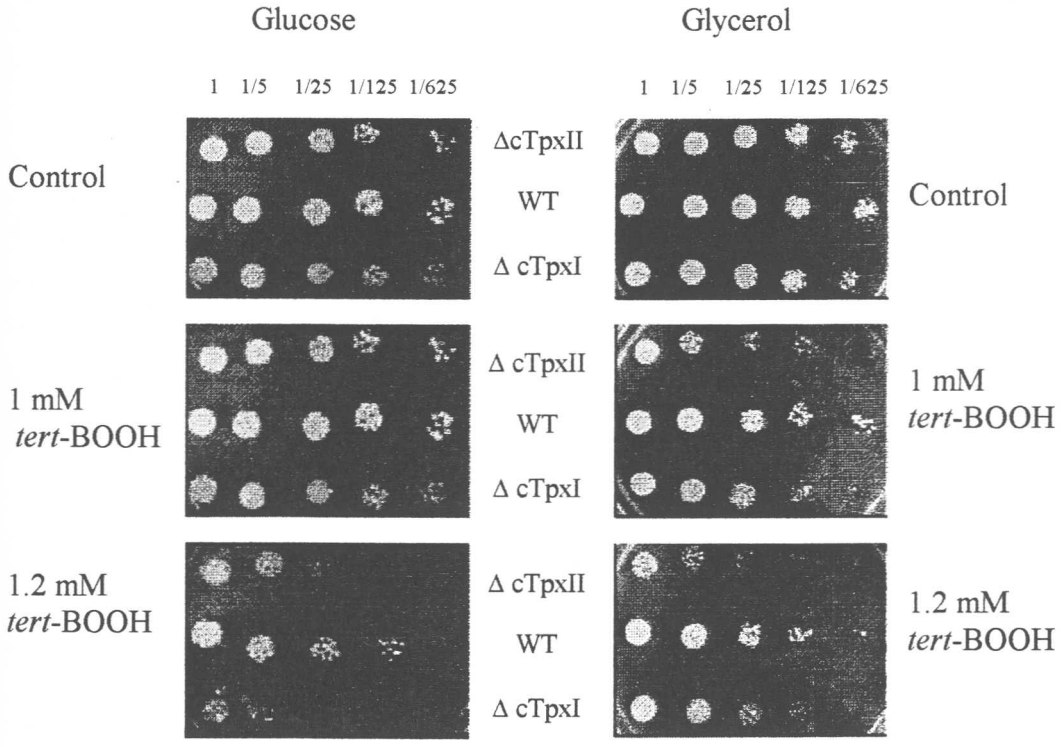
Glucose
Glycerol
1 1/5 1/25 1/125 1/625
1 1/5 1/25 1/125 1/625
Control
1 mM
tert-BOOH
1.2 mM
tert-BOOH
ΔcTpxII
WT
Δ cTpxI
Δ cTpxII
WT
Δ cTpxI
Δ cTpxII
WT
Δ cTpxI
Control
1 mM
tert-BOOH
1.2 mM
tert-BOOH

Figure 1

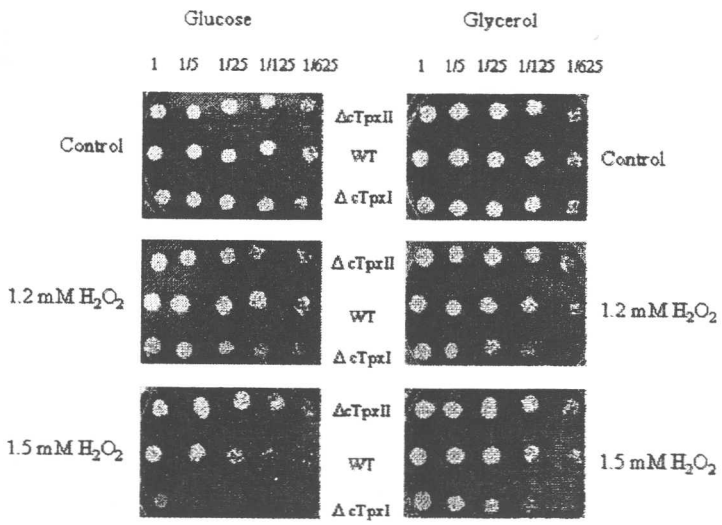
Glucose
Glycerol
1 1/5 1/25 1/125 1/625
1 1/5 1/25 1/125 1/625
Control
ΔcTpxII
WT
Δ cTpxI
Control
1.2 mM H_2O_2
ΔcTpxII
WT
Δ cTpxI
1.2 mM H_2O_2
1.5 mM H_2O_2
ΔcTpxII
WT
Δ cTpxI
1.5 mM H_2O_2

Figure 2

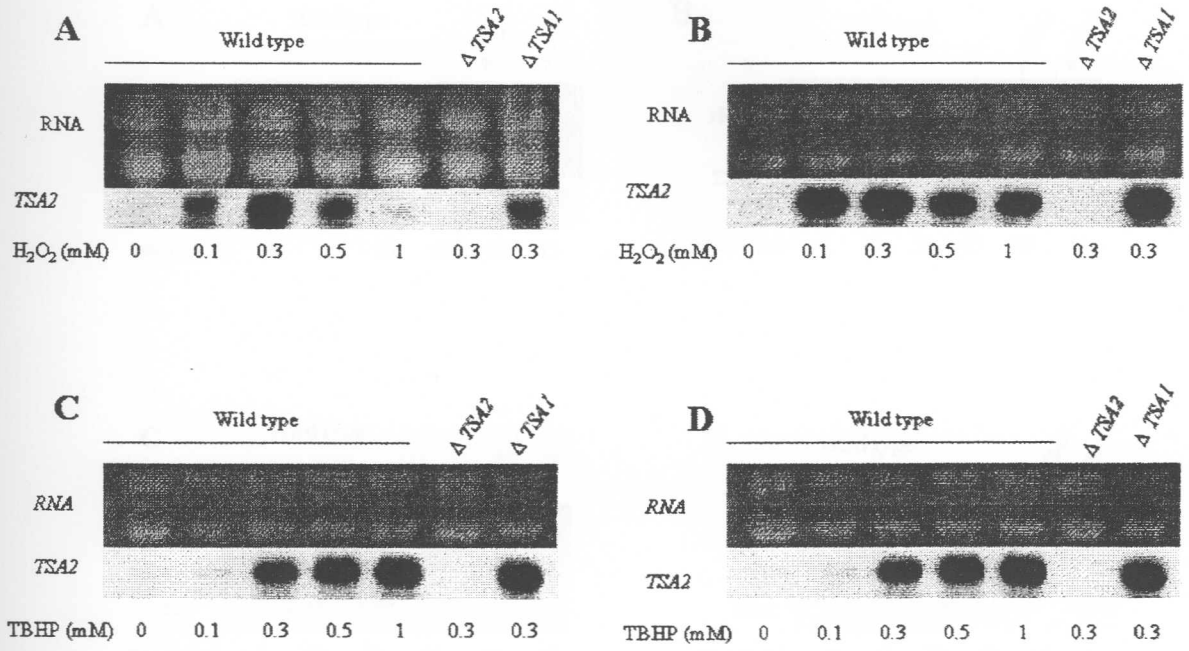
A
Wild type
Δ TSA2
Δ TSA1
RNA
TSA2
H2O2 (mM) 0 0.1 0.3 0.5 1 0.3 0.3
B
Wild type
Δ TSA2
Δ TSA1
RNA
TSA2
H2O2 (mM) 0 0.1 0.3 0.5 1 0.3 0.3
C
Wild type
Δ TSA2
Δ TSA1
RNA
TSA2
TBHP (mM) 0 0.1 0.3 0.5 1 0.3 0.3
D
Wild type
Δ TSA2
Δ TSA1
RNA
TSA2
TBHP (mM) 0 0.1 0.3 0.5 1 0.3 0.3

Figure 3

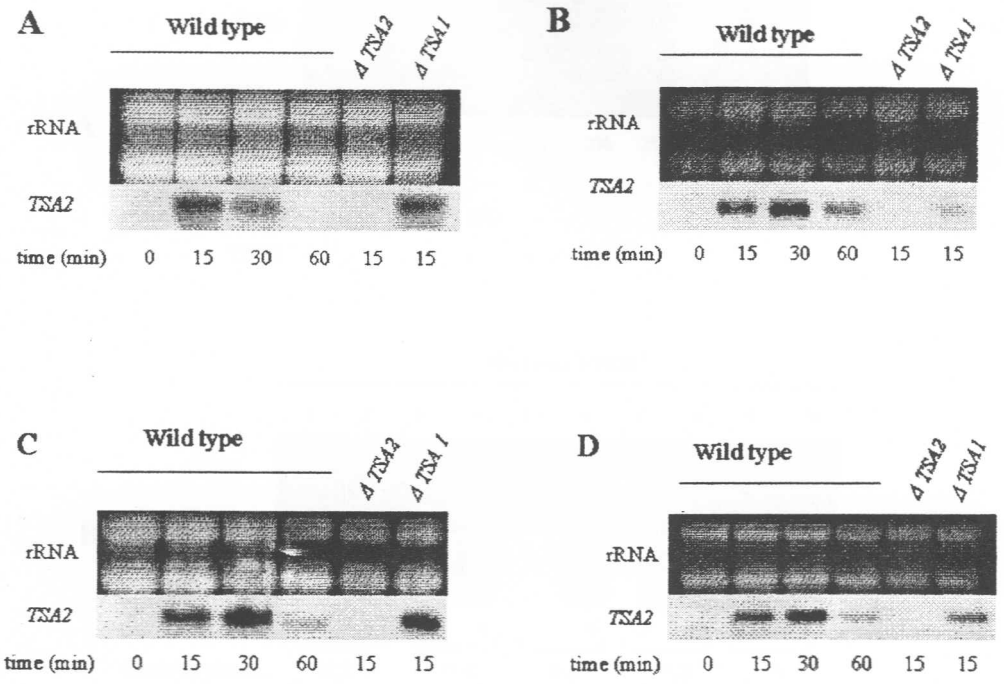
A
Wild type
Δ TSA2
Δ TSA1
rRNA
TSA2
time (min) 0 15 30 60 15 15
B
Wild type
Δ TSA2
Δ TSA1
rRNA
TSA2
time (min) 0 15 30 60 15 15
C
Wild type
Δ TSA2
Δ TSA 1
rRNA
TSA2
time (min) 0 15 30 60 15 15
D
Wild type
Δ TSA2
Δ TSA1
rRNA
TSA2
time (min) 0 15 30 60 15 15

Figure 4

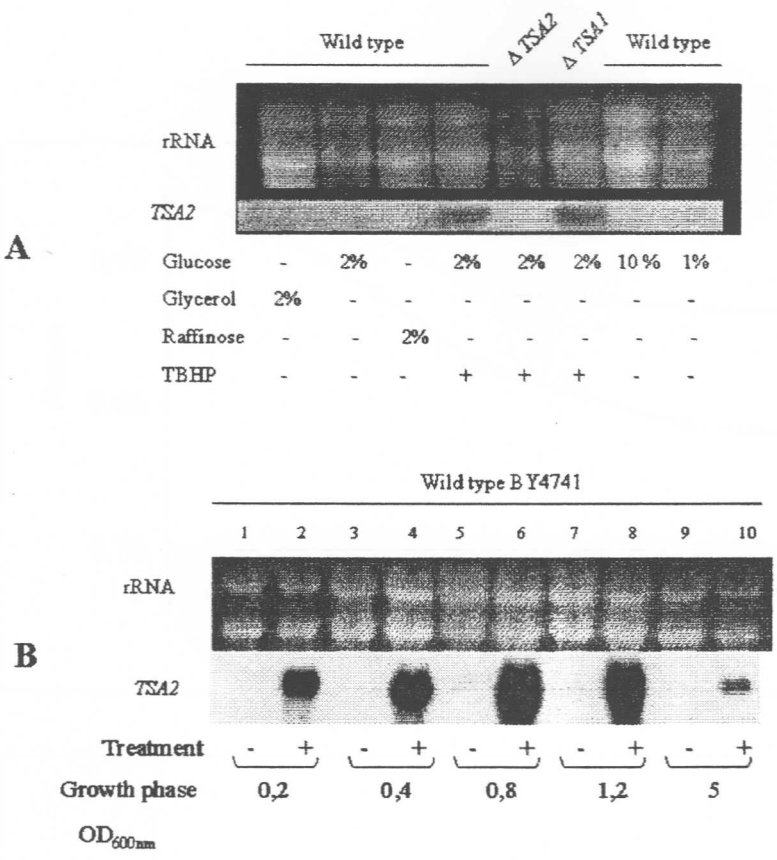
A
Wild type
Δ TSA2
Δ TSA1
Wild type
rRNA
TSA2
Glucose - 2% - 2% 2% 2% 10% 1%
Glycerol 2% - - - - - - -
Raffinose - - 2% - - - - -
TBHP - - - + + + - -
B
Wild type BY4741
1 2 3 4 5 6 7 8 9 10
rRNA
TSA2
Treatment - + - + - + - + - +
Growth phase 0,2 0,4 0,8 1,2 5
OD600nm

Figure 5

A

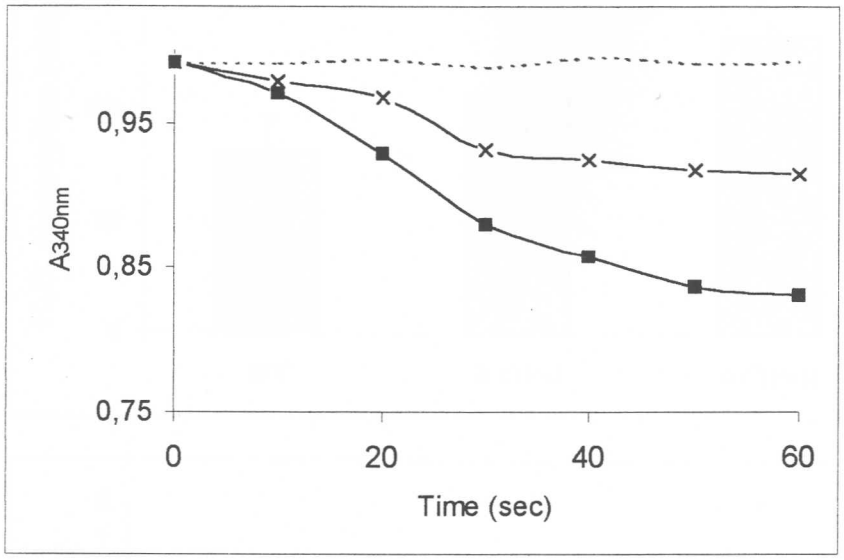
0,95
0,85
0,75
A340nm
0
20
40
60
Time (sec)

B

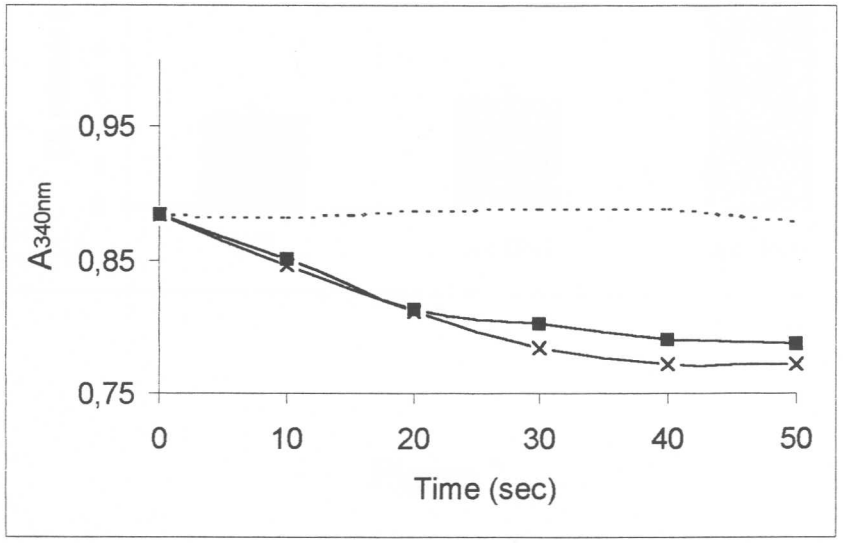
0,95
0,85
0,75
A340nm
0
10
20
30
40
50
Time (sec)

Figure 6

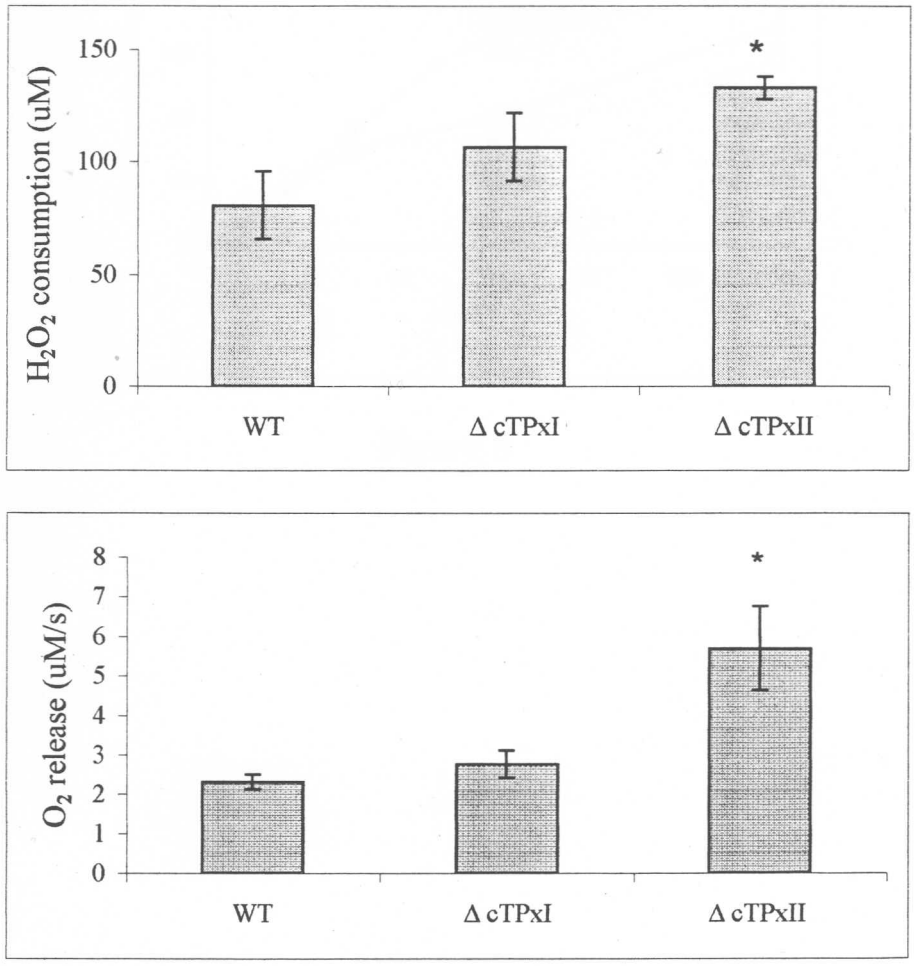
A
H_2O_2 consumption (uM)
150
100
50
0
*
WT
Δ cTPxI
Δ cTPxII
B
O_2 release (uM/s)
8
7
6
5
4
3
2
1
0
*
WT
Δ cTPxI
Δ cTPxII

Figure 7

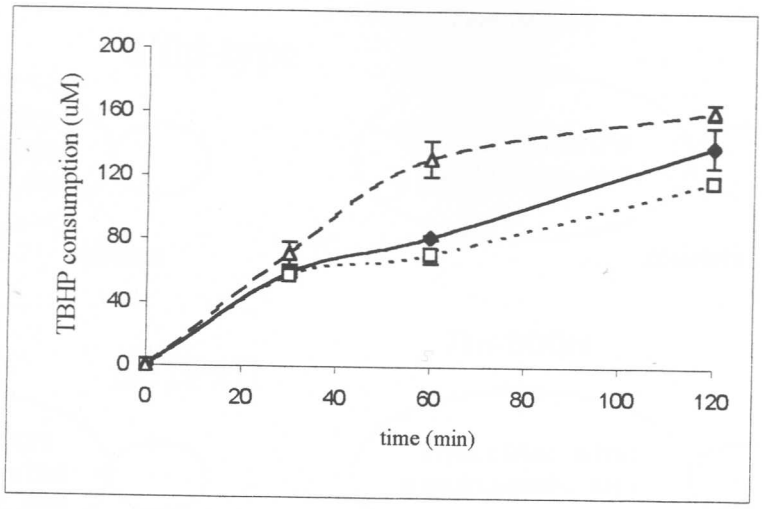
TBHP consumption (uM)
200
160
120
80
40
0
0
20
40
60
80
100
120
time (min)

Figure 8

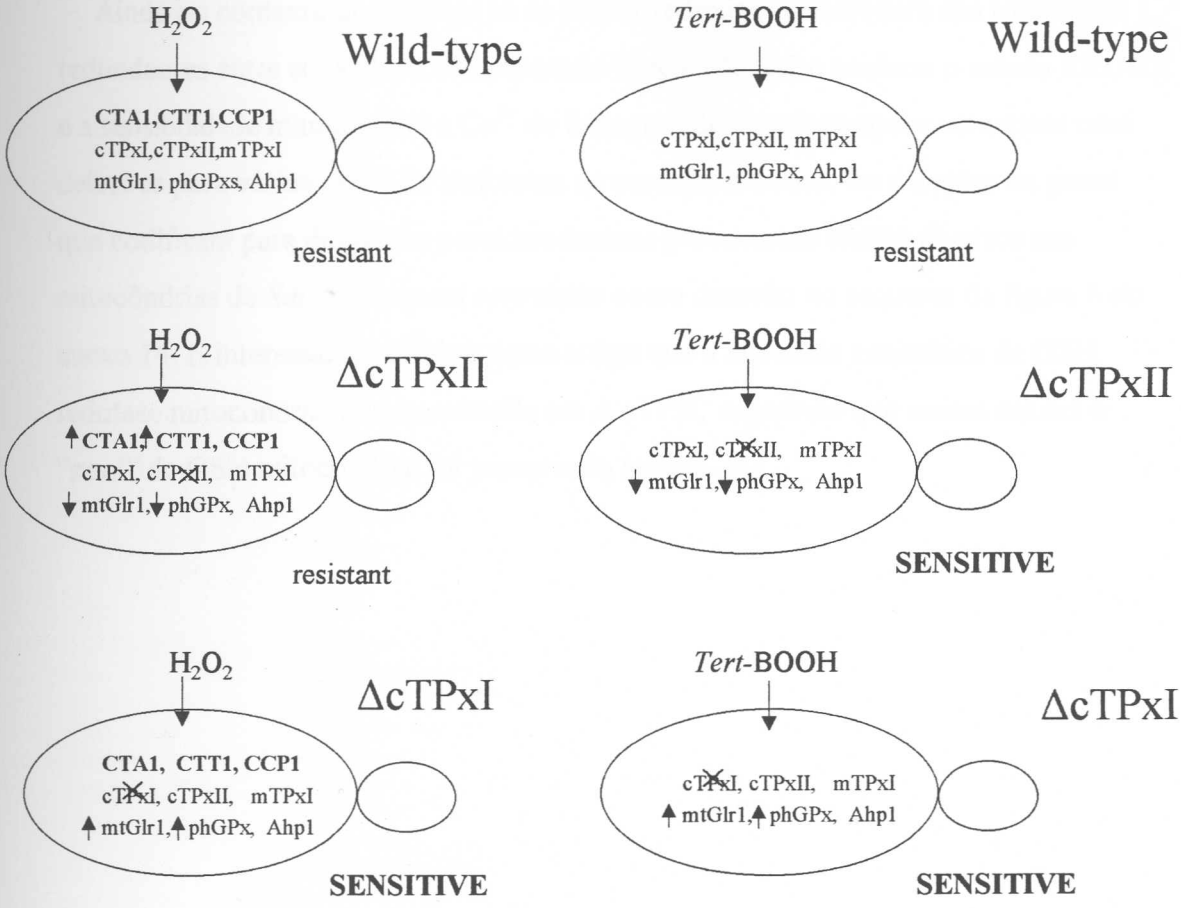
H_2O_2
Wild-type
CTA1,CTT1,CCP1
cTPxI,cTPxII,mTPxI
mtGlr1, phGPxs, Ahp1
resistant
Tert-BOOH
Wild-type
cTPxI,cTPxII, mTPxI
mtGlr1, phGPx, Ahp1
resistant
H_2O_2
ΔcTPxII
↑CTA1,↑CTT1, CCP1
cTPxI, cTPxII, mTPxI
↓mtGlr1,↓phGPx, Ahp1
resistant
Tert-BOOH
ΔcTPxII
cTPxI, cTPxII, mTPxI
↓mtGlr1,↓phGPx, Ahp1
SENSITIVE
H_2O_2
ΔcTPxI
CTA1, CTT1, CCP1
cTPxI, cTPxII, mTPxI
↑mtGlr1,↑phGPx, Ahp1
SENSITIVE
Tert-BOOH
ΔcTPxI
cTPxI, cTPxII, mTPxI
↑mtGlr1,↑phGPx, Ahp1
SENSITIVE

Figure 9

Ainda no contexto de verificar se as peroxirredoxinas de levedura são totalmente redundantes entre si, a aluna de doutorado Gisele Monteiro analisou o estado REDOX e a sensibilidade mitocôndrial a Ca^{2+} de linhagens de *Saccharomyces cerevisiae* com deleções para vários genes de isoformas de peroxirredoxinas. As deleções de genes que codificam para diferentes peroxirredoxinas provocaram efeitos diversos nas mitocôndrias de *Saccharomyces cerevisiae* como descrito no esquema da figura 8 do anexo 14. É interessante ressaltar neste artigo que a atividade enzimática de GSH redutase mitocondrial está aumentada em Δ cTPxI, sugerindo que nessas células o "pool" de GSH mitocondrial foi preservado (anexo 14).

Available online at www.sciencedirect.com
SCIENCE DIRECT®
Archives of Biochemistry and Biophysics xxx (2004) xxx–xxx
ABB
www.elsevier.com/locate/yabbi

ANEXO 14

Glutathione and thioredoxin peroxidases mediate susceptibility of yeast mitochondria to Ca^{2+}-induced damage

Gisele Monteiro,[a] Alicia J. Kowaltowski,[b] Mario H. Barros,[b] and Luis E.S. Netto[a,*]

[a] *Departamento de Biologia—Genética, Instituto de Biociências, Universidade de São Paulo, Rua do Matão 277, CEP05508-900, São Paulo, SP, Brazil*
[b] *Departamento de Bioquímica, Instituto de Química, Universidade de São Paulo, Brazil*

Received 29 December 2003, and in revised form 27 February 2004

Abstract

The effect of thioredoxin peroxidases on the protection of Ca^{2+}-induced inner mitochondrial membrane permeabilization was studied in the yeast *Saccharomyces cerevisiae* using null mutants for these genes. Since deletion of a gene can promote several other effects besides the absence of the respective protein, characterizations of the redox state of the mutant strains were performed. Whole cellular extracts from all the mutants presented lower capacity to decompose H_2O_2 and lower GSH/GSSG ratios, as expected for strains deficient for peroxide-removing enzymes. Interestingly, when glutathione contents in mitochondrial pools were analyzed, all mutants presented lower GSH/GSSG ratios than wild-type cells, with the exception of ΔcTPxI strain (cells in which cytosolic thioredoxin peroxidase I gene was disrupted) that presented higher GSH/GSSG ratio. Low GSH/GSSG ratios in mitochondria increased the susceptibility of yeast to damage induced by Ca^{2+} as determined by membrane potential and oxygen consumption experiments. However, H_2O_2 removal activity appears also to be important for mitochondria protection against permeabilization because exogenously added catalase strongly inhibited loss of mitochondrial potential. Moreover, exogenously added recombinant peroxiredoxins prevented inner mitochondrial membrane permeabilization. GSH/GSSG ratios decreased after Ca^{2+} addition, suggesting that reactive oxygen species (ROS) probably mediate this process. Taken together our results indicate that both mitochondrial glutathione pools and peroxide-removing enzymes are key components for the protection of yeast mitochondria against Ca^{2+}-induced damage.

Keywords: Calcium; Oxidative stress; Mitochondria; Thioredoxin peroxidase; Yeast; Thiol; Glutathione

Sulfhydryl groups are important components of cellular defense against oxidative stress and for the maintenance of the redox homeostasis of cells (review in [1]). In eukaryotes, the major thiol compound is the peptide glutathione (GSH)[1] [2], whereas thioredoxin and glutaredoxin are important protein sources of sulfhydryl groups in the cell. Both glutathione and thioredoxin can function as electron donors for thiol-dependent peroxidases. In the case of *Saccharomyces cerevisiae*, at least three glutathione phospholipid peroxidases and five thioredoxin peroxidase isoforms are expressed [3–5]. Glutathione and thioredoxin systems are closely linked [1]. In fact, disruption of *CTPX1* gene (also named *TSA1*) leads to increase in de novo synthesis and recycling of glutathione [3].

* Corresponding author. Fax: +55-11-30917553.
E-mail address: nettoles@ib.usp.br (L.E.S. Netto).

[1] *Abbreviations used:* cTPxI, cytosolic thioredoxin peroxidase I protein also known as Tsa1p; DTNB, 5-5′-dithiobis(2-nitrobenzoic acid); *TSA1*, cytosolic thioredoxin peroxidase I gene (ORF: *YML028w*); cTPxII, cytosolic thioredoxin peroxidase II protein also known as Tsa2p; *TSA2*, cytosolic thioredoxin peroxidase II gene (ORF: *YDR453c*); cTPxIII, cytosolic thioredoxin peroxidase III also known as Ahp1, type II TPx or TSA II (ORF: *YLR109w*); mTPxI mitochondrial thioredoxin peroxidase I also known as Prx1 (ORF: *YBL064c*); nTPxI, nuclear thioredoxin peroxidase I protein also known as DOT5 (Disruptor Of Telomeric silencing) (ORF: *YIL010w*), GSH, glutathione; GSSG, oxidized glutathione; GSH/GSSG, ratio between reduced and oxidized form of glutathione; RNS, reactive nitrogen species; ROS, reactive oxygen species; TNB, 2-nitro-5-thiobenzoic-acid; *TRR1*, thioredoxin reductase I gene (ORF: *YDR353w*); Trr1, thioredoxin reductase I protein; *TRX2*, thioredoxin 2 gene (ORF: *YGR209c*); Trx2, thioredoxin 2 protein.

0003-9861/$ - see front matter © 2003 Published by Elsevier Inc.
doi:10.1016/j.abb.2004.03.005

Among the five yeast thioredoxin peroxidases, cytosolic thioredoxin peroxidase I (cTPxI) is the most studied. It is very abundant, even under basal conditions [6]. As expected from its enzymatic activity, deletion of the *TSA1* gene (that codifies for cTPxI protein) slightly increases the sensitivity of cells to peroxides [5,7], especially when mitochondria are not functional [8]. Interestingly, besides its antioxidant role, cTPxI is also involved in the regulation of the expression and activity of several other genes such as *GSH1* (γ-glutamylcysteine synthetase), *GPX2* (glutathione peroxidase), *GLR1* (glutathione reductase), *TRX2* (thioredoxin), *TRR1* (thioredoxin reductase), and *YAP1* (transcriptional regulator) [3,9].

cTPxI belongs to a family of proteins named peroxiredoxins [10]. The other yeast peroxiredoxins are less studied. Cytosolic thioredoxin peroxidase II (cTPxII) shares 86% of identity with cTPxI and therefore they are expected to behave similarly. However, the peroxidase activity of cTPxI is about sixfold higher than the activity of cTPxII [5]. On the other hand, in vivo studies indicated that cTPxI and cTPxII are equally important in the defense of yeast against reactive oxygen species (ROS) and reactive nitrogen species (RNS) [11]. Contrary to cTPxI, cTPxII expression level is undetectable under basal conditions, but is highly inducible by peroxides [12]. The only mitochondrial peroxiredoxin in yeast, named mitochondrial thioredoxin peroxidase I (mTPxI), shares about 30% of identity with the other two peroxidases and has only one cysteine involved in the catalytic cycle [13]. The expression level of mTPxI is very low in fermentative supporting media and increases about tenfold in respiratory supporting media [14].

There are two other peroxiredoxin proteins in *S. cerevisiae*: cytosolic thioredoxin peroxidase III (cTPxIII) and nuclear thioredoxin peroxidase I (nTPxI). These two proteins also possess thioredoxin-dependent peroxidase activity, but they have very low similarity with cTPxI, cTPxII, and mTPxI [5]. cTPxIII is abundant as cTPxI, but it is at least one order of magnitude more efficient in the removal of organic peroxide than in the decomposition of H_2O_2 (because of this, cTPxIII is also named alkyl hydroperoxidase—AhpI) [15]. nTPxI also has higher peroxidase activity towards alkyl peroxides and is preferentially expressed during the stationary phase [16].

Besides the levels of antioxidant proteins, mitochondrial activity is also important for the maintenance of redox balance of eukaryotic cells since this organelle is a constant source of free radicals. Mitochondrial activity can be impaired by processes such as oxidative stress and increases in the content of cytosolic Ca^{2+}. In mammalian mitochondria, Ca^{2+} induces permeabilization of the inner mitochondrial membrane through a process known as mitochondrial permeability transition (MPT) [17,18], a phenomenon that has been implicated in processes such as cell injury and death [19]. MPT promotes swelling, a loss of the inner mitochondrial membrane potential, and the ability to produce ATP among other factors. Another important aspect related to MPT is that oxidation of thiol groups in proteins present in the inner mitochondrial membrane has been implicated as a major cause of this permeabilization [20,21]. Thiol oxidation causes protein cross-linkage, formation of large protein aggregates, and opening of a non-selective pore in the inner mitochondrial membrane [17,22,23].

Because thiols are important in both peroxiredoxin enzymatic activity and mitochondrial integrity, we are interested in the role of these proteins in the physiology of this organelle. We have shown before that yeast cTPxI and catalase cooperate in the protection of mammalian mitochondria against MPT induced by Ca^{2+} and oxidant agents [18]. Interestingly, cTPxI seems to use mitochondrial thiols as electron donors to decompose peroxides [18]. Similarly, endogenous cTPxI and catalase also protect yeast mitochondria from Ca^{2+}-promoted membrane permeabilization [24]. The experiments reported in this paper were designed to determine the relative importance of different thioredoxin peroxidase isoforms in the maintenance of mitochondrial integrity and function. Emphasis was given to cTPxII and mTPxI since these proteins share high similarity with cTPxI. The possible effect of cTPxIII was also investigated, but because mitochondria from the ΔcTPxIII strain were not more sensitive to Ca^{2+}-induced injury than wild-type mitochondria, cTPxIII was not further considered. nTPxI was not studied here because it is located farther away from mitochondria (separated by two membranes: nuclear and outer mitochondrial) and because this protein has low specific activity [5].

Interestingly, we also show in this report that deletion of genes encoding peroxiredoxins altered the metabolism of glutathione, which is in agreement with the close relationship between glutathione and thioredoxin systems [1,3].

Experimental procedures

Yeast strains and growth conditions

Yeast strains used here were obtained from EUROSCARF:

Wild type (*BY4741; Mata; his3Δ1; leu2Δ0; met15Δ0; ura3Δ0*); ΔmTPxI (*BY4741; Mata; his3Δ1; leu2Δ0; met15Δ0; ura3Δ0; YBL064c::kanMX4*); ΔcTPxI (*BY4742; Matα; his3Δ1; leu2Δ0; lys2Δ0; ura3Δ0; YML028w::kanMX4*); ΔcTPxII (*BY4741; Mata; his3Δ1; leu2Δ0; met15Δ0; ura3Δ0; YDR453c::kanMX4*); and ΔcTPxIII (*BY4741; Mata; his3Δ1; leu2Δ0; met15Δ0; ura3Δ0; YLR109w::kanMX4*).

Yeast was pre-inoculated in 10 ml YPGAL (2% galactose, 2% peptone, and 1% yeast extract) for 24 h, at 30 °C, with 250 rpm shaking. One milliliter of the culture was then inoculated in 150 ml of fresh media and incubated overnight under the same conditions. When cells were grown in YEPG (2% glycerol, 2% ethanol, 2% peptone, and 1% yeast extract), the pre-inoculated culture was incubated at 30 °C, 250 rpm for 48 h and the inoculated culture was incubated for 36 h. Yeast catalase T (cytosolic) and/or catalase A (peroxisomal) were specifically inhibited in the wild-type strain by addition of 3-amino-1,2,4-triazole (ATZ—5 mM) in the pre-inoculation and inoculation media. After this procedure, cells reached $OD_{600\,nm}$ around 6.0, therefore they were considered to be in stationary growth phase.

Determination of protein concentration

Protein concentration was determined with the Bradford reagent from BIORAD, using bovine serum albumin as a standard.

H_2O_2 removal activity

Total protein extracts from yeast cells were obtained by lysing spheroblasts previously digested with lyticase (Sigma—Lyticase from *Arthrobacter luteus*—L4025), with a buffer containing 10 mM Tris–HCl, pH 7.5, and 0.5 mM EDTA (TE buffer). Fluorimetric assays were conducted using the spheroblast samples to determine total H_2O_2 removal activity. After incubating 0.5 mg of recently (<3 h) lysed spheroblast protein in 100 μl TE buffer for 3 min with 2 mM H_2O_2, a 1 μl aliquot was taken and diluted in 2 ml of suspension buffer with 50 μM Amplex Red and 1.0 U/ml horseradish peroxidase [25]. A single reading was taken at 563 nm excitation and 587 nm emission.

Preparation of mitochondrially-enriched fractions

Yeast cultures were harvested and washed with 30 ml of 1.2 M sorbitol. Cells were then incubated with 3 ml/g of digestion buffer (1.2 M sorbitol, 75 mM sodium phosphate, 1 mM EDTA, 0.01 volume β-mercaptoethanol, and 0.4 mg/ml lyticase) and after 2 h of incubation at 37 °C, the obtained spheroblasts were harvested and washed twice with 30 ml of 1.2 M sorbitol. Pellets were then suspended in 3 ml/g lyses buffer (0.5 M sorbitol, 10 mM Tris–HCl, pH 7.5, and 1 mM EDTA) and homogenized with a potter. The suspension was harvested twice (3500*g*, 10 min, 4 °C) to precipitate the cellular debris and the supernatant was then harvested (14,000 g, 10 min, 4 °C) to obtain the mitochondrial-enriched fraction. This fraction was washed once with 10 ml of lyses buffer and the final fraction was suspended in 10 mg/ml protein in lyses buffer. The procedure described here is the same as that developed by Faye et al. [26], except for the fact that glusulase was replaced by lyticase. Quality of our mitochondrial preparations was verified by determinations of respiratory control ratio. Besides, the integrity of our mitochondrial preparations could also be demonstrated by the fact that they can mount a potential in the inner membrane and because they consume oxygen.

Measurement of mitochondrial matrix Ca^{2+} content

The procedure was carried out as described by Kowaltowski et al. [27], with some modifications. Mitochondrial-enriched fractions (650 μg/ml) were loaded with the fluorescent Ca^{2+} indicator fura-2/AM (10 μM—Sigma) in buffer containing 240 mM sucrose, 10 mM Hepes buffer, pH 7.4, 0.1 mM EGTA, and 1 mg/ml bovine serum albumin, for 30 min at 37 °C. The suspension was diluted 10-fold and washed twice at 4 °C to eliminate free extramitochondrial fura-2/AM. Fluorescence emission at 510 nm was monitored with excitations between 300 and 400 nm, and Ca^{2+} uptake was determined ratiometrically as indicated by the supplier. Maximal and minimal intramitochondrial levels were measured in each cell type by treating samples with 10 μM ionomycin plus Ca^{2+} and with 1 mM EGTA.

Measurement of thiol content

Fresh mitochondrial-enriched fractions were solubilized with 1% SDS in a buffer containing 87 mM Tris and 4 mM EDTA, pH 8.1, in the presence of 520 μM 5-5′-dithiobis(2-nitrobenzoic acid), (DTNB—also known as Ellman's reagent). These suspensions were homogenized and incubated for 30 min at room temperature in the dark. Thiol content was determined spectrophotometrically at 412 nm and calculated taking into account that 2-nitro-5-thiobenzoic-acid (TNB) possesses $\varepsilon_{412\,nm} = 13{,}600\,M^{-1}\,cm^{-1}$ [28].

Determination of GSH and GSSG

Yeast cell or mitochondrially-enriched fractions were disrupted in 1 volume of glass beads and 2 volumes of 3.5% sulfosalicylic acid. The suspension was vortexed for 20 min at 4 °C in a multifold vortex and harvested at 13,000 rpm. This procedure was repeated twice and the supernatants were combined. Total glutathione as well as GSSG were assayed as previously described [29]. Briefly, total glutathione was determined by reaction with DTNB (76 μM) in the presence of glutathione reductase (0.12 U/ml) and NADPH (0.27 mM). For GSSG determination, samples were incubated for 1 h with *N*-ethylmaleimide (NEM—5 mM) after adjusting the pH to 7 with NaOH. GSH concentration was determined by the difference between total glutathione and GSSG.

Samples were normalized by mitochondrial protein concentration (for analyses of the mitochondrial-enriched fractions) or by weight of cell pellet (for analyses of the whole cell).

Mitochondrial membrane potential ($\Delta\Psi$) measurements

Mitochondrial $\Delta\Psi$ was determined through fluorescence changes of safranin O (5 μM), recorded on a Hitachi F-4010 fluorescence spectrophotometer (Hitachi, Tokyo, Japan) operating at excitation and emission wavelengths of 495 and 586 nm, with a slit width of 5 nm [30]. The fluorescence data were transformed into $\Delta\psi$ using a K^+ distribution curve exactly as described by Kowaltowski et al. [31]. Mitochondrial-enriched fractions were incubated in buffer 1 (0.25 M sucrose, 10 mM Hepes, pH 7.5, and 2 mM Pi) containing 2.5 mM ethanol, 5 mM glutamate, and 2.5 mM succinate. $\Delta\Psi$ was continuously monitored at 30 °C with stirring. In the experiments where exogenous catalase was added, the enzyme was obtained from Sigma (C9322).

Western and Northern blot analyses

Immunoblot analysis was performed using rabbit polyclonal antibodies against cTPxI. Transfer of protein from 12% SDS–PAGE gels to nitrocellulose and processing of nitrocellulose blots were carried out in the NOVEX system. The HRP-luminol based system from ECL (RPN 2108—Amersham–Pharmacia Biotech) was used to detect cTPxI bands. Northern blot studies were carried out exactly as described by Monteiro et al. [14]. The *GSH1* fragment was obtained from yeast genomic DNA using the specific primers forward (5′-CGCGGA TCCCATATGGGACTCTTAGCTTTGGG-3′) and reverse (5′-CGCAAGCTTGGATCCTTAACATTTGCT TTCTATTGA-3′) primers. The PCR product was purified from agarose gel (0.7%) and sequenced.

Oxygen consumption measurements

Oxygen concentration was measured using a Clarke-type electrode in a glass cuvette equipped with magnetic stirring. The mitochondrial-enriched fractions were incubated in buffer 2 in the presence of 2.5 mM ethanol, 5 mM glutamate, and 2.5 mM succinate and in the absence or in the presence of 500 μM Ca^{2+}.

Expression and purification of recombinant thioredoxin peroxidases

Recombinant cTPxI, which possesses a N-terminal His-tag, was expressed in *Escherichia coli* BL21(DE3) strain transformed with pET15b-cTPxI plasmid (*CTPXI* gene was cloned into *Nde*I and *Bam*HI restriction sites of expression vector pET15b from Novagen). Recombinant mTPxI was expressed in the same *E. coli* BL21(DE3) strain from a construct kindly provided by Spyrou and co-workers [13]. In summary, *MTPXI* gene without the first 20 codons (supposedly the mitochondrial target peptide) and with a substitution of codon corresponding to Cys-38 for a codon encoding for Ser-38 was cloned into *Nde*I and *Bam*HI restriction sites of pET-15b (Novagen). Therefore, the protein expressed in this way also possesses a N-terminal His-tag. Finally, the entire *CTPXII* gene was cloned into *Nde*I and *Bam*HI restriction sites of expression vector pPROEX (Gibco) and again *E. coli* BL21(DE3) strain was utilized as the host for expression.

Cells were cultured (50 ml) overnight in LB + ampicillin (100 μg/ml) medium, transferred to 1 L of fresh LB + ampicillin medium, and cultured further until the OD_{600} reached 0.6–0.8. IPTG was then added to a final concentration of 1 mM. After 3 h of incubation, cells were harvested by centrifugation. The pellet was washed and suspended in the start buffer: 20 mM phosphate buffer, pH 7.4 (for cTPxI and cTPxII) or 20 mM Tris–HCl buffer, pH 7.4 (for mTPxI). Two cycles of 15 s of sonication (25% amplitude) following 30 s over ice were applied to cell suspension. Cell extracts were kept over ice during 1% streptomycin sulfate treatment (20 min) and the suspension was centrifuged at 31,500*g* for 30 min to remove nucleic acid precipitates. Finally, extracts were applied to a nickel-affinity column (Hi-trap from Amersham–Pharmacia Biotech). The conditions for protein purification were optimized using the gradient procedure for imidazole concentration described by the manufacturer.

Results

Redox state of yeast mutants for thioredoxin peroxidase genes

Phenotypic analysis of null mutants is sometimes difficult because compensatory effects may occur. As an example, the deletion of *CTPXI* gene in *S. cerevisiae* leads to an increase in the levels of glutathione-dependent proteins [3]. Therefore, a characterization of the redox state of yeast mutants for thioredoxin peroxidase was performed. Initially, the total H_2O_2 removal activity of yeast cells was analyzed. In all cases, the consumption of H_2O_2 dropped significantly in the mutant cells relative to control, and cTPxI mutant cells (ΔcTPxI cells) showed the most pronounced effect (Fig. 1A). These results were expected since cTPxI is very abundant, representing almost 1% of total cytosolic protein [6]. H_2O_2 removal in yeast extracts in which catalase activity was inhibited by 3-amino-1,2,4-triazole (ATZ) also dropped significantly (Fig. 1A).

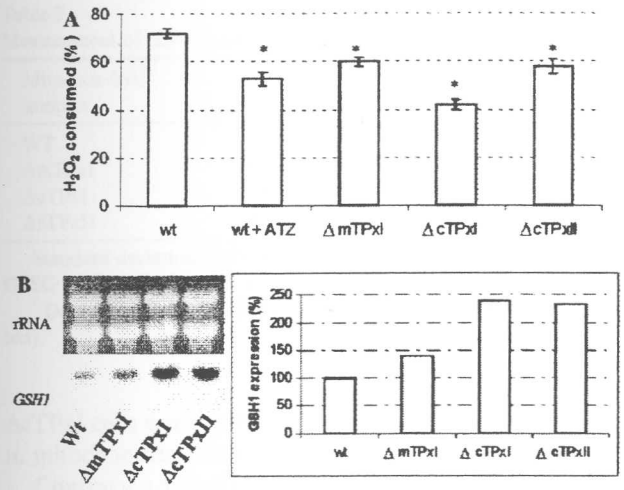

Fig. 1. (A) H_2O_2 removal activity measurement in whole cells. H_2O_2 removal activity in the different cell homogenates (wt + ATZ = wild-type cells treated with catalase inhibitor ATZ) was determined as described in Experimental procedures. The graph represents the average and standard deviation (±SD) from three independent experiments. The value 100% represents total H_2O_2 (2 mM) removal during 3 min. The differences between mutants and wild type were statistically significant for p values $\leqslant 0.01$ (determined from paired t test) as indicated by *. (B) GSH1 expression. Northern blot analyses were carried out in cells grown in galactose-containing media, until their density reached around 4.0 ($OD_{600\,nm}$). The graph represents the expression level quantified by dosimetry using Image Master equipment of Amersham–Pharmacia Biotech. Results are representative data of two similar experiments. Wild-type level was considered 100% of *GSH1* expression.

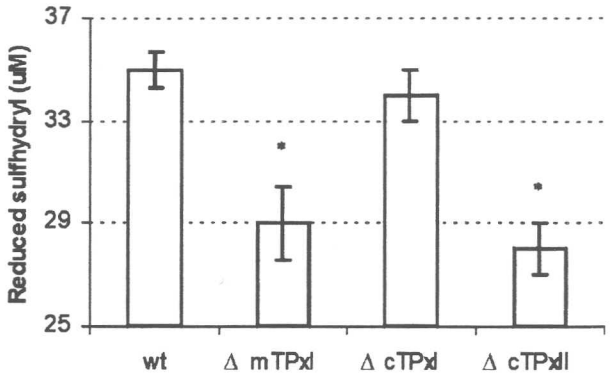

Fig. 2. Total mitochondrial thiol (protein and non-protein) content. Thiol content was determined in mitochondrially-enriched fractions, which were diluted to a concentration equal to 0.5 mg protein/ml of a solution described in Experimental procedures. The differences in total thiol content between ΔcTPxII and ΔmTPxI relative to wild-type cells were statistically significant for p values $\leqslant 0.01$ (determined from paired t test) as indicated by *. The difference between ΔcTPxI and wild-type cells was not statistically significant for p values $\leqslant 0.01$ (determined from paired t test).

To further analyze the redox state of the mutants, GSH/GSSG ratios were determined. All mutants had lower GSH/GSSG ratios than wild-type (wt) cells, although mTPxI mutant cells (ΔmTPxI cells) had lower decrease than the other two strains (Table 1). This effect can be attributed to oxidation of GSH, since the contents of total glutathione and GSH were higher in the mutant strains (Table 1). In agreement with the higher content of GSH that we observed in all mutants (Table 1), an increase in the expression of *GSH1* gene was also detected in these cells (Fig. 1B). Therefore, considering H_2O_2 removal activity, the GSH/GSSG ratios, and *GSH1* expression in whole cell, all the mutants appeared to be in more oxidizing conditions than the wild-type strain.

Next, the redox state of mitochondria was evaluated, since this organelle is the main endogenous source of free radicals in eukaryotic cells. Initially, the total sulfhydryl content (protein and non-protein) of mitochondrially-enriched fractions was measured. Interestingly, only mitochondria from ΔcTPxI cells did not show a decrease in reduced thiol content in comparison with wild type, whereas ΔmTPxI and ΔcTPxII had about the same amount of sulfhydryl groups, about 20% less than controls (Fig. 2). To further understand this phenomenon, levels of GSH and GSSG were also determined in these mitochondrially-enriched fractions. As expected from the results of Fig. 2, only mitochondria from ΔcTPxI did not show decrease in the GSH/GSSG ratio in comparison with wild type (Table 2). In fact, mitochondria from ΔcTPxI cells had higher GSH/GSSG ratios compared to controls, which is in agreement with the suggestion that glutathione system works as a backup for cTPxI [3]. This increase in GSH/GSSG ratios appears to be related to an enhancement of glutathione recycling, because GSSG contents in mitochondria from

Table 1
Measurement of GSH and GSSG in whole cells depleted of thioredoxin peroxidases

Cell strain	Total glutathione (pmol/g of cell pellet) ± SD	GSSG (pmol/g of cell pellet) ± SD	GSH (pmol/g of cell pellet) ± SD	GSH/GSSG
WT	5840 ± 275	30 ± 1.1	5810 ± 280	194 ± 13.4
ΔmTPxI	8540 ± 20*	50 ± 1*	8490 ± 10*	170 ± 4.0*
ΔcTPxI	9230 ± 20*	73 ± 0.5*	9160 ± 20*	126 ± 1.1*
ΔcTPxII	8400 ± 60*	67 ± 8*	8330 ± 50*	124 ± 7.3*

Standard deviations (SD) were calculated from three values obtained from two independent experiments. Calibration was done with commercial GSSG (from Sigma). GSH values were obtained by subtracting GSSG concentration from total glutathione.

*Denotes that the differences between mutant and wild-type strains were statistically significant for p values $\leqslant 0.01$ (determined from paired t test).

Table 2
Measurement of mitochondrial pools of GSH and GSSG

Mitochondrial samples	Total glutathione (pmol/mg of protein) ± SD	GSSG (pmol/mg of protein) ± SD	GSH (pmol/mg of protein) ± SD	GSH/GSSG
WT	870 ± 24	20 ± 3	850 ± 30	43 ± 7.2
ΔmTPxI	1140 ± 34*	56 ± 8*	1084 ± 42*	19 ± 3.32*
ΔcTPxI	870 ± 26	12 ± 2*	858 ± 28	72 ± 1.42*
ΔcTPxII	660 ± 12*	46 ± 3*	614 ± 15*	13 ± 1.06*

Standard deviations (SD) were calculated from three values obtained from two independent experiments. Calibration was done with commercial GSSG (from Sigma). GSH values were obtained by subtracting GSSG concentration from total glutathione.

* Denotes that the differences between mutant and wild-type strains were statistically significant for p values $\leqslant 0.01$ (determined from paired t test).

ΔcTPxI cells were approximately half the GSSG content in mitochondria from wild type (Table 2).

Contrary to ΔcTPxI, mitochondria from ΔcTPxII cells presented very low GSH/GSSG ratios (Table 2), which was due to both low levels of total glutathione and high amounts of GSSG. These results can account, at least in part, for the reduced amount of total sulfhydryl groups in their mitochondria (Fig. 2). In ΔmTPxI mitochondria, the amounts of total glutathione and GSH measured were slightly increased in comparison with wild type (Table 2). Therefore, the reduced amount of sulfhydryl groups observed in mitochondria from these mutants (Fig. 2) must reflect a lower content of thiols from proteins. ΔmTPxI mitochondria also showed an increase in the levels of GSSG, indicating that the recycling of glutathione is not functioning properly in these organelle (Table 2). In any case, the very low GSH/GSSG ratios observed for ΔcTPxII and ΔmTPxI indicated that the mitochondria of these strains were under more oxidizing conditions than ΔcTPxI and wild-type mitochondria. It is important to note that although GSSG values were always very low in comparison with total glutathione, we confirmed the results through three independent experiments performed in triplicate. Moreover, the differences between wild type and mutants were statistically significant with p value $\leqslant 0.01$.

In summary, our data indicated that ΔcTPxII and ΔmTPxI cells are under a more oxidizing condition than wild-type cells. In the case of ΔcTPxI, whole cells appeared to be in a more oxidizing condition, whereas their mitochondria are at least equally reduced as wild-type mitochondria. As described below, the amount of thiols measured in these mitochondrially-enriched fractions and peroxidase activity seem to be important factors involved in yeast susceptibility to Ca^{2+}-induced damage.

Mitochondrial susceptibility to stress induced by calcium

After a characterization of the redox state of whole cells and their mitochondria, the sensitivity of this organelle to inner membrane permeabilization by Ca^{2+} was studied. We have shown before that cells deficient in cTPxI and catalase are more prone to loss of mitochondrial function by Ca^{2+} [24]. Initially, the ability of mitochondria from wild type, ATZ-treated wild type, and mutant cells to keep inner membrane potential was analyzed from mitochondrially-enriched fractions of cells grown in galactose-containing media. As described previously, mitochondria from wild-type cells were resistant to Ca^{2+}-induction of inner membrane permeabilization [24,32,33] whereas mitochondria from ΔcTPxI cells and from ATZ-treated cells did suffer loss of potential [24]. Once again, the loss of potential was more pronounced in cells depleted of catalase than in ΔcTPxI cells (Fig. 3). Now, we describe for the first time that cells deficient in mTPxI and cTPxII were also susceptible to Ca^{2+}-induced permeabilization (Fig. 3). As a matter of fact, ΔmTPxI and ΔcTPxII cells are even more sensitive to loss of potential than ΔcTPxI cells, which appears to be related to the low content of thiol groups in the mitochondria of these cells (Fig. 2, Table 2). Interestingly, cells with disruption in the gene for cytosolic thioredoxin peroxidase III (ΔcTPxIII cells) did not present a Ca^{2+}-induced drop in $\Delta\Psi$ and behaved similar to wild-type mitochondria (data not shown). It is important to note that mitochondrially-enriched fractions obtained from all yeast strains analyzed here were capable to uptake the same amount of Ca^{2+}, reaching intramitochondrial concentrations of approximately 400 μM (as measured using mitochondrial loaded with fura-2/AM [27], data not shown).

As described before, the experiments shown in Fig. 3 were performed in mitochondrially-enriched fractions obtained from cells grown in galactose. Galactose, like glucose, is a fermentative supporting carbon source involved in the signaling of several biochemical pathways [34,35] and was used in most of the experiments of this work. When the yeast *S. cerevisiae* is grown in the presence of high levels of glucose, mitochondrial biogenesis and the expression of several antioxidant proteins, including some isoforms of thioredoxin peroxidases, is inhibited [8,14,34]. These processes are collectively called catabolite repression and involve several signaling pathways [35,36]. Galactose also re-

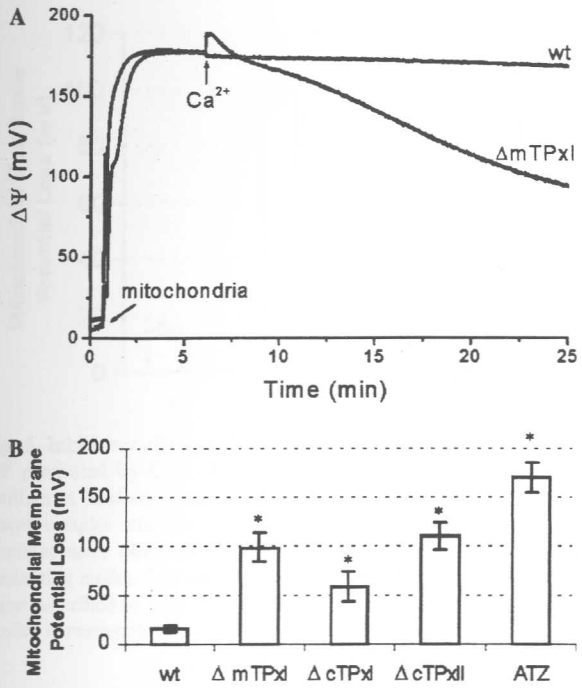

Fig. 3. Effect of thioredoxin peroxidase and catalase depletion on mitochondrial membrane potential ($\Delta\Psi$) decrease promoted by Ca^{2+}. $\Delta\Psi$ was measured in mitochondrial-enriched fractions whose protein concentration was equal to 0.5 mg/ml. (A) A representative $\Delta\Psi$ curve obtained from wild type and mTPxI null strain in the presence of Ca^{2+} (500 μM), whose addition is indicated. (B) Loss of potential in wild type (wt), in the null strains for mTPxI, cTPxI, cTPxII or in catalase-depleted cells (treated with ATZ). The values presented are averages and standard deviation from three independent experiments and represent the loss in $\Delta\Psi$ caused by Ca^{2+} addition (500 μM). The values were obtained by subtracting $\Delta\Psi$ in the absence of Ca^{2+} from the final $\Delta\Psi$ in the presence of Ca^{2+}. The differences between mutants and wild-type cells were statistically significant for p values $\leqslant 0.01$ (determined from paired t test) as indicated by *.

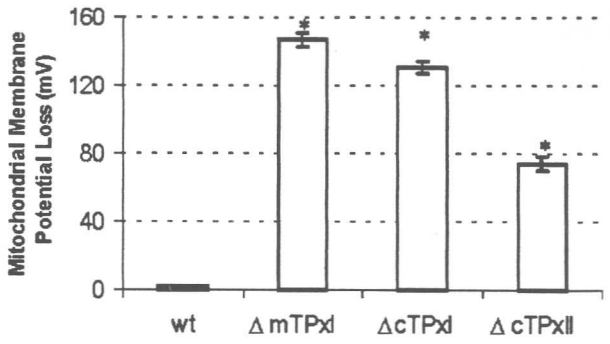

Fig. 4. Effect of thioredoxin peroxidase depletion on $\Delta\Psi$ from cells grown in respiratory conditions. The conditions in this experiment were the same as those described for Fig. 3, except that mitochondrial-enriched fractions were extracted from cells grown in glycerol/ethanol-containing media. The differences between mutants and wild type were statistically significant for p values $\leqslant 0.01$ (1) (determined from paired t test) as indicated by *.

presses several processes, but not mitochondrial proliferation [34,37].

Catalase T (cytosolic) and/or catalase A (peroxisomal) protected yeast mitochondria from Ca^{2+}-induced injury (Fig. 3 and [24]), in spite of the fact that they suffer catabolite repression [38]. It is important to observe, however, that yeast have catalase activity in cells cultured in media containing high levels of glucose [39], indicating that catabolite repression is not total in fermentative conditions.

In the specific case of mTPxI expression, galactose possesses a repressing effect that is similar to that exerted by glucose [14]. Therefore, the effect of thioredoxin peroxidase gene disruptions when cells were cultured in glycerol/ethanol media (which does not support fermentation and has no repressor effect) was also analyzed. In this case, the loss of potential was more intense in ΔmTPxI cells (Fig. 4), which can be related with the cellular location and abundance of mTPxI in respiratory adapted yeast [14].

The loss of membrane potential for ΔcTPxI mitochondria was also more intense in glycerol/ethanol than in galactose containing media (Figs. 3 and 4), which again is correlated with the fact that cTPxI is slightly more abundant in respiratory conditions [8]. It is important to note that cTPxI was present in the mitochondrially-enriched fractions analyzed here, as determined by Western blot analysis of cTPxI in different cell fractions (data not shown). Finally, in the case of ΔcTPxII cells, the loss of potential was about the same in both growth conditions (galactose or glycerol/ethanol as carbon sources) (Figs. 3 and 4). In this case, loss of membrane potential is probably related to other factors than cTPxII abundance because this protein has very low expression levels under basal conditions [12].

Involvement of ROS in yeast inner membrane mitochondrial permeability

ROS are involved in the MPT process in mammalian mitochondria [18] and in the Ca^{2+}-induced permeabilization of yeast mitochondria from cells deficient in cTPxI and catalase [24]. In agreement with these previous observations, addition of catalase to the mitochondrially-enriched fractions strongly inhibited the loss of membrane potential induced by Ca^{2+} (Fig. 5), indicating that in all cases, H_2O_2 is involved in the loss of mitochondrial function. Moreover, mitochondrial GSH/GSSG ratios decreased sharply after Ca^{2+} exposure, which indicates that these mitochondria suffered oxidative stress after the addition of this cation (Fig. 6). In wild-type mitochondrially-enriched fractions, the GSH/GSSG ratio was also reduced during Ca^{2+} exposure, but to a level that was significantly higher than GSH/GSSG ratios of mutant cells. Therefore, the drop in GSH/GSSG ratio in wild-type mitochondria appears to be not

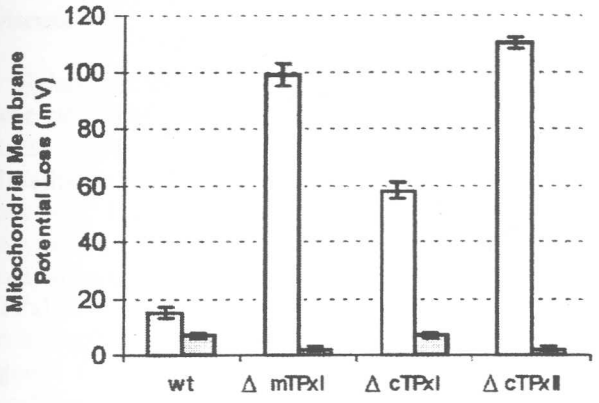

Fig. 5. Inhibitory effect of exogenously added catalase on the loss of $\Delta\Psi$ promoted by Ca^{2+}. Bovine catalase was added to the reaction medium at final concentration of 2 μM (gray bars). Empty bars represent samples with no catalase addition. Mitochondrially-enriched fractions were obtained from yeast that were grown on galactose-containing media. The conditions of this experiment were the same as those described for Fig. 3. Results are representative of series of three similar experiments.

enough to promote inner membrane permeabilization (Fig. 3).

As shown in Table 2, mitochondria from ΔmTPxI and ΔcTPxII presented low basal GSH/GSSG ratios in the absence of Ca^{2+}, indicating that they are in a chronic oxidative state and decreased even more after Ca^{2+} addition. These data suggest that redox status of yeast mitochondria seems to be a very important factor for the sensitivity of yeast mitochondria to Ca^{2+}, although other systems, such as peroxide-removing enzymes or other GSH pools, should cooperate in this process.

Besides loss of membrane potential and decrease in GSH/GSSG ratios, mitochondria from ΔmTPxI and ΔcTPxII, but not from ΔcTPxI and wild-type cells, suffered a decrease in oxygen consumption after Ca^{2+} treatment (data not shown), probably because of cytochrome *c* release secondary to non-selective inner membrane permeabilization promoted by Ca^{2+} [24]. Once again, the sensitivity of mitochondrial function to Ca^{2+} treatment correlates very well with the amount of thiol groups that this organelle possessed (Fig. 2, Table 2). In ΔcTPxI mitochondria, the loss of membrane potential (Fig. 3) and the decrease in GSH/GSSG ratios (Fig. 6) after Ca^{2+} were smaller, and respiratory rate differences were non-significant.

Not only GSH/GSSG ratios but also the lack of peroxiredoxins in mutant cells should be involved in the sensitivity of mitochondria to Ca^{2+}-induced permeabilization. Therefore, we decided to check if different recombinant peroxiredoxins could also prevent yeast mitochondria from membrane potential loss. These recombinant proteins were expressed and purified from *E. coli* and added to ΔmTPxI mitochondrially-enriched fractions (that suffered large membrane potential drop and do not possess any TPxI isoform to interfere with the assay). All of the thioredoxin peroxidase isoforms studied protected mitochondria from permeabilization induced by Ca^{2+}. mTPxI was the most protective and cTPxI the least efficient enzyme (Fig. 7). Therefore, our results indicated that mitochondrial susceptibility to loss of function induced by Ca^{2+} is very dependent on both thiol contents and on peroxide-removing enzymes.

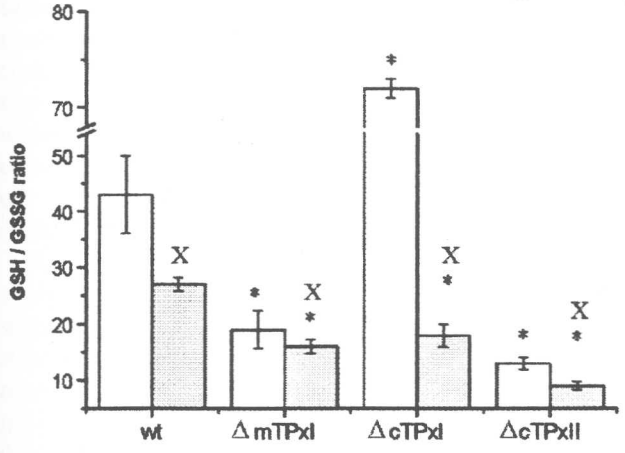

Fig. 6. Mitochondrial GSH/GSSG ratios after Ca^{2+} treatment. Mitochondrial-enriched fractions were incubated for 15 min at 30 °C with controlled stirring in buffer 2 (with respiratory substrates) in the absence (empty bars) or in the presence of 500 μM Ca^{2+} (gray bars). GSH and GSSG were determined as described in Experimental procedures. GSH/GSSG ratios represent averages of three independent experiments done in triplicate and were normalized by protein concentrations equal to 1 mg/ml. The differences between mutants and wild type (*) and the differences between mitochondrial-enriched fractions treated and non-treated with Ca^{2+} (X) were statistically significant for *p* values $\leqslant 0.01$ (determined from paired *t* test).

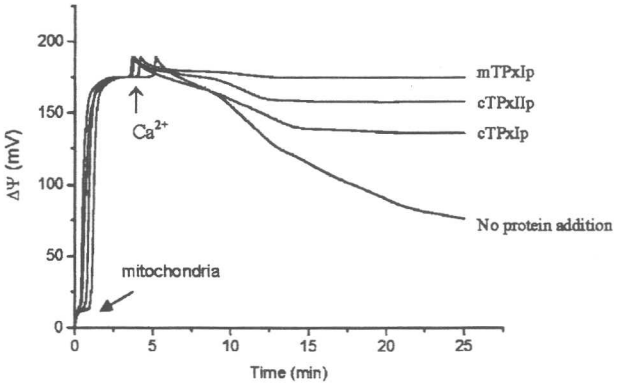

Fig. 7. Inhibitory effect of exogenously added TPxs on the loss of $\Delta\Psi$ promoted by Ca^{2+}. Conditions of this experiment were the same as described for Fig. 3. Recombinant thioredoxin peroxidases were added to the reaction medium at final concentration of 5 μM. Mitochondrially-enriched fractions were obtained from ΔmTPxI cells that were grown on galactose-containing media. These results are representative of three similar experiments performed in similar conditions.

Discussion

Eukaryotic cells possess several pathways to decompose peroxides. As an example, yeasts have two catalases, five peroxiredoxins, three phospholipid glutathione peroxidases, and one cytochrome *c* peroxidase [40]. It is reasonable to think that each of these enzymes may have a particular role in distinct cell compartments or under different conditions. Previously, cTPxI as well as peroxisomal and/or cytosolic catalases were implicated in the defense of yeast mitochondria against Ca^{2+}-promoted mitochondrial membrane permeabilization [24]. Here, we compared the protection of yeast mitochondria from Ca^{2+}-induced damage by catalase and by other peroxiredoxin isoforms.

Before the beginning of the analysis on mitochondrial function, a characterization of cellular and mitochondrial redox state was performed. The reason for this strategy is that several processes are affected in null mutants besides the absence of the gene. As a matter of fact, deletion of *CTPX1* gene promotes: (1) an induction of the *GSH1* gene (Fig. 1B), [3]; (2) an increase in glutathione reductase and glutathione peroxidase activities [3]; (3) an increase in the ability of yeast to induce cytosolic catalase expression by H_2O_2 [9]; and (4) a decrease in the ability to induce the expression of thioredoxin (*TRX2*) and cytosolic thioredoxin reductase by H_2O_2 exposure [9].

Our data showed that all TPxs mutant presented lower capacity to decompose H_2O_2 (Fig. 1A), which could increase oxidation of glutathione and consequently lead to lower GSH/GSSG ratios (Table 1). Besides, in all mutants studied here we observed an increase in the expression of the *GSH1* gene (that encodes γ-glutamylcysteine synthetase, the enzyme that catalyzes the rate-limiting step of glutathione synthesis), which could represent an attempt of mutant strains to cope with the absence of TPx isoforms. Taken together, our results indicated that mutants are in chronic oxidative stress (Fig. 1, Table 1).

After the characterization of the whole yeast cells, an analysis of the redox state of mitochondria from mutant strains was also made. In parallel to the cellular redox state, mitochondria from ΔmTPxI and ΔcTPxII cells are more oxidized than wild-type countertypes. In contrast, mitochondria from ΔcTPxI cells are at least equally reduced compared to wild-type mitochondria, since they showed the same level of total sulfhydryl groups (Fig. 2) and higher GSH/GSSG ratios (Table 2). Our data indicated that the higher level of sulfhydryl in mitochondria of ΔcTPxI cells could be attributed at least in part to the high capacity of these cells to recycle glutathione (Table 2). In fact, ΔcTPxI cells have higher GSSG reductase activities than the parental strain [3] and part of glutathione reductase protein (*GLR1*) is also located inside mitochondria [41]. An alternative explanation for the high GSH/GSSG ratio observed in ΔcTPxI cells (Table 2) could be related to the presence of a GSH transporter from cytosol to mitochondria, according to studies using mice [42].

The sensitivity of yeast mitochondria to membrane potential loss induced by Ca^{2+} appeared to be the result of the interplay of several factors. Our results identified two of them: (1) level of peroxide removing enzymes and (2) sulfhydryl levels in mitochondria. All the mutants analyzed here (and also catalase-depleted cells) were more sensitive than wild-type cells to Ca^{2+}-induced inner membrane permeabilization (Figs. 3 and 4). Interestingly, our results indicated that the sensitivities of the peroxiredoxin mutants appeared to be a consequence of different mechanisms (Fig. 8) as is discussed below. The biochemical pathways responsible for the differential effects of peroxiredoxin genes deletions on thiol redox status and total H_2O_2 removing activity are unknown. In any case these results indicate that peroxiredoxins are not totally redundant among themselves. In this regard, it is noteworthy to point out that deletion of *CTPXIII* (cytosolic thioredoxin peroxidase III gene) did not alter the sensitivity of yeast to Ca^{2+} (data not shown). In spite

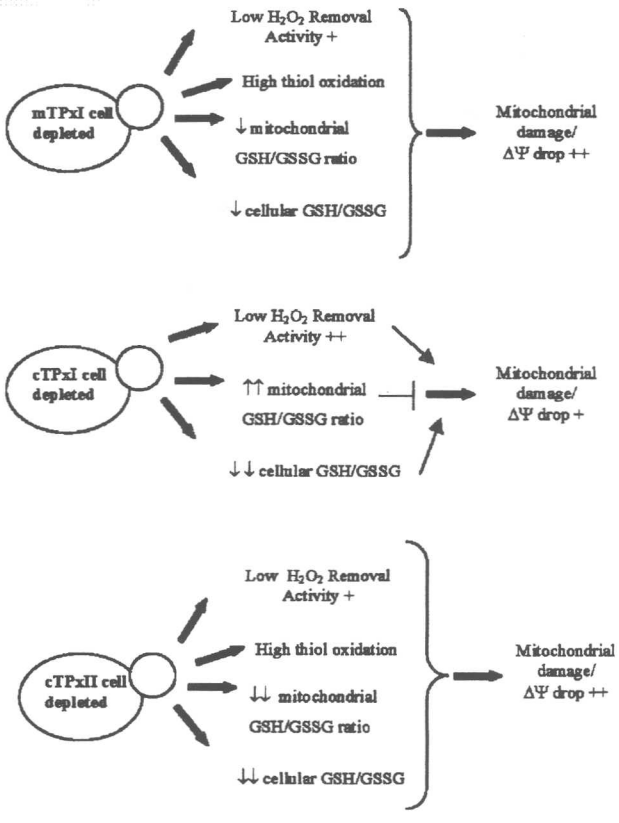

Fig. 8. Effects of deletions of TPx genes on yeast cells. Schematic representation of alterations in yeast redox status that appear to be involved in the sensitivity of strains to Ca^{2+} promoted damage in mitochondria. The signal (+) denotes the intensity of the phenomena observed. The symbols → and ⊣ indicate induction and inhibition, respectively.

of these variations in mitochondrial redox status, in all cases Ca^{2+}-induced inner mitochondrial membrane permeabilization appeared to be mediated by ROS, since catalase and TPxs strongly inhibited damage to this organelle (Figs. 5 and 7) and GSH/GSSG ratio decreased sharply after Ca^{2+} addition (Fig. 6).

In the case of ΔcTPxI mutant cells, the levels of mitochondrial GSH were about the same as the wild-type cells (Table 2) and, therefore, should not contribute significantly to the susceptibility of this strain to loss of membrane potential induced by Ca^{2+} (Figs. 3 and 4). In all cases, a large decrease of GSH/GSSG ratio occurred after Ca^{2+} treatment (Fig. 6). Since whole cellular GSH/GSSG ratios were decreased in ΔcTPxI (Table 1), we cannot exclude the possibility that other pools of GSH are also important for the maintenance of mitochondrial integrity. It is noteworthy to observe that ΔcTPxI cells possessed the lowest peroxidase activity of the all strains analyzed (Fig. 1A), indicating that the absence of the very abundant cTPxI protein should be a very important factor for the increased sensitivity to mitochondrial permeabilization in ΔcTPxI cells (Fig. 8).

Deletion of the *MTPXI* gene promotes different effects compared to *CTPXI* deletion. In this case, both mitochondrial and cytosolic GSH/GSSH ratios, as well as the total sulfhydryl content, decreased sharply (Tables 1 and 2 and Fig. 2), indicating that ΔmTPxI cells are under chronic oxidative stress (Fig. 8). Since mitochondria are highly dependent on GSH for the prevention of oxidative damage [42], the low levels of this thiol in ΔmTPxI mitochondria should be a crucial factor for the high susceptibility of these cells to Ca^{2+}. However, it is important to note that the total H_2O_2 removal activity is also decreased in ΔmTPxI cells (Fig. 1A). Moreover, the drop in inner membrane potential is higher in mitochondria derived from cells grown in glycerol/ethanol than in cells grown in galactose-containing media (Figs. 3 and 4), which correlates with the expression levels of *MTPXI* gene [14]. Therefore, our data indicate that both low sulfhydryl levels and mTPxI absence contribute significantly to the high sensitivity of ΔmTPxI cells to Ca^{2+}-induced loss of mitochondrial function (Fig. 8).

As in ΔmTPxI cells, the levels of sulfhydryl compounds in ΔcTPxII were very low in both mitochondria and in whole cells (Tables 1 and 2 and Fig. 2), which again should be related to the high sensitivity of this strain to Ca^{2+} treatment (Figs. 3 and 4). The lack of cTPxII protein would not be expected to be important in this process, since this protein is present in undetectable amounts under basal conditions [12]. In any case, it is interesting to note that cTPxII cells presented lower capacity to decompose H_2O_2 (Figs. 1A and 8). This result could directly reflect the absence of ΔcTPxII protein or the down regulation of other antioxidant enzymes. In this regard, it is important to observe that deletion of other peroxiredoxin gene, namely *CTPXI*, promotes a down regulation of *TRX2* and *TRR1* that encode other antioxidant proteins [9]. Besides, expression of *GSH1* gene in ΔcTPxII is increased in comparison to levels in wild-type cells (Fig. 1B).

As shown above, the levels of thiols in the mitochondria of peroxiredoxin mutants are an important factor in the sensitivity of yeast strains to Ca^{2+}-induced damage. In fact, several reports have highlighted the importance of depletion of mitochondrial rather than cytosolic pools of GSH in pathological processes [42–44]. Under normal conditions, the concentration of GSH within the organelle is the same as in cytoplasm, but under oxidative stress conditions, the level in the mitochondria is preserved although the cytoplasmic level is decreased [43]. Interestingly, this was the case for ΔcTPxI cells (Tables 1 and 2). Besides, GSH efflux from mitochondria is very slow even under conditions where cytoplasmic GSH contents are depleted [42]. This means that GSH may be essential for mitochondrial function and its concentration is strongly controlled in the cell [42–44].

The maintenance of mitochondrial GSH pool in ΔcTPxI cells seems to be related to the fact that their mitochondria did not lose the ability to respire, although it suffered drop of potential (Fig. 3) and had lower GSH/GSSG ratios after Ca^{2+} treatment (Fig. 6). It is important to emphasize here that the decrease of potential in ΔcTPxI cells was significantly lower than in the other two mutants (Fig. 3). Probably the loss of potential in ΔcTPxI mitochondria was not sufficient to alter oxygen consumption.

Although GSH levels are important for the maintenance of mitochondrial integrity, they are not the only factor. In fact, the importance of thiol-dependent peroxidase activity on mitochondrial protection against Ca^{2+}-induced permeabilization can be demonstrated by the exogenous addition of recombinant peroxiredoxins to mitochondrially-enriched fractions (Fig. 7). In all cases, significant protection was observed. Interestingly, all peroxiredoxins protected mitochondria, but not equally. mTPxI was the most effective, which can be related with its high enzymatic activity [5,13]. Accordingly to Park et al. [5] cTPxI is more active than cTPxII, but our results indicated that other properties rather than their enzymatic activities interfere with their protective effects. A possible hypothesis could be the differential capability to use mitochondrial thiols as electrons donors.

Thioredoxin could be another important component to maintain mitochondrial activity intact. This is because it is known that oxidative stress and decreases in glutathione content lead to the oxidation of thioredoxin in vivo [45,46]. In the absence of thioredoxin peroxidases, it is expected that thioredoxin would be oxidized slower and this could have a consequence in cell signaling. In this regard, it is important to mention that

thioredoxin, but not glutathione, is involved in regulation of yAP1p (a key transcription regulator of yeast response to oxidative stress) [3,9,45,47].

Ca^{2+}-induced inner mitochondrial membrane permeabilization in yeast possesses several similarities with MPT in mammalian mitochondria [24]. Therefore, the studies presented here may have implications in the regulation of processes that occur in higher eukaryotes, such as cell death. In fact, it has been shown before that mammalian thioredoxin, which is the substrate of TPxs, is involved in the regulation of mitochondrial membrane potential and apoptosis [48,49]. Moreover, yeast has been considered a good model for studies of human mitochondrial disorders [50]. Our results presented here indicated the existence of unknown signaling pathways that coordinate the levels of thiol compounds and peroxidases that may also be relevant to higher eukaryotes.

Acknowledgments

We thank Marilene Demasi and Gustavo Monteiro Silva for helping us with glutathione measurements, Simone Vidigal Alves for providing us with pure thioredoxin peroxidase proteins, and Victor Genu for revising the paper. We especially thank Giannis Spyrou for kindly providing us with the Ser^{38}-mPrx1p construct. We also thank Fundação de Amparo à Pesquisa do Estado de São Paulo (FAPESP) and Conselho Nacional de Desenvolvimento Científico e Tecnológico (CNPq) for financial support.

References

[1] C.M. Grant, Mol. Microbiol. 39 (2001) 533–541.
[2] M. Penninckx, Enzyme Microb. Technol. 26 (2000) 737–742.
[3] Y. Inoue, T. Matsuda, K. Sugiyama, S. Izawa, A. Kimura, J. Biol. Chem. 274 (1999) 27002–27009.
[4] A.M. Avery, S.V. Avery, J. Biol. Chem. 276 (2001) 33730–33735.
[5] S.G. Park, M-K. Cha, W. Jeong, I-H. Kim, J. Biol. Chem. 275 (2000) 5723–5732.
[6] I.H. Kim, K. Kim, S.G. Rhee, Proc. Natl. Acad. Sci. USA 86 (1989) 6018–6022.
[7] H.Z Chae, I.H. Kim, K. Kim, S.G. Rhee, J. Biol. Chem. 268 (1993) 16815–16821.
[8] A.P. Demasi, G.A.G. Pereira, L.E.S. Netto, FEBS Lett. 509 (2001) 430–434.
[9] S.J. Ross, V.J. Findlay, P. Malakasi, B.A. Morgan, Mol. Biol. Cell 11 (2000) 2631–2642.
[10] S.G. Rhee, S.W. Kang, L.E.S. Netto, M.S. Seo, E.R. Stadtman, Biofactors 10 (1999) 207–209.
[11] C.M. Wong, Y. Zhou, R.W.M. Ng, H.F. Kung, D.Y. Jin, J. Biol. Chem. 277 (2002) 5385–5394.
[12] S.K. Hong, M.K. Cha, Y.S. Choi, W.C. Kim, I.H. Kim, J. Biol. Chem. 277 (2002) 12109–12117.
[13] J.R. Pedrajas, A. Miranda-Vizuete, N. Javanmardy, J.A. Gustafsson, G. Spyrou, J. Biol. Chem. 275 (2000) 16296–16301.
[14] G. Monteiro, G.A.G. Pereira, L.E.S. Netto, Free Rad. Biol. Med. 32 (2002) 278–288.
[15] J.S. Jeong, S.J. Kwon, S.W. Kang, S.G. Rhee, K. Kim, Biochemistry 38 (1999) 776–783.
[16] M.K. Cha, Y.S. Choi, S.K. Hong, W.C. Kim, K.T. No, I.H. Kim, J. Biol. Chem. 278 (2003) 24636–24643.
[17] M. Zoratti, I. Szabò, Biochim. Biophys. Acta 1241 (1995) 139–176.
[18] A.J. Kowaltowski, L.E. Netto, A.E. Vercesi, J. Biol. Chem. 273 (1998) 12766–12769.
[19] D.G. Nicholls, S.L. Budd, Physiol. Rev. 80 (2000) 315–360.
[20] V. Petronilli, P. Costantini, L. Scorrano, R. Colonna, S. Passamonti, P. Bernardi, J. Biol. Chem. 269 (1994) 16638–16642.
[21] R.F. Castilho, A.J. Kowaltowski, A.R. Meinicke, E.J.H. Bechara, A.E. Vercesi, Free Rad. Biol. Med. 18 (1995) 479–486.
[22] M.M. Fagian, L. Pereira-da-Silva, I.S. Martins, A.E. Vercesi, J. Biol. Chem. 265 (1990) 19955–19960.
[23] D.R. Green, J.C. Reed, Science 281 (1998) 1309–1312.
[24] A.J. Kowaltowski, A.E. Vercesi, S.G. Rhee, L.E.S. Netto, FEBS Lett. 473 (2000) 177–182.
[25] M. Zhou, Z. Diwu, N. Panchuk-Voloshina, R.P. Haugland, Anal. Biochem. 253 (1997) 162–168.
[26] G. Faye, C. Kujawa, H. Fukuhara, J. Mol. Biol. 88 (1974) 185–203.
[27] A.J. Kowaltowski, R.F. Castilho, Biochim. Biophys. Acta 1322 (1997) 221–229.
[28] P.W. Riddles, R.L. Blakeley, B. Zerner, Methods Enzymol. 91 (1983) 49–60.
[29] M. Demasi, R. Shingarpure, K.J.A. Davies, Arch. Biochem. Biophys. 389 (2001) 254–263.
[30] K.E. Akerman, M.K. Wikstrom, FEBS Lett. 68 (1976) 191–197.
[31] A.J. Kowaltowski, R.G. Cosso, C.B. Campos, G. Fiskum, J. Biol. Chem. 277 (2002) 42802–42807.
[32] D.W. Jung, P.C. Bradshaw, D.R. Pfeifer, J. Biol. Chem. 272 (1997) 21104–21112.
[33] P.C. Bradshaw, D.W. Jung, D.R. Pfeiffer, J. Biol. Chem. 276 (2001) 40502–40509.
[34] A.D. Panek, J.R. Mattoon, Arch. Biochem. Biophys. 183 (1977) 306–316.
[35] J.M. Thevelein, Yeast 10 (1994) 1753–1790.
[36] J.M. Gancedo, Microbiol. Mol. Biol. Rev. 62 (1998) 334–361.
[37] D. Lohr, J. Zlatanova, FASEB J. 9 (1995) 777–787.
[38] H. Hörtner, G. Ammerer, E. Hartter, B. Hamilton, J. Rytka, T. Bilinski, H. Ruis, Eur. J. Biochem. 128 (1982) 179–184.
[39] S. Izawa, I. Inoue, A. Kimura, Biochem. J. 320 (1996) 61–67.
[40] D.J. Jamieson, Yeast 14 (1998) 1511–1527.
[41] W.K. Huh, J.V. Falvo, L.C. Gerke, A.S. Carroll, R.W. Howson, J.S. Weissman, E.K. O'Shea, Nature 425 (2003) 686–691.
[42] O.W. Griffith, A. Meister, Proc. Natl. Acad. Sci. USA 82 (1985) 4668–4672.
[43] A.G. Hall, Eur. J. Clin. Invest. 29 (1999) 238–245.
[44] D.J. O'Donovan, C.J. Fernandes, Mol. Genet. Metab. 71 (2000) 352–358.
[45] S. Kuge, M. Arita, A. Murayama, K. Maeta, S. Izawa, Y. Inoue, A. Nomoto, Mol. Cell. Biol. 21 (2001) 6139–6150.
[46] E.W. Trotter, C.M. Grant, EMBO Rep. 4 (2003) 184–188.
[47] A. Delaunay, A-D. Isnard, M.B. Toledano, EMBO J. 19 (2000) 5157–5166.
[48] A.E. Damdimopoulos, A. Miranda-Vizuete, M. Pelto-Huikko, J.A. Gustafsson, G. Spyrou, J. Biol. Chem. 277 (2002) 33249–33257.
[49] T. Tanaka, F. Hosoi, Y. Yamaguchi-Iwai, H. Nakamura, H. Masutani, S. Ueda, A. Nishiyama, S. Takeda, H. Wada, G. Spyrou, J. Yodoi, EMBO J. 21 (2002) 1695–1703.
[50] A. Barrientos, IUBMB Life 55 (2003) 83–95.

Dessa forma, analisando conjuntamente os resultados dos anexos 7 a 14, observamos que as peroxirredoxinas de *Saccharomyces cerevisiae* apesar de possuírem a mesma atividade enzimática (peroxidase dependente de tiól), têm papeis distintos no sistema antioxidante de levedura. cTPxI parece atuar preferencialmente em situações nas quais a mitocôndria não está ativa, enquanto mTPxI é importante em situações nas quais a respiração é muito ativa (quando a levedura está adaptada a baixas concentrações de glicose). Por outro lado, cTPxII parece ser um importante "backup" somente em situações nas quais a levedura estaria exposta a altas doses de peróxidos, independentemente da atividade mitocondrial.

CAPÍTULO 3

Funções de peroxidases dependentes de tiól em *Xylella fastidiosa*

A minha participação no projeto Genoma *Xylella fastidiosa* foi não somente coordenadar as atividades relacionadas a sequenciamento de DNA, mas também analisar o significado dos dados gerados ("*data mining*"). Meu interesse foi principalmente estudar os mecanismos de defesa antioxidante de *Xylella fastidiosa*, o que deve ter uma grande relevância em termos de patogenicidade, considerando que plantas e animais respondem a organismos invasores com um "*oxidative burst*" entre outros processos (anexo 3). Dessa forma, para poder invadir uma planta, *Xylella fastidiosa* tem que ser capaz de resistir a esse estresse oxidativo. Ajudei na identificação de vários sistemas antioxidantes de *Xylella fastidiosa*, como a demonstração de que essa bactéria tem genes que codificam para catalases, Mn-Superóxido Dismutase, GSH peroxidase e peroxirredoxinas. No caso de GSH peroxidase, a enzima deve ser selênio –independente, pois RNAt de seleno-cisteína somente foram encontrados em mamíferos até o momento (Halliwell e Gutteridge, 1999). Uma enzima antioxidante de *Xylella fastidiosa* que me chamou a atenção foi Ohr ("*Organic Hydroperoxide Resistance protein*"), cuja função bioquímica não era conhecida naquele momento. O gene *ohr* está presente somente em bactérias, sendo que a maior parte delas é patogênica para plantas ou mamíferos (Atichartpongkul e col., 2001).Um esquema dos sistemas antioxidantes de *Xylella fastidiosa* dentro do contexto geral da bactéria *Xylella fastidiosa* pode ser visualizada na figura 2 do anexo 15.

ANEXO 15

The genome sequence of the plant pathogen *Xylella fastidiosa*

The *Xylella fastidiosa* Consortium of the Organization for Nucleotide Sequencing and Analysis*, São Paulo, Brazil

* *A full list of authors appears at the end of this paper*

***Xylella fastidiosa* is a fastidious, xylem-limited bacterium that causes a range of economically important plant diseases. Here we report the complete genome sequence of *X. fastidiosa* clone 9a5c, which causes citrus variegated chlorosis—a serious disease of orange trees. The genome comprises a 52.7% GC-rich 2,679,305-base-pair (bp) circular chromosome and two plasmids of 51,158 bp and 1,285 bp. We can assign putative functions to 47% of the 2,904 predicted coding regions. Efficient metabolic functions are predicted, with sugars as the principal energy and carbon source, supporting existence in the nutrient-poor xylem sap. The mechanisms associated with pathogenicity and virulence involve toxins, antibiotics and ion sequestration systems, as well as bacterium–bacterium and bacterium–host interactions mediated by a range of proteins. Orthologues of some of these proteins have only been identified in animal and human pathogens; their presence in *X. fastidiosa* indicates that the molecular basis for bacterial pathogenicity is both conserved and independent of host. At least 83 genes are bacteriophage-derived and include virulence-associated genes from other bacteria, providing direct evidence of phage-mediated horizontal gene transfer.**

Citrus variegated chlorosis (CVC), which was first recorded in Brazil in 1987, affects all commercial sweet orange varieties[1]. Symptoms include conspicuous variegations on older leaves, with chlorotic areas on the upper side and corresponding light brown lesions, with gum-like material on the lower side. Affected fruits are small, hardened and of no commercial value. A strain of *Xylella fastidiosa* was first identified as the causal bacterium in 1993 (ref. 2) and found to be transmitted by sharpshooter leafhoppers in 1996 (ref. 3). CVC control is at present limited to removing infected shoots by pruning, the application of insecticides and the use of healthy plants for new orchards. In addition to CVC, other strains of *X. fastidiosa* cause a range of economically important plant diseases including Pierce's disease of grapevine, alfalfa dwarf, phony peach disease, periwinkle wilt and leaf scorch of plum, and are also associated with diseases in mulberry, pear, almond, elm, sycamore, oak, maple, pecan and coffee[4]. The triply cloned *X. fastidiosa* 9a5c, sequenced here, was derived from the pathogenic culture 8.1b obtained in 1992 in Bordeaux (France) from CVC-affected Valencia sweet orange twigs collected in Macaubal (São Paulo, Brazil) on May 21, 1992 (ref. 2). Strain 9a5c produces typical CVC symptoms on inoculation into experimental citrus plants[5], and into *Nicotiana tabacum* (S. A. Lopes, personal communication) and *Catharantus roseus* (P. Brant-Monteiro, personal communication)—two novel experimental hosts.

General features of the genome

The basic features of the genome are listed in Table 1 and a detailed map is shown in Fig. 1. The conserved origin of replication of the large chromosome has been identified in a region between the putative 50S ribosomal protein L34 and *gyrB* genes containing *dnaA*, *dnaN* and *recF*[6]. The *Escherichia coli* DnaA box consensus sequence TTATCCACA is found on both DNA strands close to *dnaA*. In addition, there are typical 13-nucleotide (ACCACCAC-CACCA) and 9-nucleotide (two TTTCATTGG and two TTTTA-TATT) sequences in other intergenic sequences of this region. This region is coincident with the calculated GC-skew signal inversion[7]. We have designated base 1 of the *X. fastidiosa* genome as the first T of the only TTTTAT sequence found between the ribosomal protein L34 gene and *dnaA*.

The overall percentage of open reading frames (ORFs) for which a putative biological function could be assigned (47%) was slightly below that for other sequenced genomes such as *Thermotoga maritima*[8] (54%), *Deinococcus radiodurans*[9] (52.5%) and *Neisseria meningitidis*[10] (53.7%). This may reflect the lack of previous complete genome sequences from phytopathogenic bacteria. Plasmid pXF1.3 contains only two ORFs, one of which encodes a replication-associated protein. Plasmid pXF51 contains 64 ORFs, of which 5 encode proteins involved in replication or plasmid stability and 20 encode proteins potentially involved in conjugative transfer. One ORF encodes a protein similar to the virulence-associated protein D (VapD), found in many other bacterial pathogens[11]. Four regions of pXF51 present significant DNA similarity to parts of transposons found in plasmids from other bacteria, suggesting interspecific horizontal exchange of genetic material.

The principal paralogous families are summarized in Table 2. The complete list of ORFs with assigned function is shown in Table 3. Seventy-five proteins present in the 21 completely sequenced genomes in the COG database[12] (as of 15th March 2000) were also found in *X. fastidiosa*. Each of these sequences was used to

Table 1 General features of the *Xylella fastidiosa* 9a5c genome

Main chromosome	
Length (bp)	2,679,305
G+C ratio	52.7%
Open reading frames (ORFs)	2,782
Coding region (% of chromosome size)	88.0%
Average ORF length (bp)	799
ORFs with functional assignment	1,283
ORFs with matches to conserved hypothetical proteins	310
ORFs without significant data base match	1,083
Ribosomal RNA operons	2 (16SrRNA-Ala-TGC-tRNA-Ile-GAT-tRNA-23SrRNA-5SrRNA)
tRNAs	49 (46 different sequences corresponding to all 20 amino acids)
tmRNA	1
Plasmid pXF51	
Length (bp)	51,158
G+C ratio	49.6%
Open reading frames (ORFs)	64
Protein coding region (% of plasmid size)	86.9%
ORFs with functional assignment	30
ORFs with matches to conserved hypothetical proteins	8
ORFs without significant data base match	24
Plasmid pXF1.3	
Length (bp)	1,285
G+C ratio	55.6%
Open reading frames (ORFs)	2
ORFs with functional assignment	1

Table 2 Largest families of paralogous genes

Family (total number of families = 312)	Number of genes (total number of genes = 853)
ATP-binding subunits of ABC transporters	23
Reductases/dehydrogenases	12
Two-component system, regulatory proteins	12
Hypothetical proteins	10
Transcriptional regulators	9
Fimbrial proteins	9
Two-component system, sensor proteins	9

generate a phylogenetic tree of the 22 organisms. In 69% of such trees, *X. fastidiosa* was grouped with *Haemophilus influenzae* and *E. coli*, consistent with a phylogenetic analysis undertaken with the 16S rRNA gene[13].

One ORF, a cytosine methyltransferase (XF1774), is interrupted by a Group II intron. The intron was identified on the basis of the presence of a reverse transcriptase-like gene (as in other Group II introns), conserved splice sites, conserved sequence in structure V and conserved elements of secondary structure[14]. Group II introns are rare in prokaryotes, but have been found in different evolutive lineages including *E. coli*, cyanobacteria and proteobacteria[15].

Transcription, translation and repair

The basic transcriptional and translational machinery of *X. fastidiosa* is similar to that of *E. coli*[16]. Recombinational repair, nucleotide and base-excision repair, and transcription-coupled repair are present with some noteworthy features. For example, no photolyase was found, indicating exclusively dark repair. Although the main genes of the SOS pathway, *recA* and *lexA*, are present, ORFs corresponding to the three DNA polymerases induced by SOS in *E. coli* (DNA polymerases II, IV and V)[17] are missing, indicating that the mutational pathway itself may be distinct.

Energy metabolism

Even though *X. fastidiosa* is, as its name suggests, a fastidious organism, energy production is apparently efficient. In addition to all the genes for the glycolytic pathway, all genes for the tricarboxylic acid cycle and oxidative and electron transport chains are present. ATP synthesis is driven by the resulting chemiosmotic proton gradient and occurs by an F-type ATP synthase. Fructose, mannose and glycerol can be utilized in addition to glucose in the glycolytic pathway. There is a complete pathway for hydrolysis of cellulose to glucose, consisting of 1,4-β-cellobiosidase, endo-1,4-β-glucanase and β-glucosidase, suggesting that cellulose breakdown may supplement the often low concentrations of monosaccharides in the xylem[18]. Two lipases are encoded in the genome, but there is no β-oxidation pathway for the hydrolysis of fatty acids, presumably precluding their utilization as an alternative carbon and energy source. Likewise, although enzymes required for the breakdown of threonine, serine, glycine, alanine, aspartate and glutamate are present, pathways for the catabolism of the other naturally occurring amino acids are incomplete or absent.

The gluconeogenesis pathway appears to be incomplete. Phosphoenolpyruvate carboxykinase and the gluconeogenic enzyme fructose-1,6-bisphosphatase, which are required to bypass the irreversible step in glycolysis, are not present. The absence of the first is compensated by the presence of phosphoenolpyruvate synthase and malate oxidoreductase, which together can generate phosphoenolpyruvate from malate. There appears, however, to be no known compensating pathway for the absence of fructose-1,6-bisphosphatase. It is possible that among the large number of unidentified *X. fastidiosa* genes there are non-homologous genes that compensate for steps in such critical pathways. Barring this possibility, however, the absence of a functional gluconeogenesis pathway implies a strict dependence on carbohydrates both as a source of energy and anabolic precursors. The glyoxylate cycle is absent and the pentose phosphate pathway is incomplete. In the latter pathway, genes for neither 6-phosphogluconic dehydrogenase nor transaldolase were identified.

Small molecule metabolism

X. fastidiosa exhibits extensive biosynthetic capabilities, presumably an absolute requirement for a xylem-dwelling bacterium. Most of the genes found in *E. coli* necessary for the synthesis of all amino acids from chorismate, pyruvate, 3-phosphoglycerate, glutamate and oxaloacetic acid[16] were identified. However, some genes in *X. fastidiosa* are bi-functional, such as phosphoribosyl-AMP cyclohydrolase/phosphoribosyl-ATP pyrophosphatase (XF2213), aspartokinase/homoserine dehydrogenase I (XF2225), imidazoleglycerolphosphate dehydratase/histidinol-phosphate phosphatase (XF2217) and a new diaminopimelate decarboxylase/aspartate kinase (XF1116) that would catalyse the first and the last steps of lysine biosynthesis. In addition, the gene for acetylglutamate kinase (XF1001) has an acetyltransferase domain at its carboxy-terminal end that would compensate for the missing acetyltransferase in the arginine biosynthesis pathway. Other missing genes include phosphoserine phosphatase, cystathionine β-lyase, homoserine *O*-succinyltransferase and 2,4,5-methyltetrahydrofolate-homocysteine methyltransferase. The first two enzymes are also absent in the *Bacillus subtilis* genome, the third is absent in *Haemophilus influenzae* and the fourth is missing in both genomes[12]. We thus presume that alternative, unidentified enzymes complete the biosynthetic pathways in these organisms and in *X. fastidiosa*.

The pathways for the synthesis of purines, pyrimidines and nucleotides are all complete. *X. fastidiosa* is also apparently capable of both synthesizing and elongating fatty acids from acetate. Again, however, some *E. coli* enzymes were not found, such as holo acyl-carrier-protein synthase (also absent in *Synechocystis* sp., *H. influenzae* and *Mycoplasma genitalium*) and enoyl-ACP reductase (NADPH) (*FabI*) (also absent from *M. genitalium, Borrelia burgdorferi* and *Treponema pallidum*)[12].

X. fastidiosa appears to be capable of synthesizing an extensive variety of enzyme cofactors and prosthetic groups, including biotin, folic acid, pantothenate and coenzyme A, ubiquinone, glutathione, thioredoxin, glutaredoxin, riboflavin, FMN, FAD, pyrimidine nucleotides, porphyrin, thiamin, pyridoxal 5′-phosphate and lipoate. In a number of the synthetic pathways, one or more of the enzymes present in *E. coli* are absent, but this is also true for at least one other sequenced Gram-negative bacterial genome in each case[12]. We therefore again infer that the missing enzymes are either not essential or replaced by unknown proteins with novel structures.

Transport-related proteins

A total of 140 genes encoding transport-related proteins were identified, representing 4.8% of all ORFs. For comparison, *E. coli*, *B. subtilis* and *M. genitalium* have around 10% of genes encoding transport proteins, whereas *Helicobacter pylori*, *Synechocystis* sp. and *Methanococcus jannaschii* have 3.5–5.4% (ref. 19). Transport systems are central components of the host–pathogen relationship (Fig. 2). There are a number of ion transporters and transporters for the uptake of carbohydrates, amino acids, peptides, nitrate/nitrite, sulphate, phosphate and vitamin B12. Many different transport

Figure 1 Linear representation of the main chromosome and plasmids pXF51 and pXF1.3 of the *Xylella fastidiosa* genome. Genes are coloured according to their biological role. Arrows indicate the direction of transcription. Genes with frameshift and point mutations are indicated with an X. Ribosomal RNA genes, the tmRNA, the principal repeats, prophages and the group II intron are indicated by coloured lines. Transfer RNAs are identified by a single letter identifying the amino acid. Pie chart represents the distribution of the number of genes according to biological role. The numbers below protein-producing genes correspond to gene IDs. ►

families are represented and include both small and large mechanosensitive conductance ion channels, a monovalent cation:proton antiporter (CAP-2) and a glycerol facilitator belonging to the major intrinsic protein (MIP) family. In addition, 23 ABC transport systems comprising 41 genes can be identified. *X. fastidiosa* appears to possess a phosphotransferase system (PTS) that typically mediates small carbohydrate uptake. There are both the enzyme I and HPr components of this system, as well as a gene supposedly involved in its regulation (*pstK* or *hprK*); however, there is no PTS permease—an essential component of the phosphotransferase complex. The functionality of the system therefore remains in question.

There are five outer membrane receptors, including siderophores, ferrichrome-iron and haemin receptors, which are all associated with iron transport. The energizing complexes, TonB–ExbB–ExbD and the paralogous TolA–TolR–TolQ, essential for the functioning of the outer membrane receptors, are also present. In all, 67 genes encode proteins involved in iron metabolism. We propose that in *X. fastidiosa* the uptake of iron and possibly of other transition metal ions such as manganese causes a reduction in essential micronutrients in the plant xylem, contributing to the typical symptoms of leaf variegation.

The *X. fastidiosa* genome encodes a battery of proteins that mediate drug inactivation and detoxification, alteration of potential drug targets, prevention of drug entry and active extrusion of drugs and toxins. These include ABC transporters and transport processes driven by a proton gradient. Of the latter, eight belong to the hydrophobe/amphiphile efflux-1 (HAE1) family, which act as multidrug resistance factors.

Adhesion

X. fastidiosa is characteristically observed embedded in an extracellular translucent matrix *in planta*[20]. Clumps of bacteria form within the xylem vessels leading to their blockage and symptoms of the disease such as water-stress leaf curling. We deduce, from our analysis of the complete genome sequence, that the matrix is composed of extracellular polysaccharides (EPSs) synthesized by enzymes closely related to those of *Xanthomonas campestris* pv *campestris* (Xcc) that produce what is commercially known as xanthan gum. In comparison with Xcc, however, we did not find *gumI* (encoding glycosyltransferase V, which incorporates the terminal mannose), *gumL* (encoding ketalase which adds pyruvate to the polymer) or *gumG* (encoding acetyltransferase which adds acetate), suggesting that *Xylella* gum may be less viscous than its *Xanthomonas* counterpart.

Positive regulation of the synthesis of extracelullar enzymes and EPS in *Xanthomomas* is effected by proteins coded by the *rpf* (regulation of pathogenicity factors) gene cluster[21]. Mutations in any of these genes in *Xanthomomas* results in failure to synthesize the EPS. In consequence, the strain becomes non-pathogenic[21]. *X. fastidiosa* contains genes that encode RpfA, RpfB, RpfC and RpfF, suggesting that both bacteria may regulate the synthesis of pathogenic EPS factors through similar mechanisms.

Fimbria-like structures are readily apparent upon electron microscopical observation of *X. fastidiosa* within both its plant and insect hosts[22]. Because of the high velocity of xylem sap passing through narrow portions of the insect foregut, fimbria-mediated attachment may be essential for insect colonization. Indeed, in the insect mouthparts the bacteria are attached in ordered arrays, indicating specific and polarized adhesion[23]. In addition, fimbriae are thought to be involved in both plant–bacterium and bacterium–bacterium interactions during colonization of the xylem itself. We identified 26 genes encoding proteins responsible for the biogenesis and function of Type 4 fimbria filaments. This type of fimbria is found at the poles of a wide range of bacterial pathogens where they act to mediate adhesion and translocation along epithelial surfaces[24]. The genes include *pilS* and *pilR* homologues, which encode a two-component system controlling transcription of fimbrial subunits, presumably in response to host cues, and *pilG*, *H*, *I*, *J* and *chpA*, which encode a chemotactic system transducing environmental signals to the pilus machinery.

In addition to the EPS and fimbriae, which are likely to have central roles in the clumping of bacteria and in adhesion to the xylem walls, we also identified outer membrane protein homologues for afimbrial adhesins. Although fimbrial adhesins are well characterized as crucial virulence factors in both plant and human pathogens[25], afimbrial adhesins, which are directly associated with the bacterial cell surface, have been hitherto associated only with human and animal pathogens, where they promote adherence to epithelial tissue. Of the three putative adhesins of this kind identified in *X. fastidiosa*, two exhibit significant similarity to each other (XF1981, XF1529) and to the *hsf* and *hia* gene products of *H. influenzae*[26]. The third (XF1516) is similar to the *uspA1* gene product of *Moraxella catarrhalis*[27]. All these proteins share the common C-terminal domain of the autotransporter family[28]. Direct experimentation will be required to establish whether these adhesins promote binding to plant cell structures or components of the insect vector foregut, or both. Nevertheless, their presence in the *X. fastidiosa* genome adds to the increasing evidence for the generality of mechanisms of bacterial pathogenicity, irrespective of the host organism[29].

We also identified three different haemagglutinin-like genes. Again, similar genes have not previously been identified in plant pathogens. These genes (XF2775, XF2196, XF0889) are the largest in the genome and exhibit highest similarity to a *Neisseria meningitidis* putative secreted protein[10].

Intervessel migration

Movement between individual xylem vessels is crucial for effective colonization by *X. fastidiosa*. For this to occur, degradation of the pit membrane of the xylem vessel is required. Of the known pectolytic enzymes capable of this function, a polygalacturonase precursor and a cellulase were identified, although the former contains an authentic frameshift. These genes exhibited highest similarity to orthologues in *Ralstonia solanacearum*—which causes wilt disease in tomatoes—where the polygalacturonase genes are required for wild-type virulence.

Toxicity

We identified five haemolysin-like genes: haemolysin III (XF0175), which belongs to an uncharacterized protein family, and four others (XF0668, XF1011, XF2407, XF2759) which belong to the RTX toxin family that contains tandemly repeated glycine-rich nonapeptide motifs at the C-terminal domain. One of these ORFs is closely related to bacteriocin, an RTX toxin also found in the plant bacterium *Rhizobium leguminosarum*[30]. RTX or RTX-like proteins are important virulence factors widely distributed among Gram-negative pathogenic bacteria[31].

There are two Colicin-V-like precursor proteins. Colicin V is an antibacterial polypeptide toxin produced by *E. coli*, which acts against closely related sensitive bacteria[32]. The precursors consist of 102-amino-acid peptides (XF0262, XF0263) that have the typical conserved leader 15-amino-acid motif, and have some similarity with Colicin V from *E. coli* at the remaining C-terminal portion. The necessary apparatus for Colicin biosynthesis and secretion is also present. Interestingly, in *E. coli* most of the genes necessary for biogenesis and export of Colicin V are in a gene cluster present in a plasmid, whereas in *X. fastidiosa* these genes are dispersed in the chromosome.

We found four genes that may function in polyketide biogenesis: polyketide synthase (PKS), pteridine-dependent deoxygenase, daunorubicin C-13 ketoreductase and a NonF-related protein. These genes belong to the synthesis pathways of frenolicin, rapamycin, daunorubicin and nonactin, respectively. These pathways

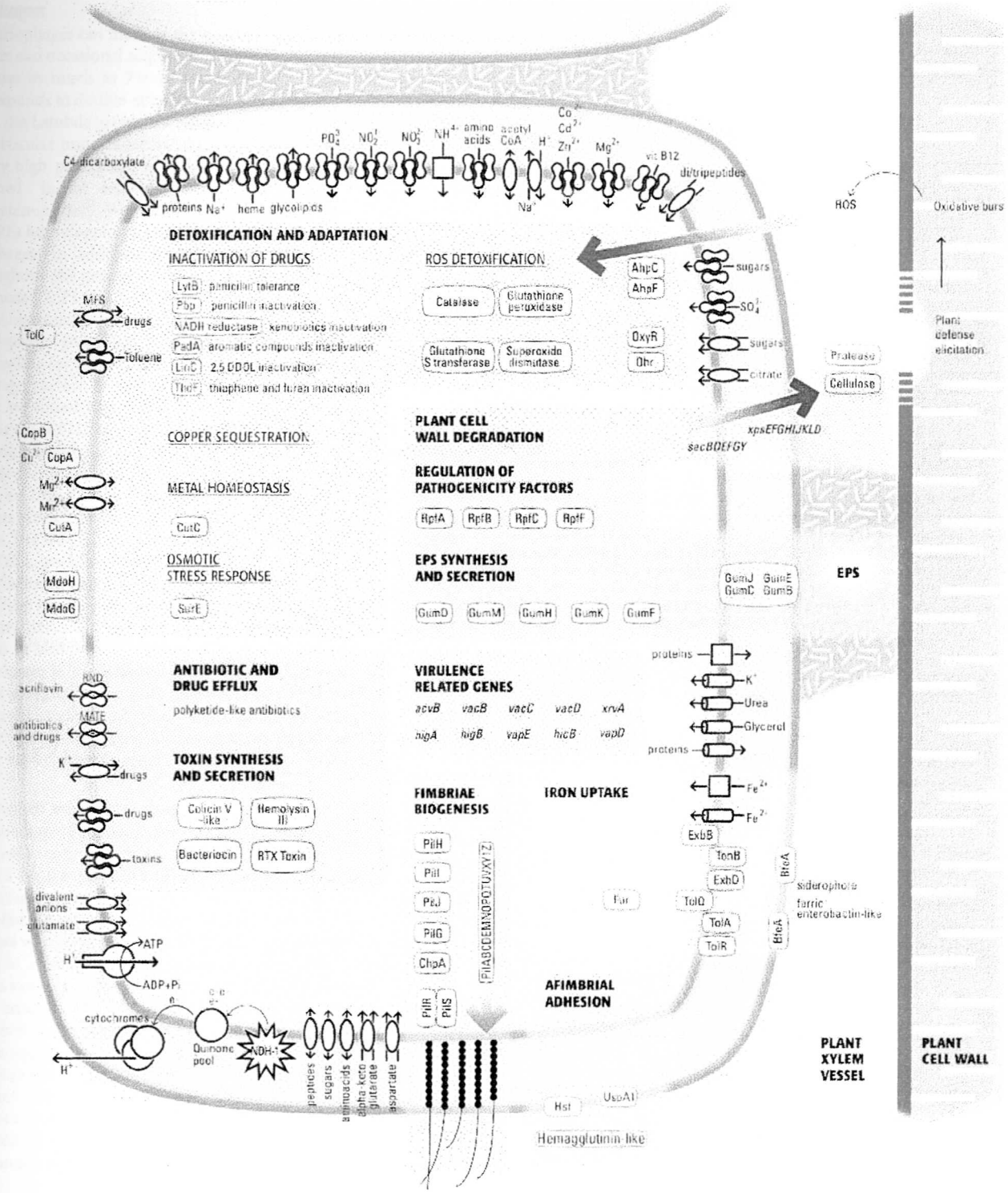

Figure 2 A comprehensive view of the biochemical processes involved in *Xylella fastidiosa* pathogenicity and survival in the host xylem. The principal functional categories are shown in bold, and the bacterial genes and gene products related to that function are arranged within the coloured section containing the bold heading. Transporters are indicated as follows: cylinders, channels; ovals, secondary carriers, including the MFS family; paired dumbbells, secondary carriers for drug extrusion; triple dumbbells, ABC transporters; bulb-like icon, F-type ATP synthase; squares, other transporters. Icons with two arrows represent symporters and antiporters (H^+ or Na^+ porters, unless noted otherwise). 2,5DDOL, 2,5-dichloro-2,5-cyclohexadiene-1,4-dol; EPS, exopolysaccharides; MATE, multi-antimicrobial extrusion family of transporters multidrug efflux gene (XF2686); MFS, major facilitator superfamily of transporters; Pbp, β-lactamase-like penicillin-binding protein (XF1621); RND, resistance-nodulation-cell division superfamily of transporters; ROS, reactive oxygen species.

include many more enzymes, which we did not find; however, some of the genes listed lie close to ORFs without significant database matches, suggesting that at least one (as yet undiscovered) polyketide pathway may be functional.

Prophages

Bacteriophages can mediate the evolution and transfer of virulence factors and occasional acquisition of new traits by the bacterial host. Because as much as 7% of the *X. fastidiosa* genome sequenced corresponds to double-stranded (ds) DNA phage sequences, mostly from the Lambda group, we suspect that this route may have been of particular importance for this bacterium. It is noteworthy that a very high percentage of phage-related sequences has also been detected in a second vascular-restricted plant pathogen, *Spiroplasma citri*[33]. We identified four regions, with a high density of ORFs homologous to phage sequences, that we considered to be prophages, in addition to isolated phage sequences dispersed throughout the genome. Two of these prophages (each ~42 kbp, designated XfP1 and XfP2) are similar to each other, lie in opposite orientations in distinct regions and appear to belong to the dsDNA, tailed-phage group. Both appear to contain most of the genes responsible for particle assembly, although we know of no reports of phage particle release from *X. fastidiosa* cultures. In prophage XfP1, we found two ORFs between tail genes V and W that are similar to ORF118 and *vapA* from the virulence-associated region of the animal pathogen *Dichelobacter nodosus*, which by homology encode a killer and a suppressor protein[34]. Interestingly, in prophage XfP2, we found two other ORFs also between tail genes V and W that are similar to hypothetical ORFs of *Ralstonia eutropha* transposon Tn4371 (ref. 35). The other two identified prophages, XfP3 and XfP4, are also similar in sequence to each other and to the *H. influenzae* cryptic prophage ϕflu (ref. 36). They both contain a 14,317-bp exact repeat. Few particle-assembly genes were found in these regions, suggesting that these prophages are defective. An ORF similar to *hicB* from *H. influenzae*, a component of the major pilus gene cluster in some isolates, was found in XfP4 (ref. 37).

The presence of virulence-associated genes from other organisms within the prophage sequences is strong evidence for a direct role for bacteriophage-mediated horizontal gene transfer in the definition of the bacterial phenotype.

Absence of avirulence genes

Phytopathogenic bacteria generally have a limited host range, often confined to members of a single species or genus. This specificity is defined by the products of the so-called avirulence (*avr*) genes present in the pathogen, which are injected directly into host cells, on infection, through a type III secretory system[38–40]. BLAST[41] searches with all known *avr* and type III secretory system sequences failed to identify genes encoding proteins with significant similarities in the genome of *X. fastidiosa*. Although the variability of *avr* genes amongst bacteria might account for this apparent lack, the high level of similarity of some components of the type III secretory system argues against this. We suspect that these genes are, in fact, not required because of the insect-mediated transmission and vascular restriction of the bacterium that obviates the necessity of host cell infection. Furthermore, if the differing host ranges of *X. fastidiosa* are molecularly defined, this may be by a quite different mechanism not involving avr proteins.

Conclusions

Before the elucidation of its complete genome sequence, very little was known of the molecular mechanisms of *X. fastidiosa* pathogenicity. Indeed, this bacterium was probably the least characterized of all organisms that have been fully sequenced. Our complete genetic analysis has determined not only the basic metabolic and replicative characteristics of the bacterium, but also a number of potential pathogenicity mechanisms. Some of these have not previously been postulated to occur in phytopathogens, providing new insights into the generality of these processes. Indeed, the availability of this first complete plant pathogen genome sequence will now allow the initiation of the detailed comparison of animal and plant pathogens at the whole-genome level. In addition, the information contained in the sequence should provide the basis for an accelerated and rational experimental dissection of the interactions between *X. fastidiosa* and its hosts that might lead to fresh insights into potential approaches to the control of CVC. □

Methods

The sequencing and analysis in this project were carried out by a network of 34 biology laboratories and one bioinformatics centre. The network is called the Organization for Nucleotide Sequencing and Analysis (ONSA)[42], and is entirely located in the state of São Paulo, Brazil.

Sequencing and assembly

The sequence was generated using a combination of ordered cosmid and shotgun strategies[43]. A cosmid library was constructed, providing roughly 15-fold genome coverage, containing 1,056 clones with average insert size of 40 kilobases (kb). High-density colony filters of the library were made, and a physical map of the genome was constructed using a strategy of hybridization without replacement[44]. A total of 113 cosmid clones was selected for sequencing on the basis of the hybridization map and end-sequence analysis. The cosmid sequences were assembled into 15 contigs covering 90% of the genome. Additionally, shotgun libraries with different insert sizes (0.8–2.0 kb and 2.0–4.5 kb) were constructed from nebulized or restricted genomic DNA cloned into plasmids, and sequenced to achieve a 3.74-fold coverage of high-quality sequence (29,140 reads). Most of the sequencing was performed with BigDye terminators on ABI Prism 377 DNA sequencers.

Cosmid and shotgun sequences were assembled into six contigs. We identified sequence gaps by linking information from forward and reverse reads, and closed either by primer walking or insert subcloning. The remaining physical gaps were closed by combinatorial PCR and by lambda clones selected from a λDash library by end-sequencing. The collinearity between the genome and the obtained sequence was confirmed by digestion of genomic DNA with *AscI*, *NotI*, *SfiI*, *SmiI* and *SrfI*, followed by comparison of the digestion pattern with the electronic digestion of the generated sequence. In addition, sequences from both ends of most cosmid clones and 236 λ clones were used to confirm the orientation and integrity of the contigs. The sequence was assembled using phred+phrap+consed[45]. All consensus bases have quality with Phred value of at least 20. There are no unexplained high quality discrepancies, each consensus base is confirmed by at least one read from each strand, and the overall error estimate is less than 1 in every 10,000 bases.

ORF prediction and annotation

ORFs were determined using glimmer 2.0 (ref. 46) and the glimmer post-processor RBSfinder (S. L. Salzberg, personal communication). A few ORFs were found by hand guided by BLAST[41] results. Annotation was carried out in a cooperative way, mostly by comparison with sequences in public databases, using BLAST[41] and tRNAscan-SE (ref. 47) and was based on the functional categories for *E. coli*[48]. Only one tmRNA was located (K. Williams, personal communication). To help annotate transport proteins, we built a custom BLAST[41] database using sequences from http://www-biology.ucsd.edu/~msaier/transport/toc.html and compared our ORFs with these sequences. Phylogenetic trees for conserved COGs[12] were built using ClustalX[49] for multiple alignment and Phylip[50]. Paralogous gene families (Table 2) were determined using BLASTX with the E-value cut-off equal to e-5 and such that at least 60% of the query sequence and at least 30% of the subject sequence were aligned.

Received 24 March; accepted 24 May 2000.

1. Rosseti, V. *et al.* Présence de bactéries dans le xylème d'orangers atteints de chlorose variégée, une nouvelle maladie des agrumes au Brésil. *C. R. Acad. Sci. Paris série III*, **310**, 345–349 (1990).
2. Chang, C. J. *et al.* Culture and serological detection of the xylem-limited bacterium causing citrus variegated chlorosis and its identification as a strain of *Xylella fastidiosa*. *Curr. Microbiol.* **27**, 137–142 (1993).
3. Roberto, S. R., Coutinho, A., De Lima, J. E. O., Miranda, V. S. & Carlos, E. F. Transmissão de *Xylella fastidiosa* pelas cigarrinhas *Dilobopterus costalimai*, *Acrogonia terminalis* e *Oncometopia facialis* em citros. *Fitopatol. Bras.* **21**, 517–518 (1996).
4. Purcell, A. H. & Hopkins, D. L. Fastidious xylem-limited bacterial plant pathogens. *Annu. Rev. Phytopathol.* **34**, 131–151 (1996).
5. Li, W. B. *et al.* A triply cloned strain of *Xylella fastidiosa* multiplies and induces symptoms of citrus variegated chlorosis in sweet orange. *Curr. Microbiol.* **39**, 106–108 (1999).
6. Ye, F., Renaudin, J., Bové, J. M. & Laigret, F. Cloning and sequencing of the replication origin (*oriC*) of the *Spiroplasma citri* chromosome and construction of autonomously replicating artificial plasmids. *Curr. Microbiol.* **29**, 23–29 (1994).
7. Francino, M. P. & Ochman, H. Strand asymmetries in DNA evolution. *Trends Genet.* **13**, 240–245 (1997).
8. Nelson, K. E. *et al.* Evidence for lateral gene transfer between Archaea and bacteria from genome sequence of *Thermotoga maritima*. *Nature* **399**, 323–329 (1999).

9. White, O. *et al.* Genome sequence of the radioresistant bacterium *Deinococcus radiodurans* R1. *Science* **286,** 1571–1577 (1999).
10. Tettelin, H. *et al.* Complete genome sequence of *Neisseria meningitidis* serogroup B strain MC58. *Science* **287,** 1809–1815 (2000).
11. Katz, M. E., Strugnell, R. A. & Rood, J. I. Molecular characterization of a genomic region associated with virulence in *Dichelobacter nodosus*. *Infect. Immun.* **60,** 4586–4592 (1992).
12. Tatusov, R. L., Galperin, M. Y., Natale, D. A. & Koonin, E. V. The COG database: a tool for genome scale analysis of protein functions and evolution. *Nucleic Acids Res.* **28,** 33–36 (2000).
13. Preston, G. M., Haubold, B. & Rainey, P. B. Bacterial genomics and adaptation to life on plants: implications for the evolution of pathogenicity and symbiosis. *Curr. Opin. Microbiol.* **1,** 589–597 (1998).
14. Knoop, V., Kloska, S. & Brennicke, A. On the identification of group II introns in nucleotide sequence data. *J. Mol. Biol.* **242,** 389–396 (1994).
15. Ferat, J. L. & Michel, F. Group II self-splicing introns in bacteria. *Nature* **364,** 358–361 (1993).
16. Blattner, F. R. *et al.* The complete genome sequence of *Escherichia coli* K-12. *Science* **277,** 1453–1474 (1997).
17. Bridges, B. A. DNA repair: Polymerases for passing lesions. *Curr. Biol.* **9,** R475–R477 (1999).
18. Brodbeck, B. V., Andersen, P. C. & Mizell, R. F. Effects of total dietary nitrogen and nitrogen form on the development of xylophagous leafhoppers. *Arch. Insect Biochem. Physiol.* **42,** 37–50 (1999).
19. Paulsen, I. T., Sliwinski, M. K. & Saier, M. H. J. Microbial genome analyses: global comparisons of transport capabilities based on phylogenies, bioenergetics and substrate specificities. *J. Mol. Biol.* **277,** 573–592 (1998).
20. Chagas, C. M., Rossetti, V. & Beretta, M. J. G. Electron-microscopy studies of a xylem-limited bacterium in sweet orange affected with citrus variegated chlorosis disease in Brazil. *J. Phytopathol.* **134,** 306–312 (1992).
21. Tang, J. L. *et al.* Genetic and molecular analysis of a cluster of *rpf* genes involved in positive regulation of synthesis of extracellular enzymes and polysaccharide in *Xanthomonas campestris* pathovar *campestris*. *Mol. Gen. Genet.* **226,** 409–417 (1991).
22. Raju, C. B. & Wells, J. M. Diseases caused by fastidious xylem-limited bacteria. *Plant Disease* **70,** 182–186 (1986).
23. Brlansky, R. H., Timmer, L. W., French, W. J. & McCoy, R. E. Colonization of the sharpshooter vectors, *Oncometopia igricans* and *Homalodisca coagulata*, by xylem-limited bacteria. *Phytopathology* **73,** 530–535 (1983).
24. Fernandez, L. A. & Berenguer, J. Secretion and assembly of regular surface structures in Gram-negative bacteria. *FEMS Microbiol. Rev.* **24,** 21–44 (2000).
25. Soto, G. E. & Hultgren, S. J. Bacterial adhesins: common themes and variations in architecture and assembly. *J. Bacteriol.* **181,** 1059–1071 (1999).
26. Geme, J. W. Molecular determinants of the interaction between *Haemophilus influenzae* and human cells. *Am. J. Respir. Crit. Care Med.* **154,** S192–S196 (1996).
27. Cope, L. D. *et al.* Characterization of the *Moraxella catarrhalis uspA1* and *uspA2* genes and their encoded products. *J. Bacteriol.* **181,** 4026–4034 (1999).
28. Henderson, I. R., Navarro-Garcia, F. & Nataro, J. P. The great escape: structure and function of the autotransporter proteins. *Trends Microbiol.* **6,** 370–378 (1998).
29. Rahme, L. G. *et al.* Common virulence factors for bacterial pathogenicity in plants and animals. *Science* **268,** 1899–1902 (1995).
30. Oresnik, I. J., Twelker, S. & Hynes, M. F. Cloning and characterization of a *Rhizobium leguminosarum* gene encoding a bacteriocin with similarities to RTX toxins. *Appl. Environ. Microbiol.* **65,** 2833–2840 (1999).
31. Lally, E. T., Hill, R. B., Kieba, I. R. & Korostoff, J. The interaction between RTX toxins and target cells. *Trends Microbiol.* **7,** 356–361 (1999).
32. Havarstein, L. S., Holo, H. & Nes, I. F. The leader peptide of colicin V shares consensus sequences with leader peptides that are common among peptide bacteriocins produced by gram-positive bacteria. *Microbiology* **140,** 2383–2389 (1994).
33. Ye, F. *et al.* A physical and genetic map of the *Spiroplasma citri* genome. *Nucleic Acids Res.* **20,** 1559–1565 (1992).
34. Billington, S. J., Johnston, J. L. & Rood, J. I. Virulence regions and virulence factors of the ovine footrot pathogen, *Dichelobacter nodosus*. *FEMS Microbiol. Lett.* **145,** 147–156 (1996).
35. Merlin, C., Springael, D. & Toussaint, A. Tn4371: A modular structure encoding a phage-like integrase, a Pseudomonas-like catabolic pathway, and RP4/Ti-like transfer functions. *Plasmid* **41,** 40–54 (1999).
36. Hendrix, R. W., Smith, M. C., Burns, R. N., Ford, M. E. & Hatfull, G. F. Evolutionary relationships among diverse bacteriophages and prophages: All the world's a phage. *Proc. Natl Acad. Sci. USA* **96,** 2192–2197 (1999).
37. Mhlanga-Mutangadura, T., Morlin, G., Smith, A. L., Eisenstark, A. & Golomb, M. Evolution of the major pilus gene cluster of *Haemophilus influenzae*. *J. Bacteriol.* **180,** 4693–4703 (1998).
38. Alfano, J. R. & Collmer, A. The type III (Hrp) secretion pathway of plant pathogenic bacteria: trafficking harpins, Avr proteins, and death. *J. Bacteriol.* **179,** 5655–5662 (1997).
39. Galan, J. E. & Collmer, A. Type III secretion machines: bacterial devices for protein delivery into host cells. *Science* **284,** 1322–1328 (1999).
40. Young, G. M., Schmiel, D. H. & Miller, V. L. A new pathway for the secretion of virulence factors by bacteria: the flagellar export apparatus functions as a protein-secretion system. *Proc. Natl Acad. Sci. USA* **96,** 6456–6461 (1999).
41. Altschul, S. F. *et al.* Gapped BLAST and PSI-BLAST: a new generation of protein database search programs. *Nucleic Acids Res.* **25,** 3389–3402 (1997).
42. Simpson, A. J. & Perez, J. F. ONSA, the São Paulo Virtual Genomics Institute. *Nature Biotechnol.* **16,** 795–796 (1998).
43. Fleischmann, R. D. *et al.* Whole-genome random sequencing and assembly of *Haemophilus influenzae* Rd. *Science* **269,** 496–512 (1995).
44. Hoheisel, J. D. *et al.* High resolution cosmid and P1 maps spanning the 14 Mb genome of the fission yeast *S. pombe*. *Cell* **73,** 109–120 (1993).
45. Gordon, D., Abajian, C. & Green, P. Consed: a graphical tool for sequence finishing. *Genome Res.* **8,** 195–202 (1998).
46. Delcher, A. L., Harmon, D., Kasif, S., White, O. & Salzberg, S. L. Improved microbial gene identification with GLIMMER. *Nucleic Acids Res.* **27,** 4636–4641 (1999).
47. Lowe, T. M. & Eddy, S. R. tRNAscan-SE: a program for improved detection of transfer RNA genes in genomic sequences. *Nucleic Acids Res.* **25,** 955–964 (1997).
48. Riley, M. Functions of the gene products of *Escherichia coli*. *Microbiol. Rev.* **57,** 862–952 (1993).
49. Thompson, J. D., Gibson, T. J., Plewniak, F., Jeanmougin, F. & Higgins, D. G. The ClustalX windows interface: flexible strategies for multiple sequence alignment aided by quality analysis tools. *Nucleic Acids Res.* **25,** 4876–4882 (1997).
50. Felsenstein, J. PHYLIP—Phylogeny Inference Package (Version 3. 2). *Cladistics* **5,** 164–166 (1989).

Supplementary information is available on *Nature*'s World-Wide Web site (http://www.nature.com), or on the author's World-Wide Web site (http://www.lbi.ic.unicamp.br/xf) or as paper copy from the London editorial office of *Nature*.

Acknowledgements

The consortium is indebted to J. F. Perez, Scientific Director of Fundação de Amparo à Pesquisa do Estado de São Paulo (FAPESP), for his strategic vision in creating and nurturing this project as well as C. A. de Pian and Juçara Parra for their administrative coordination. We thank our Steering Committee: S. Oliver, A. Goffeau, J. Sgouros, A. C. M. Paiva and J. L. Azevedo for their critical accompaniment of the work. We also thank R. Fulton and P. Minx for their timely contribution and advice. Project funding was from FAPESP, the RHAE programme of the Conselho Nacional de Desenvolvimento Científico e Tecnológico (CNPq) and Fundecitrus. For the full list of individuals who contributed to the completion of this project see (http://www.lbi. ic.unicamp.br/xf).

Correspondence and requests for materials should be addressed to J.C.S. (e-mail: setubal@ic.unicamp.br).

The sequence has been deposited in GenBank with accession numbers AE003849 (chromosome), AE003850 (pXF1.3) and AE003851 (pXF51).

Authors: A. J. G. Simpson[1], F.C. Reinach[2], P. Arruda[3], F. A. Abreu[4], M. Acencio[5], R. Alvarenga[2], L. M. C. Alves[6], J. E. Araya[7], G. S. Bala[2], C. S. Baptista[8], M. H. Barros[8], E. D. Bonaccorsi[2], S. Bordin[9], J. M. Bové[10], M. R. S. Briones[7], M. R. P. Bueno[11], A. A. Camargo[1], L. E. A. Camargo[12], D. M. Carraro[12], H. Carrer[12], N. B. Colauto[13], C. Colombo[14], F. F. Costa[9], M. C. R. Costa[15], C. M. Costa-Neto[16], L. L. Coutinho[12], M. Cristofani[17], E. Dias-Neto[1], C. Docena[2], H. El-Dorry[2], A. P. Facincani[6], A. J. S. Ferreira[2], V. C. A. Ferreira[18], J. A. Ferro[6], J. S. Fraga[4], S. C. França[19], M. C. Franco[20], M. Frohme[21], L. R. Furlan[22], M. Garnier[10], G. H. Goldman[23], M. H. S. Goldman[24], S. L. Gomes[2], A. Gruber[4], P. L. Ho[25], J. D. Hoheisel[21], M. L. Junqueira[26], E. L. Kemper[3], J. P. Kitajima[27], J. E. Krieger[26], E. E. Kuramae[28], F. Laigret[10], M. R. Lambais[12], L. C. C. Leite[25], E. G. M. Lemos[6], M. V. F. Lemos[29], S. A. Lopes[19], C. R. Lopes[13], J. A. Machado[30]†, M. A. Machado[17], A. M. B. N. Madeira[4], H. M. F. Madeira[12]†, C. L. Marino[13], M. V. Marques[8], E. A. L. Martins[25], E. M. F. Martins[18], A. Y. Matsukuma[2], C. F. M. Menck[8], E. C. Miracca[5], C. Y. Miyaki[11], C. B. Monteiro-Vitorello[12], D. H. Moon[20], M. A. Nagai[5], A. L. T. O. Nascimento[25], L. E. S. Netto[11], A. Nhani Jr[6], F. G. Nobrega[8]†, L. R. Nunes[31], M. A. Oliveira[32], M. C. de Oliveira[33], R. C. de Oliveira[31], D. A. Palmieri[13], A. Paris[13], B. R. Peixoto[2], G. A. G. Pereira[32], H. A. Pereira Jr[6], J. B. Pesquero[16], R. B. Quaggio[2], P. G. Roberto[19], V. Rodrigues[34], A. J. de M. Rosa[34], V. E. de Rosa Jr[28], R. G. de Sá[34], R. V. Santelli[2], H. E. Sawasaki[14], A. C. R. da Silva[2], A. M. da Silva[2], F. R. da Silva[3,27], W. A. Silva Jr[15], J. F. da Silveira[7], M. L. Z. Silvestri[2], W. J. Siqueira[14], A. A. de Souza[17], A. P. de Souza[3], M. F. Terenzi[23], D. Truffi[12], S. M. Tsai[20], M. H. Tsuhako[18], H. Vallada[35], M. A. Van Sluys[33], S. Verjovski-Almeida[2], A. L. Vettore[3], M. A. Zago[15], M. Zatz[11], J. Meidanis[27] & J. C. Setubal[27].

Addresses: 1, Instituto Ludwig de Pesquisa sobre o Câncer, Rua Prof. Antonio Prudente,109 - 4° andar, 01509-010, São Paulo - SP, Brazil; 2, Departamento de Bioquímica, Instituto de Química, Universidade de São Paulo, Av. Prof. Lineu Prestes, 748, 05508-900, São Paulo - SP, Brazil; 3, Centro de Biologia Molecular e Engenharia Genética, Universidade Estadual de Campinas, Caixa Postal 6010, 13083-970, Campinas - SP, Brazil; 4, Laboratório de Biologia Molecular, Departamento de Patologia, Faculdade de Medicina Veterinária e Zootecnia, Universidade de São Paulo, Av. Prof. Dr. Orlando Marques de Paiva, 87, 05508-000, São Paulo - SP, Brazil; 5, Disciplina de Oncologia, Departamento de Radiologia, Faculdade de Medicina, Universidade de São Paulo, Av. Dr. Arnaldo, 455, 01296-903, São Paulo - SP, Brazil; 6, Departamento de Tecnologia, Faculdade de Ciências Agrárias e Veterinárias de Jaboticabal, Universidade Estadual Paulista, Via

de Acesso Prof. Paulo D. Castellane s/n, Km 5, 14884-900, Jaboticabal - SP, Brazil; 7, Departamento de Microbiologia, Imunologia e Parasitologia, Escola Paulista de Medicina, Universidade Federal de São Paulo, Rua Botucatu, 862, 04023-062, São Paulo - SP, Brazil; 8, Departamento de Microbiologia, Instituto de Ciências Biomédicas, Universidade de São Paulo, Av. Prof. Lineu Prestes, 1374, 05508-900, São Paulo - SP, Brazil; 9, Hemocentro, Faculdade de Ciências Médicas, Universidade Estadual de Campinas, 13083-97, Campinas - SP, Brazil; 10, Institut National de la Recherche Agronomique et Université Victor Ségalen Bordeaux 2, 71 Avenue Edouard Bourleaux, Laboratoire de Biologie Cellulaire et Moléculaire, 33883 Vilenave d'Ornon Cedex, France; 11, Departamento de Biologia, Instituto de Biociências, Universidade de São Paulo, Rua do Matão, 277, 05508-900, São Paulo - SP, Brazil; 12, Escola Superior de Agricultura Luiz de Queiroz, Universidade de São Paulo, Av. Pádua Dias, 11, 13418-900, Piracicaba - SP, Brazil; 13, Departamento de Genética, Instituto de Biociências, Universidade Estadual Paulista, Distrito de Rubião Junior, 18618-000, Botucatu - SP, Brazil; 14, Centro de Genética, Biologia Molecular e Fitoquímica, Instituto Agronômico de Campinas, Av. Barão de Itapura, 1481, Caixa Postal 28, 13001-970, Campinas - SP, Brazil; 15, Departamento de Clínica Médica, Faculdade de Medicina de Ribeirão Preto, Universidade de São Paulo, Av. Bandeirantes, 3900, 14049-900, Ribeirão Preto - SP, Brazil; 16, Departamento de Biofísica, Escola Paulista de Medicina, Universidade Federal de São Paulo, Rua Botucatu, 862, 04023-062, São Paulo - SP, Brazil; 17, Centro de Citricultura Sylvio Moreira, Instituto Agronômico de Campinas, Caixa Postal 04, 13490-970, Cordeirópolis - SP, Brazil; 18, Laboratório de Bioquímica Fitopatológica e Laboratório de Imunologia, Instituto Biológico, Av. Cons. Rodrigues Alves, 1252, 04014-002, São Paulo - SP, Brazil; 19, Departamento de Biotecnologia de Plantas Medicinais, Universidade de Ribeirão Preto, Av. Costábile Romano, 2201, 14096-380, Ribeirão Preto - SP, Brazil; 20, Centro de Energia Nuclear na Agricultura, Universidade de São Paulo, Av. Centenário, 303, Caixa Postal 96, 13400-970, Piracicaba - SP, Brazil; 21, Funktionelle Genomanalyse, Deutsches Krebsforschungszentrum, Im Neuenheimer Feld 506, D-69120, Heidelberg, Germany; 22, Departamento de Melhoramento e Nutrição Animal, Faculdade de Medicina Veterinária e Zootecnia, Universidade Estadual Paulista, Fazenda Lageado, Caixa Postal 560, 18600-000, Botucatu - SP, Brazil; 23, Departamento de Ciências Farmacêuticas , Faculdade de Ciências Farmacêuticas de Ribeirão Preto, Universidade de São Paulo, Av. do Café s/n, 14040-903, Ribeirão Preto - SP, Brazil; 24, Departamento de Biologia, Faculdade de Filosofia, Ciências e Letras de Ribeirão Preto, Universidade de São Paulo, Av. Bandeirantes, 3900, 14040-901, Ribeirão Preto - SP, Brazil; 25, Centro de Biotecnologia, Instituto Butantan, Av. Vital Brasil, 1500, 05503-900, São Paulo - SP, Brazil; 26, Laboratório de Genética e Cardiologia Molecular/LIM 13, Instituto do Coração (InCor), Faculdade de Medicina, Universidade de São Paulo, Av. Dr. Enéas de Carvalho Aguiar, 44, 05403-000, São Paulo - SP, Brazil; 27, Instituto de Computação, Universidade Estadual de Campinas, Caixa Postal 6176, 13083-970, Campinas - SP, Brazil; 28, Departamento de Produção Vegetal, Faculdade de Ciências Agronômicas, Universidade Estadual Paulista, Fazenda Lageado, Caixa Postal 237, 18603-970, Botucatu - SP, Brazil; 29, Departamento de Biologia Aplicada à Agropecuária, Faculdade de Ciências Agrárias e Veterinárias de Jaboticabal, Universidade Estadual Paulista, Via de Acesso Prof. Paulo Donato Castellane, 14884-900, Jaboticabal - SP, Brazil; 30, Hospital do Câncer - A.C. Camargo, R. Antonio Prudente, 211, 01509-010, São Paulo - SP, Brazil; 31, Núcleo Integrado de Biotecnologia, Universidade de Mogi das Cruzes, Av. Dr. Cândido Xavier de Almeida Souza, 200, 08780-911, Mogi das Cruzes - SP, Brazil; 32, Departamento de Genética e Evolução, Instituto de Biologia, Universidade Estadual de Campinas, Caixa Postal 6010, 13083-970, Campinas - SP, Brazil; 33, Departamento de Botânica, Instituto de Biociências, Universidade de São Paulo, Rua do Matão, 277, 05508-900, São Paulo - SP, Brazil; 34, Departamento de Parasitologia, Microbiologia e Imunologia, Faculdade de Medicina de Ribeirão Preto, Universidade de São Paulo, Av. Bandeirantes, 3900, 14049-900, Ribeirão Preto - SP, Brazil; 35, Departamento de Psiquiatria, Instituto de Psiquiatria, Faculdade de Medicina, Universidade de São Paulo, Rua Dr. Ovídeo Pires de Campos s/n, Sala 4051 (3°. andar), 05403-010, São Paulo - SP, Brazil.

† *Present addresses: Novartis Seeds LTDA, Av. Prof. Vicente Rao, 90, 04706-900, São Paulo – SP, Brazil (J. A. Machado); Centro de Ciências Agrárias e Ambientais, Pontifícia Universidade Católica do Paraná, BR-376, Km 14, Caixa Postal 129, 83010-500, São José dos Pinhais – PR, Brazil (H. M. F. Madeira); Instituto de Pesquisa e Desenvolvimento, Universidade do Vale do Paraíba, Av. Shishimi Hifumi, 2911, 12244-000, São José dos Campos – SP, Brazil (F. G. Nobrega).*

O meu interesse em relação a proteína Ohr vem do fato que a deleção do seu gene em várias bactérias aumenta a sensibilidade das mesmas somente a peróxidos orgânicos mas não a H_2O_2 ou compostos que geram $O_2^{\bullet-}$ (Mongkolsuk e col, 1998; Ochsner e col, 2001). Além disso, *ohr* somente é induzido por peróxidos orgânicos como TBHP (tert-butilidroperóxido) e peróxido de cumeno. Esses dados mostram que o produto do gene *ohr* exerce uma função importante na defesa do organismo contra o estresse oxidativo induzido por peróxidos orgânicos. Análise das seqüências de proteínas da família OhrOsmC mostrou que e todas têm duas cisteínas em posições conservadas, uma das quais está presente em um motivo VCP que é característico de peroxirredoxinas tipo A (ver capítulo 2).

Dessa forma, iniciamos estudos levantando a hipótese de que a proteína Ohr é uma peroxidase dependente de tiól. O aluno de iniciação científica José Renato Rosa Cussiol construiu uma linhagem de *E.coli* que superexpressa a enzima Ohr e purificou essa proteína por cromatografia de afinidade a cauda de poli histidina. Através dos estudos apresentados no anexo 16, foi possível pela primeira vez atribuir uma função bioquímica a uma proteína da família Ohr/OsmC: Ohr é uma peroxidase dependente de tiól. Ainda neste artigo, o pós-doutorando Marcos Antonio de Oliveira construiu mutantes de Ohr (C61S e C125S) o que possibilitou mostrar que o mecanismo de ação dessa proteína. Esses estudos resultaram em uma publicação no *Journal of Biological Chemistry* (anexo 16).

THE JOURNAL OF BIOLOGICAL CHEMISTRY
© 2003 by The American Society for Biochemistry and Molecular Biology, Inc.
Vol. 278, No. 13, Issue of March 28, pp. 11570–11578, 2003
Printed in U.S.A.

Organic Hydroperoxide Resistance Gene Encodes a Thiol-dependent Peroxidase*

Received for publication, January 9, 2003
Published, JBC Papers in Press, January 22, 2003, DOI 10.1074/jbc.M300252200

José Renato Rosa Cussiol, Simone Vidigal Alves, Marco Antonio de Oliveira, and Luis Eduardo Soares Netto‡

From the Departamento de Biologia, Instituto de Biociências, Universidade de São Paulo, Rua do Matão 277, São Paulo SP Brazil 05508-900

***ohr* (organic hydroperoxide resistance gene) is present in several species of bacteria, and its deletion renders cells specifically sensitive to organic peroxides. The goal of this work was to determine the biochemical function of Ohr from *Xylella fastidiosa*. All of the Ohr homologues possess two cysteine residues, one of them located in a VCP motif, which is also present in all of the proteins from the peroxiredoxin family. Therefore, we have investigated whether Ohr possesses thiol-dependent peroxidase activity. The *ohr* gene from *X. fastidiosa* was expressed in *Escherichia coli*, and the recombinant Ohr decomposed hydroperoxides in a dithiothreitol-dependent manner. Ohr was about twenty times more efficient to remove organic hydroperoxides than to remove H_2O_2. This result is consistent with the organic hydroperoxide sensitivity of Δ*ohr* strains. The dependence of Ohr on thiol compounds was ascertained by glutamine synthetase protection assays. Approximately two thiol equivalents were consumed per peroxide removed indicating that Ohr catalyzes the following reaction: 2RSH + ROOH → RSSR + ROH + H_2O. Pretreatment of Ohr with *N*-ethyl maleimide and substitution of cysteine residues by serines inhibited this peroxidase activity indicating that both of the Ohr cysteines are important to the decomposition of peroxides. C125S still had a residual enzymatic activity indicating that Cys-61 is directly involved in peroxide removal. Monothiol compounds do not support the peroxidase activity of Ohr as well as thioredoxin from *Saccharomyces cerevisiae* and from *Spirulina*. Interestingly, dithiothreitol and dyhydrolipoic acid, which possess two sulfhydryl groups, do support the peroxidase activity of Ohr. Taken together our results unequivocally demonstrated that Ohr is a thiol-dependent peroxidase.**

The infection of both plants and animals induces a defense response that results in an oxidative burst with the increased generation of ROS[1] (1). Lipid hydroperoxides can be generated from the attack of ROS to the bacterial membrane. Organic hydroperoxides can also be formed during metabolism of certain drugs or during oxidation of n-alkanes (2). These peroxides can then react with metals or with metalloproteins leading to the production of secondary free radicals (3, 4), which may be related to the fact that organic peroxides possess bactericidal activity (5).

The alkyl hydroperoxide reductase (AhpR) is frequently considered the main enzyme responsible for the conversion of organic peroxides to the corresponding alcohols in bacteria (6, 7). This enzyme comprises two subunits, AhpF and AhpC. AhpC is a thiol-dependent peroxidase that belongs to the peroxiredoxin family (8). A cysteine residue of AhpC is oxidized to sulfenic acid (R-SOH) by peroxides. NADH reduces the sulfenic acid back to its sulfhydryl (R-SH) form in a reaction catalyzed by AhpF. AhpF is a flavo-enzyme that shares homology with thioredoxin reductase (9).

Recently a gene was isolated in *Xanthomonas campestris* pv. *phaseoli* because its deletion rendered cells highly sensitive to killing by organic peroxides but not to H_2O_2 or superoxide generators (10). Therefore, it was named *organic hydroperoxide resistance* (*ohr*) gene. *ohr* gene expression was highly induced by *t*-bOOH, weakly induced by H_2O_2, and not induced at all by superoxide (10). Recently, homologues of this gene were also characterized in other bacteria such as *Bacillus subtilis* and *Pseudomonas aeruginosa* (11, 12) among others. Interestingly, Ohr, but not AhpR, appears to play a significant role in Cu-OOH resistance in *B. subtilis* (12). In *Enterococcus faecalis*, *ohr* deletion rendered the cells more sensitive to *t*-bOOH and also to ethanol (13). Sequence analysis has shown that *ohr* homologues are widely spread among different bacteria genera, many of them pathogenic (14). Ohr also shares similarities with OsmC, which is involved in bacterial defense against osmotic stress (14).

All the Ohr and OsmC homologues have two cysteine residues located in motifs that are also very conserved. One of the cysteine residues is part of a VCP motif that is also found in peroxiredoxins. Therefore, it was postulated that Ohr could decompose peroxides directly, similarly to AhpC, a peroxiredoxin found in bacteria (14). In fact, AhpC complement *ohr* deletion in *Escherichia coli* and in *X. campestris* (10). In *P. aeruginosa*, the deletion of *ohr* rendered the cells more sensitive to organic peroxide than *ahpC* deletion, and the double mutant *ohr*, *ahpC* is more sensitive than the single mutants (11). Finally, media from mutants for Ohr contain higher levels of organic peroxides than the correspondent wild-type cells (11, 15).

Despite the suggestions that Ohr might directly detoxify organic hydroperoxides, it was not possible to rule out the possibility that Ohr is involved in other processes such as the transport of organic molecules (10) or in yet undefined signal-

* The costs of publication of this article were defrayed in part by the payment of page charges. This article must therefore be hereby marked "*advertisement*" in accordance with 18 U.S.C. Section 1734 solely to indicate this fact.

‡ To whom correspondence should be addressed. Tel.: 55-11-30917589; Fax: 55-11-30917553; E-mail: nettoles@ib.usp.br.

[1] The abbreviations used are: ROS, reactive oxygen Species; AhpC, alkyl hydroperoxide reductase, subunit C; AhpF, alkyl hydroperoxide reductase, subunit F; AhpR, alkyl hydroperoxide reductase holo-protein; DHLA, dyhydrolipoic acid; DTNB, 5,5′-dithiobis(2-nitrobenzoic acid); DTT, dithiothreitol; FOX, ferrous oxidation xylenol; NEM, *N*-ethyl maleimide; *t*-bOOH, tertbutylhydroperoxide; Cu-OOH, cumene hydroperoxide; TNB, 2-nitro-5-thiobenzoic acid.

ing pathways that lead to activation of secondary molecules that would then inactivate organic peroxides. Here, for the first time, the biochemical activity of Ohr was elucidated: Ohr from *Xylella fastidiosa* possesses a thiol-dependent peroxidase activity, which is probably responsible for the hypersensitivity of Δ*ohr* mutants to treatment with organic hydroperoxides.

MATERIALS AND METHODS

Materials—All the reagents were purchased with the highest degree of purity. DHLA was purchased in the reduced form from Sigma (T8620). DHLA is a yellow oil, and its stock solution was prepared by dilution to 50 mM concentration in 20 mM phosphate buffer, pH = 7.5 and heated at 45 °C for 30 min. DHLA concentration was ascertained by the use of the Ellman's reagent as described bellow.

Nucleic Acid Extraction, Cloning, and Nucleotide Sequencing—The *ohr* gene was PCR-amplified from the cosmid XF-07F02 that was used in the *X. fastidiosa* sequencing genome project (16). The following forward 5′-CGCGGATCCCATATGAATTCACTGGAG (Xfo1) and reverse 5′-CGCAAGCTTGGATCCTTAGTCAATCAG (Xfo2) primers were used. The underlined bases represent the *Nde*I and *Bam*HI sites, respectively. The PCR product was cloned into the pGEM-T easy vector (Promega) resulting in the pGEM/*ohr* plasmid. An *E. coli* DH5-α strain was transformed with pGEM/*ohr*, and white colonies were selected from LB-ampicillin-5-bromo-4-chloro-3-indolyl-β-D-galactopyranoside (X-gal) medium. Plasmid extraction was performed using the Rapid Plasmid Miniprep System Concert kit (Invitrogen). The plasmid PGEM/*ohr* was used to generate the two individually ohr mutant proteins, C61S and C125S, in which cysteines Cys-61 and Cys-125 were replaced by serines through PCR megaprimer methods (17, 18). In the case of the C61S construct, PCR was performed first with the mutagenic primer XfoC1 forward 5′-TTATTCTGCC**TCT**TTCATTGG-3′ and Xfo2 reverse, where the bold letters denote the mutation performed. A single band of 277 bp was eluted out from the agarose gel and used as a primer (megaprimer) along with the primer Xfo1 to the second PCR step to amplify the rest of *Ohr* gene. In the case of the C125S construct, replacement was performed in one-step PCR using the primers Xfo1 and a large terminal mutagenic primer XfoC2 5′-CGCAAGCTTGGATCCTTAGTCAATCAG-AATCAAAACGACGTCGATATTTCCACGGGTTGCATTAGAGTACG-**GAGAA**ACACGATGC-3′, where the boldface typing represents the codon mutation and the underlined bases represents the *Bam*HI restriction site. The final mutated PCR products were ligated in pGEMT easy vector to produce PGEM/*C61S* and PGEM/*C125S*, independently.

pET15b, pGEM/*ohr*, PGEM/*ohrC61S*, and PGEM/*C125S* were first digested with *Nde*I and after by *Bam*HI. The fragments generated by *NdeI*/*Bam*HI digestion of plasmids derived from pGEMs were extracted from agarose gel by the Rapid Gel Extraction Concert kit (Invitrogen) and were individually ligated to the digested pET-15b expression vector. The resulting pET15b/*ohr*, PET15b/*C61S*, and PET15b/*C125S* plasmids were sequenced in an Applied Biosystems ABI Prism 377 96 to confirm that the constructions were correct. An *E. coli* DH5-α strain was transformed with the expression vectors and cultured to increase plasmid production. Another plasmid extraction was performed, and *E. coli* Bl21(DE3) cells were transformed with the same constructs. The resulting strains were used for expression and purification of Ohr, C61S, and C125S.

Protein Expression and Purification—*E. coli* Bl21(DE3) strains transformed with pET15b/*ohr*, pET15b/*C61S*, and pET15b/*C125S* were cultured (50 ml) overnight in LB + ampicillin medium, transferred to 1 liter of fresh LB + ampicillin (100 μg/ml) medium, and cultured further until the A_{600} reached 0.6–0.8. Isopropyl-1-thio-β-D-galactopyranoside was then added to a final concentration equivalent to 1 mM. After 3 h of incubation, cells were harvested by centrifugation. The pellet was washed and suspended in the start buffer (phosphate buffer, 20 mM, pH 7.4). Seven cycles of 30 s of sonication (35% amplitude) following 30 s in ice were applied to cell suspension. The cell extracts were kept in ice during streptomycin sulfate 1% treatment for 15 min. The suspension was centrifuged at 31,500 × *g* for 30 min to remove nucleic acid precipitates. Finally cell extract was applied to a nickel affinity column (Hi-trap from Amersham Biosciences). The conditions of protein purification were optimized using the gradient procedure for imidazole concentration described by the manufacturer.

Determination of Peroxide Concentration—Peroxide concentration was determined by the ferrous oxidation xylenol (FOX) assay as previously described (3). Reactions were initiated by the addition of thiol compounds and stopped at different intervals by addition of 20 μl of HCl (1M) into 100-μl reaction mixtures. No peroxide consumption was detected in the absence of thiols. H_2O_2 concentration in stock solutions was checked by its absorbance ($\epsilon_{240\,nm}$ = 43.6 $M^{-1}\cdot cm^{-1}$).

Determination of Sulfhydryl Groups Concentration—The amount of thiol groups remaining in solution was determined by the Ellman's reagent (DTNB), using the $\epsilon_{412\,nm}$ = 13,600 $M^{-1}\cdot cm^{-1}$ for 2-nitro-5-thiobenzoic acid (TNB) (19). As described above, reactions were stopped at different intervals by addition of 20 μl of HCl (1 M) into 100-μl reaction mixtures. Samples were neutralized by dilution (1:10) in a solution containing Hepes (1 M, pH 7.4) and DTNB (5 mM). Absorbance at 412 nm was immediately recorded.

Glutamine Synthetase Protection Assay—Antioxidant activities of Ohr, OhrC61S, OhrC125S, and cTPxI were measured by their ability to protect glutamine synthetase from oxidative inactivation. Several H_2O_2-removing enzymes such as GSH peroxidase, catalase, and cTPxI can protect glutamine synthetase (20). The procedure used to determine glutamine synthetase activity was the same described by Kim *et al.* (20).

Ohr Inactivation by NEM Treatment—Recombinant Ohr (2 mg/ml) was treated with NEM (1 mM) for 1 h at room temperature and then was dialyzed against phosphate buffer (20 mM), pH 7.4. The concentration of histidine-tagged Ohr was determined using the extinction coefficient $\epsilon_{280\,nm}$ = 3960 $M^{-1}\cdot cm^{-1}$, which was determined using the software of ExPASy proteomics from Swiss Institute of bioinformatics (ca.expasy.org/tools/protparam.html).

Thrombin Proteolysis of Ohr—Histidine tag of recombinant Ohr was digested with thrombin (0.01 units/μl) using the thrombin cleavage capture kit from Novagen. The digestion was carried out for 16 h at 25 °C. The concentration of the recombinant protein without histidine tag was determined spectrophotometrically, using the same extinction coefficient $\epsilon_{280\,nm}$ = 3960 $M^{-1}\cdot cm^{-1}$ determined above because the histidine tag does not contain optically active residues.

Sulfenic Acid Formation—Determination of sulfenic acid (R-SOH) in wild-type as well as in mutant proteins was performed by the TNB anion method described by Ellis and Poole (21). In summary, TNB was prepared by incubation of an almost equimolar mixture of DTNB and DTT (1 DTNB:0.9 SH). Proteins preincubated or not with peroxides were treated with a 20-fold excess of TNB. As described before (21), TNB reacts with sulfenic acids in a 1:1 stoichiometry, generating a mixed disulfide between TNB and a cysteine residue. Excess of TNB was removed by PD-10 desalting column (Amersham Biosciences). Mixed disulfides were then treated with 10-fold excess of DTT, and the amount TNB released (which was equal to the amount sulfenic acid formed) was determined spectrophotometrically.

RESULTS

Genetic and Biochemical Analysis of Ohr—Ohr from *X. fastidiosa* possesses a very high degree of similarity with proteins from various bacteria such as *X. campestris* pv. *phaseoli* and *P. aeruginosa* (14). In general, the *ohr* gene is present in a single copy, but in some cases such as *B. subtilis*, *Mesorhizobium loti*, and *Ralstonia solanacearum* two copies of *ohr* are present (12, 22, 23). In *Streptomyces coelicolor*, three copies of ohr appear to be present (24). A blastp analysis on the *X. fastidiosa* genome using the tools available at the site aeg.lbi.ic.unicamp.br/xf/ detected only one copy of *ohr* in this bacteria located between coordinates 1,742,868 and 1,743,299 with 432 nucleotides. The predicted amino acid sequence possesses 143 residues and a molecular mass equivalent to 14.9 kDa. Among other characteristics Ohr proteins have two conserved cysteine residues that are at positions 61 and 125 in the homologue from *X. fastidiosa*. Based on sequence homology two domains of Ohr can be defined: domain 1, which contains cysteine 61 and a high number of hydrophobic residues, and domain 2, which has cysteine 125 in a VCP motif (Fig. 1*A*). The VCP motif is also present in the peroxiredoxin family, whose proteins are thiol-dependent peroxidases (25). The two proposed domains are highly conserved among Ohr homologues, especially domain 1 (14) (Fig. 1*A*). Because *ohr* deletion renders cells very sensitive to organic peroxide treatment, a hydrophobicity analysis of Ohr protein was carried out (26). Our data indicated that cysteine 61 is in a highly hydrophobic environment, whereas cysteine 125 is in a hydrophilic environment (Fig. 1*B*).

To investigate whether Ohr possesses thiol-dependent peroxidase activity, *ohr* gene from *X. fastidiosa* was expressed in

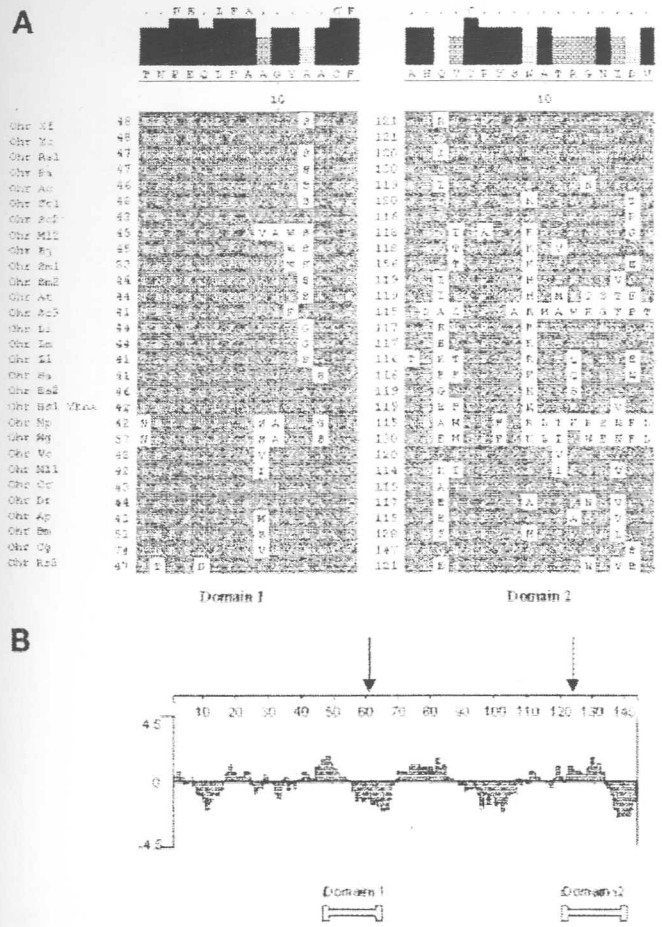

FIG. 1. **Domains of Ohr proteins that contain cysteine residues.** *A*, the sequences represented in this scheme were the consensus obtained by the Clustal W method from the MegAlign 5.01 software (DNAstar Inc.) including the Ohr proteins from: *Deinococcus radiodurans* (Ohr Dr = GI:15806857); *Caulobacter crescentus* (Ohr Cc GI: 13422184); *Mesorhizobium loti* (Ohr Ml1 = GI:14024371; Ohr Ml2 = GI:13475574); *Vibrio cholerae* (Ohr Vc = GI:15601759); *Mycoplasma genitalium* (Ohr Mg GI:1723166); *Mycoplasma pneumoniae* (Ohr Mp = GI:13508407); *B. subtilis* (Ohr Bc1or YknA = GI:16078381, Ohr Bc2 = GI:16078379); *Staphylococcus aureus* ssp. *aureus Mu50* (Ohr Sa = GI:15923818); *Lactococcus lactis* ssp. *lactis* (Ohr Ll = GI:15672574); *Listeria monocytogenes EGD-e* (Ohr Ll = GI:16804238); *Listeria innocua* (Ohr Li = GI:16801366); *S. coelicolor* (Ohr Sc1 = GI:6562797, Ohr Sc2 = GI:7546676, Ohr Sc3 = GI:9885209); *Agrobacterium tumefaciens* (Ohr At GI:15888188); *Sinorhizobium meliloti* (Ohr Sm1 = GI:16263744, Ohr Sm2 = GI:15964715); *Bradyrhizobium japonicum* (Ohr Bj = GI:8708902); *Acinetobacter calcoaceticus* (Ohr Ac = GI: 7531260); *Pseudomonas aeruginosa* (Ohr Pa = GI:15598046); *Ralstonia solanacearum* (Ohr Rs1 = GI:17549328, Ohr Rs2 = GI:17548547); *Xanthomonas campestris* pv. *phaseoli* (Ohr Xc = GI:7531169); *Xylella fastidiosa* (Ohr Xf = GI:15838425). The letters in *shade* represent residues that match the consensus. The histogram shows the strength of the residues belonging to the two domains. *B*, hydrophilicity plot according to Ref. 26. In this scheme, the amino acid sequence of Ohr from *X. fastidiosa* is displayed in the *x*-axis,whereas hydrophilicity values are displayed in the *y*-axis. According to this method, hydrophilic residues have positive values, whereas hydrophobic residues have negative values. The *arrows* show the positions of cysteines in Ohr sequence.

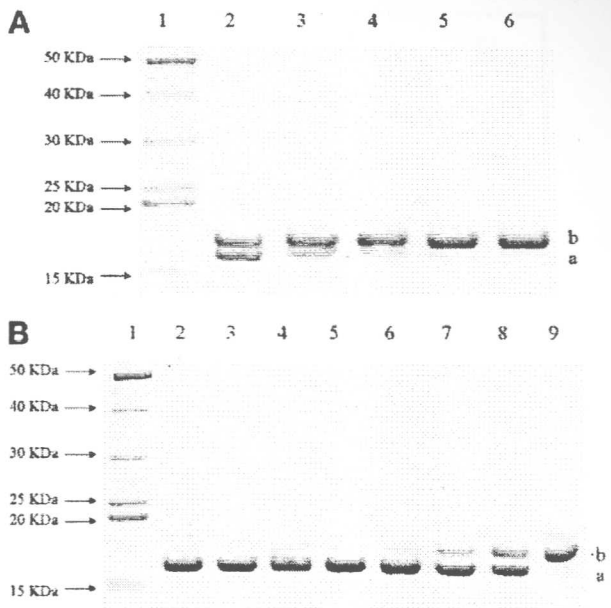

FIG. 2. **SDS-PAGE analysis of purified recombinant Ohr from *X. fastidiosa*.** Recombinant Ohr was expressed in *E. coli* and purified as described under "Material and Methods." Treatments were carried out for 1 h at room temperature. *A*, *lane 1*, molecular mass standard (BenchMark™ Protein Ladder, Invitrogen); *lane 2*, untreated Ohr; *lanes 3–6* represent Ohr treated with the following concentrations of DTT: 60 μM, 1 mM, 10 mM, and 100 mM, respectively. *B*, *lane 1*, molecular mass standard (BenchMark™ Protein Ladder, Invitrogen); *lanes 2–5* represent Ohr treated with the following concentrations of H_2O_2: 60 μM, 0.5 mM, 1 mM, and 10 mM, respectively; *lanes 6–9* represent Ohr treated with the following concentrations of *t*-bOOH: 60 μM, 0.5 mM, 1 mM, and 10 mM, respectively. Letters *a* and *b* denote the *lower* and *upper band*, respectively.

E. coli and purified by nickel affinity chromatography (see "Materials and Methods"). A histidine tag recombinant Ohr was obtained with high degree of purity as ascertained by SDS-PAGE (Fig. 2). Two bands corresponding to Ohr were observed, both of which migrate closely to 17 kDa, as expected for a monomer (Fig. 2*A*). Removal of histidine tag by thrombin proteolysis also resulted in two bands both of which migrated at ~15 kDa (data not shown). The abundance of each band was dependent on the oxidative condition to which Ohr was exposed (Fig. 2) and was independent of the presence of the histidine tag (data not shown). Bands corresponding to dimers did not appear even after treatments of Ohr with H_2O_2 or organic hydroperoxide at various concentrations (Fig. 2*B*) indicating that no disulfide bond was formed between two Ohr molecules. Since the two bands observed in Fig. 2 have approximately the monomer size, they should represent different configurations of Ohr monomers. The lower band (*band a*) should correspond to an oxidized state of Ohr, which is generated after H_2O_2 treatment or at mild concentrations of *t*-bOOH (Fig. 2*B*). On the other side, the upper band (*band b*) may represent a mixture of reduced and oxidized states of Ohr. This is because Ohr treatment with increasing concentrations of DTT provoked augment of *band b* intensity (Fig. 2*A*) as well as Ohr treatment with high organic peroxide concentrations (Fig. 2*B*). The meanings of these two bands are further discussed below, after the description of results with Ohr site-specific mutants. In any case, it is important to emphasize that different monomeric configurations were also observed before for cTPxI, a thiol-dependent peroxidase from *Saccharomyces cerevisiae* (27).

Thiol-dependent Peroxidase Activity of Ohr—Recombinant Ohr decomposed peroxides only if DTT was also present in the reaction mixture (Fig. 3). Because the substrates were present in a 350–4100-excess over the protein, it is reasonable to think that Ohr was acting catalytically. In the conditions described in Fig. 3, the specific activity of Ohr was 20.0, 17.0, and 1.3 μM/min/ng when, respectively, *t*-bOOH, Cu-OOH, and H_2O_2 were considered the substrates. This indicates that Ohr was 10–20 times more efficient in the removal of organic peroxides than in the removal of H_2O_2. These results are consistent with the high susceptibility of Δ*ohr* mutants to organic peroxides but not to H_2O_2 (Ref. 14 and references cited herein). In any case, Ohr did decompose H_2O_2 when DTT was present in the

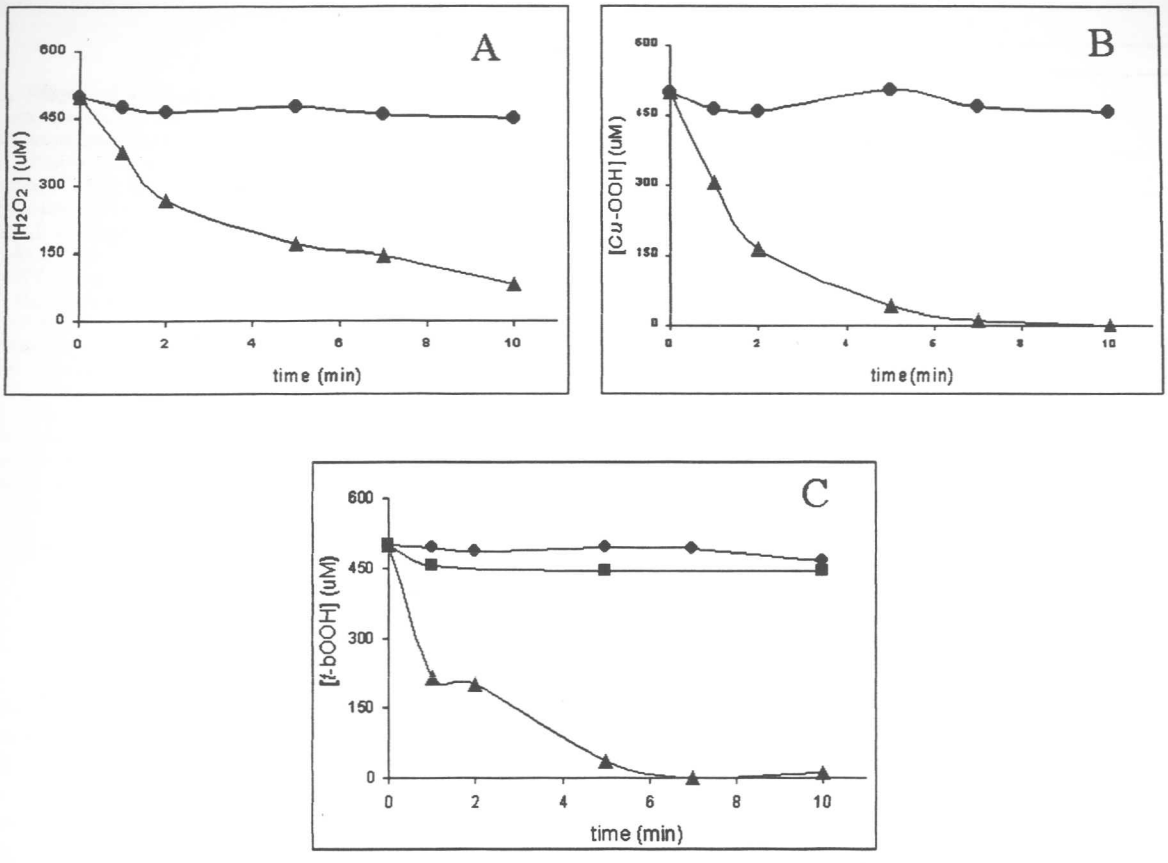

FIG. 3. **Thiol-dependent peroxidase activity of Ohr.** Peroxide concentration was determined at different periods by FOX assay as described under "Material and Methods." The reactions were carried out in Hepes buffer 50 mM, pH 7.4, in the presence of azide (1 mM) and DTPA (0.1 mM). The concentration of peroxides at time zero was 500 μM. Reactions were initiated by the addition of DTT (0.5 mM). *A* represents the kinetics of H_2O_2 decomposition in the presence of Ohr (100 ng/μl). *B* and *C* represent the kinetics of Cu-OOH and *t*-bOOH decomposition, respectively, in the presence of Ohr (10 ng/μl). ● represents the reaction mixture without Ohr (DTT + peroxide); ▲ represents the full system (DTT + peroxide + Ohr). Reaction mixtures without DTT did not show any decomposition of peroxides even in the presence of Ohr. The symbol ■ in *C* represents Ohr whose cysteine residues were previously alkylated with NEM.

reaction mixture. This ability of Ohr to decompose peroxides was dependent on the integrity of its cysteine residues because pretreatment of Ohr with NEM inhibited its peroxidase activity (Fig. 3*C*). Therefore, it is reasonable to think that Cys-61, Cys-125, or both are directly involved in the decomposition of peroxides by Ohr.

Ohr also possesses antioxidant property as demonstrated by its capacity to protect glutamine synthetase from inactivation by thiol-containing oxidative system composed of DTT/Fe^{3+}/O_2 or composed of DHLA/Fe^{3+}/O_2 (Fig. 4*A*). Probably, this protection was due to the thiol-dependent peroxidase activity of Ohr because other thiol-dependent peroxidase such as GSH peroxidase and cTPxI also protect glutamine synthetase from inactivation (20). In fact, the glutamine synthetase protection assay has been used to investigate whether proteins possess peroxide-removing activity (28, 29). Ohr did not protect glutamine synthetase against the ascorbate/Fe^{3+}/O_2 system, indicating that this protein is a thiol-specific antioxidant protein (Fig. 4*A*). The protective activity of Ohr was dependent on the concentration of protein and is comparable to the cTPxI activity (Fig. 4*B*). Removal of histidine tag by thrombin treatment did not alter the enzymatic characteristics of Ohr nor its ability to protect glutamine synthetase (data not shown).

When H_2O_2 was used as substrate, the specific activity of Ohr (Fig. 3) was similar to cTPxI (data not shown). These results are consistent with the glutamine synthetase assays (Fig. 4*B*) where these two proteins were also equally protective. The oxidative inactivation of glutamine synthetase is dependent on H_2O_2 formation by metal catalyzed oxidation systems

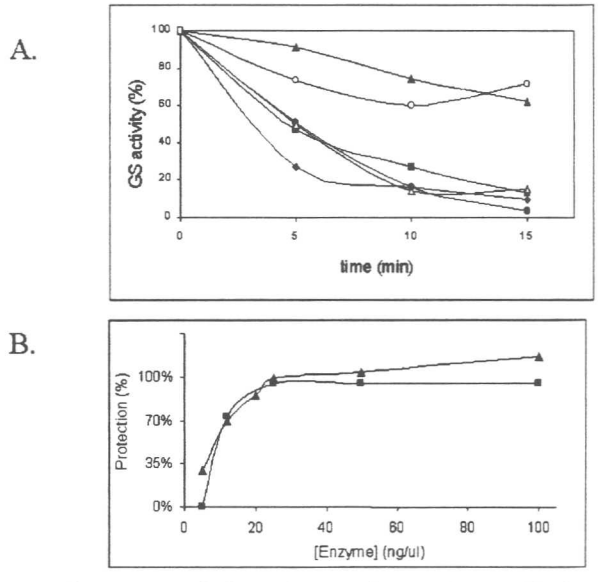

FIG. 4. **Ohr protected glutamine synthetase from oxidative inactivation.** Glutamine synthetase (*GS*) protection assay was performed as described under "Material and Methods." All reaction mixtures contain: Fe^{3+} = 1 μM; glutamine synthetase 1 mg/ml; azide = 1 mM in Hepes buffer 50 mM, pH 7.4. *A*, the symbols represent: ● (DTT 10 mM addition); ▲ (DTT 10 mM + Ohr 100 ng/μl addition); ◆ (ascorbate 10 mM addition); ■ (ascorbate 10 mM + Ohr 100 ng/μl addition); △ (DHLA 10 mM addition); ○ (DHLA 10 mM + Ohr 100 ng/μl addition). *B*, reactions were carried out for 15 min. The symbols represent: ▲ = Ohr and ■ = cTPxI at the concentrations described in the *x*-axis.

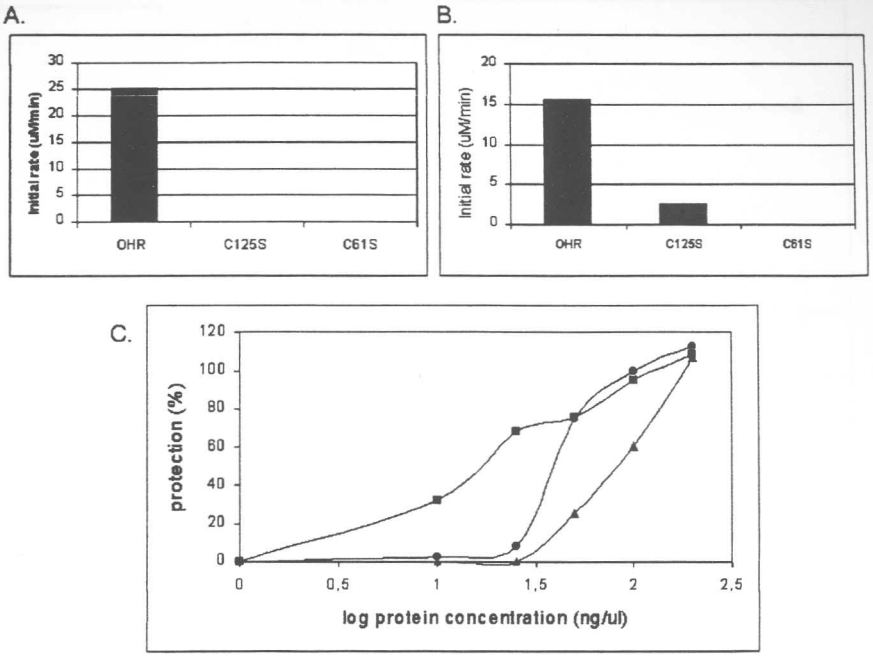

FIG. 5. **Effect of Ohr cysteine removal on peroxide decomposition and on glutamine synthetase protection.** *A*, initial rate of *t*-bOOH decomposition by Ohr, C125S, and C61S measured by the FOX assay. Protein concentrations were 2 ng/μl, and initial peroxide concentration was 200 μM. Reactions were initiated by DTT (0.5 mM) addition. *B*, initial rate of H_2O_2 decomposition by Ohr, C125S, and C61S measured by the FOX assay. Protein concentrations were 50 ng/μl, and initial peroxide concentration was 200 μM. Reactions were initiated by DTT (0.5 mM) addition. *C*, glutamine synthetase protection assay. All reaction mixtures contain: Fe^{3+} = 1 μM; glutamine synthetase 1 mg/ml; azide = 1 mM in Hepes buffer 50 mM, pH 7.4. Reactions were carried out for 30 min. The symbols represent: ■ Ohr, ● C125S, ▲ C61S.

and by its posterior conversion to hydroxyl radical through the Fenton reaction (30). Therefore protection of glutamine synthetase from inactivation probably occurs through the removal of H_2O_2 by antioxidant enzymes (31).

Analysis of Cysteine Replacements on Ohr Activity—The role of Ohr cysteines in peroxide reduction was strongly suggested since treatment of Ohr with NEM lead to protein inactivation (Fig. 3). To specifically investigate the roles of Cys-61 and Cys-125 on Ohr catalysis these two residues were individually replaced by serine generating, respectively, C61S and C125S. Initially, the capacity of the mutant proteins to decompose hydroperoxides was investigated. C61S and C125S had no detectable peroxidase activity when *t*-bOOH was used as a substrate (Fig. 5*A*). When H_2O_2 was the substrate, C125S had a residual activity, whereas C61S did not decompose any peroxide (Fig. 5*B*). These results indicated that both cysteine residues are important for catalysis. Replacement of either Cys-61 or Cys-125 also provoked great decreases in the ability of Ohr to protect glutamine synthetase from oxidative inactivation (Fig. 5*C*). C61S only showed some protective effect at very high doses, which might be attributable to nonspecific activity. Interestingly, replacement of two of the cysteines of human peroxiredoxin V (prx V), which forms a stable intramolecular disulfide intermediate during its catalytic cycle, produced similar effects (32). Therefore, the results described in Fig. 5 represented an initial suggestion that an intramolecular disulfide is also a reaction intermediate of wild-type Ohr. Further evidences are presented below.

The migration of Ohr mutants was also analyzed by SDS-PAGE (Fig. 6) under both reducing and non-reducing conditions to understand the meaning of the two monomeric bands observed in Fig. 2. As standards for mutant proteins, wild-type Ohr was treated with peroxides (60 μM) and with DTT (100 mM), which provoked the appearance of the monomeric lower (*band a*) and upper band (*band b*) respectively. Interestingly, neither C61S nor C125S, in any condition tested, migrated at the same position that the wild-type protein treated with peroxides (60 μM) (*band a*) (Fig. 6). Therefore, *band a* observed for the wild-type protein (Fig. 2) should represent an intramolecular intermediate since any of the mutants can form an intramolecular disulfide bond. This was expected since an intramolecular disulfide bond should lead to a more compact

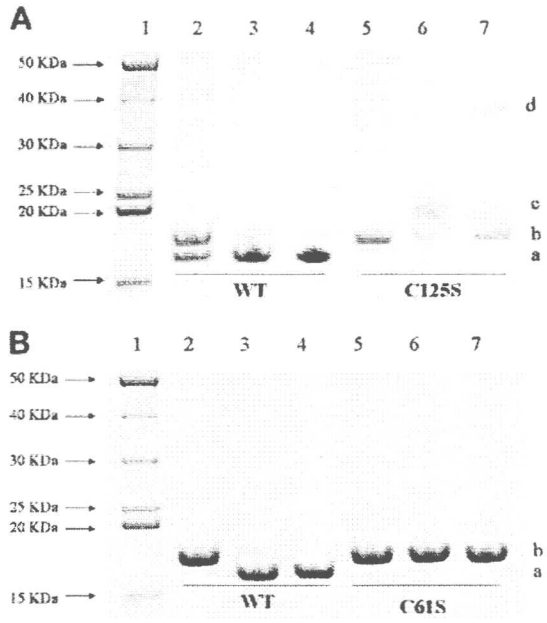

FIG. 6. **Migration of mutant proteins in SDS-PAGE.** Treatments were carried out for 1 h. *A*, *lane 1*, molecular mass standard (BenchMark™ Protein Ladder, Invitrogen); *lanes 2–4* represent wild-type Ohr treated with DTT (100 mM), *t*-bOOH (60 μM) and H_2O_2 (60 μM), respectively; *lanes 5–7* represent C125S treated with DTT (100 mM), *t*-bOOH (60 μM), and H_2O_2 (60 μM), respectively; *B*, *lane 1*, molecular mass standard (BenchMark™ Protein Ladder, Invitrogen); *lanes 2–4* represent wild-type Ohr treated with DTT (100 mM), *t*-bOOH (60 μM), and H_2O_2 (60 μM), respectively; *lanes 5–7* represent C61S treated with DTT (100 mM), *t*-bOOH (60 μM), and H_2O_2 (60 μM), respectively. Letters *a*, *b*, *c*, and *d* refer to the bands described under "Results."

protein configuration that would migrate faster than the other REDOX states.

Interestingly, two other bands, named *c* and *d*, could also be observed in C125S exposed to oxidative conditions (Fig. 6*A*). Band *d* was detected in non-treated C125S (data not shown) as well as in C125S submitted to mild oxidative conditions (Fig. 6*A*, *lane 7*). Under stronger oxidative conditions, *band c* became predominant and *band d* disappeared (Fig. 6*A*, *lane 6* and data not shown). Sometimes a band of ~30 kDa was observed in

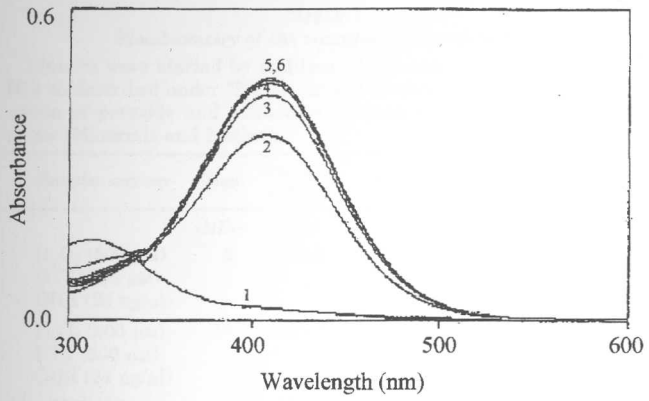

FIG. 7. **Sulfenic acid formation in C125S.** Sulfenic acid in C125S was measured by its reaction with TNB. C125S (100 μM) with no pretreatment was incubated with TNB (4 mM) for 15 min at room temperature. A mixed disulfide C125S-TNB was prepared as described under "Material and Methods." Release of TNB from the mixed disulfide was recorded after 1, 3, 5, 10, and 30 min after addition of 10-fold excess of DTT, which corresponds to the spectra 2–6. Spectrum 1 corresponds to the mixed disulfide before DTT addition.

substitution of *band c* after C125S treatment with organic peroxides (data not shown). The meaning of *band c* is unknown and could be attributed to proteolysis or to generation of cross-links in the dimer.

Since *band d* should correspond to a dimer of two C125S proteins bound through their Cys-61, it appears that this sulfhydryl group is relatively reactive toward peroxides. As expected for a dimer exposed to reducing condition, when C125S was treated with DTT in denaturing conditions, only a monomeric band (*band b*) was detected (Fig. 6*A*, *lane 5*).

On the contrary, C61S migrated preferentially as a monomer (Fig. 6*B*). Only after treatment of cells with very high peroxide concentrations could a dimer be observed (data not shown), indicating that Cys-125 is not very oxidizable by peroxides.

The possible formation of stable sulfenic acid intermediates (R-SOH) in Ohr, C125S, and C61S was also analyzed. Using the compound TNB, we could only clearly detect sulfenic acid intermediates in C125S protein (Fig. 7). This result further indicated that Cys-61 but not Cys-125 is very reactive.

Thiol Substrate Specificity—The possibility that other thiol compounds besides DTT support the peroxidase activity of Ohr was also analyzed. No decomposition of *t*-bOOH by Ohr was detected when DTT was replaced by monothiols such as GSH, 2-mercaptoethanol (Fig. 8*A*), and cysteine (data not shown). It is important to note that even when GSH was added at a concentration 10-fold higher than DTT no peroxidase activity could be observed (Fig. 8*A*). Therefore, Ohr does not possess GSH peroxidase activity.

To check if thioredoxin could be the biological substrate for Ohr, thioredoxin was added to the reaction mixture containing DTT, *t*-bOOH, and Ohr. In the case of cTPxI, addition of thioredoxin to the reaction mixture increased the specific activity of this protein (28). The addition of thioredoxin from *Spirulina* or from *S. cerevisiae* did not increase significantly the ability of Ohr to decompose *t*-bOOH, taking into account the decomposition of peroxides by thioredoxin itself (Fig. 8*B*). The peroxidase activity of Ohr may be specific for thioredoxin from *X. fastidiosa*. Alternatively, other thiol compound than thioredoxin can be the reducing agent of Ohr.

Interestingly, Ohr was also capable of decomposing peroxides (Fig. 8*A*) and protecting glutamine synthetase from inactivation (Fig. 4*A*) if DHLA was present in the reaction mixture. Like DTT, DHLA is also a dithiol compound. Enzymes required for DHLA biosynthesis are present in *X. fastidiosa* (XF1269, XF1270) in an operon configuration indicating that this thiol

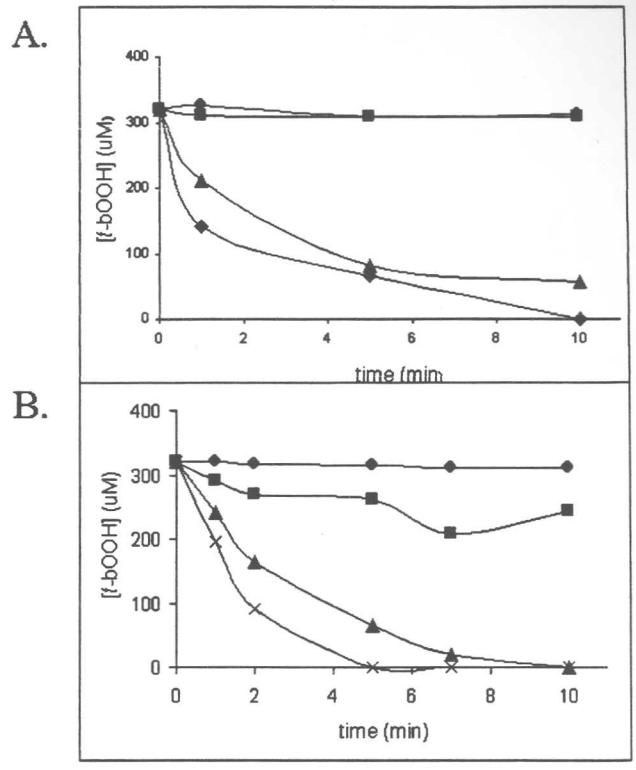

FIG. 8. **Thiol specificity of the Ohr peroxidase activity.** *t*-bOOH concentration was determined by the FOX assay as described under "Material and Methods." Reactions were initiated by addition of thiol compounds and terminated by addition of 20 μl of HCl (1 M) into 100-μl reaction mixtures. Reactions were carried out in Hepes buffer 50 mM, pH 7.4 in the presence of azide (1 mM) and DTPA (0.1 mM). *A*, symbols represent the reactions with the following thiol compounds: ● (GSH = 5 mM), ■ (2-mercaptoethanol = 10 mM), ▲ (DTT = 0.5 mM), and ◆ (DHLA = 0.5 mM). *B*, the symbols represent: ● (no further addition); ■ (thioredoxin 80 ng/μl); ▲ (Ohr 5 ng/μl); and X (thioredoxin + Ohr).

compound should be present in this bacteria. The possibility that DHLA is the *in vivo* reducing power of Ohr is discussed below.

Because the ability of Ohr to decompose peroxides is dependent on the presence of DTT, the stoichiometry of the reaction catalyzed by this protein was investigated as described before for cTPxI (31). The data described in Table I indicated that the ratio of thiol consumption per peroxide consumption is around 2, which is consistent with the same reaction catalyzed by proteins belonging to the peroxiredoxin family: 2RSH + ROOH $\rightarrow$ RSSR + ROH − H_2O. Therefore, Ohr is a thiol-dependent peroxidase.

DISCUSSION

The present report attribute for the first time a biochemical function for a protein belonging to the Ohr/OsmC family. Taken together, our results demonstrate unequivocally that Ohr from *X. fastidiosa* possesses thiol-dependent peroxidase activity. This biochemical activity is consistent with the increased sensitivity to organic peroxides observed for several bacterial species in which this gene is deleted (10–13, 15).

Ohr possesses a very high specific activity for organic peroxides in comparison with peroxiredoxins. In our hands, the specific activity of Ohr is approximately 10–20 times higher than the specific activity of cTPxI when organic peroxides were used as substrates (data not shown). AhpC is the other thiol-dependent peroxidase present in *X. fastidiosa* and in several other bacteria. AhpC belongs to the peroxiredoxin family like cTPxI, and therefore they are expected to behave similarly. Results showing that mutation of *ohr* renders cells more sen-

TABLE I
Stoichiometry of the reaction catalyzed by Ohr

Kinetics were started by addition of peroxide and were stopped by HCl as described under "Materials and Methods." Assays for determination of peroxide and sulfhydryl concentrations are also described under "Materials and Methods."

Reaction mixture	Time	Peroxide removed	-SH consumed	-SH/peroxide ratio
	(MIN)	*(μM)*	*(μM)*	
H_2O_2 (500 μM) DTT (500 μM) OHR (24 ng/μl)	5	283.6	547.2	1.93
H_2O_2 (500 μM) DTT (500 μM) OHR (24 ng/μl)	10	382.4	756	1.98
t-BHP (500 μM) DTT (500 μM) OHR (2 ng/μl)	5	435.4	799.2	1.83
t-BHP (500 μM) DTT (500 μM) OHR (2 ng/μl)	10	465.9	892.8	1.91

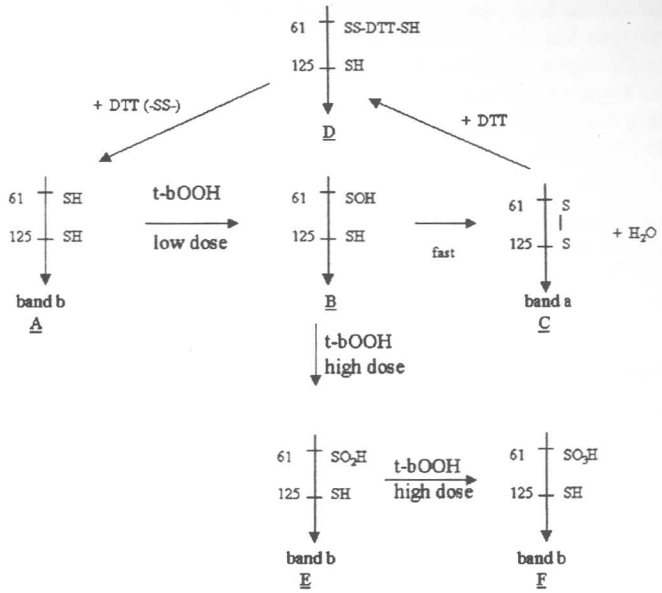

FIG. 9. **Proposed scheme for the enzymatic mechanism of Ohr.** The reduced form of Ohr (*A*) can react with peroxides leading to the formation of Cys-61-SOH intermediate (*B*), which can then be rapidly converted to an intramolecular disulfide intermediate after reaction with Cys-125 (*C*). The intramolecular disulfide can be reduced back to (*A*) by DTT or DHLA. In the presence of high amounts of organic peroxides, Cys-61-SOH can be further oxidized to Cys-61-SO_2H (*E*) or Cys-61-SO_3H (*F*), which co-migrates with the reduced form of Ohr in the position corresponding to the *band b* in the gels of Figs. 2 and 6.

sitive to organic peroxide killing than *ahpC* deletion (11, 12) lead us to speculate that this probably occurs because Ohr has higher specific activity toward organic peroxides than peroxiredoxins, but this suggestion awaits experimental confirmation.

The relationship between Ohr and AhpCF proteins has been studied in other bacteria. AhpC acts in concert with AhpF (a thioredoxin reductase homologue) to reduce peroxides to the corresponding alcohols at the expense of NADH (9). It is well known that the expression of *ahpC* and *ahpF* are regulated by OxyR, a transcriptional regulator that is activated by H_2O_2 (33). This should also occur in *X. fastidiosa* because *ahpC*, *ahpF*, and *oxyR* genes are contiguous and therefore probably belong to the same operon (aeg.lbi.ic.unicamp.br/xf/). On the other hand, the expression of *ohr* genes in *B. subtilis* and *X. campestris* are not regulated by OxyR but by OhrR (12, 34). OhrR is a member of the MarR family of transcriptional repressors. No OhrR homologue was found in a search through the site of *X. fastidiosa* genome suggesting that *ohr* is regulated by a different mechanism in this microorganism.

X. fastidiosa contains several peroxide-removing enzymes as analyzed by the bioinformatic tools available at aeg.lbi.ic.unicamp.br/xf/and using the sequencing data generated by the genome project supported by FAPESP (16). Besides *ahpC* (XF1530), two other genes codify for proteins that contain AhpC/TSA domains as defined by the pFAM analysis. Additionally, one catalase and one GSH peroxidase homologue are also present. Each one of these peroxide-removing enzymes may utilize different substrates or may act during specific stress conditions.

Ohr is also capable of decomposing H_2O_2 although with a lower efficiency compared with the removal of organic peroxides (Fig. 3). Probably Ohr does not play an important role in the defense of *X. fastidiosa* against this oxidant. In other related bacteria, Δ*ohr* mutants are not hypersensitive to H_2O_2 (10, 11, 15). Moreover, in *X. campestris* pv. *phaseoli* and in *B. subtilis* *ohr* expression is not regulated by OxyR, which is activated by H_2O_2 (12, 34). Catalases appear to be the primary defense of *Xanthomonas* against exogenous H_2O_2 (35, 36). *X. fastidiosa* possesses at least one catalase (XF2232), similar to HPI, (katG) from *E. coli*, which is OxyR-regulated (33) and should be a key component of the antioxidant defense against exogenous H_2O_2. On the other side, several studies indicate that AhpR should be an important component in the removal of H_2O_2 endogenously generated in bacteria (37–39).

The reduction of peroxides by Ohr requires at least one of its cysteine residues because NEM pretreatment abolishes its peroxidase activity (Fig. 3*C*). Ohr has two cysteine residues that are present in all of its homologues (Fig. 1*A*) and therefore potentially could be involved in peroxide reduction. Substitution of Cys-61 or Cys-125 by serine dramatically reduces the ability of Ohr to decompose peroxides (Fig. 5), indicating that both cysteine residues are important for the catalytic activity. However, it is important to note that C125S, but not C61S, still has a residual peroxidase activity, suggesting an essential role for Cys-61. In fact, Cys-61, but not Cys 125, was easily oxidized by any of the peroxides (Fig. 6), and it appears that Cys-61 is directly involved on peroxide reduction, whereas Cys-125 is the resolving cysteine. Our data fit very well in the scheme described in Fig. 9. At low concentrations of organic peroxides, Cys-61 could be oxidized to sulfenic acid, which should be rapidly converted to the intramolecular disulfide intermediate (electrophoretic *band a*). In support with this model, we could only detect sulfenic acid intermediate in C125S protein (Fig. 7). Cys-61-SOH should be more stable in C125S than in wild-type Ohr because the mutant protein lacks Cys-125 to react with Cys-61-SOH. At high levels of organic peroxides, sulfenic acid of Cys-61 should react first with another peroxide molecule and not with Cys-125 sulfhydryl group, leading to the formation of a cysteine sulfinic acid (R-SO_2H). Further reaction of Cys-61-SO_2H with another organic peroxide molecule can provoke the formation of Cys-61 sulfonic acid (R-SO_3H). Both Cys-61-SO_2H and Cys-61-SO_3H should correspond to the electrophoretic *band b* observed in Fig. 2 when Ohr was exposed to high concentrations of organic peroxides.

Disulfide intermediates are stable compounds among other factors because they can not be overoxidized as sulfenic acids can be (40). Therefore is tempting to speculate that Cys-125 prevents Ohr inactivation by avoiding Cys-61 overoxidation to sulfinic or sulfonic acids. It is well described that overoxidation of peroxiredoxin provoked their inactivation (41). In the case of the mutant protein C125S, in addition to overoxidation of Cys-61, dimer formation (Fig. 6*A*) could represent another pathway of protein oxidation.

Band b was never observed when Ohr was treated with H_2O_2 (Fig. 2), indicating that this peroxide has lower capacity than organic peroxides to overoxidize Cys-61 to sulfinic or sulfonic acids. In fact, H_2O_2 had lower ability than organic peroxides to induce dimer formation in the mutant protein C125S (data not shown). Cys-61 is located in a very hydrophobic environment (Fig. 1*B*), which is probably ideal to accommodate an organic peroxide but not H_2O_2. This hypothesis would explain the higher specific activity of Ohr toward organic peroxides in comparison with H_2O_2 (Fig. 3).

The biological-reducing substrate of Ohr is still unknown. GSH should be present in *X. fastidiosa* because this bacteria contains homologues for the two genes (*gsh1* and *gsh2*) involved in its biosynthesis (aeg.lbi.ic.unicamp.br/xf/). However, this thiol was not capable of reducing peroxides in the presence of Ohr, even when it was present in a concentration ten times higher than DTT concentration (Fig. 8*A*). Thioredoxin from neither *Spirulina* (data not shown) nor from *S. cerevisiae* (Fig. 8*B*) increased the rate of peroxide removal by Ohr. We can not exclude, however, the possibility that thioredoxin or glutaredoxin systems of *X. fastidiosa* specifically reduces Ohr.

In addition to DTT, DHLA supported the peroxidase activity of Ohr (Figs. 4*A* and 8*A*). Therefore, Ohr utilized only dithiols, but not monothiols, as substrate. Dithiols such as DTT and DHLA have very negative redox potentials, which indicate that these compounds have very high reducing power. The redox potentials for dithiols are in the range from -0.31 to -0.33, whereas for monothiols such as GSH and cysteine the redox potentials are in the range of -0.24 to -0.25 (42). Probably the intramolecular disulfide bond of Ohr is very stable, and only very strong reducing agents are able to convert them to the reduced form. Another possibility is related to possible structural constrains of the Ohr active site. According to our results, the active site of this protein is very hydrophobic and may not be capable of accommodating two monothiols but can interact with only one dithiol molecule. This is because in the case of dithiols only one molecule would be enough to reduce Ohr back to the dithiol configuration according to Reaction 1.

$$Ohr(-SS-)+R\text{-}(SH)_2 \rightarrow Ohr-[Cys\text{-}61]\text{-}SSR\text{-}SH \rightarrow Ohr-(SH)_2+RSSR$$

REACTION 1

In the case of monothiols, two molecules would be required to fully reduce Ohr. First, a mixed disulfide between Ohr and the monothiol would be generated (Reaction 2), which would then be reduced to the Ohr dithiol configuration by other monothiol molecule and the release of a disulfide compound (Reaction 3).

$$Ohr(-SS-)+R\text{-}SH \rightarrow Ohr-SSR$$

REACTION 2

$$Ohr-SSR+R\text{-}SH \rightarrow Ohr-SH-RSSR$$

REACTION 3

The possibility that DHLA is the biological substrate of Ohr is supported by the fact that its biosynthetic pathway is present in *X. fastidiosa* (XF 1269,XF1270). Interestingly, Bryk *et al.* (43) characterized a peroxidase system dependent on lipoic acid in *Mycobacterium tuberculosis*. Bryk *et al.* (43) demonstrated that lipoic acid utilized came from a thiol linked through an amide linkage dihydrolipoamide succinyltransferase, a component of α-ketoacid oxidases, and was reduced by NADH in a reaction catalyzed by dihydrolipoamide dehydrogenase. Both dihydrolipoamide succinyltransferase (XF1549) and dihydrolipoamide dehydrogenase (XF1548) enzymes are also present in *X. fastidiosa* (aeg.lbi.ic.unicamp.br/xf/). Several reducing systems from *X. fastidiosa* are in the process to be expressed to find the reducing substrate of Ohr. In any case, our data suggest that Ohr may be a dihydrolipoic acid peroxidase.

Contrary to peroxiredoxins, GSH peroxidase, and catalases, Ohr belongs to a family of proteins that are present only in bacteria, most of them pathogenic to plants or mammals. Thus Ohr may be promising as a target for drug development in agriculture and medicine, considering the fact that plant and mammal defenses against pathogens involves generation of oxidative burst (1).

Acknowledgments—We thank Gisele Monteiro for revising the manuscript and Fundação de Amparo à Pesquisa do Estado de São Paulo (FAPESP) and Pró-Reitoria de Pesquisa da Universidade de São Paulo for financial support.

REFERENCES

1. Tenhaken, R., Levine, A., Brisson, L. F., Dixon, R. A., and Lamb, C. (1995) *Proc. Natl. Acad. Sci. U. S. A.* **92,** 4158–4163
2. Maeng, J. H., Sakai, Y., Tani, Y., and Kato, N. (1996) *J. Bacteriol.* **178,** 3695–3700
3. Jiang, Z-Y., Hunt, J. V., and Wolff, S. P. (1992) *Anal. Biochem.*, **202,** 384–389
4. Barr, D. P., and Mason, R. P. (1995) *J. Biol. Chem.* **270,** 12709–12716
5. Akaike, T., Sato, K., Ijiri, S., Miyamoto, Y., Kohno, M., Ando, M., Maeda, H. (1992) *Arch. Biochem. Biophys.* **294,** 55–63
6. Bsat, N., Chen, L., and Helmann, J. D. (1996) *J. Bacteriol.* **178,** 6579–6586
7. Jacobson, F. S., Morgan, R. W., Christman, M. F., and Ames, B. N. (1989) *J. Biol. Chem.* **264,** 1488–1496
8. Chae, H. Z., Robison, K. Poole, L. B. Church, G., Storz, G., and Rhee, S. G. (1994) *Proc. Natl. Acad. Sci.* **91,** 7017–7021
9. Poole, L. B., and Ellis, H. R. (1996) *Biochemistry* **35,** 56–64
10. Mongkolsuk, S., Praituan, W., Loprasert, S., Fuangthong, M., Chamnongpol, S. (1998) *J. Bacteriol.* **180,** 2636–2643
11. Ochsner, U. A., Hassett, D. J., and Vasil, M. L. (2001) *J. Bacteriol.* **183,** 773–778
12. Fuangthong, M., Atichartpongkul, S., Mongkolsuk, S., and Helmann, J. D. (2001) *J. Bacteriol.* **183,** 4134–4141
13. Rince, A., Giard, J. C., Pichereau, V., Flahaut, S., and Auffray, Y. (2001) *J. Bacteriol.* **183,** 1482–1488
14. Atichartpongkul, S., Loprasert, S., Vattanaviboon, P., Whangsuk, W., Helmann, J. D., and Mongkolsuk, S. (2001) *Microbiology* **147,** 1775–1782
15. Shea, R. J., and Mulks, M. H. (2002) *Infect. Immun.* **70,** 794–802
16. Simpson, A. J. G., Reinach, F. C., Arruda, P., Abreu, F. A., Acencio, M., Alvarenga, R., Alves, L. M., Araya, J. E., Baia, G. S., Baptista, C. S., Barros, M. H., Bonaccorsi, E. D., Bordin, S., Bove, J. M., Briones, M. R., Bueno, M. R., Camargo, A. A., Camargo, L. E., Carraro, D. M., Carrer, H., Colauto, N. B., Colombo, C., Costa, F. F., Costa, M. C., Costa-Neto, C. M., Coutinho, L. L., Cristofani, M., Dias-Neto, E., Docena, C., El-Dorry, H., Facincani, A. P., Ferreira, A. J., Ferreira, V. C., Ferro, J. A., Fraga, J. S., Franca, S. C., Franco, M. C., Frohme, M., Furlan, L. R., Garnier, M, Goldman, G. H., Goldman, M. H., Gomes, S. L., Gruber, A., Ho, P. L., Hoheisel, J. D., Junqueira, M. L., Kemper, E. L., Kitajima, J. P., Krieger, J. E., Kuramae, E. E., Laigret, F., Lambais, M. R., Leite, L. C. C., Lemos, E. G., Lemos, M. V., Lopes, S. A., Lopes, C. R., Machado, J. A., Machado, M. A., Madeira, A. M., Madeira, H. M., Marino, C. L., Marques, M. V., Martins, E. A., Martins, E. M., Matsukuma, A. Y., Menck, C. F., Miracca, E. C., Miyaki, C. Y., Monteiro-Vitorello, C. B., Moon, D. H., Nagai, M. A., Nascimento, A. L., Netto, L. E. S., Nhani, A., Jr., Nobrega, F. G., Nunes, L. R., Oliveira, M. A. de Oliveira, M. C., de Oliveira, R. C., Palmieri, D. A., Paris, A., Peixoto, B. R., Pereira, G. A. G., Pereira, H. A., Jr., Pesquero, J. B., Quaggio, R. B., Roberto, P. G., Rodrigues, V., de M. Rosa, A. J., de Rosa, V. E., Jr., de Sa, R. G., Santelli, R. V., Sawasaki, H. E., da Silva, A. C., da Silva, A. M., da Silva, F. R., da Silva, W. A., Jr., da Silveira, J. F., Silvestri, M. L., Siqueira, W. J., de Souza, A. A., de Souza, A. P., Terenzi, M. F., Truffi, D., Tsai, S. M., Tsuhako, M. H., Vallada, H., Van Sluys, M. A., Verjovski-Almeida, S., Vettore, A. L., Zago, M. A., Zatz, M., Meidanis, J., Setubal, J. C. (2000) *Nature* **406,** 151–159
17. Sarkar, G., Sommer, S. S. (1990) *BioTechniques* **4,** 404–407
18. Datta, A. K. (1995) *Nucleic Acids Res.* **21,** 4530–4531
19. Riddles, P. W., Robert, L. B., and Zerner, B. (1983) *Methods Enzymol.* **91,** 49–60
20. Kim, K., Kim, I. H., Lee, Ki-Y., Rhee, S. G., and Stadtman, E. R. (1988) *J. Biol. Chem.* **263,** 4704–4711
21. Ellis, H. R., and Poole, L. B. (1997) *Biochemistry* **36,** 13349–13356
22. Kaneko, T., Nakamura, Y., Sato, S., Asamizu, E., Kato, T., Sasamoto, S., Watanabe, A., Idesawa, K., Ishikawa, A., Kawashima, K., Kimura, T., Kishida, Y., Kiyokawa, C., Kohara, M., Matsumoto, M., Matsuno, A., Mochizuki, Y., Nakayama, S., Nakazaki, N., Shimpo, S., Sugimoto, M., Takeuchi, C., Yamada, M., and Tabata, S. (2000) *DNA Res.* **7,** 331–338
23. Salanoubat, M., Genin, S., Artiguenave, F., Gouzy, J., Mangenot, S., Arlat, M., Billault, A., Brottier, P., Camus, J. C., Cattolico, L., Chandler, M., Choisne, N., Claudel-Renard, C., Cunnac, S., Demange, N., Gaspin, C., Lavie, M., Moisan, A., Robert, C., Saurin, W., Schiex, T., Siguier, P., Thebault, P., Whalen, M., Wincker, P., Levy, M., Weissenbach, J., and Boucher, C. A. (2002) *Nature* **415,** 497–502
24. Redenbach, M., Kieser, H. M., Denapaite, D., Eichner, A., Cullum, J., Kinashi, H., and Hopwood, D. A. (1996) *Mol. Microbiol.* **21,** 77–96
25. Rhee, S. G., Kang, S. W., Netto, L. E. S., Seo, M. S., and Stadtman, E. R. (1999) *Biofactors* **10,** 207–209
26. Kyte, J., and Doolittle, R. F. (1982) *J. Mol. Biol.* **157,** 105–132
27. Chae, H. Z., Uhm, T. B., and Rhee, S. G. (1994) *Proc. Natl. Acad. Sci. (U. S. A.)* **91,** 7022–7026

28. Lee, S. P., Hwang, Y. S., Kim, Y. J., Kwon, K. S., Kim, H. J., Kim, K., and Chae, H. Z. (2001) *J. Biol. Chem.* **276,** 29826–29832
29. Yamashita, H., Avraham, S., Jiang, S., London, R., Van Veldhoven, P. P., Subramani, S., Rogers, R. A., Avraham, H. (1999) *J. Biol. Chem.* **274,** 29897–29904
30. Stadtman, E. R. (1990) *Free Rad. Biol. Med.*, **9,** 315–325
31. Netto, L. E. S., Chae, H. Z., Kang, S. W., Rhee, S. G., and Stadtman, E. R. (1996) *J. Biol. Chem.* **271,** 15315–15321
32. Seo, M. S., Kang, S. W., Kim, K., Baines, I. C., Lee, T. H., and Rhee, S. G. (2000) *J. Biol. Chem.* **275,** 20346–20354
33. Storz, G., and Imlay, J. A. (1999) *Curr. Opin. Microbiol.* **2,** 188–194
34. Sukchawalit, R., Loprasert, S., Atichartpongkul, S., and Mongkolsuk, S. (2001) *J. Bacteriol.* **183,** 4405–4412
35. Sriprang, R., Vattanaviboon, P., and Mongkolsuk, S. (2000) *Appl. Environ. Microbiol.* **66,** 4017–4021
36. Vattanaviboon, P., and Mongkolsulk, S. (2000) *Gene* **241,** 259–265
37. Mongkolsuk, S., Whangsuk, W., Vattanaviboon, V., Loprasert, S., and Fuangthong, M. (2000) *J. Bacteriol.* **182,** 2636–2643
38. Ochsner, U. A., Vasil, M. L., Alsabbagh, E., Parvatiyar, K., and Hassett, D. J. (2000) *J. Bacteriol.* **182,** 4533–4544
39. Seaver, L. C., and Imlay, J. A. (2001) *J. Bacteriol.* **183,** 7173–7181
40. Radi, R., Beckman, J. S., Bush, K. M., and Freeman, B. A. (1991) *J. Biol. Chem.* **266,** 4244–4250
41. Yang, K. S., Kang, S. W., Woo, H. A., Hwang, S. C., Chae, H. Z., Kim, K., and Rhee, S. G. (2002) *J. Biol. Chem.* **277,** 38029–38036
42. Lees, W. J., and Whitesides, G. M. (1993) *J. Org. Chem.* **251,** 642–647
43. Bryk, R., Lima, C. D., Erdjument-Bromage, H., Tempst, P., and Nathan, C. (2002) *Science* **295,** 1073–1077

Os nossos estudos sobre o mecanismo de ação de Ohr mostraram ainda que a cisteína peroxidásica (Cys-S_p) dessa proteína está no motivo $AC_{61}F$ e não no motivo $VC_{125}P$ como postulado anteriormente (anexo 16). A cisteína do motivo $VC_{125}P$ atuaria como uma "resolving cysteine" (Cys-S_p) ao atacar o acido sulfênico presente na Cys 61, originado um dissulfeto intramolecular. Dessa forma, o mecanismo de catálise de Ohr seria similar ao das peroxirredoxinas atípicas (figura 3C – capítulo 2). Outra peculiaridade de Ohr é o fato dessa enzima somente utilizar ditióis e não monotióis como substrato redutor (anexo 16). Todavia, Ohr tem outras características similares às peroxirredoxinas: tem atividade peroxidásica dependente de tiól e independente de heme e tem um tiolato no sítio ativo (Cys 61 no caso de Ohr de *Xylella fastidiosa*).

Dessa forma, analisei se a seqüência primária de amino ácidos de Ohr apresentava alguma similaridade com alguma das cinco classes de peroxirredoxinas. Inicialmente fiz alguns alinhamentos utilizando a ferramenta Blast P (http://www.ncbi.nlm.nih.gov/BLAST/Blast.cgi) e somente proteínas da família OsmC/Ohr apresentaram similaridade significativa com Ohr de *Xylella fastidiosa*. Posteriormente, utilizei a ferramenta "BLAST 2 SEQUENCES" (http://www.ncbi.nlm.nih.gov/blast/bl2seq/) que alinha duas seqüências de cada vez. Analisando Ohr contra peroxirredoxinas de todos os tipos, não foi possível encontrar similaridade significativa (dados não mostrados). Finalmente, tentei alinhar Ohr com várias peroxirredoxinas utilizando a ferramenta clustal W do software MegAling 5.01 e neste caso poucos amino acidos apresentaram similaridade, sendo que as cisteínas peroxidásicas (Cys_p) não foram alinhadas pelo referido algorítimo. Finalmente, para tentar mais uma vez verificar se Ohr poderia ter alguns daqueles quatro amino ácidos presentes em todas as peroxirredoxinas (figura 4-capítulo 2), alinhei manualmente as cisteínas peroxidásicas de Ohr e AhpC de *Xylella fastidiosa*, após resultado obtido pelo Clustal W. Fazendo outros alinhamentos manuais pelo software MegAling 5.01, consegui que no máximo três dos quatro resíduos conservados em todas as peroxirredoxinas fossem alinhados entre essas duas proteínas (figura 5).

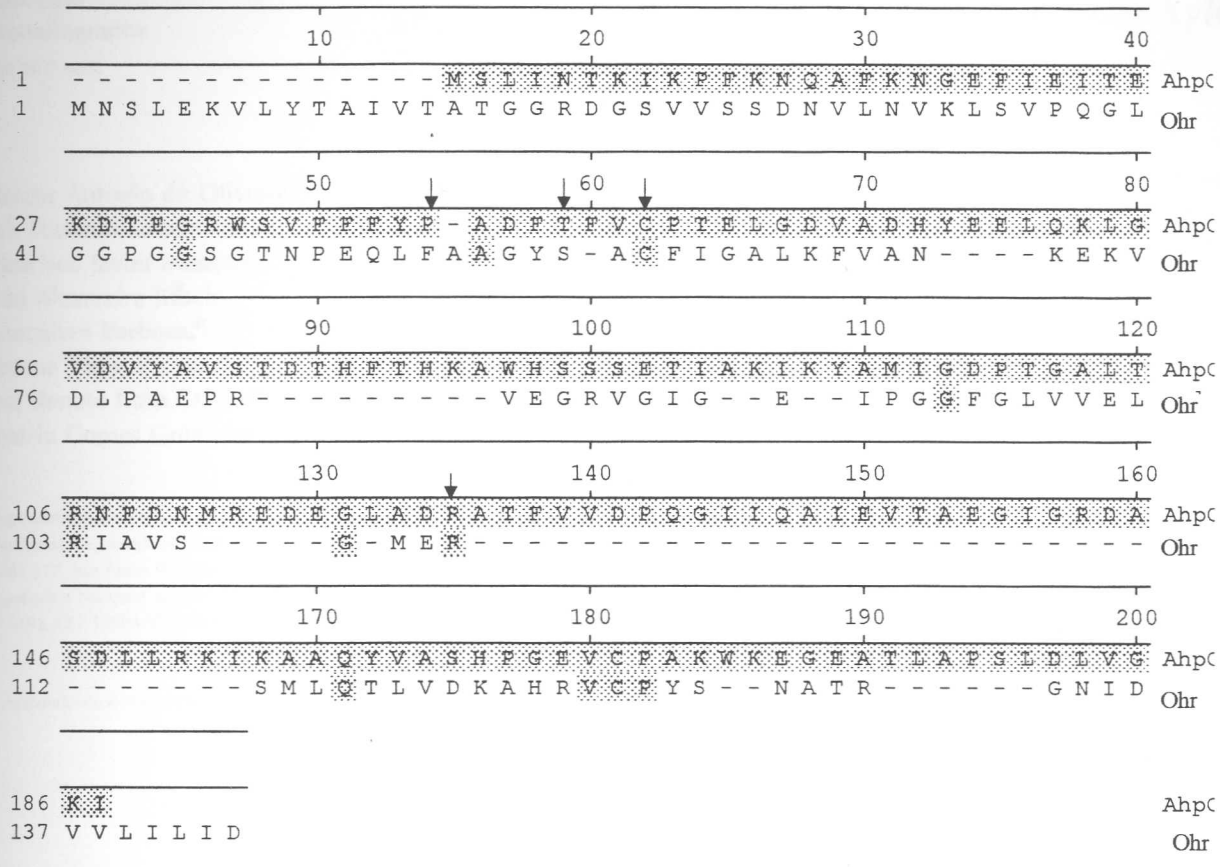

Figura 5 – **Alinhamento Ohr e AhpC de *Xylella fastidiosa*.** As setas indicam os quatro resíduos que são conservados em todas as peroxirredoxinas descritas. Desses quatro resíduos, somente não foi possível alinhar a prolina 40 de AhpC com uma prolina de Ohr.

Analisando os resultados descritos acima em conjunto, parece que Ohr não pode ser considerado uma peroxirredoxina devido à baixa similaridade e a algumas características funcionais (Ohr não aceita monotióis como substrato como peroxirredoxinas). Como todas peroxirredoxinas com estruturas resolvidas até o momento tem um domínio denominado "thioredoxin fold" (Wood e col., 2003a) , seria interessante verificar se Ohr também teria essa característica estrutural. Dessa forma, em colaboração com a equipe de cristalógrafos do Centro de Biologia Molecular Estrutural (Laboratório Nacional de Luz Sincronton-LNLS) tentamos obter cristais de Ohr de *Xylella fastidiosa*. Como Ohr apresenta diversas configurações oxidadas e reduzidas que apresentam diferentes migrações em SDS-PAGE (anexo 16), resolvemos realizar ensaios de cristalizações com proteínas que foram previamente tratadas com diversos agentes redutores e oxidantes, de forma a ter preparações mais homogeneas. Em proteínas tratadas com TBHP (10mM) obtivemos cristais hexagonais que difrataram a luz sincronton com alta resolução (1,8 Å),(anexo 17).

Acta Crystallographica Section D
Biological Crystallography
ISSN 0907-4449

Crystallization and preliminary X-ray diffraction analysis of an oxidized state of Ohr from *Xylella fastidiosa*

Marcos Antonio de Oliveira,[a] Luis Eduardo Soares Netto,[a] Francisco Javier Medrano,[b] João Alexandre Ribeiro Gonçalves Barbosa,[b] Simone Vidigal Alves,[a] José Renato Rosa Cussiol[a] and Beatriz Gomes Guimarães[b]*

[a]Departamento de Biologia, Instituto de Biociências, Universidade de São Paulo, Rua do Matão 277, São Paulo SP, Brazil, and [b]Laboratório Nacional de Luz Síncrotron, CP 6192, CEP 13084-971, Campinas SP, Brazil

Correspondence e-mail: beatriz@lnls.br

Received 30 September 2003
Accepted 21 November 2003

Xylella fastidiosa organic hydroperoxide-resistance protein (Ohr) is a dithiol-dependent peroxidase that is widely conserved in several pathogenic bacteria with high affinity for organic hydroperoxides. The protein was crystallized using the hanging-drop vapour-diffusion method in the presence of PEG 4000 as precipitant after treatment with organic peroxide (*t*-butyl hydroperoxide). X-ray diffraction data were collected to a maximum resolution of 1.8 Å using a synchrotron-radiation source. The crystal belongs to the hexagonal space group $P6_522$, with unit-cell parameters $a = b = 87.66$, $c = 160.28$ Å. The crystal structure was solved by molecular-replacement methods. The enzyme has a homodimeric quaternary structure similar to that observed for its homologue from *Pseudomonas aeruginosa*, but differs from the previous structure as the active-site residue Cys61 is oxidized. Structure refinement is in progress.

1. Introduction

An increase in reactive oxygen species (ROS) is an important component of the defence response against microbial infection in plants and animals. ROS can cause damage to macromolecules such as DNA, lipids and proteins (Akaike *et al.*, 1992; Tenhaken *et al.*, 1995). This host response has led bacteria to evolve several complex mechanisms to detoxify ROS such as hydrogen peroxide (H_2O_2), superoxide anion radicals ($O_2^{-\cdot}$) and organic hydroperoxides (OHPs). The cellular enzymatic defences for detoxification of free radicals and H_2O_2 are well characterized and several structures of proteins involved in this mechanism have been solved. However, the structures of bacterial proteins involved in OHP metabolism are comparatively poorly characterized. Alkyl hydroperoxide reductase (AhpR) is frequently considered to be the main protein in OHP metabolism (Wood *et al.*, 2002). This enzyme has the ability to convert OHPs into their respective alcohols at the expense of NADH or NADPH. AhpR consists of two subunits: the reductase subunit F (AhpF) and the catalytic subunit C (AhpC) (Poole & Ellis, 1996; Poole, 1996). AhpC is a thiol-dependent peroxidase that belongs to a large family of peroxidases named peroxiredoxins (Chae *et al.*, 1994). Mongkolsuk *et al.* (1998) characterized a novel gene in the phytopathogen *Xanthomonas campestris* pv. *phaseoli* involved in OHP detoxification, denominated *ohr* (organic hydroperoxide resistance). The deletion of this gene in *X. campestris* rendered the mutants highly sensitive to OHPs but not to other oxidants. Additionally, the expression of *ohr* was highly induced by OHPs, but was not induced by a superoxide generator and was only weakly induced by H_2O_2. Recently, it was observed that organic hydroperoxide-resistance protein (Ohr) but not AhpR seemed to play a significant role in OHP resistance in *Bacillus subtilis* (Fuangthong *et al.*, 2001) and that *ohr* overexpression in an *Escherichia coli ahpC-ahpF* double mutant caused it to revert to the hypersensitive to OHPs phenotype (Mongkolsuk *et al.*, 1998).

At present, several proteins similar to Ohr have been characterized in other organisms. Ohr belongs to a family of proteins that are present only in bacteria, most of which are pathogenic to plants or animals (Ochsner *et al.*, 2001; Fuangthong *et al.*, 2001; Rince *et al.*, 2001; Cussiol *et al.*, 2003).

Analysis of Ohr-protein sequences from several bacteria showed that all homologues possess two conserved cysteine residues located in domains that show different characteristics in their amino-acid composition (Cussiol *et al.*, 2003). The C-terminal cysteine (Cys125 in *X. fastidiosa*) is located among several hydrophilic residues and is part of a Val-Cys-Pro motif which is also present in all proteins of the peroxiredoxin family (Mongkolsuk *et al.*, 1998; Cussiol *et al.*, 2003). On the other side, the cysteine residue located at the N-terminus (Cys61 in *X. fastidiosa*) is surrounded by several hydrophobic residues and is inserted into a new motif: Ala-Cys-Phe.

DOI: 10.1107/S0907444903026799

Acta Crystallographica Section D
Biological Crystallography
ISSN 0907-4449

Crystallization and preliminary X-ray diffraction analysis of an oxidized state of Ohr from *Xylella fastidiosa*

Marcos Antonio de Oliveira,[a] Luis Eduardo Soares Netto,[a] Francisco Javier Medrano,[b] João Alexandre Ribeiro Gonçalves Barbosa,[b] Simone Vidigal Alves,[a] José Renato Rosa Cussiol[a] and Beatriz Gomes Guimarães[b]*

[a]Departamento de Biologia, Instituto de Biociências, Universidade de São Paulo, Rua do Matão 277, São Paulo SP, Brazil, and [b]Laboratório Nacional de Luz Síncrotron, CP 6192, CEP 13084-971, Campinas SP, Brazil

Correspondence e-mail: beatriz@lnls.br

Received 30 September 2003
Accepted 21 November 2003

Xylella fastidiosa organic hydroperoxide-resistance protein (Ohr) is a dithiol-dependent peroxidase that is widely conserved in several pathogenic bacteria with high affinity for organic hydroperoxides. The protein was crystallized using the hanging-drop vapour-diffusion method in the presence of PEG 4000 as precipitant after treatment with organic peroxide (*t*-butyl hydroperoxide). X-ray diffraction data were collected to a maximum resolution of 1.8 Å using a synchrotron-radiation source. The crystal belongs to the hexagonal space group $P6_522$, with unit-cell parameters $a = b = 87.66$, $c = 160.28$ Å. The crystal structure was solved by molecular-replacement methods. The enzyme has a homodimeric quaternary structure similar to that observed for its homologue from *Pseudomonas aeruginosa*, but differs from the previous structure as the active-site residue Cys61 is oxidized. Structure refinement is in progress.

1. Introduction

An increase in reactive oxygen species (ROS) is an important component of the defence response against microbial infection in plants and animals. ROS can cause damage to macromolecules such as DNA, lipids and proteins (Akaike *et al.*, 1992; Tenhaken *et al.*, 1995). This host response has led bacteria to evolve several complex mechanisms to detoxify ROS such as hydrogen peroxide (H_2O_2), superoxide anion radicals ($O_2^{-\cdot}$) and organic hydroperoxides (OHPs). The cellular enzymatic defences for detoxification of free radicals and H_2O_2 are well characterized and several structures of proteins involved in this mechanism have been solved. However, the structures of bacterial proteins involved in OHP metabolism are comparatively poorly characterized. Alkyl hydroperoxide reductase (AhpR) is frequently considered to be the main protein in OHP metabolism (Wood *et al.*, 2002). This enzyme has the ability to convert OHPs into their respective alcohols at the expense of NADH or NADPH. AhpR consists of two subunits: the reductase subunit F (AhpF) and the catalytic subunit C (AhpC) (Poole & Ellis, 1996; Poole, 1996). AhpC is a thiol-dependent peroxidase that belongs to a large family of peroxidases named peroxiredoxins (Chae *et al.*, 1994). Mongkolsuk *et al.* (1998) characterized a novel gene in the phytopathogen *Xanthomonas campestris* pv. *phaseoli* involved in OHP detoxification, denominated *ohr* (organic hydroperoxide resistance). The deletion of this gene in *X. campestris* rendered the mutants highly sensitive to OHPs but not to other oxidants. Additionally, the expression of *ohr* was highly induced by OHPs, but was not induced by a superoxide generator and was only weakly induced by H_2O_2. Recently, it was observed that organic hydroperoxide-resistance protein (Ohr) but not AhpR seemed to play a significant role in OHP resistance in *Bacillus subtilis* (Fuangthong *et al.*, 2001) and that *ohr* overexpression in an *Escherichia coli ahpC-ahpF* double mutant caused it to revert to the hypersensitive to OHPs phenotype (Mongkolsuk *et al.*, 1998).

At present, several proteins similar to Ohr have been characterized in other organisms. Ohr belongs to a family of proteins that are present only in bacteria, most of which are pathogenic to plants or animals (Ochsner *et al.*, 2001; Fuangthong *et al.*, 2001; Rince *et al.*, 2001; Cussiol *et al.*, 2003).

Analysis of Ohr-protein sequences from several bacteria showed that all homologues possess two conserved cysteine residues located in domains that show different characteristics in their amino-acid composition (Cussiol *et al.*, 2003). The C-terminal cysteine (Cys125 in *X. fastidiosa*) is located among several hydrophilic residues and is part of a Val-Cys-Pro motif which is also present in all proteins of the peroxiredoxin family (Mongkolsuk *et al.*, 1998; Cussiol *et al.*, 2003). On the other side, the cysteine residue located at the N-terminus (Cys61 in *X. fastidiosa*) is surrounded by several hydrophobic residues and is inserted into a new motif: Ala-Cys-Phe.

DOI: 10.1107/S0907444903026799

Both cysteines are essential for the peroxidase activity of Ohr (Lesniak *et al.*, 2002; Cussiol *et al.*, 2003).

Recently, the X-ray structure of homodimeric Ohr from *P. aeruginosa* with a novel α/β fold was reported (Lesniak *et al.*, 2002). The Ohr structure contains two active-site pockets on opposite sides of the dimer. The two conserved cysteines (Cys60 and Cys124) in each active site come from the same monomer and the distance between the S atoms is 3.6 Å. The entrances to the pockets are rich in hydrophobic side chains, which may be related to the high specificity of Ohr towards OHPs. Cys124 is located at the bottom of the cavity, while the side chain of Cys60 is solvent-exposed. The three-dimensional structure of *P. aeruginosa* Ohr was solved using crystals grown in the presence of dithiothreitol (DTT) and the electron-density maps showed a DTT molecule bound to each active site near Cys60. The N^{ε} atom of Arg18 makes a hydrogen bond to a DTT O atom. Arg18 is highly conserved among Ohr proteins and has been shown to play a role in catalysis, since its replacement by glutamine led to a significant decrease in OHP reduction (Lesniak *et al.*, 2002).

X. fastidiosa is the causative agent of a number of economically important crop and citrus diseases and possesses an Ohr protein (Simpson *et al.*, 2000). Two-dimensional gel-electrophoresis/mass-spectrometry analysis revealed that Ohr is highly abundant in whole cell extract and in the extracellular fraction (Smolka *et al.*, 2003), indicating an important role in pathogen resistance to host defences. Ohr from *X. fasdidiosa* is a thiol-dependent peroxidase and catalyzes the following reaction: $2RSH + ROOH \rightarrow RSSR + ROH + H_2O$ (Cussiol *et al.*, 2003). The enzyme is able to decompose hydroperoxides and is about 10–20 times more efficient in the removal of organic hydroperoxide than of hydrogen peroxide. Additionally, Ohr only decomposes peroxides in the presence of dithiols such as DTT. No decomposition of peroxides is detected when DTT was replaced by monothiols such as GSH, 2-mercaptoethanol or cysteine (Cussiol *et al.*, 2003).

We report here the crystallization and preliminary X-ray analysis of Ohr from *X. fastidiosa* in an oxidized state. The structure was solved by molecular-replacement methods and structure refinement is in progress. The analysis of the Ohr structure in the oxidized state should provide insights into the enzymatic mechanism of this protein and may provide reasons for the higher efficiency of this protein towards organic hydroperoxides as well as towards dithiol compounds.

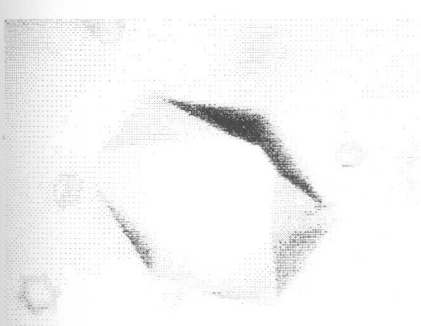

Figure 1
Crystal of Ohr from *X. fastidiosa*.

2. Methods

2.1. Cloning

The 432 base-pair *ohr* gene (NP_299113.1) was amplified by PCR from the cosmid XF-07F02 used in the *X. fastidiosa* genome-sequencing project (Simpson *et al.*, 2000) and cloned in the pET15b vector (Novagen) using *Nde*I–*Bam*HI restriction sites. The resulting pET15b/*ohr* was sequenced in an Applied Biosystems ABI Prism 377 96 to confirm that the construction was correct.

2.2. Expression and purification

Escherichia coli BL21 (DE3) strain harbouring pET15b/*ohr* plasmid was grown (50 ml) overnight in LB medium containing 100 μg ml^{-1} ampicillin at 310 K and transferred to 1 l of fresh LB/amp medium and cultured further at 310 K until the OD_{600} reached 0.6–0.8. Expression was induced with 1 m*M* of IPTG and the cells were harvested after 4 h of incubation at 310 K. The cell pellet was resuspended in starting buffer (20 m*M* sodium phosphate buffer pH 7.4). Seven cycles of 30 s sonication followed by 30 s on ice were applied to the cell suspension. The cell extract was kept on ice during treatment with 1% streptomycin sulfate for 15 min. The suspension was centrifuged at 31 500*g* for 30 min to remove nucleic acid precipitate. Finally, the cell extract was applied to a nickel-affinity column and purified with an imidazole gradient as described by the manufacturer (Hi-trap column; Amersham-Pharmacia Biotech). We obtained ~50 mg of pure protein from 1 l of cell culture. The purity of the protein was confirmed by SDS–PAGE and the peroxidase activity was measured using the FOX method (Wolf, 1994). The purified protein was concentrated to 10 mg ml^{-1} in 5 m*M* Tris–HCl pH 7.5.

2.3. Crystallization

After treatment with 10 m*M* *t*-butyl hydroperoxide (*t*-BOOH) at 310 K for 1 h, the samples were used in crystallization trials by the hanging-drop vapour-diffusion method. Initial screening was performed at 293 K using Crystal Screen and Crystal Screen II from Hampton Research, mixing equal volumes (2 μl) of protein solution (10 mg ml^{-1} in 5 m*M* Tris–HCl) and reservoir solution. Several conditions were refined and the optimal conditions were obtained with the reservoir solution consisting of 25% PEG 4000 and 0.1 *M* Tris–HCl pH 8.7. The crystals reached dimensions of 0.25 × 0.25 × 0.05 mm after two weeks (Fig. 1).

2.4. Data collection and processing

A crystal cryoprotected with 20% glycerol was cooled to 110 K and X-ray diffraction data were collected using synchrotron radiation at the protein crystallography beamline D03B-CPR at the Laboratório Nacional de Luz Síncrotron (LNLS), Campinas, Brazil. The wavelength was set to 1.453 Å and a MAR CCD detector was used to record the oscillation data with $\Delta\varphi = 1.0°$. The data set was processed using the programs *MOSFLM* (Leslie, 1992) and *SCALA* (Kabsch, 1988; Blessing, 1995) from the *CCP*4 package (Collaborative Computational Project, Number 4, 1994).

3. Results and discussion

Ohr crystallization trials using protein without OHP treatment resulted in crystals of poor diffraction quality. In previous work, Cussiol *et al.* (2003) showed the existence of two bands of purified protein on SDS–PAGE and that the amount of each band was dependent on the redox state of Ohr. We found that pre-treatment of Ohr with 10 m*M* *t*-BOOH resulted in the formation of several crystal forms of high quality. *t*-BOOH treatment was chosen because this experimental condition converts Ohr to a highly homogenous oxidized state (Cussiol *et al.*, 2003). These data and those obtained by Lesniak *et al.* (2002) suggest that treatment of Ohr with reductants or oxidants is important in order to maintain the protein in a homogeneous state suitable for crystallization procedures. The crystals studied here were obtained from protein exposed to a large excess of peroxide. Therefore, we expect that after treatment with 10 m*M* *t*-BOOH, Ohr will be in a highly oxidized state, probably as the sulfinic acid (R-SO_2) or sulfonic acid (R-SO_3).

The best crystal diffracted to 1.8 Å resolution and belonged to space group $P6_522$, with unit-cell parameters $a = b = 87.66$, $c = 160.28$ Å. Table 1 summarizes the data-collection statistics.

The protein structure was solved by molecular-replacement methods with the program *AMoRe* (Navaza, 2001) from the *CCP*4 package using the atomic coordinates of *P. aeruginosa* Ohr (Lesniak *et al.*, 2002) as the search model (PDB code 1n2f; 58% sequence identity). The solution shows one dimer in the asymmetric unit, in agreement with the Matthews coefficient calculation (Matthews, 1968), giving $V_M = 2.8$ Å^3 Da^{-1} and a solvent content of 55.4%. Initial rigid-body refinement was carried out using *AMoRe*, yielding an *R* factor of 0.470. Model completion and refinement are currently in progress.

The *X. fastidosa* Ohr tertiary and quaternary structures are similar to those observed for its counterpart from *P. aeruginosa*, but differ in the redox state of the N-terminal active-site residue. In our case the N-terminal cysteine (Cys61) is oxidized, while in the previous structure of *P. aeruginosa* the corresponding residue (Cys60) is in a reduced state. We expect that the structure of *X. fastidiosa* Ohr will assist in understanding the catalytic mechanism concerning the high specificity for OHPs and dithiol compounds in this important protein family.

Table 1
Data-collection statistics.

Values in parentheses are for the outer resolution shell.

Space group	$P6_522$
Unit-cell parameters (Å)	$a = b = 87.66$, $c = 160.28$
Resolution limits (Å)	34.3–1.80 (1.90–1.80)
Total No. reflections	372394
No. unique reflections	34390
Completeness (%)	99.9 (99.9)
Multiplicity	10.8 (11.1)
R_{sym} (%)	7.4 (32.8)
$\langle I/\sigma(I)\rangle$	6.2 (2.2)

This work was supported by grant 01/07539-5, the Structural Molecular Biology Network (SMOLBnet), from the Fundação de Amparo à Pesquisa do Estado de São Paulo (FAPESP).

References

Akaike, T., Sato, K., Ijiri, S., Miyamoto, Y., Kohno, M., Ando, M. & Maeda, H. (1992). *Arch. Biochem. Biophys.* **294**, 55–63.

Blessing, R. H. (1995). *Acta Cryst.* A**51**, 33–38.

Chae, H. Z., Robison, K., Poole, L. B., Church, G., Storz, G. & Rhee, S. G. (1994). *Proc. Natl Acad. Sci. USA*, **91**, 7017–7021.

Collaborative Computational Project, Number 4 (1994). *Acta Cryst.* D**50**, 760–763.

Cussiol, J. R., Alves, S. V., Oliveira, M. A. & Netto, L. E. S. (2003). *J. Biol. Chem.* **180**, 2636–2643.

Fuangthong, M., Atichartpongkul, S., Mongkolsuk, S. & Helmann, J. D. (2001). *J. Bacteriol.* **183**, 4134–4141.

Kabsch, W. (1988). *J. Appl. Cryst.* **21**, 916–924.

Leslie, A. G. W. (1992). *Jnt CCP4/ESF–EAMCB Newsl. Protein Crystallogr.* **26**.

Lesniak, J., Barton, W. A. & Nikolov, D. B. (2002). *EMBO J.* **21**, 6649–6659.

Matthews, B. W. (1968). *J. Mol. Biol.* **33**, 491–497.

Mongkolsuk, S., Praituan, W., Loprasert, S., Fuangthong, M. & Chamnongpol, S. (1998). *J. Bacteriol.* **180**, 2636–2643.

Navaza, J. (2001). *Acta Cryst.* D**57**, 1367–1372.

Ochsner, U. A., Hassett, D. J. & Vasil, M. L. (2001). *J. Bacteriol.* **183**, 773–778.

Poole, L. B. (1996). *Biochemistry*, **35**, 65–75.

Poole, L. B. & Ellis, H. R. (1996). *Biochemistry*, **35**, 56–64.

Rince, A., Giard, J. C., Pichereau, V., Flahaut, S. & Auffray, Y. (2001). *J. Bacteriol.* **183**, 1482–1488.

Simpson, A. J. *et al.* (2000). *Nature (London)*, **406**, 151–159.

Smolka, M. B., Martins D., Winck, F. V., Santoro, C. E., Castellari, R. R., Ferrari, F., Brum, I. J., Galembeck, E., Della Coletta Filho, H., Machado, M., Marangoni, S. & Novello, J. C. (2003). *Proteomics*, **2**, 224–237.

Tenhaken, R., Levine, A., Brisson, L. F., Dixon, R. A. & Lamb, C. (1995). *Proc. Natl Acad. Sci. USA*, **92**, 4158–4163.

Wolf, S. (1994). *Methods Enzymol.* **233**, 182–189.

Wood, Z. A., Poole, L. B., Hantigan, R. R. & Karplus, A. (2002). *Biochemistry*, **17**, 5493–5504.

Paralelamente, Lesniak e col. (2002) descreveram a estrutura de Ohr de *Peudomonas aeroginosa* na forma reduzida. Apesar das semelhanças funcionais com peroxirredoxinas, Ohr é muito distinto estruturalmente, não possuindo o "thioredoxin fold" característico dessas proteínas. Além disso, Ohr é um dímero fortemente enovelado que apresenta um "fold" nunca antes descrito que foi denominado alfa/beta (Lesniak e col., 2002). Os resíduos de cisteína de Ohr de *Pseudomonas aeruginosa* localizam-se muito próximos entre si, a uma distância de 3,6 Å o que possibilitaria a formação de um dissulfeto intramolecular, como proposto no anexo 16.

Apesar da alta semelhança entre as seqüências de amino ácidos das proteínas de *Xylella fastidiosa* e *Pseudomonas aeroginusa* (66% de identidade e 74% de similaridade), decidimos continuar a resolver a estrutura de Ohr porque o cristal da mesma se encontra na forma oxidada (anexo 17). Recentemente, concluímos a estrutura de Ohr de *Xylella fastidiosa*. Trata-se de um homodímero de forma oval sendo que cada subunidade é estruturalmente idêntica (Figuras 6 e 7). As interações entre os monômeros se dão principalmente por interações de Van der Waals entre as duas maiores alfa hélices de cada monômero no centro hidrofóbico da enzima, onde estão situados os resíduos de cisteínas catalíticos. Duas grandes folhas beta circundam as grandes hélices centrais, sendo que cada folha beta é constituída de seis fitas beta pregueadas, três derivadas de um monômero e as restantes do outro. Como as cisteínas se encontram dentro do centro hidrofóbico formado pela junção dos monômeros, parece claro que a dimerização é necessária para a atividade enzimática (Figura 6) .

Os resíduos de cisteína se encontram em uma fenda da molécula (figura 6). A entrada da fenda é guardada por diversos aminoácidos hidrofóbicos o que explica a a alta especificidade de Ohr por peróxidos orgânicos quando comparados com H_2O_2 (anexo 16). Cys 61 se apresenta na forma de ácido sulfônico (Cis-SO_3) devido ao pré-tratamento da proteína com altas doses TBHP (Figuras 6 e 7). Cys61 e Cys125 estão separadas por uma distância de 4.2 Å e muito provavelmente podem interagir para formação de um dissulfeto intramolecular.

A estrutura da Ohr determinada de *Xylella fastidiosa* é muito similar a de *Pseudomonas aeruginosa*, no entanto a Cys-S_p de *Pseudomonas* (Cys 60) se encontra reduzida ao passo que na estrutura de Ohr de *X. fastidiosa* a Cys-S_p (C61) está totalmente oxidada.

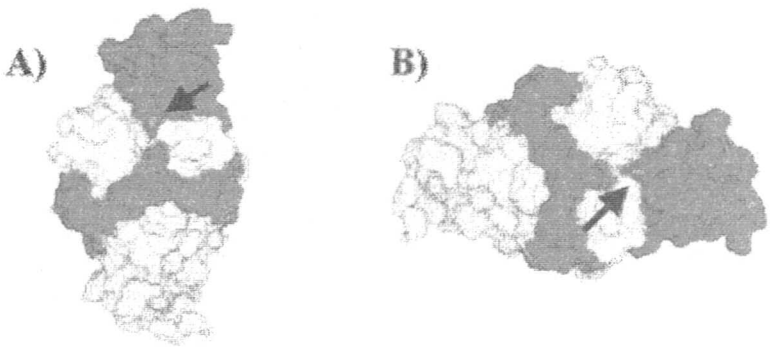

Figura 6 - Representação da superfície da molécula de Ohr de *X. fastidiosa*. A) Estrutura do dímero de Ohr. Um monômero está representado em cinza e o outro em púrpura. B) Equivalente a estrutura da figura A que sofreu rotação de 90 °. As setas indicam a fenda onde está localizado o sítio ativo. Notar em vermelho que correspondem aos oxigênios da cisteína oxidada (Cis-SO_3H).

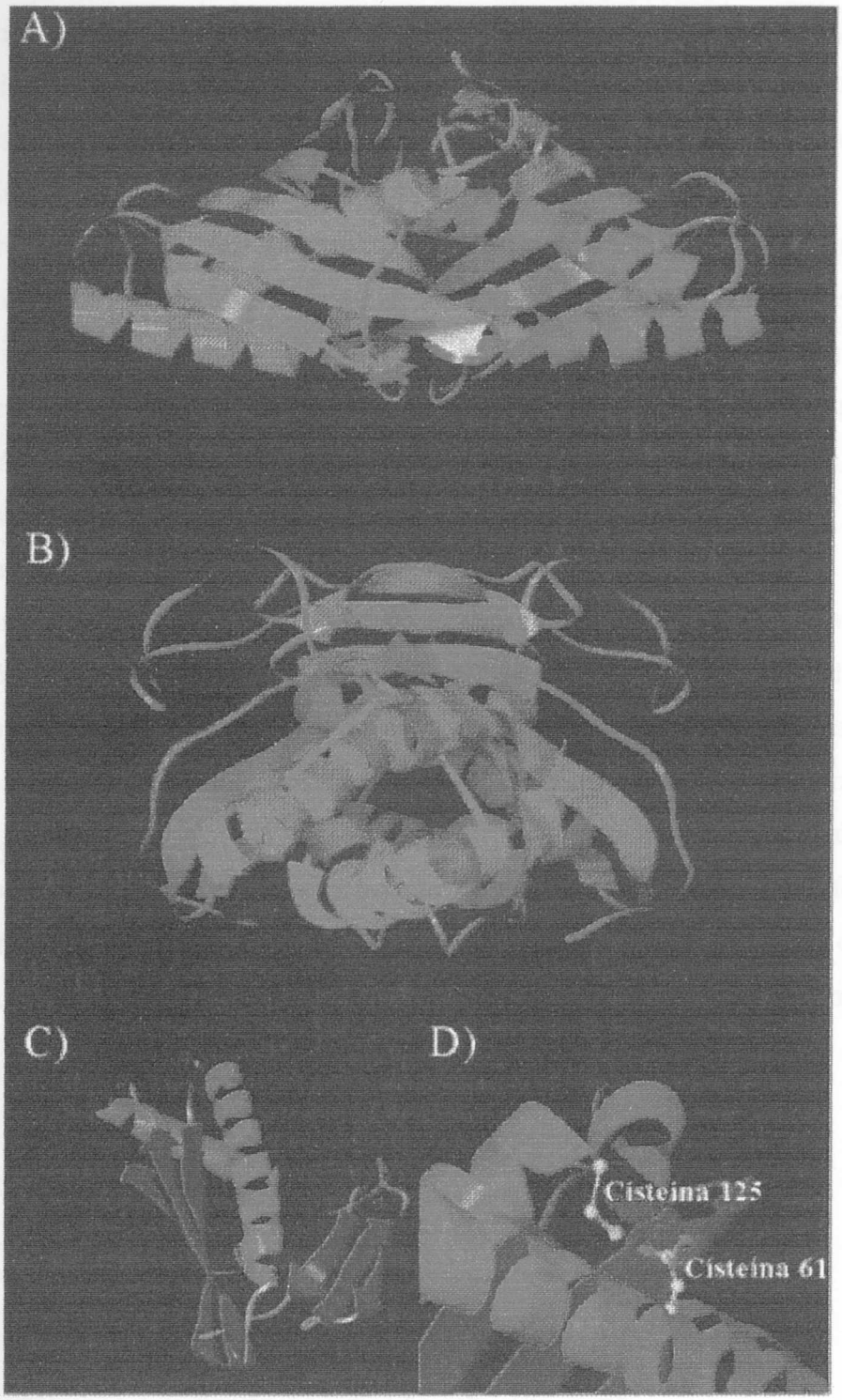

Figura 7 - Estrutura de Ohr de *X. fastidiosa*. A) Estrutura do dímero de Ohr. Um monômero está representado em vermelho e o outro em púrpura. Notar a forma elíptica. B) Equivalente a estrutura da figura A que sofreu rotação de 90 °. C) Monômero de Ohr. As alfa hélices estão representadas em vermelho e as fitas beta em azul. D) Detalhe do monômero com as duas cisteínas do sítio catalítico, sendo que a Cys61 está fortemente oxidada (Cys-SO_3H).

Como descrito anteriormente, Ohr e peroxirredoxinas apresentam características estruturais distintas. Ohr tem o domínio alfa/beta, enquanto peroxirredoxinas têm o domínio "thioredoxin fold". Apesar dessas diferenças, outras semelhanças poderiam ser detectadas através da sobre posição das estruturas de proteínas dessas duas classes depositadas no pdb (protein databank). Todavia, Ohr de *X. fastidiosa* só possui similaridade estrutural com proteínas pertencentes à família Ohr/OsmC. Tanto OsmC quanto Ohr foram relacionadas como proteínas envolvidas na degradação de peróxidos orgânicos. Estas proteínas não possuem grande similaridade com nenhuma outra proteína eucariótica ou procariótica conhecida. A identidade na seqüência de aminoácidos das subfamílias OsmC e Ohr varia entre 40-70% dentro de cada sub-família e aproximadamente 20 % entre elas (Atichartpongkul e col., 2001).

Atualmente existem coordenadas atômicas somente de três proteínas da família Ohr/OsmC depositadas no pdb: Ohr de *P. aeruginosa*, OsmC de *E. coli* e OsmC de *Mycobacterium pneumoniae* (Choi e col., 2003). Utilizamos as coordenadas das três proteínas para fazer um alinhamento estrutural preliminar. A sobreposição estrutural da cadeia principal de aminoácidos de Ohr de *X. fastidiosa* com os representantes citados acima mostra uma elevada semelhança estrutural (figura 8). Esta similaridade é também extremamente evidente na estrutura quaternária destas proteínas (figura 9). É importante notar que apesar de pequenas diferenças existentes entre os ângulos formados entre as alfa hélices e extensão de folhas beta elas apresentam a mesma forma e possuem elementos estruturais em posições equivalentes (Figura 9).

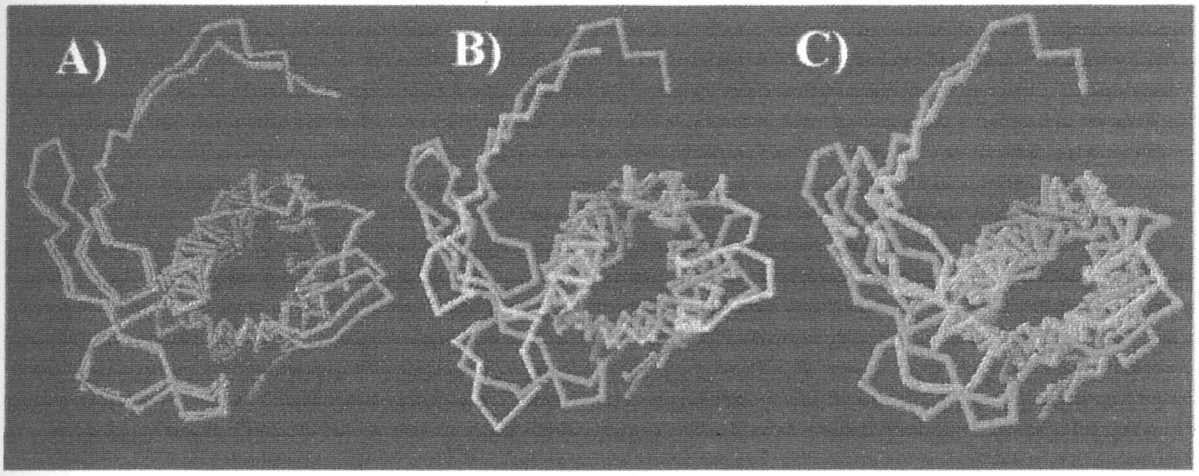

Figura 8 - Sobreposição de estruturas monoméricas de proteínas da família Ohr/OsmC. Alinhamento da cadeia principal do monômero de Ohr de *X. fastdiosa* (verde) com: A) Ohr de *P. aeruginosa* (código pdb: 1N2F), b) OsmC de *E. coli* (código pdb: 1QWI) e C) OsmC de *M. pneumoniae* (código pdb: 1LQL). A orientação é a mesma nas três sobreposições.

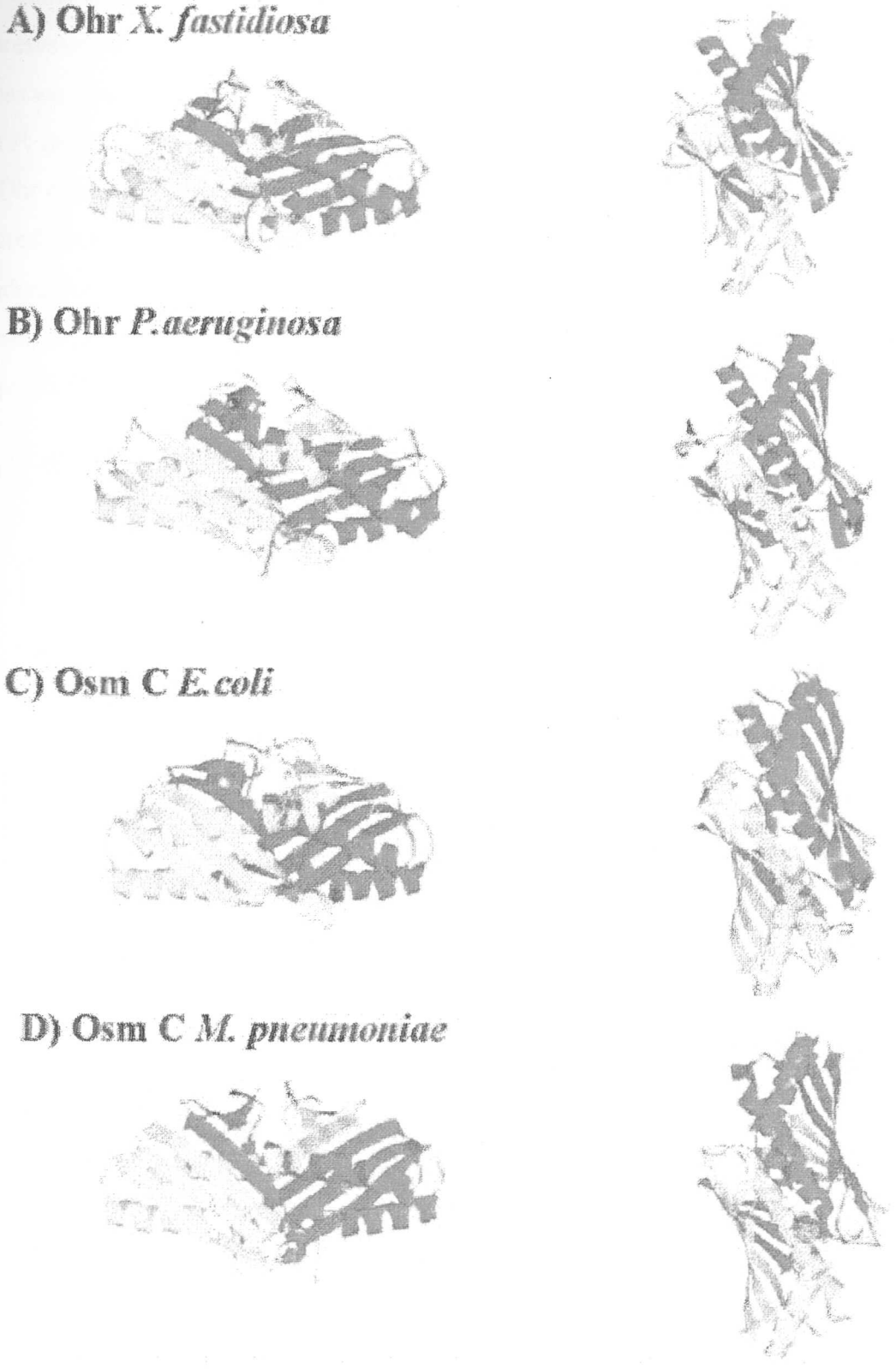

Figura 9 - Sobreposição de estruturas diméricas de proteínas da família Ohr/OsmC Comparação das estruturas do dímericas de Ohr de *X. fastidiosa* proteínas com proteínas com alta similaridade e coordenadas depositadas no pdb (http://www.rcsb.org).

Como mencionado anteriormente, as proteínas Ohr de *X. fastidiosa* e *P. aeruginosa* apresentam extensa homologia estrutural. A principal diferença entre o sítio ativo das duas estruturas reside no estado REDOX de cada uma delas. Enquanto que a molécula de *P. aeruginosa* se apresenta reduzida, com uma molécula de DTT próxima a $CysS_p$, a Ohr de *X. fastidiosa* se encontra oxidada a ácido sulfônico (Cys-SO_3H - Figura 10). Acreditamos que uma análise comparativa cuidadosa do sítio ativo das duas proteínas poderá fornecer informações importantes no que concerne ao mecanismo catalítico desta enzima. Uma das questões iniciais que serão analisadas será o motivo da especificidade por ditióis apresentada por esta proteína (Anexo 16).

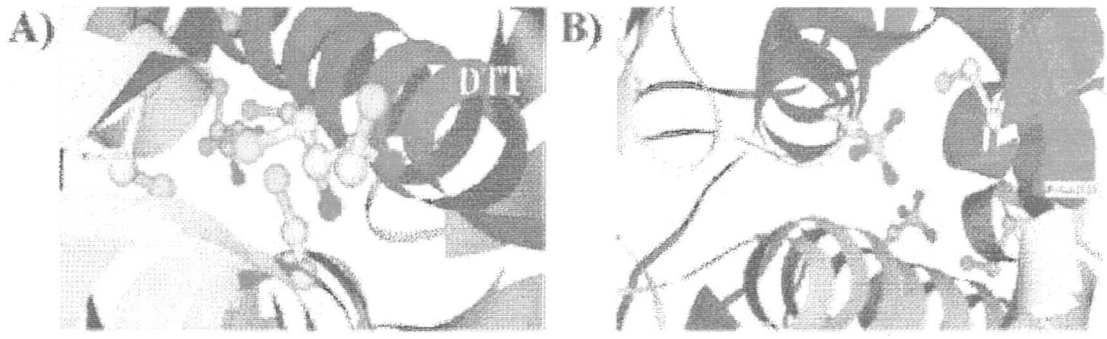

Figura 10 - Detalhe das cisteínas do sítio ativo de Ohr de *X. fastidiosa* e *P.aeruginosa* (A) Ohr de *P.aeruginosa*. A seta vermelha indica uma molécula de DTT próxima a cisteína 60. B) Ohr de *X. fastidiosa* altamente oxidada com formação de ácido sulfônico (Cys-SO_3H).

O provável mecanismo de ação de Ohr envolve a oxidação do tiolato de Cys 61 (Cys-S_p^-) por peróxidos orgânicos, levando a formação de um ácido sulfênico (Cys-SOH), o qual seria rapidamente atacado pela Cys 125 (Cys-S_r) gerando dissulfeto intramolecular. Entretanto, em altas concentrações de peróxidos orgânicos, Cys61-SOH poderia ser oxidada por outra molécula de peróxido orgânico formando ácido sulfínico (Cys61-SO_2H) e o ataque por outra molécula de peróxido levaria a formação de ácido sulfônico (Cys61-SO_3H) (Anexo 16). Dessa forma, era esperado o aparecimento de Cys61-SO_3H em Ohr tratada com grande excesso de TBHP (1mol TBHP :1 mol de Ohr). A formação de Cys-SO_2H ou Cys-SO_3H é considerada um processo de inativação de proteínas porque estes estados oxidados não podem ser reduzidos por moléculas como DTT, 2- mercaptoetanol ou tiorredoxina (revisado por Wood e col., 2003a).

Entretanto ensaios enzimáticos realizados pelo aluno de iniciação científica José Renato Rosa Cussiol indicaram que não ocorre inibição extensiva de Ohr na presença de altas concentrações de *t*-BOOH (10mM), (Figura 11). Nesses ensaios, utilizamos um sistema redutor composto por NADH, lipoamida desidrogenase e lipoamida e medimos a queda de absorbância a 340nm. Utilizando proporções de TBHP/Ohr superiores a utilizada para obter o cristal (17 TBHP:1 Ohr) descrito no anexo 17, não obtivemos evidência de inibição significativa como seria esperado, caso Cys61-SO_3H fosse formado.

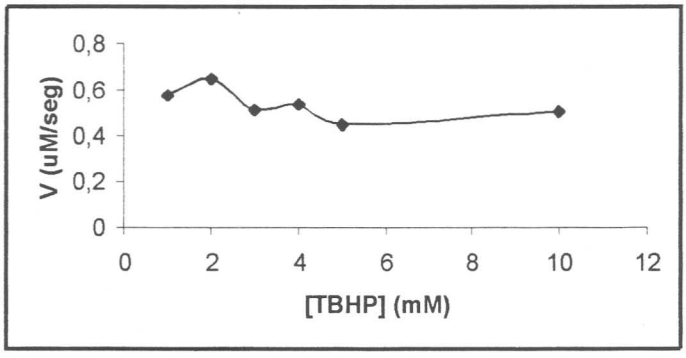

Figura 11- Análise da atividade enzimática de Ohr Foi utilizado o ensaio de consumo de NADH através do sistema Ohr/Lipoamida/Lpd/NADH. Foi utilizado para este ensaio Ohr numa Cf de 10ng/ul (0,6uM). Reações foram feitas em tampão fosfato de potássio (50mM) pH 7,0; EDTA (0,1 mM) pH 8,0; NADH (0,2mM) Lipoamida (50uM), LpD de boi (0,4 U/ml) (SIGMA); Ohr e TBHP foram adicionados para uma mistura de reação de Vf= 1ml à 25°C.

Uma hipótese para tentar conciliar esses resultados seria que para o Cys61-SO_3H ser formado, seria necessário um longo tempo de exposição (~1 semana) de Ohr a TBHP (10mM), como ocorreu durante os ensaios de cristalização, mas não durante os ensaios enzimáticos descritos na figura 11. Para testar essa hipótese, tratamos Ohr com altas concentrações de H_2O_2 ou TBHP e removemos o excesso de peróxidos por cromatografia de exclusão molecular. Resultados prévios indicavam que somente TBHP, mas não H_2O_2, seria capaz de oxidar Cys61-Sp a Cys61-SO_3H (anexo 16). De

fato, Ohr foi inibida quando pré-tratada com altas doses de TBHP (mas não H_2O_2) por períodos equivalentes aos utilizados no ensaio de cristalizaram (figura 12). De qualquer forma, para esclarecer esse fenômeno inequivocamente, pretendemos realizar experimentos de espectrometria de massa. Dessa forma, poderemos verificar se as unidades de massa de Ohr variam como esperado pelos tratamentos com diferentes peróxidos por diferentes períodos de tempo.

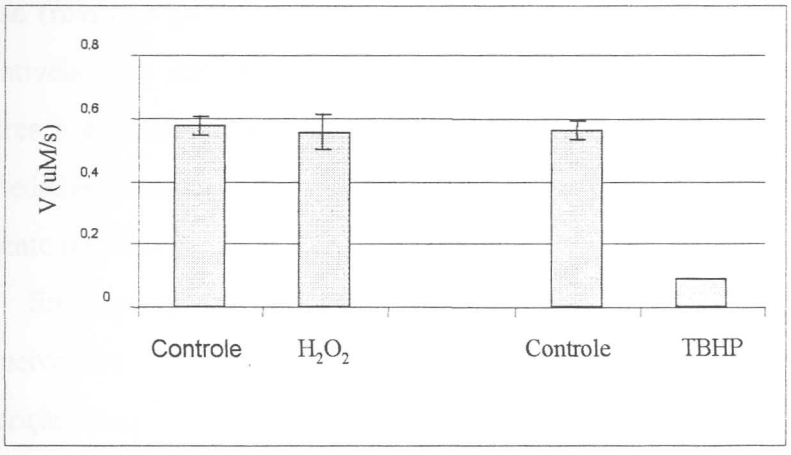

Figura 12 – **Atividade de Ohr pré-tratada com peróxidos por uma semana**. Ohr foi incubada com peróxidos (H_2O_2 e *TBHP* numa Cf de 300uM) durante 1 semana à 4°C nas seguintes condições: Para H_2O_2 temos Ohr uma Cf de 100ng/ul e para TBHP numa Cf de 10ng/ul. DTPA (0,1mM) foi adicionado em ambas as incubações. Após a incubação foi realizado o ensaio de consumo de NADH pelo sistema OHR/Lipoamida/Lpd/NADH (ver condições na figura 11).

Em resumo, nossos resultados indicam que Ohr de *Xylella fastidiosa* é membro de uma classe de enzimas antioxidantes distinta das enzimas antioxidantes tradicionais (catalase, superóxido dismutase e GSH peroxidase), bem como das peroxirredoxinas. Estamos no momento, buscando os redutores biológicos de Ohr em *Xylella fastidiosa* (ver capítulo 5).

CAPÍTULO 4

Regulação REDOX por peróxidos e tiolatos

Analisamos nos capítulos anteriores vários sistemas antioxidantes e, portanto, EROS foram consideradas como agentes patológicos que devem ser eliminados pelas células. Porém, é crescente a visão de que EROS e particularmente H_2O_2 podem atuar também como sinalizadores celulares. Este interesse tem aumentado pela descoberta de que células não fagocitárias têm complexos protéicos com atividade de NADPH oxidase (revisado por Bokoch e Knaus, 2003). Além disso, H_2O_2 tem propriedades compatíveis com um sinalizador celular: é capaz de se difundir entre membranas celulares e é relativamente estável. Portanto, H_2O_2 é comparável com NO nas suas propriedades físico-químicas e por poder ser produzido por um sistema enzimático altamente regulável (Stone, 2004).

Em organismos mais simples como bactérias e leveduras está bem estabelecido que peróxidos são capazes de realizar sinalização celular ao ativar fatores de transcrição (capítulo 1). Todos os sistemas regulados por peróxidos que foram bem caracterizados até o momento dependem de tiolatos (RS^-), como é o caso de OxyR (bactérias) e Yap1 (*Saccharomyces cerevisiae*). Em mamíferos, tem sido proposto que vários sistemas podem ser regulados por peróxidos, mas esses fenômenos são ainda controversos (Stone, 2004).

Muita atenção tem sido dada às Proteínas Tirosinas Fosfatases (PTP) como sistemas que poderiam ser sensores celulares de H_2O_2. Inicialmente, foi demonstrado que H_2O_2 reage com cisteínas do sítio ativo de PTPs, gerando um ácido sulfênico (Cys-SOH) e foi posteriormente proposto que essas fosfatases poderiam ser reguladas através do par REDOX sulfidrila (Cys-SH) – ácido sulfênico (Cys-SOH) (Lee e col., 1998). Mais recentemente, dois grupos independentes resolveram estruturas de PTPs que tinham um grupo sulfenil-amida (Salmeen e col., 2003; Van Montfort e col., 2003). Sulfenil-amida foram geradas em PTPs pelas reações descritas abaixo:

RS^- (cys 215) + H_2O_2 → RSOH + H_2O (reação 7)

R^1SOH + R^2-NH_3 (ser 216) → R^1S-NR^2H_2 (reação 8)

A forma sulfenil-amida de PTP é inativa, o que deve promover um aumento nos níveis de fosforilação de tirosina. Dessa forma, alvos prováveis de PTPs como

MAP quinases seriam fosforilados em tirosinas. As estruturas de PTPs oxidadas a ácidos sulfínico (Cys-SO_2H) e sulfônico (Cys-SO_3H) também foram determinadas a partir de preparações tratadas com grande excesso de H_2O_2 (Van Montfort e col., 2003). Ao contrário das formas sulfínico (Cys-SO_2H) e sulfônico (Cys-SO_3H), as sulfenil amidas podem ser reduzidas de volta a sulfidrila original (Salmeen e col., 2003; Van Montfort e col., 2003). Dessa forma, por ser uma inibição reversível, esse formação e destruição de sulfenil-amidas foi sugerida como uma via de sinalização por H_2O_2.

Porém, a regulação de REDOX de PTPs é controversa entre outros motivos porque a reação de H_2O_2 com fosfatases é lenta (~$10M^{-1}$ s^{-1}). Como a concentração intracelular de H_2O_2 varia entre 1 a 700nM e os níveis de GSH na célula são da ordem de 1-10 mM, para oxidar um possível alvo de sinalização, a constante de reação deve ser bem mais alta (Stone, 2004). Para efeitos de comparação, a reação de H_2O_2 com OxyR (Cys 199) é aproximadamente $2x10^5$ M^{-1} s^{-1} (Aslund e col., 1999). No caso de OxyR e outras proteínas que têm tiolatos altamente reativos, enovelamentos apropriados fazem com que o pKa da cisteína fique muito mais baixo do que o pKa cisteína livre (pKa ~8,0). Dessa forma, essas cisteínas estariam desprotonadas em pH fisiológico. Portanto, de acordo com Stone (2004), um alvo de regulação por H_2O_2 teria que reagir com esse oxidante com velocidades dessa ordem de grandeza.

Neste contexto, um dos possíveis sensores biológicos de H_2O_2 seriam peroxirredoxinas que são proteínas que reagem com peróxidos com constantes de reação da ordem de 10^5 M^{-1} s^{-1} (Baker e col., 2001). De fato, existem várias sugestões que peroxirredoxinas poderiam ser sensores de H_2O_2 (Wood e col., 2003b). Recentemente, foi observado que peroxirredoxinas do tipo A de bactérias são cerca de cem vezes mais resistentes que proteínas equivalentes de eucariontes (revisto por Wood e col., 2003b). Em ambos os casos, a inativação dessas proteínas se deve À oxidação adicional da Cys S_p de ácido sulfênico (Cys-SOH) a sulfínico (Cys-SO_2H) (Woo e col., 2003). Na tentativa de encontrar características distintas entre peroxirredoxinas sensíveis e robustas, Wood e col. (2003b) alinharam várias dessas sequências e observaram que todas as peroxirredoxinas sensíveis a inativação têm em comum dois motivos: GGLG (entre alfa hélice 4 e estrutura beta 5) e YF (localizado na alfa hélice 7, estrutura secundária que só aparece nas proteínas sensíveis). Portanto, parece que a alta sensibilidade de peroxirredoxinas de eucariontes a peróxidos não é

uma limitação do mecanismo de catálise, mas uma propriedade que foi selecionada durante a evolução dos eucariontes (Wood e col., 2003b). A hipótese levantada para explicar esse mecanismo de regulação seria que em condições basais, baixas doses de H_2O_2 estariam presentes na célula entre outros motivos porque peroxirredoxinas sensíveis poderiam decompor esse oxidante. Em situações nas quais os níveis de peróxido aumentam (por exemplo: tratamento com TNF = "*Tumor Necrosis Factor*"), as peroxirredoxinas do tipo A seriam inativadas, possibilitando que outros alvos protéicos sejam oxidados por peróxidos, como Orp1/Gpx3 de *Saccharomyces cerevisiae* (Delaunay e col., 2002; Wood e col., 2003b) e PTPs.

Outra observação que reforça a hipótese descrita acima foi que ácido sulfínico (Cys-SO_2H) gerados em cisteínas peroxidásicas são regenerados *in vivo* em peroxirredoxinas sensíveis (Woo e col., 2003). É importante ressaltar que peroxirredoxinas oxidadas a ácido sulfínico (Cys-SO_2H) não são reduzidas *in vitro* por redutores clássicos como DTT ou tiorredoxina. Mais recentemente ainda, foi identificado em *Saccharomyces cerevisiae*, o sistema enzimático dependente de ATP responsável pela redução de peroxirredoxinas do tipo A *in vivo*(Biteau e col., 2003). Trata-se de uma proteína de 13kDa denominada sulfirredoxina que é conservada em eucariontes superiores e que anteriormente não tinha função conhecida. O mecanismo de catálise proposto envolve atividades de fosfo-transferase e tiól-transferase. Sulfirredoxina é capaz de formar pontes dissulfeto mistas com peroxirredoxinas de *Saccharomyces cerevisiae* o que também está relacionado com o ciclo catalítico dessas proteínas. O significado da formação e redução de ácido sulfínico em peroxirredoxinas ainda não é claro mas aponta uma co-evolução com sulfirredoxinas. Se de fato a inativação de peroxirredoxina a ácido sulfínico representa uma etapa de sinalização, sua reversão dependente de sulfirredoxina pode representar um nível adicional de regulação (Biteau e col., 2003).

O significado desses estudos recentes sobre oxidação de peroxirredoxinas a ácido sulfínico ainda não está bem estabelecido. De qualquer forma, o envolvimento de peroxirredoxinas em sinalização celular foi reforçado pelo fato de que a atividade dessas enzimas também pode ser regulada por fosforilação através de quinases dependentes de ciclinas (Chang e col., 2002).

Em colaboração com Marilene Demasi, temos investigado em *Saccharomyces cerevisiae* outra possível via de sinalização de peróxidos: a glutatiolação de

proteassoma. O proteassoma é um grande complexo protéico responsável por grande parte da atividade protéica das células. Como mencionado no capítulo 1, em situações de estresse a biossíntese de macromoléculas é inibida e concomitantemente, a degradação é estimulada. De fato, estudos realizados em escala proteômica mostraram que a expressão de algumas das subunidades do proteassoma é induzida por H_2O_2 (Lee e col., 1999a). Por outro lado, estudos da Dra. Demasi com proteassoma de mamíferos mostraram que esse complexo protéico é glutatiolado e que a adição desse tiól modula a atividade proteolítica desse complexo (Demasi e col., 2001). Demonstramos que proteassoma de *Saccharomyces cerevisiae* também é regulado por glutatiolação *in vitro* e demonstramos que esse mecanismo envolve a formação de ácido sulfênico (RSOH) no complexo proteolítico (anexo 18). Além disso, pela primeira vez mostramos que proteassoma é glutatiolado *in vivo* é que essa modificação pós-traducional resulta em alteração de sua atividade enzimática. No momento estamos buscando caracterizar possíveis sistemas enzimáticos responsáveis pela adição e remoção de GSH em proteassoma. Estamos preparando um artigo para submissão cujos resultados indicam que glutarredoxina 2 é capaz de catalisar a remoção de GSH de proteassoma (anexo 19).

ANEXO 18

THE JOURNAL OF BIOLOGICAL CHEMISTRY
Vol. 278, No. 1, Issue of January 3, pp. 679–685, 2003
Printed in U.S.A.

20 S Proteasome from *Saccharomyces cerevisiae* Is Responsive to Redox Modifications and Is *S*-Glutathionylated*

Received for publication, September 10, 2002, and in revised form, October 24, 2002
Published, JBC Papers in Press, October 29, 2002, DOI 10.1074/jbc.M209282200

Marilene Demasi‡, Gustavo Monteiro Silva, and Luis Eduardo Soares Netto

From the Departmento de Biologia, Instituto de Biociências, Universidade de São Paulo, Rua do Matão, 277 São Paulo, São Paulo 05508-900, Brazil

The 20 S proteasome core purified from *Saccharomyces cerevisiae* is inhibited by reduced glutathione (GSH), cysteine (Cys), or the GSH precursor γ-glutamylcysteine. Chymotrypsin-like activity was more affected by GSH than trypsin-like activity, whereas the peptidylglutamyl-hydrolyzing activity (caspase-like) was not inhibited by GSH. Cys-sulfenic acid formation in the 20 S core was demonstrated by spectral characterization of the Cys-*S*(*O*)-4-nitrobenzo-2-oxa-1,3-diazole adduct, indicating that 20 S proteasome Cys residues might react with reduced sulfhydryls (GSH, Cys, and γ-glutamylcysteine) through the oxidized Cys-sulfenic acid form. *S*-Glutathionylation of the 20 S core was demonstrated *in vitro* by GSH-biotin incorporation and by decreased alkylation with monobromobimane. Compounds such as *N*-ethylmaleimide (-S-sulfhydril H alkylating), dimedone (-SO sulfenic acid H reactant), or 7-chloro-4-nitrobenzo-2-oxa-1,3-diazole (either -SH or -SOH reactant) highly inhibited proteasomal chymotrypsin-like activity. *In vivo* experiments revealed that 20 S proteasome extracted from H_2O_2-treated cells showed decreased chymotrypsin-like activity accompanied by *S*-glutathionylation as demonstrated by GSH release from the 20 S core after reduction with $NaBH_4$. Moreover, cells pretreated with H_2O_2 showed decreased reductive capacity assessed by determination of the GSH/oxidized glutathione ratio and increased protein carbonyl levels. The present results indicate that at the physiological level the yeast 20 S proteasome is regulated by its sulfhydryl content, thereby coupling intracellular redox signaling to proteasome-mediated proteolysis.

The proteasome is an essential proteolytic complex in eukaryotic cells where it is responsible for the degradation of many cellular proteins. It plays an important role in cell-cycle regulation, cell signaling, including apoptosis, and elimination of abnormal proteins generated by mutation (1, 2) and oxidative damage (3–5).

In recent years, many publications have reported the reversible *S*-glutathionylation of a discrete number of proteins (6). Protein *S*-glutathionylation seems to play an essential role in redox regulation. This form of regulation has direct effects on both enzyme activity and the ability of transcription and replication factors to bind DNA targets. The mechanism of protein glutathionylation has evolved in recent years from the strict belief that this event would take place solely when intracellular GSSG[1] levels increased upon oxidative stress, with the formation of mixed disulfides between protein Cys-SH residues and GSSG (7, 8), to the present and more complete understanding of protein sulfhydryl chemistry and evidence showing formation of protein-Cys-SOH derivatives (9) that are prone to *S*-glutathionylation by reduced GSH (10).

Either individual enzyme activity or global cellular responses can be rapidly controlled by the oxidation of protein-Cys-SH residues (reviewed in Ref. 6) generating Cys-SOH, Cys-SO_2H, and Cys-SO_3H acid forms (11), where Cys-SOH is susceptible to *S*-thionylation and reversibly reduced to Cys-SH (11–14). Cys-SOH formation and *S*-glutathionylation during enzyme catalysis and redox signaling are novel cofactors in the context of redox regulation (14).

In a recent publication (15) it was demonstrated that the reduced and oxidized forms of GSH modulate the chymotrypsin-like activity of purified 20 S proteasome extracted from mammalian cells. In the present report we show that the activity of the 20 S proteasome purified from the yeast *Saccharomyces cerevisiae* is also sensitive to GSH, though in a different way from that observed in the mammalian proteasome. The 20 S proteasome extracted from yeast is inhibited by reduced GSH and *S*-glutathionylated *in vitro*, as well as *in vivo*, when cells are submitted to oxidative challenge. Considering that the proteasome plays important role in cell signaling regulation by hydrolysis of many proteins involved in cascade events of the cellular regulatory pathways, it is not surprising that its activity may be regulated by its Cys-SH residues redox status.

MATERIALS AND METHODS

Chemicals and Reagents—Diethylenetriaminepentaacetic acid (DTPA), dimedone (5,5-dimethyl-1,3-cyclo-hexanedione), dinitrophenylhydrazine, dithionitrobenzoic acid (DTNB), *N*-ethylmaleimide (NEM), fluorogenic substrates succinyl-Leu-Leu-Val-Tyr-MCA (s-LLVY-MCA) and *t*-butoxycarbonyl-Gly-Lys-Arg-MCA, γ-glutamylcysteine (GC), and streptavidin immobilized on 4% beaded agarose were purchased from Sigma. The fluorogenic substrate carbobenzoxy-Leu-Leu-Glu-MCA, the proteasome inhibitors lactacystin and tri-leucine vinyl sulfone, and monobromobimane (mBrB) were purchased from Calbiochem. 7-Chloro-4-nitrobenzo-2-oxa-1,3-diazole (NBD) was purchased from Aldrich. All other reagents used were of analytical grade, and the water was purified with the Milli-Q system.

Yeast Strains and Growth—*S. cerevisiae* BY4741 strain (MATa *his*3Δ1 *leu*2Δ0 *met*15Δ0 *ura*3Δ0) was obtained from Euroscarf, Frankfurt,

* This work was supported by Fundação de Amparo à Pesquisa do Estado de São Paulo. The costs of publication of this article were defrayed in part by the payment of page charges. This article must therefore be hereby marked "*advertisement*" in accordance with 18 U.S.C. Section 1734 solely to indicate this fact.

‡ To whom correspondence should be addressed. Tel.: 55-11-3091-7589; Fax: 55-11-3091-7553; E-mail: mari_mais@hotmail.com.

[1] The abbreviations used are: GSSG, oxidized glutathione; Cys-SH, reduced cysteine; Cys-SOH, Cys-sulfenic acid; Cys-SO_2H, Cys-sulfinic acid; Cys-SO_3H, Cys-sulfonic acid; DTNB, dithionitrobenzoic acid; DTPA, diethylenetriaminepentaacetic acid; DTT, dithiothreitol; GC, γ-glutamylcysteine; GSH, reduced glutathione; mBrB, monobromobimane; MCA, 4-methylcoumarin-7-amide; NBD, 7-chloro-4-nitrobenzo-2-oxa-1,3-diazole; NEM, *N*-ethylmaleimide; s-LLVY-MCA, succinyl-Leu-Leu-Val-Tyr-MCA; HPLC, high pressure liquid chromatography; ANOVA, analysis of variance.

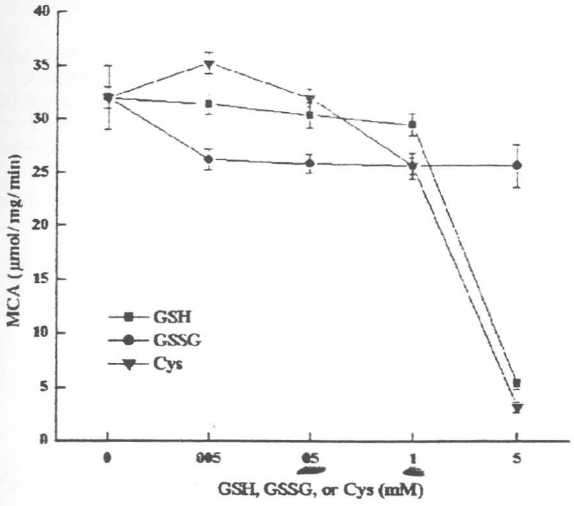

FIG. 1. **Chymotrypsin-like activity of the 20 S proteasome extracted from yeast determined in the presence of GSH, GSSG, and Cys.** The 20 S proteasome (1–3 μg/ml) isolated from *S. cerevisiae*, as described under "Materials and Methods," was preincubated in standard buffer for 10 min at room temperature in the presence of 0–5 mM Cys, GSH, or GSSG, followed by a further 1-h incubation at 37 °C with 10 μM s-LLVY-MCA. Results are expressed as means ± S.D. of four independent experiments.

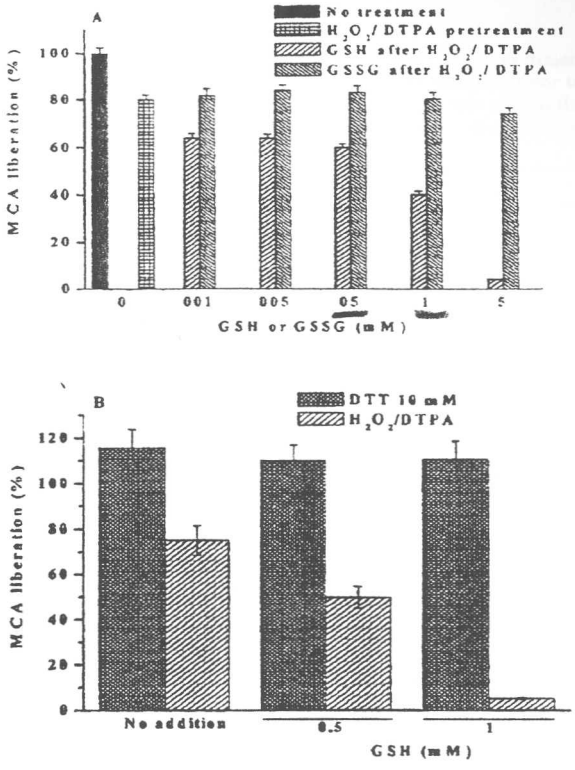

FIG. 2. *A*, H_2O_2/DTPA pretreatment of 20 S proteasome sensitizes chymotrypsin-like activity to GSH inhibition. 20 S proteasome was pretreated with H_2O_2 in the presence of DTPA, as described under "Materials and Methods." Aliquots of H_2O_2-treated samples (1–3 μg) were taken and incubated with GSH or GSSG, as described in the legend for Fig. 1, followed by a hydrolysis assay with s-LLVY-MCA. *B*, DTT preincubation followed by oxidation with H_2O_2/DTPA increases 20 S core sensitization to GSH inhibition. 20 S proteasome (100 μg) was preincubated for 30 min at room temperature in standard buffer in the presence of 10 mM DTT. After incubation, DTT was washed out by filtration through Microcon CM-10 filters. Protein recovered from the filter was treated with H_2O_2/DTPA, as described under "Materials and Methods." Aliquots of H_2O_2-treated samples (1–3 μg) were taken and incubated with GSH or GSSG, as per the legend for Fig. 1, followed by a hydrolysis assay with s-LLVY-MCA. Results are represented as percentage of control samples (no treatment) set as 100 and are expressed as means ± S.D. of four independent experiments.

To test this hypothesis, purified 20 S proteasome preparations were incubated in the presence of 5 mM H_2O_2 and 100 μM DTPA. The iron chelator DTPA was used to prevent the Fenton reaction and consequently the generation of the very reactive hydroxyl radical, which may produce nonspecific protein oxidation, in addition to iron-catalyzed thiol oxidation and generation of several protein-sulfur derivatives (21). Thus, in the absence of iron or another transition metal, sulfhydryl oxidation to Cys-SOH may prevail, though further oxidation of Cys-SOH to Cys-SO_2H and Cys-SO_3H is expected (11). According to our results, 20 S proteasome treatment with H_2O_2 in the presence of DTPA decreased chymotrypsin-like activity to 80% of the original level (Fig. 2*A*), whereas when H_2O_2 treatment was performed in the absence of DTPA the activity was reduced to 60% (data not shown). When 20 S proteasome was pretreated with H_2O_2 plus DTPA the chymotrypsin-like activity was much more affected by GSH (Fig. 2*A*). In fact, after H_2O_2/DTPA pretreatment, inhibition by GSH occurred at concentrations as low as 0.01 mM (35% inhibition), and GSH at 1 mM promoted stronger inhibition (60%; see Fig. 2*A*) than that verified without pretreatment (Fig. 1). In contrast, GSSG did not affect 20 S proteasome activity (Fig. 2*A*). These results are in agreement with our hypothesis in the reaction shown above.

In contrast to H_2O_2, DTT treatment enhanced proteasomal activity by about 15–20% (Fig. 2*B*). Moreover, it sensitized the proteasome to GSH incorporation after H_2O_2 treatment. When 20 S proteasome samples were treated with 10 mM DTT, followed by incubation with H_2O_2/DTPA, the chymotrypsin-like activity was even more sensitive to GSH when compared with samples not preincubated with DTT (Fig. 2*A*). In this condition, proteasomal activity was decreased to 50 and 5% in the presence of 0.5 or 1 mM GSH, respectively (Fig. 2*B*), whereas when the same GSH concentrations were employed without DTT pretreatment, chymotrypsin-like activity was decreased only to 60 and 40%, respectively (Fig. 2*A*). Cys-SOH already present in 20 S proteasome was probably reduced to Cys-SH by DTT, with the consequent prevention of hyperoxidation of Cys-SOH to Cys-SO_2H or Cys-SO_3H by H_2O_2 treatment.

As expected according to our hypothesis described in the reaction shown above, when the 20 S core was pretreated only with DTT, no alteration by GSH was observed in its activity (Fig. 2*B*). Also, proteasome reduced by DTT was not inhibited by GSSG (result not shown) as could be expected, because GSSG is able to react with sulfhydryl groups to form mixed disulfides (7, 8). Reduced Cys-20 S might be prevented from reacting with GSSG by structural constraints imposed by nearby groups.

Proteasomal Activity Is Inhibited by Cys-SH and Cys-SOH Reactants—To demonstrate that modification of Cys-20 S core residues is responsible for the inhibition of chymotrypsin-like activity, we next tested this activity in the presence of Cys-SH and Cys-SOH reactants, such as NBD, dimedone, and NEM (Table I). We observed that chymotrypsin-like activity was inhibited 40 and 30% by 50 μM NBD and 1 mM NEM, respectively. NEM alkylates Cys-SH whereas NBD is incorporated into both Cys-SH and Cys-SOH. This might be, at least in part, the reason why NBD is more potent than NEM in terms of chymotrypsin-like activity inhibition. After inhibition by NBD, 20 S proteasomal activity was recovered by incubation with 5 mM DTT (result not shown). Because DTT treatment leads to NBD release (9), this result indicates that inhibition was promoted by Cys conjugation.

The specific Cys-SOH reagent dimedone (9) produced low inhibition when compared with the former reagents. Dimedone

TABLE I

Effect of Cys-SH and Cys-SOH reactants on proteasomal activity

The 20 S proteasome (1–3 μg/ml) was preincubated, as per Fig. 1, for 30 min at room temperature in the presence of NBD, NEM, or dimedone, at the indicated concentrations, followed by a further 1-h incubation at 37 °C with 10 μM s-LLVY-MCA. H_2O_2/DTPA-treated samples, prior to the hydrolysis assay or dimedone incubation, samples were treated with 5 mM H_2O_2 and 100 μM DTPA, as described under "Materials and Methods," followed by incubation with dimedone and the assay with the fluorogenic substrate. The s-LLVY-MCA hydrolysis assay is described under "Materials and Methods." Results are means ± S.D. of three independent experiments.

Proteasome incubation		MCA release
		$\mu mol \times min^{-1} \times mg^{-1}$
Control (no addition)		25.4 ± 1.4
H_2O_2/DTPA-treated samples		20.3 ± 1.5[a]
NBD	50 μM	15.7 ± 0.8[a]
Dimedone	1 mM	24.1 ± 1.1
	5 mM	22.6 ± 1.8
	10 mM	19.6 ± 1.8[a]
H_2O_2/DTPA-treated samples plus 10 mM dimedone		11.6 ± 1.0[a]
NEM	1 mM	17.6 ± 1.0[a]
	5 mM	10.4 ± 0.8[a]
	10 mM	7.6 ± 0.6[a]

[a] $p \leq 0.0001$ (ANOVA).

promoted 23% inhibition only at 10 mM concentration. On the other hand, when purified 20 S proteasome preparations were pretreated with H_2O_2/DTPA prior to incubation with dimedone, we observed increased proteolytic inhibition compared with the inhibition observed in the absence of H_2O_2/DTPA pretreatment followed by dimedone incubation (results shown in *italics* in Table I). Upon H_2O_2 pretreatment, 10 mM dimedone decreased chymotrypsin-like activity to 50% of that observed in H_2O_2 control samples.

Taken together, the results reported thus far indicate that any group located in Cys residues of the 20 S core decreases its hydrolytic activity, at least the chymotrypsin-like activity, which is considered the strongest of its activities (1). It seems that Cys residues in the 20 S proteasome must be reduced as much as possible to allow maximum activity. Nevertheless, these residues appear to oxidize easily to Cys-SOH.

Cys-SOH Formation and S-Glutathionylation—To demonstrate that Cys residues in the 20 S proteasome structure are oxidized to Cys-SOH, 20 S proteasome preparations were incubated with NBD. This compound reacts with Cys-SH, as well as with Cys-SOH. NBD adducts of Cys-SOH and Cys-SH can be distinguished by their spectra (9). The proteasome-Cys-*S*(*O*)-NBD adduct was generated by 20 S proteasome pretreatment with H_2O_2/DTPA followed by NBD incubation (Fig. 3, *dashed line spectrum*). This adduct showed maximum absorbance at 345 nm whereas the purified 20 S core not oxidized by H_2O_2 yielded the NBD adduct with a maximum absorbance at 420 nm (Fig. 3, *solid line spectrum*).

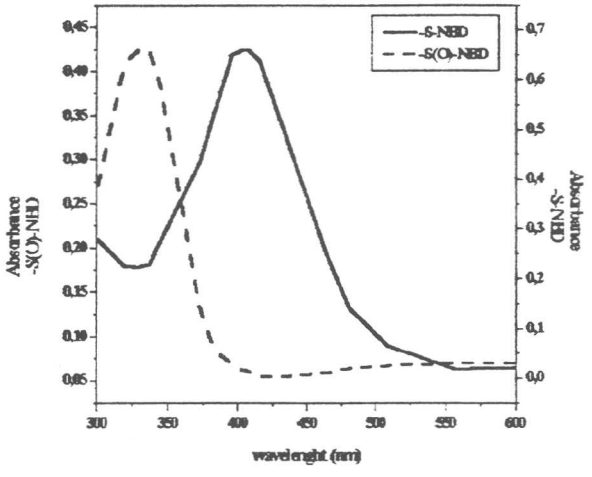

FIG. 3. **NBD-modified 20 S proteasome UV-visible spectra.** The Cys-*S*(O)-NBD conjugate (*dashed line*) was generated by incubating denatured 20 S proteasome (40 μg) in standard buffer with H_2O_2/DTPA, as described under "Materials and Methods," followed by incubation with 100 μM NBD for 30 min. All reagents were washed out by filtration through Microcon CM-10 filters prior to absorbance measurements. The Cys-S-NBD conjugate (*solid line*) was generated by incubating denatured 20 S proteasome (40 μg) in standard buffer with 100 μM NBD. Proteasome was denatured by preincubation in 5 M guanidine solution buffered in 50 mM Tris/HCl, pH 7.5. Spectra were recorded with a Hitachi spectrophotometer.

We also reacted denatured 20 S proteasome preparations with the –SH reactant mBrB (22). Denatured 20 S proteasome samples were preincubated with DTT or GSH. After incubation, DTT and GSH were removed, and the samples were treated overnight with 150 μM mBrB. Proteasome-Cys-bimane conjugates were detected by fluorescence emission recorded after removal of mBrB. DTT-reduced samples showed fluorescence emission at least twice as high as control samples, whereas GSH-treated samples showed reduced fluorescence, probably because 20 S proteasome mixed disulfides could not conjugate with mBrB (Fig. 4). This result indicates that GSH does not play the role of a reducing compound as DTT, but probably GSH was incorporated into the protein structure by *S*-conjugation.

To demonstrate effectively that the effect of GSH on proteasomal activity is because of *S*-glutathionylation, 20 S proteasome preparations were incubated with the GSH-biotin derivative according to the protocol described in the literature (18). This method allows the direct determination of protein *S*-glutathionylation, because biotinylated GSH-proteasome complexes can be isolated by the streptavidin affinity procedure. 20 S proteasome pretreatment with H_2O_2 increased GSH incorporation (Fig. 5). The protein concentration determined after protein elution from the streptavidin-agarose beads was 4-fold higher in samples pretreated with H_2O_2. Protein recovered from control and H_2O_2-treated samples after elution from the streptavidin beads was 10 and 40.5 μg, respectively (the amount of protein reacted with GSH-biotin was the same in both samples, *i.e.* 300 μg). This result is direct proof that 20 S proteasome is susceptible to *S*-glutathionylation by means of GSH addition to Cys-SOH. Because a significant amount of *S*-glutathionylated 20 S proteasome was detected in the control sample, part of its Cys residues were probably already oxidized to Cys-SOH (Fig. 5). It should be emphasized that the reaction with GSH-biotin was performed under non-denaturing conditions. The preparation was brought to denaturing conditions only after incubation with and removal of GSH-biotin to displace the 20 S core from the streptavidin-agarose beads. Thus the results described in Fig. 5 do not allow us to predict how many or which subunits of the 20 S core were *S*-glutathiony-

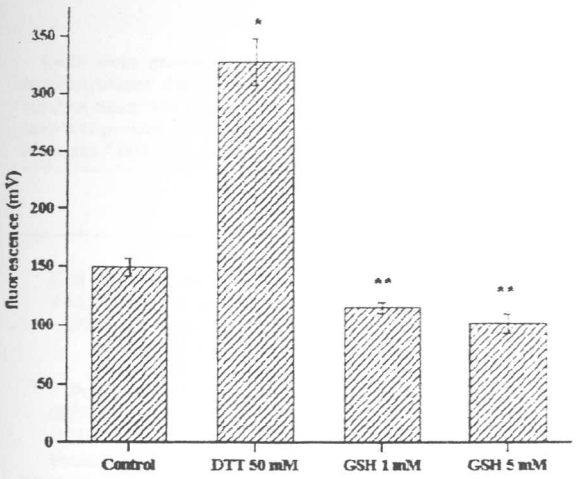

FIG. 4. **mBrB incorporation into the 20 S core after DTT and GSH preincubation.** 20 S proteasome (10 μg) was incubated in standard buffer for 30 min with DTT or for 10 min with GSH at room temperature at the indicated concentrations. GSH or DTT was removed, and protein samples were washed in standard buffer by filtration. The Cys-mBrB conjugate was generated by overnight incubation with 150 μM mBrB at 4 °C in the dark. After incubation, 20 S proteasome was precipitated with 20% trichloroacetic acid followed by washing three times with 10% trichloroacetic acid. The protein was dissolved in 5 M guanidine buffered in 0.1 M Tris/HCl, pH 7.5. Fluorescence emission was recorded at 476 nm (excitation at 400 nm). Results are expressed as means ± S.D. of three independent experiments. *, $p <$ 0.000025. **, p at least 0.001 (ANOVA).

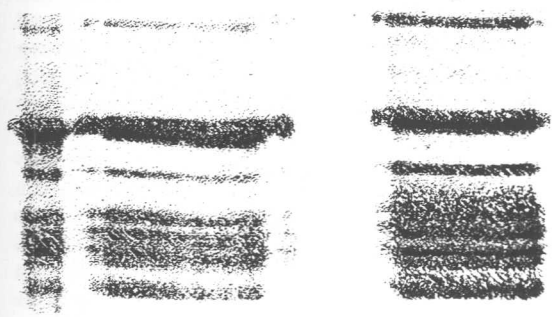

FIG. 5. **20 S proteasome S-glutathionylation by GSH-biotin.** Glutathionylated 20 S proteasome was purified from control (300 μg) and H_2O_2-treated (300 μg) samples after incubation with GSH-biotin followed by SDS-PAGE. The complete experimental procedure is described under "Materials and Methods." The *gel* shown is representative of three independent experiments. The *left lane* refers to 5 μg of a standard preparation of 20 S proteasome, and the *middle* and *right lanes* refer to the GSH-biotin-incubated control (10 μg) and to H_2O_2-treated samples (40.5 μg), respectively.

lated. We tried to denature the proteasome just after incubation with GSH-biotin and prior to the streptavidin incubation to determine approximately how many and which subunits would be *S*-glutathionylated. However, under these conditions, the proteasome concentration of control and H_2O_2-treated samples recovered from the agarose beads was not sufficient to be detected on the gel by Coomassie Blue staining. This is an indication that perhaps very few or even only one subunit might be *S*-glutathionylated.

Comparative Catalytic Regulation by GSH among 20 S Proteasome Structures—Chymotrypsin-like activity of 20 S proteasome from *Methanosarcina thermophila*, an Archaeon bacterium, was assayed in the presence of GSH and NEM for comparison to its counterpart, the yeast 20 S proteasome. The Archaeon proteasome was not affected by GSH and was inhibited slightly by NEM (Table II). In the case of mammalian 20 S

TABLE II

Effect of Cys modification on Archaeon proteasome activity

Archaeon proteasome was purchased from ICN Biomedical Research Products. 25–50 μg/ml was preincubated for 10 or 30 min at room temperature in the presence of GSH or NEM, respectively, at the indicated concentrations, followed by a further 1-h incubation at 37 °C with 10 μM s-LLVY-MCA. Hydrolysis determination was described under "Materials and Methods." Results are means ± S.D. of three independent experiments.

		s-LLVY-MCA hydrolysis
	mM	MCA μmol × min^{-1} × mg^{-1}
No addition		8.8 ± 0.5
GSH	5	9.0 ± 0.5
	10	10.2 ± 0.9
NEM	1	8.7 ± 0.6
	5	7.5 ± 0.7
	10	6.2 ± 0.4[a]

[a] $p \leq 0.001$ (ANOVA).

proteasome, both GSH and GSSG at micromolar concentrations activated the chymotrypsin-like activity, whereas it was inhibited by millimolar concentrations (15). Moreover, 20 S mammalian proteasomal activity was inhibited strongly by NEM. On the other hand, the yeast 20 S core is inhibited only by reduced GSH (Fig. 1) and is inhibited strongly by NEM (Table I) whereas the Archaeon proteasome is not affected by any GSH form and is only affected slightly by NEM (Table II).

These results indicate a possible role of Cys residues inside the 20 S core controlling its catalytic activity. Comparing Cys residue content among archaeon, yeast, and mammalian (human) 20 S proteasomes, 28, 74, and 100 (108 total Cys) reduced Cys residues are found, respectively. Most likely the differential effect of GSH addition on proteasome activity is related to non-conserved Cys residues. Our belief is that the 20 S proteasome core has evolved as an important sensor of cellular redox status by modification in its catalytic activity brought about by changes in its Cys residues, promoting the cellular response to redox alterations.

In Vivo 20 S Proteasome Glutathionylation—Our next approach was to search for *in vivo* 20 S proteasome *S*-glutathionylation. Our hypothesis was that proteasome would be sensitive to intracellular reductive capacity, being more active as the cell reductive environment is maximized. This might be an additional way for cells to trigger the signaling response to oxidative alterations. To test this hypothesis, we treated cells with increasing H_2O_2 concentrations. After treatment, the hydrolysis of the fluorogenic substrate s-LLVY-MCA was determined in preparations of 20 S proteasome isolated from the cell extract with the anti-FLAG system and in the proteasome-free cell extract obtained after 20 S proteasome extraction. The 20 S core-anti-FLAG antibody complex bound to agarose beads was assayed for the hydrolysis of the fluorogenic peptide s-LLVY-MCA before and after incubation in the presence of 20 mM $NaBH_4$ to reduce the S-S bridges formed by mixed disulfides or to reduce Cys-SOH to Cys-SH. $NaBH_4$ can also reduce carbonyl groups or Schiff bases formed by the oxidation of some specific amino acid residues to alcohol derivatives (23). Our purpose in using $NaBH_4$ was to reduce oxidized Cys residues inside the 20 S core, thereby recovering proteasome sulfhydryls and promoting GSH release from the core. GSH was assayed in the supernatant recovered after reduction with $NaBH_4$, as described under "Materials and Methods."

The reductive cellular capacity was evaluated by the determination of the GSH/GSSG ratio. We also determined cell viability and the formation of carbonyl protein as a marker of oxidative stress (Table III).

H_2O_2 treatment leads to a significant increase in the formation of protein carbonyl when added to the culture medium at

TABLE III

Proteasomal activity and redox parameters upon H_2O_2 cell treatment

Cells were grown in YPD medium to A_{600} of 0.6–0.8 followed by a further 1-h incubation with H_2O_2 added to the medium at the final concentrations shown. After incubation, aliquots were taken for cell viability assay. The remaining cells were harvested by centrifugation and washed twice with water. Cell extract preparation, 20 S proteasome purification by immunoprecipitation, reduction with $NaBH_4$, and measurements of proteolysis, total and oxidized glutathione, GSH released from 20 S proteasome, and carbonyl proteins are described under "Materials and Methods." ND, not determined.

	No addition	H_2O_2		
		0.1	0.5	1
		mM		
Cell viability, no. of colonies	62 ± 2	62 ± 2	28 ± 2[a]	19 ± 1[a]
s-LLVY-MCA hydrolysis, %				
20 S proteasome fraction[b,c]				
Before $NaBH_4$ reduction	100 ± 6	102 ± 3	50 ± 3[a]	36 ± 2[a]
After $NaBH_4$ reduction	110 ± 7	ND	70 ± 4[a]	ND
Proteasome-free cell extract[b,d]	100 ± 4	128 ± 9[a]	160 ± 7[a]	165 ± 8[a]
GSH, nmol/mg[e]	Not detected	ND	1.40 ± 0.05	ND
GSH/GSSG	54 ± 3	66 ± 2[a]	37 ± 9[a]	29 ± 1[a]
Protein carbonyl formation, nmol/mg[f]	20 ± 2	24 ± 2	27 ± 1[g]	ND

[a] $p \leq 0.00027$ (ANOVA).

[b] Results are expressed as percentage of control samples (No addition), set as 100.

[c] 20 S proteasome was purified from the cell extract by immunoprecipitation and assayed for proteolysis before and after reduction with $NaBH_4$.

[d] Proteolysis was determined in the cell extract, free of the 20 S proteasome particle, recovered after incubation two times with anti-FLAG antibody.

[e] GSH was released from samples of 20 S proteasome after reduction with $NaBH_4$, as described in footnote c.

[f] The protein fraction from cell extracts was precipitated with 20% trichloroacetic acid. All results are means ± S.D. of four to five independent experiments.

[g] $p = 0.027$ (ANOVA).

a concentration of at least 0.5 mM (Table III). At this concentration, H_2O_2-promoted oxidative stress was accompanied by decreased reductive capacity of the cell, as evaluated by the GSH/GSSG ratio, which dropped to 68.5% compared with that found in control cells. Under the same conditions, proteasomal activity decreased 50% before incubation with $NaBH_4$ and was partially recovered after reduction with $NaBH_4$ to 70% of control samples (Table III). Hydrolysis of the fluorogenic peptide s-LLVY-MCA, determined in the proteasome-free extract, increased by 60%. Reports in the literature (24–26) show that mammalian cells under oxidative stress show increased proteolysis. The cited authors assume that increased proteolysis is because of increased proteasomal activity such as that seen *in vitro* when oxidized substrates show increased hydrolysis levels by purified 20 S proteasome preparations from mammalian cells (3). However, our results show that yeast 20 S proteasome is highly affected by oxidative stress whereas hydrolysis not dependent on proteasome is increased (Table III).

The reason for the partial recovery of proteasome activity after $NaBH_4$ treatment (Table III) is probably the reduction of Cys-SOH or Cys-SSG to Cys-SH. However, other oxidative processes are responsive to reduction by $NaBH_4$, *e.g.* formation of carbonyl and Schiff bases (19), but in this case the original amino acid structures are not regenerated as expected for Cys-SOH and Cys-SSG. GSH release from the 20 S core after reduction with $NaBH_4$ (Table III) is strong evidence that proteasomal activity might be regulated by *S*-glutathionylation under intracellular oxidative conditions, and consequently decreased reductive capacity, here attested by a reduced GSH/GSSG ratio upon H_2O_2 cell treatment.

Taken together, results obtained *in vivo* after cell treatment with H_2O_2 indicate that loss of reductive cellular capacity, according to GSH/GSSG ratios and protein carbonyl levels, is associated with loss of 20 S proteasomal activity and with its *S*-glutathionylation. These data are an indication of redox modulation of 20 S proteasome activity.

DISCUSSION

It is becoming increasingly apparent that many oxidant-sensitive proteins are *S*-glutathionylated in response to intracellular redox status (6, 18, 27) (reviewed in Ref. 28). Cys-SOH is an intermediate form involved in redox regulation and catalysis by protein sulfhydryl groups (reviewed in 6). Distinct fates for protein Cys-SOH have been considered (11, 14) whereby *S*-glutathionylation would be one of the mechanisms modulating protein activity. Protein *S*-glutathionylation is a reversible process, and there is considerable evidence that GSH release is controlled enzymatically, probably by glutaredoxin (29).

In this manuscript we describe the mechanism by which 20 S proteasome is glutathionylated *in vitro*. Taken together, those results indicate that during moderate oxidative stress Cys residues inside the 20 S proteasome core might be oxidized to Cys-SOH, reversibly protected by *S*-glutathionylation, and most likely deglutathionylated after cellular recovery from oxidative stress.

From the data in Table III we calculated that one to two molar GSH was released per mol of 20 S proteasome, considering that the molecular mass of the yeast protease is ~700 kDa. GSH was not detected in 20 S proteasome samples obtained from control cells, probably because of the sensitivity of the assay utilized for GSH detection. The low GSH concentration released from the 20 S core is a suggestion that *S*-glutathionylation of 20 S proteasome at the physiological level is highly specific; probably very few Cys residues in the core are prone to *S*-glutathionylation during metabolic processes. Our hypothesis is that *S*-glutathionylation of the 20 S proteasome is coupled to the oxidation of sulfhydryls, according to the reaction shown above.

Comparing the results described here about the effect of GSH and GSSG on proteasomal activity from yeast (see Figs. 1 and 2) and *M. thermophila* (Table II) to earlier results (15) obtained for mammalian 20 S proteasome, it is clear that the 20 S proteasome homologues respond differentially to changes in redox conditions. In this regard, it is important to observe that the mammalian counterpart has either long- or short-lived proteins as substrates, and its localization inside cells is widespread; it is found in the cytoplasm and nucleus (30). On the other hand, the yeast proteasome is associated with the degradation of short-lived proteins and localized mainly inside the cell nucleus, and perhaps not more than 20% occurs in the

cytoplasm associated with the nuclear endoplasm reticulum network (31).

It is interesting to point out that GSH distribution inside yeast cells is still not clear. Although it has been demonstrated already that GSH is distributed inside the mammalian nucleus at concentrations as high as in the cytoplasm (32), its presence inside the yeast nucleus is not clear, neither is the distribution of glutarredoxin isoforms inside yeast cells clear thus far. A mammalian nuclear isoform was described already (33, 34) whereas information on yeast nuclear isoforms is still lacking. Because glutaredoxin activity is coupled to direct GSH consumption, its presence inside the nucleus would be strong evidence of GSH distribution in the nucleus. Considering proteasome distribution and its role in the yeast cell, as discussed above, elucidation of GSH distribution inside yeast cells is an important matter to corroborate the findings discussed here.

Another important difference suggested in the literature (30, 31) is that yeast proteasome is always capped by the 19 S regulatory unit in contrast to the finding that its counterpart, the mammalian 20 S proteasome, is found in 3–4-fold excess over the 19 S regulatory unit. In our opinion, even if it is true that the yeast proteasome is always capped with the 19 S regulator, this does not rule out the possibility that the catalytic unit represented by 20 S proteasome is regulated independently of either protein ubiquitinylation or substrate recognition by the 26 S proteasome. Our results indicated that redox regulation by glutathionylation is important *in vivo* (Table III). Other examples of redox regulation and *S*-glutathionylation have been described for other metabolic processes (27, 35, 36). Our results lead us to speculate that 20 S proteasomal activity can be modulated by *S*-glutathionylation through the increased presence of oxidants, which would be used in signaling processes. Besides, transient 20 S proteasome inhibition would decrease the hydrolysis of proteins responsible for redox signaling, *e.g.* AP-1-like factors. AP-1-like proteins are sensors of the redox state of the cell (37) and, as already demonstrated in mammalian cells, are degraded by the proteasome (38). The metabolic advantage of protein *S*-glutathionylation in redox signaling is the prevention of irreversible oxidation of the Cys thiol group to Cys-SO_2H or Cys-SO_3H, permitting protein reactivation by reduction. Such mechanism might work in parallel to the main mechanism controlling proteasome-mediated proteolysis, *i.e.* ubiquitinylation. The relationship between proteasome glutathionylation and ubiquitinylation of substrates remains to be established.

REFERENCES

1. Coux, O., Tanaka, K., and Goldberg, A. F. (1996) *Annu. Rev. Biochem.* **65,** 801–847
2. Bochtler, M., Ditzel, L., Groll, M., Hatmann, C., and Huber, R. (1999) *Ann. Rev. Biophys. Biomol. Struct.* **28,** 295–317
3. Giulivi, C., Pacifici, R. E., and Davies, K. J. A. (1994) *Arch. Biochem. Biophys.* **311,** 329–341
4. Berlett, B. S., and Stadtman E. R. (1997) *J. Biol. Chem.* **272,** 20313–20316
5. Ullrich, O., Reinheckel, T., Sitte, N., Hass, R., Grune, T., and Davies, K. J. A. (1999) *Proc. Natl. Acad. Sci. U. S. A.* **6,** 6223–6228
6. Claiborne, A., Mallett, T. C., Yeh, J. I., Luba, J., and Parsonage, D. (2001) *Adv. Prot. Chem.* **58,** 215–276
7. Gilbert, H. F. (1995) *Methods Enzymol.* **251,** 8–28
8. Thomas, J. A., Poland, B., and Honzatko, R. (1995) *Arch. Biochem. Biophys.* **319,** 1–9
9. Ellis, H. R., and Poole, L. B. (1997) *Biochemistry* **36,** 15013–15018
10. Barrett, W. C., DeGnore, J. P., Keng, Y. F., Zhang, Z. Y., Yim, M. B., and Chock, P. B. (1999) *J. Biol. Chem.* **274,** 34543–34546
11. Yang, K. S., Kang, S. W., Woo, H. A., Hwang, S. C., Chae, H. Z., Kim, K., and Rhee, S. G. (2002) *J. Biol. Chem.* **277,** 38029–38036
12. Benitez, L. V., and Allison, W. S. (1973) *Arch. Biochem. Biophys.* **159,** 89–96
13. Allison, W. S. (1976) *Acc. Chem. Res.* **9,** 293–299
14. Claiborne, A., Yeh, J. I., Mallett, T. C., Luba, J., Crane, E. J., Charrier, V., and Parsonage, D. (1999) *Biochemistry* **38,** 15407–15416
15. Demasi, M., Shringarpure, R., and Davies, K. J. A. (2001) *Arch. Biochem. Biophys.* **389,** 254–263
16. Verma, R., Chen, S., Feldman, R., Schieltz, D., Yates, J., Dohmen, J., and Deshaies, R. J. (2000) *Mol. Biol. Cell* **11,** 3425–3439
17. Hough, R., Pratt, G., and Rechsteiner, M. (1987) *J. Biol. Chem.* **262,** 8303–8313
18. Sullivan, D. M., Wehr, N. B., Fergusson, M. M., Levine, R. L., and Finkel, T. (2000) *Biochemistry* **39,** 11121–11128
19. Levine, R. L., Williams, J. A., Stadtman, E. R., and Shacter, E. (1994) *Methods Enzymol.* **233,** 346–357
20. Radi, R., Beckman, J. S., Bush, K. M., and Freeman, B. A. (1991) *J. Biol. Chem.* **266,** 4244–5250
21. Netto, L. E. S., and Stadtman, E. R. (1996) *Arch. Biochem. Biophys.* **333,** 233–242
22. Kosower, E. M., and Kosower, N. S. (1995) *Methods Enzymol.* **251,** 133–148
23. Stadtman, E. R. (1993) *Annu. Rev. Biochem.* **62,** 797–821
24. Grune, T., Reinheckel, T., and Davies, K. J. A. (1995) *J. Biol. Chem.* **270,** 2344–2351
25. Grune, T., Reinheckel, T., and Davies, K. J. A. (1996) *J. Biol. Chem.* **271,** 15504–15509
26. Reinheckel, T., Sitte, N., Ullrich, O., Kuckelkorn, U., Davies, K. J. A., and Grune, T. (1998) *Biochem. J.* **335,** 637–642
27. Fratelli, M., Demol, H., Puype, M., Casagrande, S., Eberin, I., Salmona, M., Bonetto, V., Mengozzi, M., Duffieux, F., Miclet, E., Bachi, A., Vandekerckhove, J., Gianazza, E., and Ghezzi, P. (2002) *Proc. Natl. Acad. Sci. U. S. A.* **99,** 3505–3510
28. Cotgreave, I. A., and Gerdes, R. G. (1998) *Bioch. Biophys. Res. Comm.* **242,** 1–9
29. Cotgreave, I. A., and Gerdes, R. G., Schuppe-Koistinen, I., and Lind, C. (2002) *Methods Enzymol.* **348,** 175–182
30. Brooks, P., Fuertes, G., Murray, R. Z., Bose, S., Knecht, E., Rechsteiner, M. C., Hendil, K. B., Tanaka, K., Dyson, J., and Rivett, J. (2000) *Biochem. J.* **346,** 155–161
31. Russell, S. J., Steger, K. A., and Johnston, A. S. (1999) *J. Biol. Chem.* **274,** 21943–21952
32. Bellomo, G., Palladini, G., and Vairetti, M. (1997) *Microsc. Res. Tech.* **36,** 243–252
33. Bandyopadhyay, S., Starke, D. W., Mieyal, J. J., and Gronostaiski, R. M. (1998) *J. Biol. Chem.* **273,** 392–397
34. Lundberg, M., Johansson, C., Chandra, J., Enoksson, M., Jacobsson, C., Ljung, J., Johansson, M., and Holmgren, A. (2001) *J. Biol. Chem.* **276,** 26269–26275
35. Nulton-Persson, A. C., and Szweda, L. I. (2001) *J. Biol. Chem.* **276,** 23357–23361
36. Nulton-Persson, A. C., and Szweda, L. I. (2002) *Free Radic. Biol. Med.* **33,** S90
37. Toone, W. M., Morgan, B. A., and Jones, N. (2001) *Oncogene* **20,** 2336–2346
38. Acquaviva, C., Brockly, F., Ferrara, P., Bossis, G., Salvat, C., Jariel-Encontre, I., and Piechaczyk, M. (2001) *Oncogene* **20,** 7563–7572

ANEXO 19

(Manuscrito em fase final de preparação para submissão)

REDOX MODIFICATION OF 20S PROTEASOME IN *S. CEREVISIAE* IS REGULATED BY THE DETHIOLASE ACTIVITY OF GLUTAREDOXIN*

Marilene Demasi[1, §, #], Gustavo M. Silva[1,§], Felicia P. Cavalher[1,§], José A. Bárcena[2], Clelia R. A. Bertoncini[3] and Luis E. S. Netto[1]

From the [1]Departamento de Biologia, Instituto de Biociências, Universidade de São Paulo, BRASIL; [2]Departamento de Bioquímica y Biología Molecular, Universidad de Córdoba, SPAIN; [3]CEDEME, Universidade Federal do Estado de São Paulo, BRAZIL

*This work was supported by FAPESP, Fundação de Amparo à Pesquisa do Estado de São Paulo

[§]These authors contributed equally to this work

[#]To whom correspondence should be addressed. E-mail: mari_masi@hotmail.com

R. do Matão, 277. São Paulo – SP. BRASIL 05508-900

Fax. 55 11 3091 7553

Phone: 55 11 3091 7589

RUNNING TITLE: YEAST 20S PROTEASOME REDOX REGULATION

ABSTRACT

Chymotrypsin-like activity of the 20S proteasome core purified from *S. cerevisiae* is affected by the redox state of its cystein (Cys) residues. Redox alterations observed *in vitro* and *in vivo* refer to the oxidation of Cys residues (Cys-SH) to Cys-sulfenic acid (-SOH) followed, or not, by S-glutathionylation (CyS-SG). This mechanism is described for other proteins and thereafter deglutathionylation occurs through glutaredoxin activity, as attested by some few examples in the literature. In the present work we describe experiments showing that glutaredoxin2 is able to release glutathione from 20S proteasome core followed by recovering of its chymotrypsin-like activity. Experiments performed *in vivo* showed that the specific activity of 20S proteasome isolated from cells grown to stationary phase in glycerol-containing medium was 5-fold the activity found in 20S proteasome preparations isolated from cells grown to stationary phase in glucose-containing medium. These findings were positively correlated to the levels of glutaredoxin2 expression and to the reductive intracellular capability accessed by the determination of GSH/GSSG ratio at the same growth conditions. These results are in agreement with our early hypothesis that 20S core activity is regulated by redox modifications.

INTRODUCTION

Oxidation of protein Cys[1] residues to sulfenic acid (Cys-SOH) and the subsequent S-thiolation of those residues during enzyme catalysis and redox signaling have been increasingly accepted as important cofators during redox regulation (Ellis & Poole, 1997; Barrett et al, 1999; Claiborne et al, 1999 and 2001; Yang et al, 2002; Nulton-Persson & Szweda, 2001 and 2002; Demasi et al, 2003). This reversible mechanism is supposed to play a role upon enzyme catalysis and binding of transcription or replication factors to DNA targets. The advantage of this kind of regulation is the protection of Cys residues by S-glutathionylation when intracellular reductive ability is decreased, concomitantly to redox signaling effectuation.

The first step of protein-Cys-SH oxidation generates sulfenic acid (Cys-SOH), prone to S-thionylation by sulfhydryls, *e.g.* glutathione (GSH), otherwise the oxidation continuous further generating Cys-sulfinic (Cys-SO_2H) and Cys-sulfonic (Cys-SO_3) acid forms (Yang et al, 2002; Georgiou & Masip, 2003). As discussed next, reduced protein sulfhydryls are recovered by S-deglutathionylation of protein mixed disulfides and recent publications in the literature show that yeast peroxiredoxin-Cys-SO_2H forms can also be reduced *in vivo* regenerating Cys-SH (Chevallet et al, 2003; Woo et al, 2003; Biteau et al, 2003).

Many lines of investigation conducted in recent years have shown that S-deglutathionylation of protein Cys residues is an enzymatic process. Glutaredoxins (Luikenhuis et al, 1998; Shenton et al, 2002), as well as, thioredoxins (Garrido & Grant, 2002) are postulated to be directly responsible for S-dethiolation in yeast cells. The first function assigned to glutaredoxins was the reduction of the intramolecular disulfide bond in

ribonucleotide reductase of *E. coli* (Holmgren, 1976). Since that, biochemical and genetic approaches have brought out evidence for a protective role of glutaredoxins under oxidative conditions and during redox signaling, *e.g.* the GSH-dependent reduction of protein mixed disulfides by means of its so-called dethiolase or deglutathionylase activity in different eukaryote cells (Jung & Thomas, 1996; Davis et al, 1997; Bandyopadhyay et al, 1998; Luikenhuis et al, 1998; Rodríguez-Manzaneque et al, 1999; Shenton et al, 2002).

Yeast glutaredoxin isoforms consist of two dithiol proteins: Grx1 and Grx2 and three monothiol proteins: Grx3, Grx4 and, Grx5. These isoforms differ in their location inside cell and cellular response to oxidative stress (Gan, 1992; Luikenhuis et al, 1998; Rodríguez-Manzaneque et al, 1999; Grant et al, 2000; Pedrajas et al, 2002). Evidences in the literature indicate that the reduction of protein mixed disulfides in the yeast cells is a primary function of Grx2 whereas Grx1 as well as Grx5 would play a secondary role as mixed disulfide-dethiolase enzymes and may be required during certain stress conditions or after the formation of particular mixed disulfides substrates (Luikenhuis et al, 1998; Shenton et al, 2002).

In a previous report (Demasi et al, 2003) we have shown that yeast Cys-20S proteasomal residues are S-glutathionylated by reduced glutathione afterwards oxidation to Cys-SOH. Moreover, this mechanism was seen to be responsible for a decrease of proteasomal chymotrypsin-like activity. In the present work our goal was to search for an enzymatic process accounting for reduction of Cys-S-thionylated residues of the 20S proteasome core. We report that the yeast dithiolic Grx2 deglutathionylates the 20S proteasome followed by the recover of its chymotrypsin-like activity. We also found that specific proteasome chymotrypsin-like activity was positively correlated to intracellular

reductive capability and to glutaredoxin expression suggesting a coupled mechanism for the redox regulation of 20S proteasome.

EXPERIMENTAL PROCEDURES

Chemicals and reagents. Diethylenetriaminepentaacetic acid (DTPA); dithionitrobenzoic acid (DTNB); *N*-ethylmaleimide (NEM) and, fluorogenic substrate succinyl-Leu-Leu-Val-Tyr-MCA (s-LLVY-MCA) were purchased from SIGMA. 7-Chloro-4-nitrobenzo-2-oxa-1,3-diazole (NBD) was purchased from ALDRICH. Glutathione reductase (120 U/mg) was purchased from ICN. All other reagents used were of analytical grade and the water was purified with the Milli-Q system.

Cloning and expression of recombinant yeast GRX2. The cloning of yeast *GRX2* and its expression in *E. coli* are described in Pedrajas et al (2002). Grx2 purification from *E. coli* was performed by growing cells at 37 °C until an OD_{600} of 0.5 was attained; the recombinant protein was induced with 0.5 mM isopropyl β-D-thiogalactoside (IPTG), and the cells were allowed to continue growing at 37 °C for 4 h. Collection, lysis and crude extract preparation was performed as described previously (Pedrajas et al, 1999). Histidine-tagged Grx2 was purified from the extract by chromatography on a TALON® Metal Affinity Resin column (Clontech), as described previously (Pedrajas et al, 2000). Purified Grx2 was analyzed by SDS-PAGE and by 8% non-denaturing polyacrylamide gel according to the protocol enclosed in the kit of Nondenatured Protein Molecular Weight Marker from SIGMA.

Assay of Grx2 activity. Grx2 activity was determined spectrophotometrically by monitoring for 5 min the disappearance of 2 mM NADPH at 340 nm in the presence of 0.5 mM cystine (Aldrich Chemicals), 1 mM GSH and 0.5 unit of yeast glutathione reductase (ICN), at 30°C (modified from Pedrajas et al, 2002).

Yeast strains and growth. S. cerevisiae RJD1144 (MATa *his*3Δ200 *leu*2-3,112, *lys*2-801 *trp*1Δ63 *ura*3-52 *PRE*1^{FH}::*Ylplac*211 *URA*3) derived from strain JD47-13C was kindly donated by Dr. Raymond Deshaies, Division of Biology, Caltech, Pasadena, CA. This strain has the 20S proteasome Pre1 subunit tagged with the *flag* peptide sequence and a polyhistidine tail (Verma et al, 2000). Cells were cultured in minimum medium containing 2% glucose or 2% glycerol plus 2% ethanol at 30 °C for 96 h with reciprocal shaking. Cells were harvested at the optical density of the culture at 600 nm (OD_{600}) of 2.5-3.5.

Extraction and purification of the 20S proteasome. The 20S proteasome was purified by affinity chromatography according to the protocol described previously (Demasi et al, 2003) or by immunoprecipitation with the ANTI-FLAG® M2 Affinity Gel Freezer-safe (SIGMA) antibody immobilized on agarose beads according to the manufacturer's protocol.

Hydrolysis assay of the fluorogenic peptide s-LLVY-MCA - 20S proteasome (0.5-3 μg) was incubated at 37 °C in 10 mM Tris/HCl buffer, pH 7.8, containing 20 mM KCl and 5 mM $MgCl_2$, here referred to as standard buffer. Incubation was started by the addition of 10-25 μM of the peptide s-LLVY-MCA. The reaction was stopped by adding 4 volumes of 0.1 M

sodium borate, pH 9. Fluorescence emission was recorded at 430 nm (excitation at 365 nm). MCA liberated from the substrates was calculated from a standard curve of free MCA.

Oxidation and S-glutathionylation of 20S proteasome - When specified, preparations of purified 20S proteasome were treated with H_2O_2 for oxidation. Proteasome concentration in these experiments was typically 200-300 μg. The preparation was incubated for 30 min at room temperature in the presence of 5 mM H_2O_2 with 100 μM DTPA in standard buffer. After incubation, excess H_2O_2 was removed by two cycles of centrifugation and redilution with standard buffer through Microcon CM-100 filters (AMICON). An aliquot of oxidized 20S proteasome (100 μg) was incubated at room temperature for 20 min in the presence of 1-5 mM GSH. Afterwards, excess GSH was removed by cycles of centrifugation and redilution through microfilters, as described above. Aliquots of oxidized or S-gluathionylated 20S proteasome were taken for further incubation or for hydrolysis assay after determination of protein concentration.

Incubation of S-gluathionylated 20S proteasome with Grx2. S-gluathionylated 20S proteasome (20-30 μg) was incubated at 37 ^{0}C for 30-60 min in 0.2 mL standard buffer in the presence of Grx2 (0.5-1 μg) added of 2 mM NADPH, 1 mM GSH and 84 mU glutathione reductase. After incubation, Grx2, glutathione reductase and the other reagents were removed by four cycles of centrifugation and redilution in standard buffer through CM-100 microfilters, as described above. Aliquots of Grx2-treated 20S proteasome were taken for hydrolysis assay after determination of protein concentration. Control samples

(non-Grx2 incubated samples) were incubated in the same conditions in buffer containing all reagents except Grx2.

GSH determination – Intracellular GSH and GSSG extraction and determination were performed as described previously (Demasi et al, 2003).

Isolation of total RNA and semi-quantitative analysis by RT-PCR. Total RNA was extracted as described by Ausubel et al (1998). RNA was quantified by optical density measurement at 260 and 280 nm. RNA integrity was confirmed by running 1 μg RNA on a 1% agarose gel. RT-PCR analysis was performed in 20 μl reaction mixture containing 800 ng total RNA, 400 nmol foward and reverse primers, and the other reagents supplied by the cMaster RT- Plus PCR kit (Eppendorf). The reactions for c-DNA first strand synthesis were carried out according to the manufacturer's protocol (Eppendorf). The PCR primers were synthesized by Invitrogen. They were designed strictly using Primer 3 software according to the DNA sequence of the genes: *ACT 1* (Ng & Abelson, 1980), *GRX2* (Pedrajas et al., 2002) and *PRE2* (Heinemeyer et al., 1993). Table 1 summarizes sequences of the primers and the expected size of PCR products. Program parameters for one step RT-PCR were 50°C for 35 min, 94°C for 2 min followed by 40 cycles of 94°C for 15 s, followed by 58 °C for 20 s and 68°C for 35 s. PCR products were run on a 1.5% agarose gel containing ethidium bromide and the bands captured under UV by the Video Documentation System (Pharmacia). The PCR signal intensities were semi-quantified using Totalab 1D software. *GRX2* and *PRE2* volumes of densitometry measurements were normalized by *ACT1* (yeast

actin 1) band and results expressed as means ± SD. PCR products were confirmed by sequencing analysis.

Protein determination - Protein concentration was determined with the Bradford® reagent (BIORAD)

RESULTS

S-glutathionylated 20S proteasome is deglutathionylated by Grx2. We conducted the present work to investigate whether S-glutathionylated 20S proteasome is dethiolated by an enzymatic mechanism. S-glutathionylation of the proteasome catalytic subunit had been previously verified *in vitro* by H_2O_2-oxidation followed by GSH incubation of purified preparations of 20S proteasome and *in vivo* when cells were treated with H_2O_2 (Demasi et al, 2003). Based on reports in the literature indicating Grx2 as one of the enzymes responsible for a GSH-dependent dethiolase activity in the yeast cells (Luikenhuis et al, 1998), in the present work we initially tested *in vitro* the ability of recombinat Grx2 to S-dethionylate 20S proteasome preparations. To evaluate this effect, purified 20S proteasome was treated with 5 mM H_2O_2 in the presence of the iron chelator DTPA to avoid unspecific protein oxidation, followed by incubation with 5 mM GSH in order to S-glutathionylate the 20S core. These preparations were afterwards incubated in the presence of recombinant Grx2 as described in the legend of Figure 1. Preparations obtained at each step were reacted with NBD, a sulfhydryl and sulfenic acid reagent. The formation of -Cys–S-NBD, -Cys–S(O)-NBD adducts or the disappearance of those adducts was followed by spectral

characterization. As depicted in the spectra (Fig. 1A), when 20S core is oxidized with H_2O_2, there is the formation of the Cys-S(O)-NBD adduct (solid line). The sulfenic form of the 20S core Cys residues completely disappeared when H_2O_2-oxidized 20S preparations were treated with GSH (dot line). This result is consistent with the idea that in this condition Cys residues of 20S core were protected from NBD modification by S-glutathiolation. On the other hand, S-glutathionylated 20S core was almost completely reduced to Cys-SH as observed by the formation of Cys–S-NBD adduct next to incubation with Grx2 (dashed line). In all the three conditions tested the protein concentration was the same. These results are direct evidence that Grx2 is able to S-dethiolate GSH-mixed-20S proteasome disulfides.

In another set of experiments, we followed NADPH consumption as indicative of Grx2 activity upon purified 20S proteasome by incubating S-glutathionylated 20S core in the presence of Grx2 (Fig 1B). As seen, NADPH consumption was started just after the addition of Grx2 to the medium. According to the results obtained from control samples run in the same set of experiments, NADPH was not significantly consumed in the absence of either S-thionylated 20S core or of Grx2 (result not shown).

The incubation of S-glutathionylated 20S proteasome with Grx2 was followed by increased chymotrypsin-like activity that had greatly been lost after oxidation of purified 20S core preparations with H_2O_2 followed by S-thionylation with GSH (Fig. 2). As depicted in Figure 2, chymotrypsin-like activity after the oxidation of purified 20S proteasome preparations with H_2O_2 decreased to 80% the activity found in control samples whereas after S-thionylation of the same preparations the activity was decreased to less than 35% from activity found in control samples. The incubation of S-thionylated preparations with Grx2 promoted the recovering of chymotrypsin-like activity to 80% of

the activity observed in control samples. The chymotrypsin-like activity was not significantly increased after 60 min incubation in the presence of Grx2 when compared to the activity observed after 30 min of incubation (Fig 2).

This set of experiments clearly show that S-glutathionylated 20S proteasome is reduced by Grx2 (Fig 1) and that its chymotrypsin-like activity, profoundly decreased by S-thionylation, was significantly recovered after incubation with Grx2.

Role of Grx2 upon maintainance of proteasome chymotrypsin-like activity in vivo. An earlier observation from several *in vivo* experiments conducted in our laboratory had suggested to us that 20S core extracted from cells grown at different conditons of carbon source in the medium (glucose or glycerol/ethanol) or growth phases (log and stationary), presented variable specific chymotrpsyn-like activity (concentration of MCA release / mg proteasomal protein / min). Our hypothesis for that was the correlation between proteasomal activity and intracellular reductive capability, as we had already observed upon H_2O_2-cell treatment (Demasi et al, 2003). To test this hypothesis, in the present work we determined GSH content and GSH/GSSG ratio from cells grown to stationary phase in glucose- and glycerol/ethanol – containing medium as a parameter of intracellular reductive capability and to demonstrate *in vivo* the role of Grx2 upon maintenaince of proteasomal activity by keeping it in the reduced form, we determined *GRX2* expression, concomitantly to the determination of specific proteasomal activity. All these experiments were conducted by growing cells to the stationary phase in glucose and glycerol/ethanol-containing media. The cells were grown for 96 h and monitored by a growth curve (result not shown).

We found that the specific activity of purified 20S proteasome obtained from cells grown in glycerol/ethanol was 5-fold the specific activity of those preparations obtained

from cells grown in glucose-containing medium (Table 2). As a control of proteasome levels, its expression in both conditions, glucose and glycerol/ethanol, was evaluated by RT-PCR accessed by the expression of *PRE2* gene encoding the Pre2 catalytic subunit (Fig. 3). According to these results, *PRE2* expression did not vary in both conditions. On the other hand, *GRX2* expression verified in cells grown in glycerol / ethanol-containing medium was two-fold the expression observed when cells were grown in glucose-containing medium (Fig. 3). These results were accompanied by increased GSH/GSSG ratio (Table 2) in the same growth condition where *GRX2* expression and proteasomal activity were augmented (Fig. 3 and Table 2, respectively). GSH/GSSG ratio obtained from cells grown in glycerol/ethanol – containing medium was at least 2-fold the ratio found in cells grown in glucose whereas total glutathione levels were found to be 30% higher in cells grown in glycerol/ethanol (Table 2). Taken together, these results are indicative of the higher reductive ability of cells grown in glycerol/ethanol-containing medium most probably due to the fact that *GSH1*, the gene encoding the enzyme that catalyzes the rate limiting step in GSH synthesis, is repressed by glucose (Maris et al, 2001).

As known, expression of several antioxidant enzymes is repressed by glucose (reviewed by Jamieson, 1998 and Moradas-Ferreira & Costa, 2000). When glucose is consumed from the culture medium yeast cells suffer great physiological and biochemical changes in order to produce ATP mainly by oxidative phosphorylation with consequent ROS generation besides of the lower levels of antioxidant enzymes expression. Thus, it is expected decreased intracellular reductive capacity during growth into glucose-containing medium. Therefore, by changing the carbon source in the media, bioenergetics of yeast is profoundly affected as well as the antioxidant parameters, as herein reported for cells grown into glycerol-containing medium. Most likely, this is the reason we found a positive

correlation among proteasomal activity, total glutathione concentration, GSH/GSSG ratio and Grx2 expression (Table 2).

We also tested the effect of recombinant Grx2 upon the activity of 20S proteasome purified from cells grown as described above. Proteasomal activity determined in 20S proteasome preparations obtained from cells grown in glucose was 85% higher after incubation with recombinant Grx2 than specific activty obtained from Grx2 non-treated preparations (Table 2). On the other hand, specific activity determined in preparations obtained from cells grown in glycerol/ethanol was less than 10% increased after incubation with Grx2 (Table 2). These results are an evidence that 20S proteasome extracted from cells grown in glucose-containing medium are most likely more S-thiolated than samples extracted from cells grown in glycerol. Moreover, these data are in agreement with *GRX2* expression and GSH/GSSG ratio obtained from cells grown in same conditions (Fig. 3 and Table 2, respectively).

Taken together, present results show that intracellular reductive capability between both cellular growth conditions was quite different. Moreover, intracellular reductive parameters (GSH content, GSH/GSSG ration and *GRX2* expression) were found to be positively correlated to chymotrypsin-like proteasome activity. The finding that 20S core extracted from cells grown in glucose medium had its chymotrypsin-like activity increased 85% after incubation with Grx2 (Table 2) is an indicative of more susceptible oxidative environment in cells grown in glucose than in glycerol-containing medium. In the latter condition, extracted 20S proteasome showed only 10% increased chymotrypsin-like activity after incubation with Grx2 (Table 2). According to our hypothesis, reductive cell ability, Grx2 function and proteasome activity are coupled mechanisms inside cells.

DISCUSSION

Our conclusion from a previous work (Demasi et al, 2003) was that reductive intracellular environment was positively associated to the chymotrypsin-like proteasomal activity. In the present work our goal was to extend this observation and search for other intracellular redox parameters associated to the modulation of 20S proteasome chymotrypsin-like activity. According to reports in the literature, Grx2 is responsible for the GSH-dependent dethiolase activity of most protein mixed-disulfides (Luikenhuis et al, 1998). We started this investigation trying the dithiolic glutaredoxin Grx2 and the monothiolic Grx5 as possible dethiolase enzymes of S-glutathionylated 20S core. Our results showed that only Grx2 was able to recover chymotrypsin-like proteasomal activity of S-glutathionylated 20S proteasome. Grx2 was also able to dethiolate 20S proteasomal mixed disulfides generated by cysteine or by the GSH precursor, γ-glutamyl-cysteinyl (results not shown). Although reports in the literature have shown dethiolase activity of the monothiolic glutaredoxin Grx5 upon protein-mixed disulfides (Shenton et al, 2002), we have not found *in vitro* any effect on the chymotrypsin-like proteasomal activity when purified preparations of S-glutathionylated 20S proteasome were incubated with Grx5 extracted and purified from yeast cells (result not shown), as seen when S-glutathionylated proteasome preparations were incubated in the presence of Grx2 (Fig 2).

The GSH-dependent dethiolase Grx2 activity upon the maintenance of 20S proteasomal activity by a redox mechanism may be dependent *in vivo* on GSH/GSSG ratio. Most probably, at the intracellular level Grx2 coupled to the reduced glutathione pool, variable according to GSH/GSSG ratio oscillation, might be responsible for the redox

regulation of 20S proteasomal activity. Accordingly, our results showed a positive correlation among these parameters as reported in Table 2.

One question raised from present study was how is the mechanism by which Grx2 exerts its dethiolase effect upon such a complex protein structure like is the 20S proteasome. Pedrajas et al (2002) have demonstrated that Grx2 of the yeast *S. cerevisiae* is expressed in two isoforms localized into mitochondria and cytosolic fraction. These isoforms differ in an N-terminal extension targeting to mitochondria and consequently they differ in their size: 15.9 and 11.9 kDa. Both isoforms were found in mitochondria. On the other hand, only the long form is prominent in microsomes and the short one in the cytosol. It was not demonstrated so far whether the cytosolic form would result from differential processing of one single translation product or by different initiation codon. Anyway, both isoforms might interact to the proteasome considering its distribution inside yeast cell (Enenkel et al, 1998). In the present study, recombinant Grx2 assayed *in vitro* was the 11.9 kDa and according to the results obtained from non-denaturing gel electrophoresis this Grx2 isoform is a dimer complex (results not shown). The dimer may present a globular shape able to get into the 20S chamber, interact with those S-thionylated Cys residues and afterwards get out the chamber. On that, Grx2 was completely rescued after its incubation with S-glutathionylated 20S proteasome (same conditions described in Figure 1B), according to results obtained from SDS-PAGE (not shown). These data demonstrated that Grx2 neither bound covalently to the proteasome nor was degraded by it. To confirm the degradative ability of 20S proteasome peparations utilized in the present work, we run in parallel samples of 20S proteoasome incubated with cytochrome c, a low molecular weight protein, and in this case we detected significant lower concentration of this protein on SDS-PAGE gels. This result suggests that cytochrome c was degraded by the proteasome since

no alteration on its concentration on the gel was detected when the incubation was performed in the presence of the proteasome inhibitor lactacystin (result not shown).

Our hypothesis based on studies conducted so far (Demasi et al, 2003 and present work) is that redox modulation of 20S proteasome is a widespread mechanism, most likely involving different sulfhydryl compounds, such as Cys, γ-GluCys and GSH depending on their availability inside cell, as well as, the S-dethionylation may be performed by different enzymes as earlier postulated for other mixed disulfides protein complexes (Garrido & Grant, 2002). Thioredoxin (Trx) systems are supposed to play an S-dethiolase role as glutaredoxins do (Garrido & Grant, 2002). On that, preliminary results showed that yeast recombinant Trx1 and Trx2 tested in the presence of NADPH and yeast recombinant thioredoxin reductase showed similar ability *in vitro* to rescue chymotrypsin-like activity of S-glutathionylated 20S proteasome core (results not shown). This result was considered as indicative of the ability of Trx1 and Trx2 to reduce S-thionylated 20S proteasome as here demonstrated for Grx2 (Fig 1). These studies are subjects of our ongoing investigations.

Extensive protection of protein Cys residues from oxidation has been demonstrated by recent findings showing the existence of a sulfinic reductase, named sulphoredoxin. This enzyme reduces Cys-SO_2H residues from the yeast family of peroxiredoxins (Biteau & Masip, 2003). Although we have not demonstrated further oxidation of 20S proteasome Cys-SOH, but only S-thionylation, we believe on the occurrence of other 20S proteasome Cys-oxidized forms, as well. On that, our hypothesis is that many mechanisms inside yeast cells participate on redox regulation of the 20S core and these remain subjects of future studies.

Bibliography

Ausubel, FM, Brent, R, Kingston, RE, Moore, DD, Geidman, JG, Smith, AJ and Struhl, K (1998) **In:** *Current Protocols in Molecular Biology.* Ed. John Wiley & Sons Inc., New York, USA

Bandyopadhyay, S, Starke, DW, Mieyal, JJ, and Gronostajski, RM (1998) *J Biol Chem* **273,** 392-397

Barrett, W.C., DeGnore, J.P., Keng, Y.F., Zhang, Z.Y., Yim, M.B., and Chock, P.B. (1999) *J. Biol. Chem.* **274,** 34543-34546

Biteau, B, Labarre, J, and Toledano, MB (2003) *Nature* **425:** 980-984

Chevallet, M, Wagner, E, Luche, S, van Dorsselaer, A, Leize-Wagner, E, Rabilloud, T. (2003) *J Biol Chem.* **278,** 37146-37153.

Claiborne, A., Yeh, J.I., Mallett, T.C., Luba, J., Crane, E.J., Charrier, V., and Parsonage, D. (1999) *Biochemistry* **38,** 15407-15416

Claiborne, A., Mallett, T.C., Yeh, J.I., Luba, J., and Parsonage, D. (2001) *Adv. Prot. Chem.* **58,** 215-276

Davis, DA, Newcomb, FM, Starke, DW, Ott, DE, Mieyal, JJ, and Yarchoan, R (1997) *J Biol Chem* **272,** 25935-25940

Demasi, M, Silva, GM, and Netto, LES (2003) *J Biol Chem* **278,** 679-685

Ellis, H.R. and Poole, L.B. (1997) *Biochemistry* **36,** 15013-15018

Enenkel, C, Lehmann, A, Kloetzel, PM. (1998) *EMBO J.* **17**:6144-54.

Gan, ZR (1992) *Biochem Biophys Res Commun* **187,** 949-955

Garrido, EO and Grant, CM (2002) *Mol Microbiol* **43,** 993-1003

Georgiou, G & Masip, L (2003) *Science* **300:** 592-594

Grant, CM, Luikenhuis, S, Beckhouse, A, Soderbergh, M and Dawes, IW (2000) *Biochem Biophys Acta* **1490:** 33-42

Heinemeyer, W, Gruhler, A, Mohrle, V, Mahe, Y, and Wolf, DH. (1993) *J Biol Chem.* **268,** 5115-5120.

Holmgren, A (1976) *Proc Natl Acad Sci USA* **73,** 2275-2279

Jamieson, D.J. (1998) *Yeast* **16**:1511-1527

Jung, CH and Thomas, JA (1996) *Arch Biochem Biophys* **335,** 61-72

Luikenhuis, S, Perrone, G, Dawes, IW, and Grant, CM (1998) *Mol Biol Cell* **9,** 1081-1091

Maris AF, Assumpcao AL, Bonatto D, Brendel M, Henriques JA. (2001). *Curr Genet.* **39:** 137-49.

Moradas-Ferreira, P., and Costa, V. (2000) *Redox Rep.* **5**: 277-285.

Ng, R. and Abelson, J. (1980) *Proc Natl Acad Sci U S A.* **77,** 3912-3916.

Nulton-Persson, A.C. and Szweda, L.I. (2001) *J. Biol. Chem.* **276** 23357-23361

Nulton-Persson, A.C. and Szweda, L.I. (2002) *Free Rad. Biol. Med.* **33,** S90

Pedrajas, JR, Kosmidou, E, Miranda-Vizuete, A, Gustafsson, JÁ, Wright, AP and Spyrou, G (1999) *J Biol Chem* **274:** 6366-6373

Pedrajas, JR, Miranda-Vizuete, A, Javanmardy, N, Gustafsson, JÁ and Spyrou, G (2000) *J Biol Chem* **275:** 16296-16301

Pedrajas, JR, Porras, P, Martínez-Galisteo, E, Padilla, CA, Miranda-Vizuete, A, and Bárcena, JA (2002) *Biochem J* **364,** 617-623

Rodríguez-Manzaneque, MT, Ros, J, Cabiscol, E, Sorribas, A, and Herrero, E (1999) *Mol Cel Biol* **19,** 8180-8190

Shenton, D, Perrone, G, Quinn, KA, Dawes, IW, and Grant, CM (2002) *J Biol Chem* **277,** 16853-16859

Yang, K.S., Kang, S.W., Woo, H.A., Hwang, S.C., Chae, H.Z., Kim, K., and Rhee, S.G. (2202) *J. Biol. Chem* **277,** 38029-38036.

Verma, R., Chen, S., Feldman, R., Schieltz, D., Yates, J., Dohmen, J., and Deshaies, R.J. (2000) *Mol. Biol. Cell* **11,** 3425-3439

Woo, HA, Chae, HZ, Hwang, SC, Yang, KS, Kang, SW, Kim, K, Rhee SG. (2003) *Science* **300,** 592-594

FOOTNOTES

[1]Abbreviations used are: Cys, cysteine; Cys-SOH, cysteine sulfenic acid; Cys-SO_2H, cysteine sulfinic acid; Cys-SO_3H, cysteine sulfonic acid; DTNB, dithionitrobenzoic acid; DTPA, diethylenetriaminepentaacetic acid; Grx, glutaredoxin; GSH, glutathione; GSSG, oxidized glutathione; γ-GluCys, γ-glutamyl-cysteinyl; IPTG, isopropyl β-D-thiogalactoside; NBD, 7-Chloro-4-nitrobenzo-2-oxa-1,3-diazole; NEM, *N*-ethylmaleimide; s-LLVY-MCA, succinyl-Leu-Leu-Val-Tyr-MCA; SO_2H-Rx, sulphoredoxin; ROS, Reactive Oxygen Species; Trx, thioredoxin

Table 1 –Sequences of primers used in RT-PCR analysis of *ACT1*, *GRX2* and *PRE2* mRNA

GENE	Acession	Sequence	Location	Size of PCR products (pb)
ACT1	L00026	TGTCACCAACTGGGACGATA	675	
	gi:170985	CCAAACCCAAAACAGAAGGA	1258	584
GRX2	YDR513W	ATCACGTTGTTTGCCACAAG	49	
	gi:|37362627	GTTACCACCAATGTGCTTGC	366	318
PRE2	X6866	ATTCTGCGTTGGTTCAGGTC	979	
	gi:4220	TCCTCTTCCTTGACCTTCCA	1212	234

Table 2 – Proteasomal activity and antioxidant parameters at stationary phase of yeast cells grown in glucose- and glycerol-containing medium

	Glucose	*Glycerol*
GSH/GSSG	40 ± 7	91.5 ± 15*
Total GSH (μmoles / g wet pellet)	6.6 ± 2.0	9.2 ± 1.5*
[1]20S proteasomal specific activity (MCA μmoles x min^{-1} x mg^{-1})	35 ± 1.5	192 ± 22*
[2]Grx2 effect upon20S proteasome (MCA μmoles x min^{-1} x mg^{-1})	65 ± 3	211 ± 25*

Cells were grown in minimum medium containing 2% glucose or 2% glycerol plus 2% ethanol and harvested after 96-h incubation. At both conditions, cell incubation started at OD_{600} of 0.1. Glutathione determination is described in Demasi et al (2003). [1, 2]20S proteasome was purified from cell extracts by immunoprecipitation with the ANTI-FLAG system and assayed for hydrolysis (0.5-1 μg) by incubation in the presence of fluorogenic substrate. [1]Results shown refer to hydrolysis assay performed immediately after 20S proteasome purification from cells grown at the specified conditions. [2]Prior to incubation with the fluorogenic substrate, purified 20S proteasome (20-30 μg) was incubated for 60 min at 37 °C in standard buffer containing 0.75 mM GSH, 2 mM NADPH, 84 mU glutathione reductase and recombinant Grx2 (1-2 μg). After incubation, all reagents were washed out by 4 cycles of centrifugation and redilution in standard buffer. Final suspension was assayed for hydrolysis. All results shown are means ± SD of 3-4 independent experiments. *p at least ≤ 0.0021

Fig. 1. 20S Proteasome deglutathionylation by Grx2 according to NBD-modified 20S proteasome Cys residues. **(A)** The Cys-S(O)-NBD conjugate (solid line) was generated by incubating 20S proteasome (300 μg) in standard buffer with H_2O_2/DTPA, as described in Materials and Methods, followed by resuspension in 5 M guanidine and incubation with NBD. An aliquot (100 μg) of oxidized-20S proteasome was taken for incubation with GSH. After removing GSH by cycles of filtration and redilution through Microcon CM-100 filters, S-glutathionylated-20S proteasome was resuspended in 5 M guanidine and incubated with NBD (dot line). The Cys–S-NBD conjugate (dashed line) was generated by incubation of S-glutathionylated 20S proteasome (50 μg) for 30 min with Grx2 (1 μg), as described in Materials and Methods, followed by NBD treatment after 20S proteasome denaturation in 5 M guanidine. Incubation with 5 M guanidine solution buffered in 50 mM Tris/HCl, pH 7.5, was performed in order to denature 20S proteasome prior to NBD incubation. Samples were incubated with 100 μM NBD for 30 min in the dark at room temperature. After incubation, excess NBD was washed out by 4 cycles of filtration and redilution through Microcon CM-10 filters. Spectra were recorded with a HITACHI spectrophotometer. Results shown are representative of 3 independent experiments of three independent proteasome purifications. **(B)** Purified 20S proteasome preparations were treated with H_2O_2 followed by GSH as described above. Afterwards, 5 μg of S-glutathionylated proteasome were incubated in the presence of 0.75 mM GSH and 2 mM NADPH followed by the addition of 1 μg recombinant Grx2, as indicated. NADPH disappearance was followed spectrophotometrically, as shown.

Fig. 2. Chymotrypsin-like activity of S-glutathionylated 20S proteasome was rescued after incubation with recombinant Grx2. Purified 20S proteasome preparations were treated with H_2O_2 and GSH at same conditions as per Fig 1. Afterwards, 5 μg of S-glutathionylated proteasome were incubated at 37 °C for 30 and 60 min in the presence of 0.75 mM GSH, 2 mM NADPH and 1 μg recombinant Grx2. After incubation, all the reagents were washed out by three cycles of filtration and redilution through Microcon CM-100 filters, followed by the hydrolytic activity assay with the s-LLVY-MCA substrate, as described in Materials and Methods. Results shown are means ± standard deviation and represent six independent experiments.

*p = 0.000012, compared to S-glutathionylated samples not incubated with Grx2.

Fig.3. Analysis by RT-PCR of the expression of GRX2 and PRE2 in cells grown to stationary phase in glucose- and glycerol-containing medium. Cells were grown for 96 h in minimal medium containing glucose or glycerol / ethanol as described in Materials and Methods **(A)** Expression of *GRX2* and *PRE2* proteasomal subunit were evaluated by RT-PCR as described in Materials and Methods. Blots shown are representative of 4 independent experiments. Expression of *ACT1* was used as Control. **(B)** Values shown in the plot are given as relative RNA expression of the *GRX2* and *PRE2* genes *versus* the expression of *ACT1* gene. Results are expressed as means ± SD of 4 independent experiments.

*p = 0.00068

FIGURE 1

A

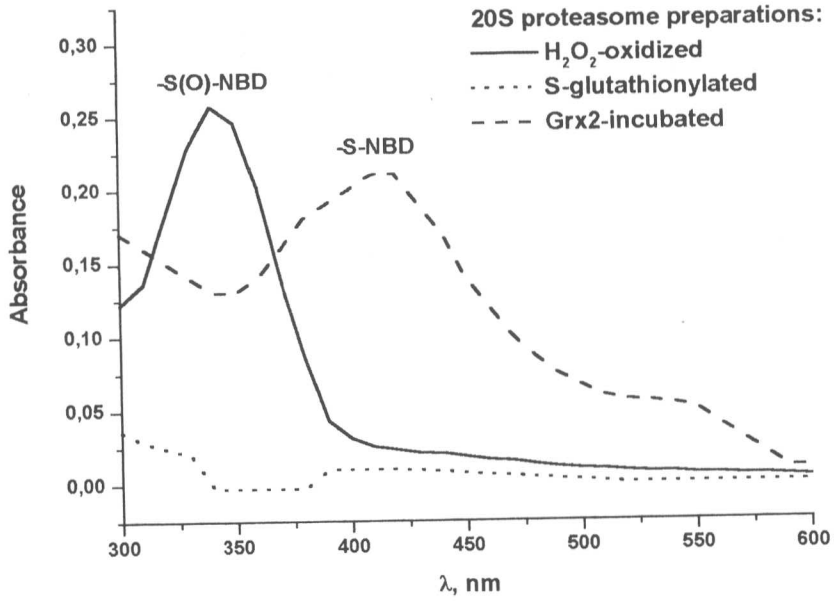
20S proteasome preparations:
H_2O_2-oxidized
S-glutathionylated
Grx2-incubated
-S(O)-NBD
-S-NBD
Absorbance
0,30
0,25
0,20
0,15
0,10
0,05
0,00
300
350
400
450
500
550
600
λ, nm

B

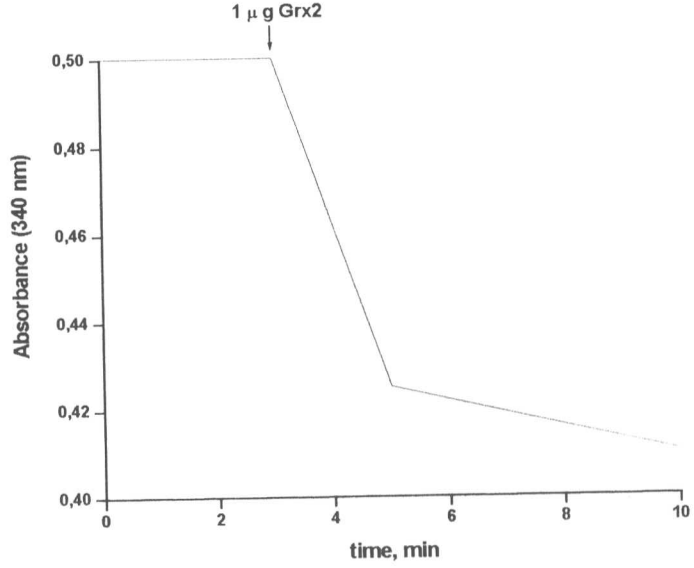
1 μ g Grx2
Absorbance (340 nm)
0,50
0,48
0,46
0,44
0,42
0,40
0
2
4
6
8
10
time, min

FIGURE 2

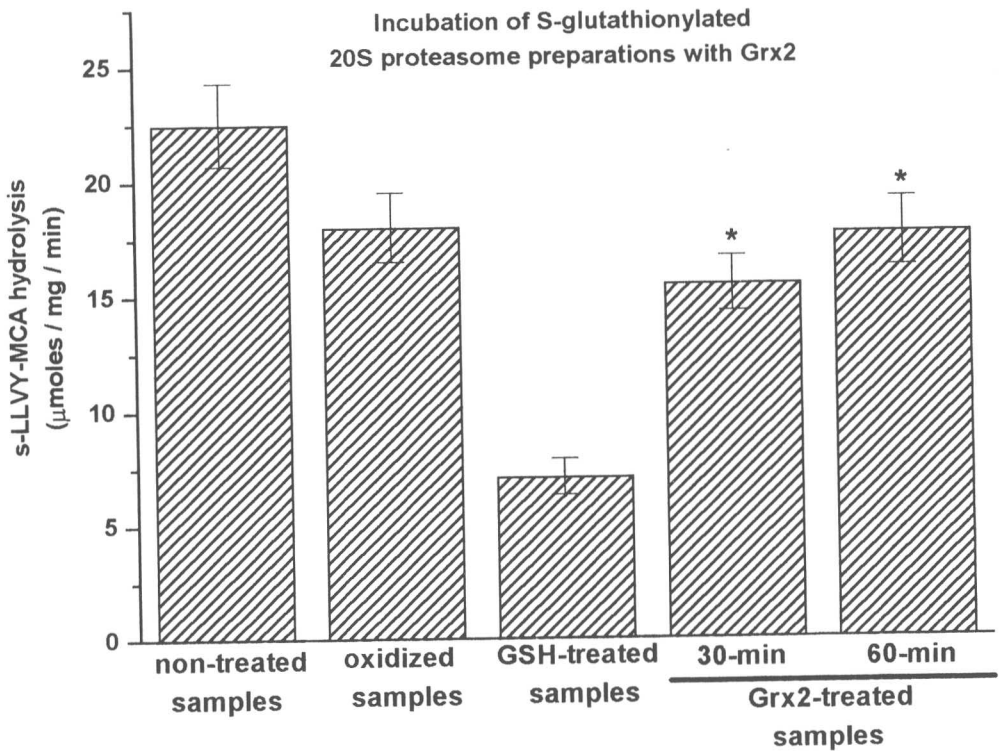
Incubation of S-glutathionylated
20S proteasome preparations with Grx2
s-LLVY-MCA hydrolysis
(μmoles / mg / min)
25
20
15
10
5
0
*
*
non-treated samples
oxidized samples
GSH-treated samples
30-min
60-min
Grx2-treated samples

FIGURE 2

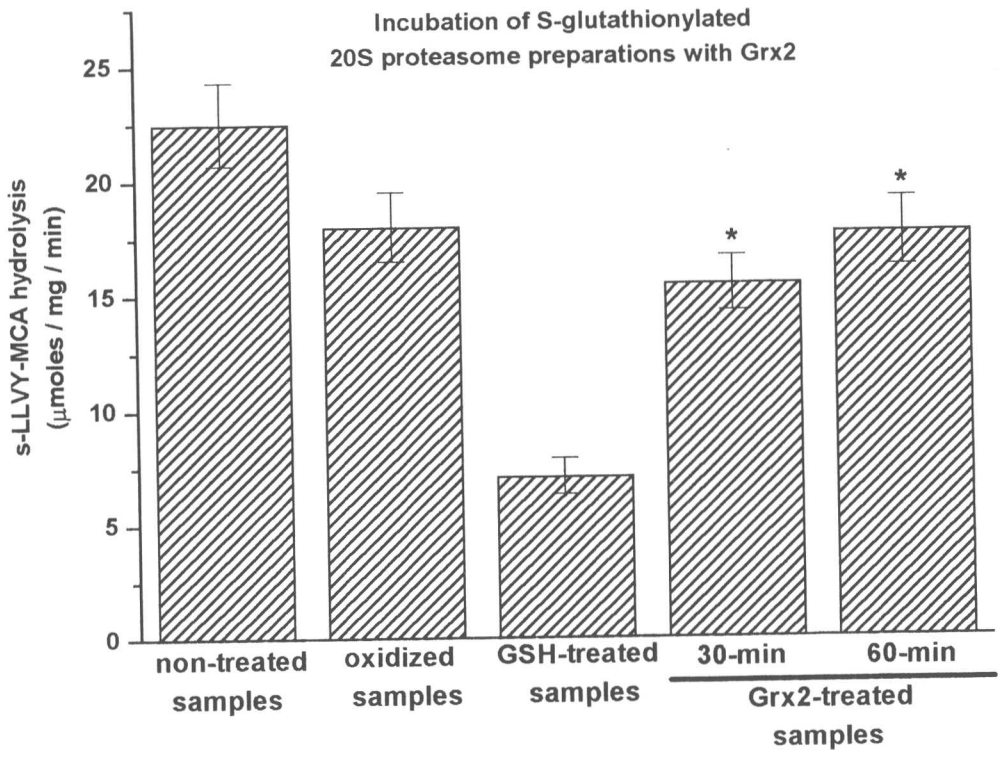
Incubation of S-glutathionylated
20S proteasome preparations with Grx2
s-LLVY-MCA hydrolysis
(μmoles / mg / min)
25
20
15
10
5
0
*
*
non-treated samples
oxidized samples
GSH-treated samples
30-min
60-min
Grx2-treated samples

FIGURE 3

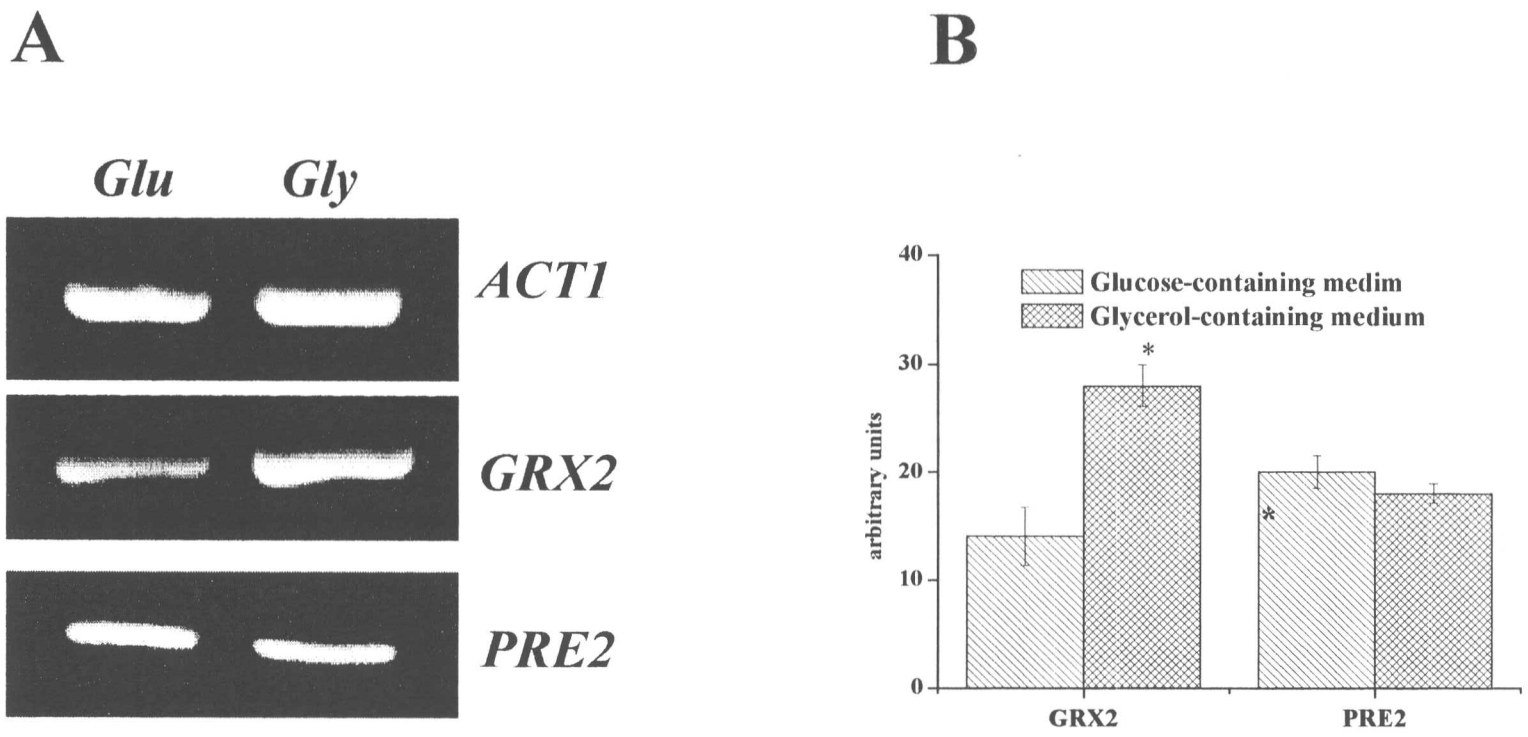
A
Glu
Gly
ACT1
GRX2
PRE2
B
40
30
20
10
0
arbitrary units
Glucose-containing medim
Glycerol-containing medium
*
*
GRX2
PRE2

CAPÍTULO 5

Perspectivas

No ano de 2001, meu grupo se juntou a Rede de Biologia Molecular Estrutural (SmolBNet), coordenada pelo Centro de Biologia Molecular Estrutural do Laboratório Nacional de Luz Sincontron e financiada pela FAPESP. Estou muito empolgado com esse programa e acredito que o mesmo possibilitará um grande salto qualitativo dos trrabalhos a serem gerados, ao possibilitar relacionar dados de estruturais e funcionais.

Mesmo antes do programa SmolBNet, já estava interessado com a possibilidade de realizar estudos relacionando estrutura com função de proteínas. Nesse sentido, iniciei colaboração com o Dr. Fabio de Almeida da UFRG no sentido de resolver a estrutura de proteínas por ressonância paramagnética nuclear (NMR). Nossos estudos se centraram nas proteínas Trx1 e Trx2 pelo fato de serem bastante solúveis, ter protocolo de purificação bastante simples e serem de baixo peso molecular. Dessa forma, utilizando Trx2 como objeto de estudo, tive a oportunidade ser co-autor de um artigo do Dr. Fabio C.L. Almeida que representou um avanço em estudos de Genômica Estrutural (anexo 20). Nesse artigo, um método é apresentado para ter idéia se as ressonâncias de uma proteína em extrato celular são promissoras para estudos posteriores de NMR. Esse protocolo baseia-se no uso de rimpaficina para inibir a síntese de proteínas não recombinantes, aumentando a marcação de proteínas recombinantes por isótopos ^{15}N e ^{13}C.

Journal of Magnetic Resonance 148, 142–146 (2001)
doi:10.1006/jmre.2000.2213, available online at http://www.idealibrary.com on IDEAL®

ANEXO 20

Selectively Labeling the Heterologous Protein in *Escherichia coli* for NMR Studies: A Strategy to Speed Up NMR Spectroscopy

F. C. L. Almeida,*[,1] G. C. Amorim,* V. H. Moreau,* V. O. Sousa,* A. T. Creazola,* T. A. Américo,* A. P. N. Pais,* A. Leite,† L. E. S. Netto,‡ R. J. Giordano,§ and A. P. Valente*[,1]

*Centro Nacional de Ressonância Magnética Nuclear, Departamento de Bioquímica Médica, ICB, CCS, Universidade Federal do Rio de Janeiro–UFRJ, Cidade Universitária, Rio de Janeiro, RJ 21941-590, Brazil; †Universidade de Campinas UNICAMP, Campinas, SP, Brazil; ‡Instituto de Biologia, Universidade de São Paulo–USP, São Paulo, SP, Brazil; and §M.D. Anderson Cancer Center, GU Medical Oncology Department, University of Texas, Houston, Texas

Received June 27, 2000

Nuclear magnetic resonance is an important tool for high-resolution structural studies of proteins. It demands high protein concentration and high purity; however, the expression of proteins at high levels often leads to protein aggregation and the protein purification step can correspond to a high percentage of the overall time in the structural determination process. In the present article we show that the step of sample optimization can be simplified by selective labeling the heterologous protein expressed in *Escherichia coli* by the use of rifampicin. Yeast thioredoxin and a coix transcription factor Opaque 2 leucine zipper (LZ) were used to show the effectiveness of the protocol. The $^{1}H/^{15}N$ heteronuclear correlation two-dimensional NMR spectrum (HMQC) of the selective ^{15}N-labeled thioredoxin without any purification is remarkably similar to the spectrum of the purified protein. The method has high yields and a good $^{1}H/^{15}N$ HMQC spectrum can be obtained with 50 ml of M9 growth medium. Opaque 2 LZ, a difficult protein due to the lower expression level and high hydrophobicity, was also probed. The ^{15}N-edited spectrum of Opaque 2 LZ showed only the resonances of the protein of heterologous expression (Opaque 2 LZ) while the ^{1}H spectrum shows several other resonances from other proteins of the cell lysate. The demand for a fast methodology for structural determination is increasing with the advent of genome/proteome projects. Selective labeling the heterologous protein can speed up NMR structural studies as well as NMR-based drug screening. This methodology is especially effective for difficult proteins such as hydrophobic transcription factors, membrane proteins, and others. © 2001 Academic Press

Key Words: NMR; Opaque 2; rifampicin; selective labeling; thioredoxin.

INTRODUCTION

Protein NMR[2] studies need high protein concentration and purity. Purification of proteins that behave well in solution is straightforward. On the other hand, some proteins can aggregate and be very difficult to handle in solution. The majority of proteins in the cell can be difficult and the methodology used to deal with them needs improvement. For those proteins, purification can be the most time-consuming step for structure determination by NMR. Poor yields during purification and protein aggregation are problems that often occur and can be avoided by working with salt, pH, and temperature and sometimes by the addition of cosolvents or even by making protein complexes.

Protein expression in the presence of rifampicin enables labeling of only the heterologous proteins. This occurs since cells self protein synthesis is inhibited but not heterologous expression. Rifampicin binds to the bacterial β-subunit of RNA polymerase, inhibiting transcription initiation (*1*). On the other hand, rifampicin does not inhibit T7 RNA polymerase, which is used for expression of the heterologous protein. This is a well-known methodology for labeling with specific amino acids (*2, 3*).

The present work shows a simple and cheap methodology using rifampicin to simplify NMR sample optimization for structural determination. The growth is done in nonlabeled M9 medium. Rifampicin is added, inhibiting the cell self protein synthesis. The cells are then pelleted and resuspended in ^{15}N-labeled M9 medium with isopropyl-β-D-thiogalactopyranoside (IPTG) and rifampicin. The use of rifampicin in the M9 medium with IPTG permits the selective labeling of protein with heterologous expression. The labeling was monitored by the comparison of the proton spectrum and the $^{1}H/^{15}N$ HMQC spectrum. Yeast thioredoxin type 2 (*4*) (TRX, 12 kDa) and Opaque 2 leucine zipper (LZ, 9 kDa), a transcription factor from coix (*5*), were used to test the rifampicin protocol. The nonpurified NMR samples showed a HMQC spectrum that was remarkably similar to those of the purified protein and consistent with the expected properties.

[1] To whom correspondence should be addressed at Av. Brigadeiro Trompowiski s/n, CCS-ICB, Bloco E sala 10, Cidade Universitaria, Rio de Janeiro, RJ 21941-590, Brasil. Fax: (5521) 2708647. E-mail: valente@cnrmn.bioqmed.ufrj.br; fameida@cnrmn.bioqmed.ufrj.br.

[2] Abbreviations used: HMQC, heteronuclear multiple quantum coherence; NMR, nuclear magnetic resonance; TPPI, time proportional phase increment; TRX, thioredoxin.

1090-7807/01 $35.00

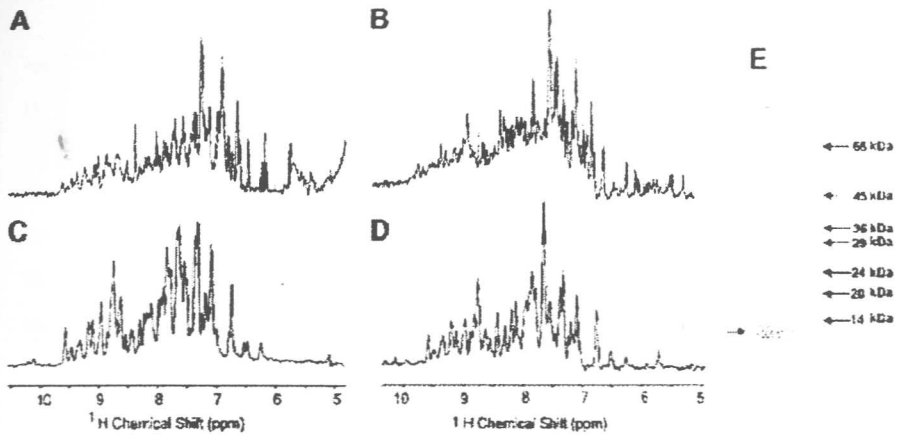

FIG. 1. ^{1}H spectra (A, B) and ^{15}N-edited ^{1}H spectra (C, D) of TRX. Spectra of purified TRX are shown in A and C. The samples obtained using rifampicin protocol samples are shown in B and D. E shows the SDS–PAGE of the rifampicin NMR sample, the same as spectra B and D.

RESULTS

The effectiveness of the rifampicin protocol was tested by comparing the spectra of purified and nonpurified TRX, prepared using the rifampicin protocol. The comparison of the ^{1}H spectrum and the one edited for ^{15}N enables the evaluation of the selectiveness of the labeling, since ^{1}H spectra will show the resonances from all proteins in the cell and the edited spectrum will show resonances only from the labeled protein. In Fig. 1 we show the ^{1}H spectra of the purified TRX and the sample obtained with the rifampicin protocol. Several proton resonances show up in the sample prepared with rifampicin (Fig. 1B) when compared with the purified TRX (Fig. 1A), since resonances from cell self proteins also appear in this spectrum. Different results are obtained for the ^{15}N-edited spectra (Figs. 1C and 1D). The spectra in Figs. 1C and 1D are remarkably similar, showing that the use of rifampicin methodology stops cell self protein synthesis and enables the ^{15}N labeling of, exclusively, TRX.

Figure 2 confirms the observation in Fig. 1 but with more details. The two-dimensional HMQC of the purified TRX (Fig. 2A) is almost the same as the nonpurified TRX (Fig. 2B). The threshold was set low in spectrum B to show the absence of weak extra peaks. The spectra of the purified TRX were obtained from 1 L of growth medium and the one with rifampicin was obtained with 50 mL (see the legend to Fig. 2 for experimental details).

As shown in the SDS–PAGE in Fig. 1E, TRX has a high expression level. It may represent more than 50% of all proteins in the cell. Since in an NMR spectrum the low-molecular-weight proteins give rise to the most intense peaks, it is expected that the spectra of the TRX grown always in labeled media has the great majority of peaks from TRX. The spectrum in Fig. 2C shows this important control. The supernatant of the lysed cells grown all the time in ^{15}N-labeled M9 shows that several proteins other than TRX are also labeled (Fig. 2C). Of course, TRX resonances are clearly prominent. However, several extra peaks also appear in the amide region. This control shows the importance of using rifampicin to get selectivity in the labeling of the heterologous protein even if the protein is well behaved in solution and the clone has very high expression levels.

It is important to show the effectiveness of the rifampicin protocol for a difficult protein. Opaque 2 LZ is a transcription factor from coix (*5*). This protein has an unknown structure. It is a leucine zipper with a probable coiled coil structure. It is highly hydrophobic and the expression yield is low. The rifampicin protocol was performed and a step of ultrafiltration was included for sample concentration and semi-purification. The Opaque 2 LZ is 9 kDa and passes through the 30-kDa membrane and is retained in the 3.5 kDa membrane (Fig. 3C).

The material retained in the 3.5-kDa membrane (where Opaque 2 LZ is present) was checked for ^{15}N labeling. The differences between the ^{1}H and ^{1}H/^{15}N HMQC spectra clearly show that the heterologous protein is the one that is being labeled (Fig. 3). The SDS–PAGE in Fig. 3C shows that even after ultrafiltration steps, the sample has several proteins other than Opaque 2 LZ.

The two-dimensional ^{1}H/^{15}N HMQC spectrum (Fig. 4) is consistent with a leucine zipper, with low dispersion similar to GCN4 (*6*) although the protein has a sign of partial aggregation. At this moment, we are improving sample conditions. This protein has 86 amino acids and we can count approximately 70 cross peaks (Fig. 4). It is important to mention that there are no cross peaks from free amino acids or small peptides, since the sample was ultrafiltrated in a membrane of 3.5-kDa molecular weight cutoff.

Another way to control the selectiveness of the labeling is to check the presence of labeled proteins with higher molecular weights (retained on the 30-kDa cutoff ultrafiltration membrane). When the induction is performed in the presence of rifampicin, no ^{15}N signal could be measured in the sample retained in the 30-kDa membrane (Fig. 5B). In contrast, in the

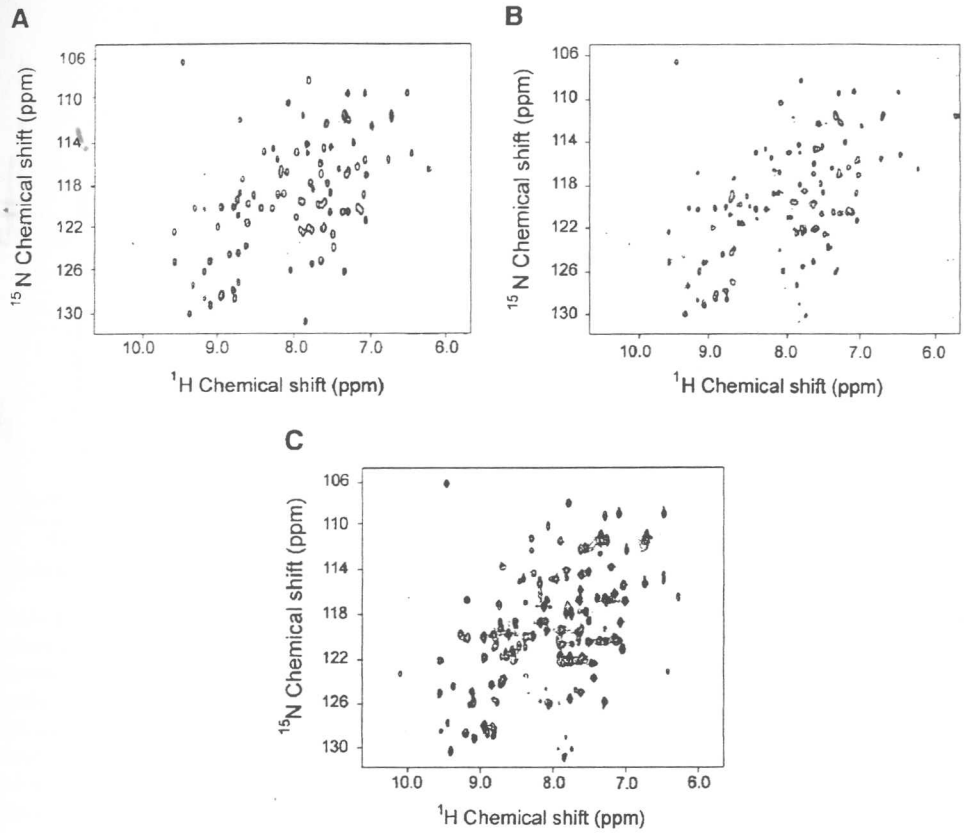

FIG. 2. Two-dimensional ^{15}N, ^{1}H-HMQC spectra of TRX. Purified TRX (A), rifampicin protocol sample (B), and totally labeled control (C) HMQC spectra were analyzed. The spectra were obtained at 303 K. The threshold was set low in spectrum B to show the absence of extra weak peaks. All spectra were acquired with 1024 × 200 points, 256 scans, and a recycle delay of 1.2 s. The processing was performed with zero filling and a square sine multiplication shifted by 90° in both dimensions. The States–TPPI method was used for quadrature detection in the indirect dimension (*12*). GARP was used to decouple ^{15}N during acquisition (*13*) and WATERGATE for water supression (*14*).

sample obtained when the cells grew all the time in labeled medium, a strong ^{15}N signal is present. These results show that rifampicin drives the labeling to the heterologous protein (Fig. 5A).

DISCUSSION AND CONCLUSION

The rifampicin protocol simplifies the protein labeling for NMR studies. The first steps of NMR sample optimization are facilitated. The first NMR spectrum can be obtained after growing, cleaving the cells and acquiring a ^{15}N-edited spectrum.

The two-dimensional ^{15}N HMQC of the rifampicin protocol sample spectrum is very similar to those of the purified protein. ^{13}C labeling and ^{15}N/^{13}C double labeling also give good results (data not shown). Gronenborn and Clore proposed a similar procedure by using an overexpressed protein (*7*). The strategy presented here is also simple, offers high yields and, most importantly, the rifampicin protocol can also be used for difficult low-expressing proteins. The rifampicin protocol can make the protein preparation cheaper by reducing the amounts of ^{13}C-glucose and $^{15}NH_4^+$ to be used. A 250-ml growth medium culture is sufficient to perform three-dimensional experiments. Lee *et al.* used a similar protocol to specifically label proteins with selected amino acids for NMR studies (*2*). In the present work we show that such a methodology has broader uses.

For the Opaque 2 LZ we have performed a fast prepurification step by using ultrafiltration membranes. This procedure is fast, with almost no loss of protein. It is important because, by selecting only the low-molecular-weight proteins, it enables solubilization at the concentrations necessary for NMR purposes.

The rifampicin protocol can also be used to follow proteins during purification by screening the ^{15}N signal on column fractions or in the supernatant of protein precipitation. This procedure can be easily done through a one-dimensional HMQC spectrum.

Several genome projects are being carried out nowadays. These projects consist of the identification and isolation of many novel genes. The next step will be the proteome projects. These include the elucidation of expression control, structure, and function of proteins coded by the large number of gene

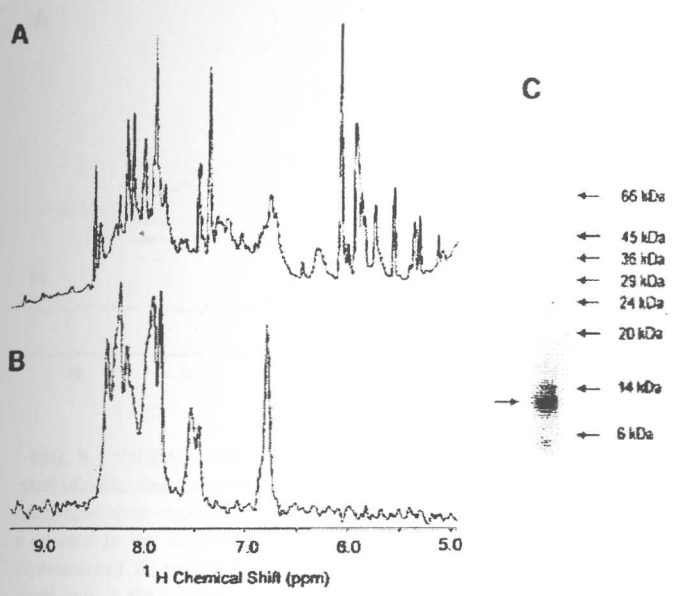

FIG. 3. ^{1}H spectrum (A) and ^{15}N-edited ^{1}H spectrum (B) of Opaque 2 LZ. The ^{15}N-edited ^{1}H spectrum shows low dispersion and is consistent with a leucine zipper (*6*). The proton spectrum shows several different peaks with higher dispersion. This spectrum was obtained with 250 ml of growth medium. The sample was prepared using the Amicon by passing 250 ml through a membrane of 30-kDa molecular cutoff and then concentrating it to 500 μl using a membrane of 3.5 kDa. C shows the SDS–PAGE of the rifampicin NMR sample used to obtain spectra A and B.

sequences. The investigation of these new proteins demands fast methodology for structural studies. Different methodologies have been proposed (*8, 9*). Selective labeling of the heterologous protein can speed up the screening of clones that leads to folded proteins for NMR structural studies.

HMQC spectrum analysis can also be used to monitor changes in protein structure upon drug addition. This will make rational drug design faster as the screening can be performed quickly.

We strongly believe that there might be cases where protein purification in high amounts is difficult and the structure determination could be elucidated by using the rifampicin protocol.

EXPERIMENTAL

NMR experiments. NMR spectra were made at 303 K in a Bruker Avance DRX 600 MHz, using 5-mm triple-resonance probes. Bruker XWINNMR software and NMRView (*10*) were used for data acquisition and processing and for data analysis, respectively. The sample preparation includes the addition of 10% D_2O for lock. All spectra were recorded at pH 7.0.

All reagents were of analytical grade purity.

Selective protein labeling: Rifampicin protocol samples. Escherichia coli BL21(DE3) with plasmids (pET) containing TRX or Opaque 2 LZ were grown in 100 ml of nonlabeled M9 growth medium (*11*) at 37°C and were shaken at 200 rpm up to mid-log phase (OD about 0.7 at 600 nm). At this point 1 mM of IPTG was added. This enabled the induction of T7 RNA polymerase. A small amount of unlabeled TRX or Opaque 2 LZ will be obtained. After 5 min, 200 μg/ml of rifampicin was added. The cells grew for 15 more min and then were centrifuged to pellet. This time interval is necessary in order to let rifampicin diffuse into the cell, inhibiting self synthesis while still in the unlabeled medium. The cells were then resuspended in 100 ml of ^{15}N-labeled M9 growth medium containing 1 mM IPTG and 200 μg/ml rifampicin. The induced cells grew for 2 to 3 h more and were cleft by freezing and thawing in cleavage buffer (1 ml TRX and 15 ml Opaque2 LZ per 100 ml of growth medium). The samples were then centrifuged and the superna-

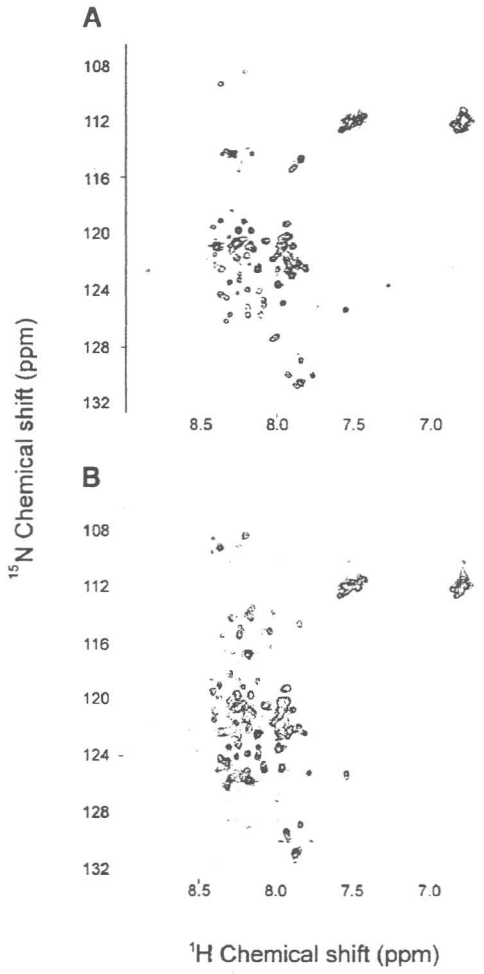

FIG. 4. Two-dimensional ^{15}N, ^{1}H-HMQC spectra of Opaque 2 LZ obtained with (A) and without (B) rifampicin. The 2D spectrum (A) shows 70 peaks while the primary sequence has 86 amino acids. The dispersion is very similar to the one obtained for GCN4 (*6*). The sample obtained without rifampicin shows several extra peaks. The sample was prepared as described in Fig. 3. All spectra were acquired with 1024 × 512 points, 64 scans, and a recycle delay of 1.3 s. The processing was performed with zero filling and a square sine multiplication shifted by 90° in both dimensions. The States–TPPI method was used for quadrature detection in the indirect dimension (*12*). GARP was used to decouple ^{15}N during acquisition (*13*) and WATERGATE for water supression (*14*).

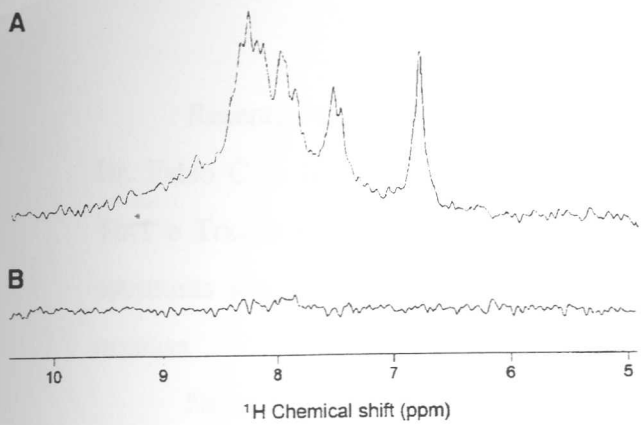

FIG. 5. ^{15}N-Edited ^{1}H spectrum of the sample retained in the 30-kDa cutoff ultrafiltration membrane prepared with (B) and without rifampicin (A). The spectra were obtained with the same number of scans of the material that is retained in the Amicon of the 30-kDa cutoff membrane (for details see Experimental). As expected, the sample prepared with rifampicin shows a ^{15}N signal only in the fraction where the Opaque 2 LZ is present (low molecular weight). The ^{1}H signal has the same intensity in the two samples (not shown).

ant containing the specifically labeled protein was used to perform NMR experiments. In the case of TRX, the sample was dialyzed in a membrane of molecular weight cutoff of 3.5 kDa to remove low-molecular-weight compounds (free amino acids). In the case of Opaque 2 LZ, a step for sample concentration was included and is described below.

Controls were made to probe the efficiency of the rifampicin protocol: bacterium cells grew always in labeled M9 medium. Briefly, the cells grew up to an OD (600 nm) of 0.7 when protein expression is induced with 1 mM IPTG, in the absence of rifampicin. The cells grew for 2 to 3 h more. Sample preparation is exactly the same as for samples made with the rifampicin protocol. These samples were called "totally labeled control."

The cleavage buffer used was 20 mM phosphate buffer, pH 7.0; 10 mM β-mercaptoethanol; 40 μg/ml PMSF.

Opaque 2 LZ sample preparation. The protein was expressed as described above. Cells grown in 250 ml of growth medium were cleaved with 50 ml of cleavage buffer (described above). The supernatant was ultrafiltrated at a molecular weight cutoff of 30 kDa. The flow-through was collected and applied to another ultrafiltration step, but now with a molecular weight cutoff of 3.5 kDa, in order to concentrate the sample and free it of low-molecular-weight compounds (such as peptides and free amino acids). The sample was concentrated to 500 μL and 100 mM of KCl was added.

Thioredoxin purification. The purified thioredoxin was obtained by cleaving the cells as described above, the supernatant was applied to a Toyopearl-650M column (ion exchange) at pH 8, and the fraction eluted with 50 mM NaCl was collected, dialyzed, and applied to the same column. TRX is eluted with 50 mM NaCl. Sample purity and expression were confirmed by SDS–PAGE.

ACKNOWLEDGMENTS

The authors thank PRONEX, CAPES, CNPq, FAPERJ, and ICGEB–International Center for Genetic Engineering and Biotechnology. We also thank Dr. C. Griesinger for helpful discussions.

REFERENCES

1. A. Travers, Control of transcription in bacteria, *Nature (London) N. Biol.* **229,** 69 (1971).
2. K. M. Lee, E. J. Androphy, and J. D. Baleja, A. novel method for selective isotope labeling of bacterially expressed proteins, *J. Biomol. NMR* **5,** 93–96 (1995).
3. W. W. Gao and E. Goldman, Use of sodium dodecyl sulfate–polyacrylamide gel eletrophoresis to resolve mRNA and its protein product in one gel, *FASEB J.* **11,** 1153–1156 (1997).
4. A. Holmgren, Thioredoxin, *Annu. Rev. Biochem.* **54,** 237–271 (1985).
5. A. L. Vettore, J. A. Yunes, G. C. Neto, M. J. Silva, P. Arruda, and A. Leite, The molecular and functional characterization of a Opaque2 homologue gene from Coix and a new classification of plant bZIP proteins, *Plant Mol. Biol.* **36,** 249–263 (1998).
6. C. Bracken, P. Carr, J. Cavanagh, and A. G. Palmer, Temperature dependence of intramolecular dynamics of the basic leucine zipper of GCN4: Implications for the entropy of association with DNA, *J. Mol. Biol.* **285,** 2133–2146 (1999), doi: 10.1006/jmbi.1998.2429.
7. A. M. Gronenborn and G. M. Clore, Rapid screening for structural integrity of expressed proteins by heteronuclear NMR spectroscopy, *Protein Sci.* **5,** 174–177 (1996).
8. D. T. Jones, GenTHREADER: An efficient and reliable protein fold recognition method for genomic sequences, *J. Mol. Biol.* **287,** 797–815 (1999), doi: 10.1006/jmbi.1999.2583.
9. C. C. Wang and C. L. Tsou, Post-genome study—Proteomics, *Acta Biochim. Biophys. Sin.* **30,** 533–539 (1998).
10. B. A. Johnson and R. A. Blevins, NMR View—A computer-program for the visualization and analysis of NMR data, *J. Biomol. NMR* **4,** 603–614 (1994).
11. J. Sambrook, E. F. Fritsch, and T. Maniatis, "Molecular Cloning—A Laboratory Manual," Cold Spring Harbor Laboratory Press, Cold Spring Harbor, New York, 1989.
12. D. Marion, M. Ikura, R. Tschudin, and A. Bax, Rapid recording of 2D NMR spectra without phase cycling-application to the study of hydrogen exchange in proteins, *J. Magn. Reson.* **85,** 393–399 (1989).
13. A. J. Shaka, P. B. Barker, and R. Freeman, Computer-optimized decoupling scheme for wideband applications and low-level operation, *J. Magn. Reson.* **64,** 547–552 (1985).
14. M. Piotto, V. Saudek, and V. Sklenar, Gradient-tailored excitation for single-quantum NMR-spectroscopy of aqueous solutions, *J. Biomol. NMR* **2,** 661–665 (1992).

Recentemente dois alunos de mestrado orientados pelo Grupo liderado pelo Dr. Fabio C.R. Almeida e Ana Paula Valente conseguiram resolver as estruturas de Trx1 e Trx2 e estão em fase final de refinamento. Como era de se esperar as duas estruturas são muito semelhantes, mas parecem existir diferenças nas dinâmicas das mesmas.

Nesse sentido, Simone Vidigal Alves (técnica de nível superior alocada em meu laboratório) iniciou estudos comparando a atividade de tiorredoxina redutase 1 (TRR1) de *Saccharomyces cerevisiae*, utilizando as duas tiorredoxinas como substrato. Os resultado obtidos indicam que existe uma diferença considerável na afinidade de TRR1 pelos duas isoformas de tiorrexina (figura 13, tabela II).

A

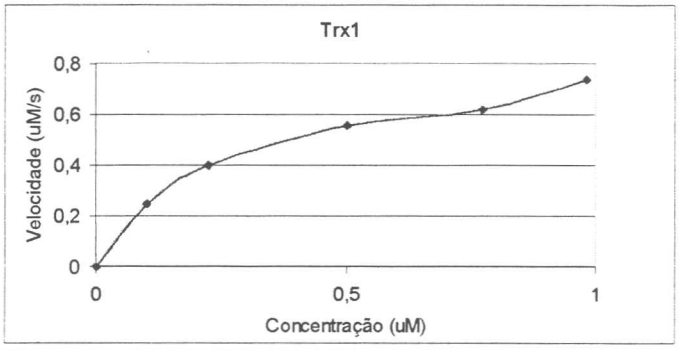

B

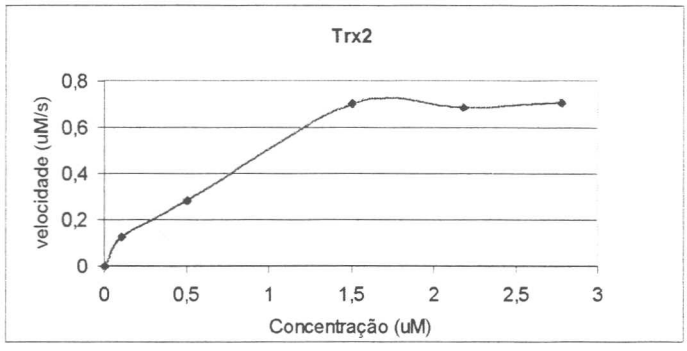

Figura 13 – Em A, gráfico mostrando a cinética enzimática de TRR1(75nM) e Trx1(0,1-0,98mM); em B, gráfico mostrando a cinética enzimática de TRR1(75nM) e Trx2 (0,1-2,78mM).

Tabela II Paramêtros enzimáticos de TRR1

Substrato	K_M (uM)	Vmax (uM/s)	Kcat (s^{-1})	Kcat /K_M (M^{-1} s^{-1})
Trx1	0,2	0,8	11,2	$4,8 \times 10^7$
Trx2	0,5	0,8	10,3	$1,9 \times 10^7$

Dentro do programa SmolBNet, conseguimos vários cristais da proteína TRR1 a qual difratou raios X com resolução razoável (2.3 Å). Esperamos com esses dados resolver a estrutura de TRR1 pela técnica de substituição molecular utilizando tiorredoxina redutase de *Arabdopsis thaliana* como referência. Tentaremos encontrar características estruturais em TRR1, Trx1 e Trx2 que possam explicar os dados funcionais apresentados resumidamente na figura 13 e Tabela II.

Pretendemos utilizar abordagens semelhantes para entender interações enzimas substratos. Mais especificamente, estamos interessados em investigar as interações entre diferentes tiorredoxinas redutase e tiorredoxinas e entre diferentes tiorredoxina e tiorredoxinas peroxidases, tanto no aspecto funcional como no estrutural.

No caso de Ohr de *Xylella fastidiosa*, estamos procurando o sistema responsável por doar elétrons necessários a redução de peroxidos orgânicos. Nesse sentido, é importante destacar resultado descrito no anexo 16: Ohr não aceita elétrons oriundos de tiorredoinas de *Saccharomyces cerevisiae* e nem de tiorredoxina de *Spirulina*. Recentemente, o aluno de iniciação científica José Renato Rosa Cussiol clonou, expressou e purificou uma tiorredoxina de *Xylella fastidiosa* (TSNC). A atividade específica de Ohr para TBHP foi aumentada em cerca de cinco vezes indicando que essa TSNC é doador de elétrons biológico para Ohr (figura 14). Dada a especificidade da interação TSNC-Ohr, esse ponto pode constituir-se em um potencial alvo de quimioterapia no futuro.

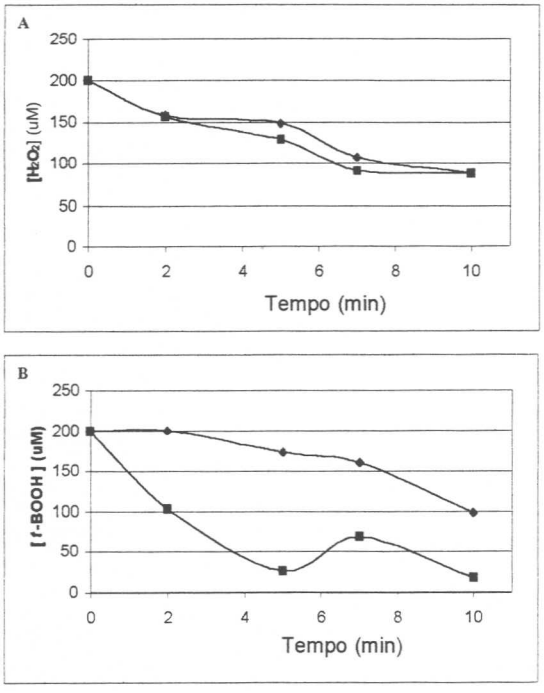

Figura 14 **Atividade específica de Ohr na presença e na ausência de TSNC.** Concentração de TBHP e H_2O_2 foi determinada através do ensaio FOX (ver anexo 16). A reação foi iniciada após a adição de DTT (500uM) e terminada pela adição de HCl (0,1M). Reações ocorreram em tampão Hepes (50mM) pH 7,4 na presença de azida (1mM) e DTPA (0,1mM). Em A, a reação ocorreu na presença de H_2O_2 (200uM) e Ohr (30ng/ul); em B, a reação ocorreu na presença de *t*-BOOH (200uM) e Ohr (1ng/ul). Para ambas as reações os símbolos representam: ♦¨ (Ohr sem adição de TSNC); ■ (Ohr + TSNC).

Também dentro do programa SMolBnet, obtivemos cristais de TSNC que estão em fase de refinamento. De posse das estruturas de Ohr e TSNC esperamos ser possível correlacionar resultados funcionais e estruturais que talvez possam permitir o desenho de inibidores dessa via de destoxificação de peróxidos orgânicos. Além TRR1 de *Saccharomyces cerevisiae* e Ohr e TSNC de *Xylella fastidiosa* vários outros cristais de proteína foram obtidos nos nossos estudos dentro do programa SMOLBNET, sendo um desses cristais difrataram raios X com boa resolução. A tabela III apresenta os progressos de nosso grupo dentro do Programa SMOLBNET.

Tabela III. Resumo dos resultados obtidos no SMolBNet.

Gene/MW/ Organism	Clonagem	Expressão	Purificação	Cristalização (Tratamento)	Refinamento	Difração	Estrutura
Ohr (17 kDa) *X. fastidiosa*	pET15b (Novagen)	~20mg/L de cultura	His tag		Em andamento	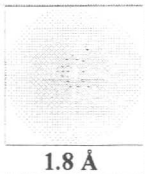 1.8 Å	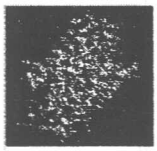
TRR1 (30kDa) *S. cerevisiae*	pET15b (Novagen)	~10mg/L de cultura	His tag	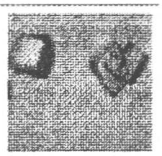 (H_2O_2)	Em andamento	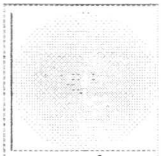 2.3 Å	
Ahp1 (25kDa) *S. cerevisiae*	pET15b (Novagen)	~30mg/L de cultura	His tag	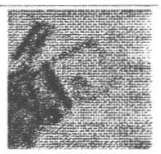 (S/T e *t*-BOOH)	Em andamento	 3.2 Å	
Grx2 (12kDa) *S. cerevisiae*	pET15b (Novagen)	~10mg/L de cultura	His tag	 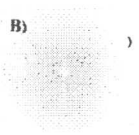		 1.8	
cTPxI (30kDa) *S. cerevisiae*	pET15b (Novagen)	~10mg/L de cultura	FPLC	 (S/T e H_2O_2)	Em andamento		
cTPxII (25kDa) *S. cerevisiae*	pPROEX (Invitrogen)	~5mg/L de cultura	Em andamento	 (H_2O_2)	Em andamento		
TSNC (13.5kDa) *X. fastidiosa*	pET15b (Novagen)	~20mg/L de cultura	His tag	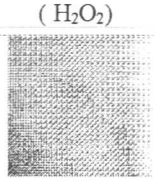 (H_2O_2)	Em andamento		
mTPxI (30kDa) *S. cerevisiae*	pET15b (Novagen)	~5mg/L de cultura	FPLC	Em andamento			
nTPx (30kDa) *S. cerevisiae*	TOPO	Em andamento					
TRR (80kDa) *X. fastidiosa*	PET15b (Invitrogen)	Em andamento					
XF2394 (30kDa) *X. fastidiosa*	pET15b (Novagen)	Em andamento					

Ainda dentro do programa SMOlbNet, estamos interessados também na identificação de estruturas quartenárias de peroxidases dependentes de tiól. No caso de peroxirredoxinas do tipo A, foi demonstrado que estas proteínas podem assumir configurações do tipo decamérica (pentameros de homodímeros) dependendo do estado de oxidação dessas proteínas (revisado por Wood e col., 2003a). No caso de AhpC, a proteína reduzida se encontra na forma decamérica como demonstrado por experimentos de ultrafiltração e de difração de raios X (SAXS). Por outro lado, dados de ultrafiltração revelam que a proteína assume a configuração dimérica quando oxidada. A proteína TrypB também se apresenta como um decâmero quando reduzida(revisado por Wood e col., 2003a). Apesar desses estudos, pouco se sabe sobre o significado biológico destas estruturas diméricas e decaméricas. Tem-se postulado que esses estados de oligomerização poderiam ser um nível adicional de regulação de peroxirredoxinas por H_2O_2 (revisado por Wood e col., 2003a).

Dessa forma, temos interesses em estudar o grau de oligomerização de outras peroxidases dependentes de tiól. Já iniciamos estudos com Ohr de *Xylella fastidiosa* realizando experimentos de DLS ("*Dynamic Light Scattering*") o qual pode determinar o raio de giro de uma partícula em solução e com base destes dados é possível calcular o peso molecular das partículas. Neste experimento analisamos a possibilidade de Ohr formar estruturas quaternárias de acordo com o estado redox. Para tanto a proteína foi tratada com H2O2 , TBHP e DTT.

O resultado de DLS aponta uma partícula de massa estimada em 31KDa para a proteína sem tratamento prévio com agentes oxidante ou redutor. A proteína tratada com peróxidos apresentou um peso molecular de 36kDa (H_2O_2) e 32kDa (TBHP) enquanto que para a proteína tratada previamente com DTT a massa foi de 35 kDa. O que indica que em solução Ohr se apresenta como um dímero independente de seu estado redox (Figura 15). Para a confirmação destes resultados pretendemos realizar experimentos de SAXs ("*Small Angle X-ray Scattering*") em colaboração com a Dra. Íris Torriani,

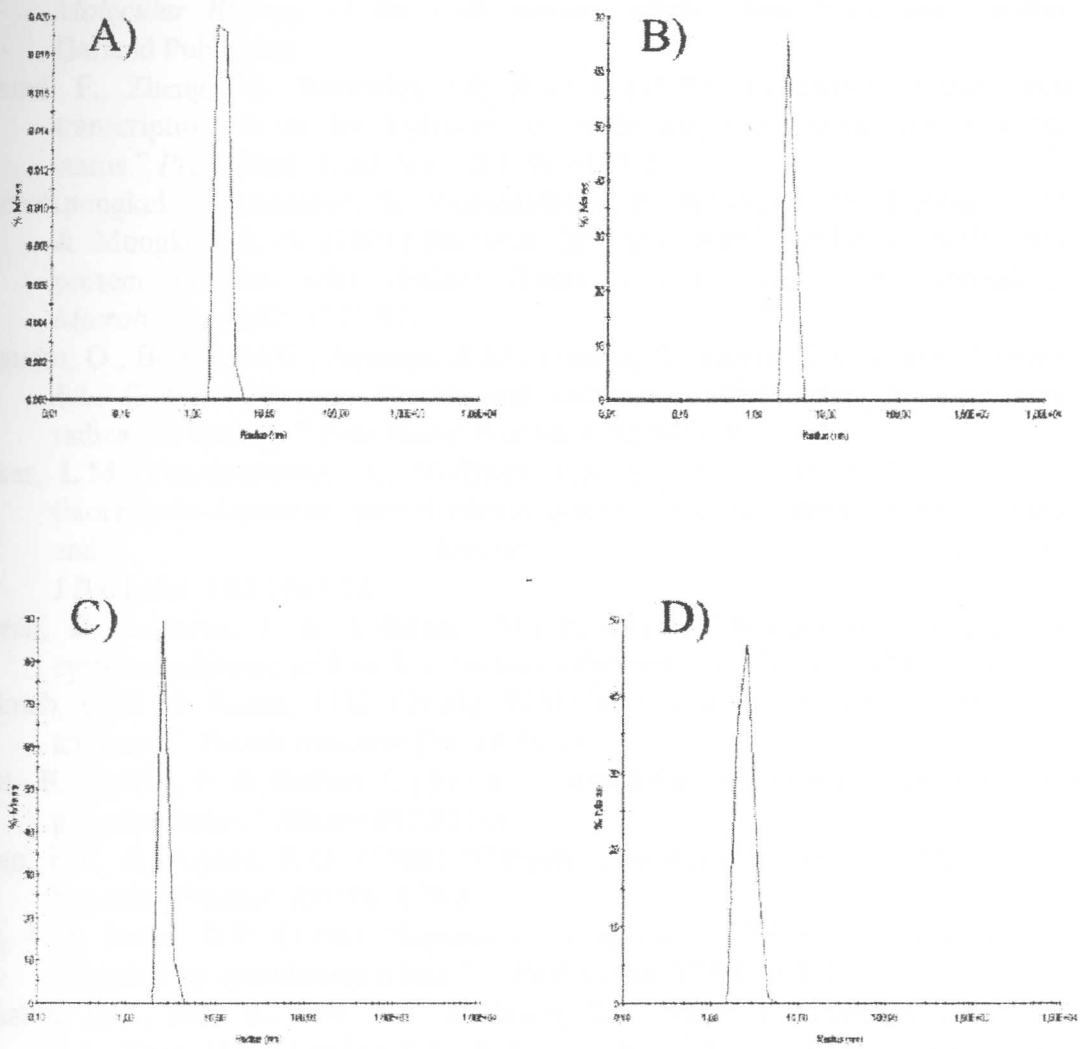

Figura 15 - Resultado de espalhamento de luz dinâmica para a proteína Ohr a concentração de proteína foi fixada em 600μM em todas as condições testadas. A) Proteína sem tratamento prévio; B) Ohr previamente tratada com DTT 1mM 1h/37°C; C) Ohr tratada com H_2O_2 (0,1mM) 1h/37°C e D) Ohr tratada com TBHP (1mM) 1h/37°C. Todos os resultados indicam uma partícula de aproximadamente 34 KDa que corresponde à forma dimérica de Ohr.

Referências

Alberts, B., Bray, D., Lewis, J., Raff, M., Roberts, K. & Watson, J. D. (1994) em *Molecular Biology of the Cell*, terceira edição, New York and London: Garland Publishing.

Aslund, F., Zheng, M., Beckwith, J.& Storz G.(1999) "Regulation of the OxyR transcription factor by hydrogen peroxide and the cellular thiol-disulfide status." *Proc. Natl. Acad. Sci. USA*. **96**:6161-5.

Atichartpongkul, S., Loprasert, S., Vattanaviboon, P., Whangsuk, W., Helmann, J.D. & Mongkolsuk, S. (2001)"Bacterial Ohr and OsmC paralogues define two protein families with distinct functions and patterns of expression." *Microbiology* **147**: 1775-82.

Augusto, O., Bonini, M.G., Amanso, A.M., Linares, E., Santos, C.C. & De Menezes, S.L. (2002) "Nitrogen dioxide and carbonate radical anion: two emerging radicals in biology." *Free Radic Biol Med*. **32**:841-59.

Baker, L.M., Raudonikiene, A., Hoffman, P.S. & Poole, L.B. (2001) "Essential thioredoxin-dependent peroxiredoxin system from Helicobacter pylori: genetic and kinetic characterization. J Bacteriol. **183**:1961-73.

Biteau, B., Labarre, J. & Toledano, M.B.(2003) "ATP-dependent reduction of cysteine-sulphinic acid by S. cerevisiae sulphiredoxin." *Nature*. **425**:980-4.

Bokoch, G.M. & Knaus, U.G. (2003) "NADPH oxidases: not just for leukocytes anymore!" *Trends Biochem Sci*. **28**:502-8.

Bryk, R., Griffin, P. & Nathan, C.(2000) "Peroxynitrite reductase activity of bacterial peroxiredoxins." *Nature* **407**:211-5.

Bunn, H.F. & Poyton, R.O. (1996) "Oxygen sensing and molecular adaptation to hypoxia" *Physiol. Rev.***76**: 839-85.

Cai, J. & Jones, D.P. (1998) "Superoxide in apoptosis. Mitochondrial generation triggered by cytochrome c loss." *J. Biol. Chem*. **273**:11401-4.

Causton, H.C., Ren, B., Koh, S.S., Harbison, C.T., Kanin, E., Jennings, E.G., Lee, T.I., True, H.L., Lande,r E.S. & Young, R.A. (2001) "Remodeling of yeast genome expression in response to environmental changes." *Mol. Biol. Cell*. **12**:323-37.

Chae, H.Z., Kim, I. H., Kim, K. & Rhee, S.G. (1993), "Cloning, sequencing, and Mutation of Thiol Specific Antioxidant gene of TSA" *J. Biol. Chem*. **268**:16815-21.

Chae, H.Z., Robison, K. Poole, L.B. Church, G., Storz, G. & Rhee, S.G. (1994a), "Cloning and sequencing of thiol-specific antioxidant from mammalian brain: alkylhydroperoxide reductase and thiol-specific antioxidant define a large family of antioxidant enzymes" *Proc. Natl. Acad. Sci*. **91**: 7017-21.

Chae, H.Z., Uhm. T.B. & Rhee, S.G. (1994b) "Dimerization of thiol-specific antioxidant and the essential role of cysteine 47" *Proc. Natl. Acad. Sci. USA* **91**: 7022-26.

Chang, T.S., Jeong, W., Choi, S.Y., Yu, S., Kang ,.S.W. & Rhee SG. (2002) "Regulation of peroxiredoxin I activity by Cdc2-mediated phosphorylation." *J. Biol. Chem*. **277**:25370-6.

Choi, I.G., Shin, D.H., Brandsen, J., Jancarik, J., Busso, D., Yokota, H., Kim, R. & Kim S.H. (2003) "Crystal structure of a stress inducible protein from

Mycoplasma pneumoniae at 2.85 A resolution." *J Struct Funct Genomics.* **1**:31-34.

Christman, M.F., Morgan, R.W., Jacobson, F.S. & Ames, B.N. (1985) "Positive control of a regulon for defenses against oxidative stress and some heat-shock proteins in *Salmonella typhimurium*" *Cell*, **41**: 753-62.

Delaunay, A., Pflieger, D., Barrault, M.B., Vinh, J. & Toledano, MB.(2002) "A thiol peroxidase is an H_2O_2 receptor and redox-transducer in gene activation." Cell. **111**:471-81.

Demasi, M., Shringarpure, R & Davies, K.J. (2001) "Glutathiolation of the proteasome is enhanced by proteolytic inhibitors." *Arch. Biochem. Biophys.* **389**: 254-63.

Dietz, K.J., Horling, F., Konig, J. & Baier, M. (2002) "The function of the chloroplast 2-cysteine peroxiredoxin in peroxide detoxification and its regulation." *J. Exp. Bot.* **53**:1321-9.

Dinkova-Kostova, A.T., Holtzclaw, W.D., Cole, R.N., Itoh, K., Wakabayashi, N., Katoh, Y., Yamamoto, M. & Talalay, P. (2002) "Direct evidence that sulfhydryl groups of Keap1 are the sensors regulating induction of phase 2 enzymes that protect against carcinogens and oxidants." *Proc. Nat.l Acad. Sci. USA* **99**:11908-13.

Estruch F. (2000) "Stress-controlled transcription factors, stress-induced genes and stress tolerance in budding yeast." *FEMS Microbiol Rev.* **24**:469-86.

Fernandes, L., Rodrigues-Pousada, C. & Struhl, K. (1997) "Yap, a novel family of eight bZIP proteins in *Saccharomyces cerevisae* with distinct biological functions." *Molec.Cell. Biol.* **17**: 6982-6993.

Gasch, A.P., Spellman, P.T., Kao, C.M., Carmel-Harel, O., Eisen, M.B., Storz, G., Botstein, D. & Brown P.O. (2000) "Genomic expression programs in the response of yeast cells to environmental changes." *Mol. Biol. Cell.* **11**:4241-57.

Godon, C., Lagniel, G., Lee, J., Buhler, J-M., Kieffer, S., Perrot, M., Boucherie, H., Toledano, M.B. & Labarre, J. (1998) "The H_2O_2 stimulon in *Saccharomyces cerevisiae*" *J. Biol. Chem.*, **273**, 22480-89.

Gorner, W., Durchschlag, E., Wolf, J., Brown, E.L., Ammerer, G., Ruis, H. & Schuller, C.(2002) "Acute glucose starvation activates the nuclear localization signal of a stress-specific yeast transcription factor." *EMBO J.* **21**:135-44.

Halliwell, B & Gutteridge, J.M.C. (1999) em *Free Radicals in biology and Medicine* (Hallywell, B e Gutteridge, J.M.C., eds.), third edition, Claredon Press, Oxford.

Hasan, R., Leroy, C., Isnard, A.D., Labarre, J., Boy-Marcotte, E. & Toledano, M.B.(2002) "The control of the yeast H_2O2 response by the Msn2/4 transcription factors." *Mol. Microbiol.* **45**:233-41.

Hong, S.K., Cha, M.K., Choi, Y.S., Kim, W.C. & Kim, IH. (2002) "Msn2p/Msn4p act as a key transcriptional activator of yeast cytoplasmic thiol peroxidase II" *J. Biol. Chem.* **277**:12109-17.

Isoyama, T., Murayama, A., Nomoto A. & Kuge S. (2001) "Nuclear import of the yeast AP-1-like transcription factor Yap1p is mediated by transport receptor Pse1p, and this import step is not affected by oxidative stress." *J. Biol. Chem.* **276**:21863-9.

Jeong, J.S., Kwon, S.J., Kang, S.W., Rhee, S.G. & Kim, K. (1999) Purification and characterization of a second type Thioredoxin peroxidase (type II TPx) from *Saccharomyces cerevisiae*. *Biochemistry* **38**: 776-83.

Kim, K., Kim, I.H., Lee, Ki-Y., Rhee, S.G. & Stadtman, E.R. (1988) "The isolation and purification of a specific "protector" protein which inhibits enzyme

inactivation by a thiol/Fe(III)/O_2 mixed-function oxidation system" *J. Biol. Chem.* **263**: 4704-4711.

Kim, I.H., Kim, K. & Rhee, S.G.(1989) "Induction of an antioxidant protein of *Saccharomyces cerevisae* by O_2, Fe(III), or 2-mercaptoethanol" *Proc. Natl. Acad. Sci. USA* **86:** 6018-6022.

Korshunov, S.S., Krasnikov, B.F., Pereverzev, M.O. & Skulachev, V.P. (1999) "The antioxidant functions of cytochrome c" *FEBS Lett.* **462**:192-8.

Korshunov, S.S., Skulachev, V.P., Starkov, A.A. (1997) "High protonic potential actuates a mechanism of production of reactive oxygen species in mitochondria." *FEBS Lett.***416**:15-8.

Kowaltowski, A.J., Castilho, R.F. & Vercesi, [a]E. (2001) "Mitochondrial permeability transition and oxidative stress." *FEBS Lett.* **495**: 12-5.

Laval, F. (1988) "Pretreatment with oxygen species increases the resistance of mammalian cells to hydrogen peroxide and X-rays" *Mutat. Res.* **201**: 73-9.

Lee, J., Godon, C., Lagniel, G., Spector, D., Garin, J., Labarre, J. & Toledano M.B.(1999a) "Yap1 and Skn7 control two specialized oxidative stress response regulons in yeast." *J. Biol. Chem.* **274**:16040-6.

Lee, J., Romeo, A. & Kosman, D. J. (1996) "Transcriptional remodeling and G1 arrest in dioxygen stress in *Saccharomyces cerevisiae*" *J. Biol. Chem.* **271**: 24885-93.

Lee, J., Spector, D., Godon, C., Labarre, J. & Toledano, M.B. (1999b) "A new antioxidant with alkyl hydroperoxide defense properties in yeast." *J. Biol. Chem.* **274**:4537-44.

Lee S.R., Kwon K.S., Kim S.R. & Rhee S.G. (1998) "Reversible inactivation of protein-tyrosine phosphatase 1B in A431 cells stimulated with epidermal growth factor." *J. Biol. Chem.* 273:15366-72.

Lesniak, J., Barton, W.A. & Nikolov, D.B.(2002) "Structural and functional characterization of the Pseudomonas hydroperoxide resistance protein Ohr" *EMBO J.* **21**:6649-59.

Lu, D., Maulik, N., Moraru, I.I., Kreutzer, D.L., & Das, D.K. (1993) "Molecular adaptation of vascular endothelial cells to oxidative stress" *Am. J. Physiol.*, 264, C715-C722.

Madeo, F., Herker, E., Maldener, C., Wissing, S., Lachelt, S., Herlan, M., Fehr, M., Lauber, K., Sigrist, S.J., Wesselborg, S. & Frohlich K.U. (2002) "A caspase-related protease regulates apoptosis in yeast." *Mol Cell* **9**:911-7.

Mo, J.Y., Maki, H. & Sekiguchi, M. (1992) "Hydrolytic elimination of a mutagenic nucleotide, 8-oxodGTP, by human 18-kilodalton protein: sanitization of nucleotide pool." *Proc Natl Acad Sci U S A* **89**:11021-5.

Mongkolsuk, S., Praituan, W., Loprasert, S., Fuangthong, M. & Chamnongpol, S. (1998) "Identification and characterization of a new Organic Hydroperoxide Resistance Gene (*ohr*) with a novel pattern of oxidative stress regulation from *Xanthomonas campestris pv.phaseoli*" *J Bacteriol.* **180**:2636-43.

Morgan, B.A., Banks, G.R., Toone, W.M., Raitt, D., Kuge, S. & Johnston, L.H. (1997) "The Skn7 response regulator controls gene expression in the oxidative stress response of the budding yeast *Saccharomyces cerevisiae*" *The EMBO J.*, **16**:1035-44.

Ochsner, U.A., Hassett, D.J. & Vasil, M.L.(2001) "Genetic and physiological characterization of *ohr*, encoding a protein involved in organic hydroperoxide resistance in *Pseudomonas aeruginosa*" *J. Bacteriol.* **183**:773-778.

Paget, M.S. & Buttner, M.J. (2003) "Thiol-based regulatory switches." *Annu. Rev. Genet.* **37**:91-121.

Park, S.G., Cha, M.K., Jeong, W, & Kim, I.H. (2000). "Distinct physiological functions of thiol peroxidase isoenzymes in *Saccharomyces cerevisiae*." *J. Biol. Chem.* **275**:5723-5732.

Pedrajas, J.R., Miranda-Vizuete, A., Javanmardy, N., Gustafsson, J.A. & Spyrou, G. (2000) "Mitochondria of Saccharomyces cerevisiae contain one-conserved cysteine type peroxiredoxin with thioredoxin peroxidase activity." *J. Biol. Chem.* **26**: 16296-16301.

Pomposiello, P.J. & Demple, B.(2001) "Redox-operated genetic switches: the SoxR and OxyR transcription factors." *Trends Biotechnol.* **19**:109-14.

Ravagnan, L., Roumier, T. & Kroemer, G. (2002) "Mitochondria, the killer organelles and their weapons" *J Cell Physiol.* **192**:131-7.

Rhee, S.G.(1999)"Redox signaling: hydrogen peroxide as intracellular messenger. *Exp Mol Med.* **31**:53-9.

Rouhier, N., Gelhaye, E. & Jacquot J.P. (2002) "Glutaredoxin-dependent peroxiredoxin from poplar: protein-protein interaction and catalytic mechanism." *J. Biol. Chem.* **277**:13609-14.

Salmeen, A., Andersen, J.N., Myers, M.P., Meng, T.C., Hinks, J.A., Tonks, N.K. & Barford, D. (2003) "Redox regulation of protein tyrosine phosphatase 1B involves a sulphenyl-amide intermediate." *Nature* **423**:769-73.

Seo, M.S., Kang, S.W., Kim, K., Baines, I.C., Lee, T.H. & Rhee S.G. (2000) "Identification of a new type of mammalian peroxiredoxin that forms an intramolecular disulfide as a reaction intermediate." *J. Biol. Chem.* **275**:20346-54.

Skulachev, V.P. (1998) "Cytochrome c in the apoptotic and antioxidant cascades." *FEBS Lett*, **423**:275-80

Spitz, D.R., Dewey, W.C. & Li, G.C. (1987) "Hydrogen peroxide or heat shock induces resistance to hydrogen peroxide in Chinese hasmster fibroblasts" *J. Cell. Physiol.* **131**:364-373.

Stadtman, E.R. (1990) "Metal ion-catalyzed oxidation of proteins: biochemical mechanism and biological consequences" *Free Rad. Biol. Med.* **9**:315-325.

Stone, J.R. (2004) "An assessment of proposed mechanisms for sensing hydrogen peroxide in mammalian systems" *Arch. Biochem. Biophys.* **422**:119-24.

Storz, G., Jacobson, F.S., Tartaglia, L.A., Morgan, R.W., Silveira, L.A. & Ames B.N. (1989) "An alkyl hydroperoxide reductase induced by oxidative stress in *Salmonella typhimurium* and *Escherichia coli*: genetic characterization and cloning of ahp." *J. Bacteriol.* **171**:2049-55.

St-Pierre, J., Buckingham, J.A., Roebuck, S.J. Brand, M.D.(2002) "Topology of superoxide production from different sites in the mitochondrial electron transport chain." *J. Biol. Chem.* **277**:44784-90.

Szallies, A., Kubata, B.K. & Duszenko, M. (2002) "A metacaspase of *Trypanosoma brucei* causes loss of respiration competence and clonal death in the yeast *Saccharomyces cerevisiae*" *FEBS Lett* **517**:144-50.

Trivelli, X., Krimm, I., Ebel, C., Verdoucq, L., Prouzet-Mauleon, V., Chartier, Y., Tsan, P., Lauquin, G., Meyer, Y. & Lancelin, J.M. (2003) "Characterization of the yeast peroxiredoxin Ahp1 in its reduced active and overoxidized inactive forms using NMR." Biochemistry. **42**:14139-49.

Van Montfort, R.L., Congreve, M., Tisi, D., Carr, R. & Jhoti, H. (2003) "Oxidation state of the active-site cysteine in protein tyrosine phosphatase 1B." *Nature* **423**:773-7.

Veal, E.A., Ross, S.J., Malakasi, P., Peacock, E. & Morgan, BA. (2003) "Ybp1 is required for the hydrogen peroxide-induced oxidation of the Yap1 transcription factor." *J. Biol. Chem.* **278**:30896-904.

Veinot-Drebot, L.M., Singer, R.A. & Johnston, G.C. (1989) "Heat-shock causes transient inhibition of yeast rRNA gene transcription" *J. Biol. Chem.*, **264:** 19473-19474.

Verdoucq, L., Vignols, F., Jacquot, J.P., Chartier, Y. & Meyer Y.(1999) "In vivo characterization of a thioredoxin h target protein defines a new peroxiredoxin family." *J. Biol. Chem.* **274**:19714-22.

Werner-Washburne, M., Braun, E., Johnston, G.C. & Singer, R.A. (1993) "Stationary-phase in the yeast *Saccharomyces cerevisae*" *Microbiol. Rev.*, **57**: 383-401.

Wiese, A.G., Pacifici, R.E. & Davies, K J.A. (1995) "Transient adaptation to oxidative stress in mammalian cells" *Arch. Biochem. Biophys.* **318**:231-240.

Wong, C.M., Zhou, Y., Ng, R.W., Kung, H.F. & Jin D.Y.(2002) "Cooperation of yeast peroxiredoxins Tsa1p and Tsa2p in the cellular defense against oxidative and nitrosative stress." *J. Biol. Chem.* **277**:5385-94.

Woo, H.A, Chae, H.Z., Hwang, S.C., Yang, K.S., Kang, S.W., Kim, K. & Rhee S.G.(2003) "Reversing the inactivation of peroxiredoxins caused by cysteine sulfinic acid formation." *Science* **300**:653-6.

Wood, Z.A, Schroder, E., Harris, J.R. & Poole, L.B. (2003a) "Structure, mechanism and regulation of peroxiredoxins" *Trends in Biochem. Sci.* **28**: 32-40.

Wood, Z.A, Poole, L.B. & Karplus, P.A.(2003b) "Peroxiredoxin evolution and the regulation of hydrogen peroxide signaling." *Science* **300**:650-3.

Wu, A., Wemmie, J.A., Edgington, N.P., Goebl, M., Guevara, J.L. & Moye-Rowley ,W.S. (1993) "Yeast bZip proteins mediate drug and metal resistance" *J. Biol. Chem.*, **268**:18850-8.

Yim, M.B., Chae, H.Z., Rhee, S.G., Chock, P.B. & Stadtman, E.R. (1994) "On the protective mechanism of the Thiol Specific Antioxidant enzyme against the oxidative damage of biomolecules" , *J. Biol. Chem.*, **269**: 1621-1626.

Zhang, P., Liu, B., Kang, S.W., Seo, M.S., Rhee, S.G. & Obeid, L.M. (1997) "Thioredoxin peroxidase is a novel inhibitor of apoptosis with a mechanism distinct from that of Bcl-2" *J Biol Chem.* **272**:30615-8.

Zhao, Y., Wang, Z.B. & Xu, J.X. (2003) "Effect of cytochrome c on the generation and elimination of $O_2^{\bullet-}$ and H_2O_2 in mitochondria". *J Biol Chem.* **278**:2356-60.

Zheng, M. & Storz, G. (2000) "Redox sensing by prokaryotic transcription factors." *Biochem. Pharmacol.* **59**:1-6.

Zoratti, M. & Szabo, I. (1995) "The mitochondrial permeability transition." *Biochim. Biophys. Acta* **1241**:139-76.